Adsorption on platinum (110): reflection-absorption infra-red studies

Robinson, Andrew William

Award date:
1988

Awarding institution:
University of Bath

Adsorption on Platinum(110):

Reflection-Absorption Infra-red Studies

submitted by Andrew William Robinson
for the degree of PhD
of the University of Bath
1988

A W Robinson

ProQuest LLC
789 East Eisenhower Parkway
P.O. Box 1346
Ann Arbor, MI 48106-1346

SUMMARY

Adsorption of CO and co-adsorption of CO with potassium on Pt(110)-(1 x 2) has been studied using reflection-absorption infra-red spectroscopy (RAIRS), temperature programmed desorption and low energy electron diffraction (LEED).

For adsorption of CO on Pt(110)-(1 x 2) at 300K, the (1 x 2) reconstruction is lifted to form a (1 x 1) LEED pattern at θ_{CO}=0.5. The C-O stretch exhibits a single absorption peak at all CO coverages, increasing in frequency with coverage from 2085 cm^{-1} to 2132 cm^{-1}. CO isotope mixture experiments demonstrate that the coverage dependent frequency shift is due solely to dipole-dipole interactions. The intensity of the absorption band reaches a maximum at θ_{CO}=0.5 and declines thereafter. To account for the reduction in absorption coefficient, a model of adsorption where the CO molecular axis tilts away from the surface normal at θ_{CO}>0.5 is proposed. A similar intensity decline has been observed for CO/Ru(001) at θ_{CO}>0.33; an adsorption model for CO/Ru(001) at $0.33<\theta_{CO}<0.66$ is proposed, based on three domains of tilted CO in a $(2\sqrt{3} \times \sqrt{3})R30^{o}$ structure.

RAIRS spectra following CO adsorption at 100K are similar to those observed at 300K, despite no lifting of

the surface reconstruction. It is concluded that the surface geometry of the (1 x 2) surface is similar to the (1 x 1) surface and a rumpled surface model is proposed to account for this.

When CO is co-adsorbed with potassium (Θ_K=0.1) on Pt(110)-(1 x 2) at 300K, the RAIRS band is shifted down to 1985-2030 cm^{-1} and is broadened. Coverage dependent frequency shift and intensity behaviour remain similar to CO/Pt(110)-(1 x 2). Isotope mixture experiments show no extra contribution to the frequency shift due to chemical effects. It is concluded that the overall downward frequency shift is due to interaction of the electric field associated with potassium ions with the CO dipole. An electrostatic model is applied to qualitatively demonstrate the downward frequency shift and broadening of the absorption band.

To my parents.

ACKNOWLEDGEMENTS

I would like to thank the following people for their assistance in carrying out this work. Firstly, my supervisor, Dr. B.E. Hayden, for his help and encouragement in this project. I am also grateful to the following for technical assistance: Mr. G. Venn and his workshop staff and Mr. J. Stainer, the chief technician in physical chemistry. There are also several colleagues working in the laboratory who have helped me either to obtain results or sustained my enthusiasm for the subject, in particular Miss D.C. Godfrey, Mr. D.A. Slater, Miss C. Lamont and Miss L. Bricknell. I am also indebted to Dr. S.C. Parker for a critical reading of this thesis. Finally I must thank my parents for all of their support during the last few years.

CONTENTS page

Introduction

1.1 Platinum as a catalyst

Platinum is an important catalyst for a wide variety of syntheses in both heterogeneous and homogeneous catalysis. As a heterogeneous catalyst, platinum is often supported on oxides such as alumina or silica. These adsorption systems may be rather complex as there may be interaction of the metal with the support, spillover of reactants or reaction intermediates onto the support, as well as chemical activity on the metal particles [1]. The structure of the support may also change both reactivity and product distribution [2].

In order to simplify the adsorption system, an increasing number of studies have been carried out on more idealised adsorption systems. These include well ordered metal films or foils and on single crystals of the metal with well ordered surfaces [3]. It has been demonstrated that such model systems can be used to determine the nature of catalytic processes on supported metal catalysts under more realistic temperatures and pressures than those available in the laboratory [4,5].

The production of well characterised surfaces of metal single crystals requires the attainment of ultra-high vacuum (UHV) conditions, with pressures of less

than 10^{-9} mbar. The maintainence of a contamination free surface for a sufficient period of time to carry out useful experiments also requires UHV conditions. In addition some of the experimental techniques used to probe surface structures and interactions at the surface, principally those involving interactions of electrons with the surface or adsorbate, also require the maintainence of a vacuum to prevent the scattering of electrons.

Many catalytic processes can be promoted by the addition of small quantities of other elements to the metal. One of the most important class of promoters used to dope catalysts are the alkali metals. The benefits of adding such a dopant to the catalyst include increase in activity of the catalyst, improving the selectivity of reaction products and increasing the effective lifetime of the catalyst [6]. The causes of these beneficial effects may be due to the promoter changing the nature of the metal, by perturbation of electronic states of either the adsorbates or the metal itself, or by changing the nature of the support, for example by neutralising acidic centres or by creation of basic centres on the support [6].

The primary objective of this study was to investigate the interaction of an important promoter,

potassium, adsorbed on a well characterised platinum surface, with the co-adsorbate CO. One reason for the choice of CO as the co-adsorbate is that it is one of the reactants for important syntheses such as the hydogenation of CO to form methanol or long-chain hydrocarbons [7].

The main experimental probe used was that of Reflection Absorption Infra-red Spectroscopy (RAIRS or IRAS). The C-O stretching vibrational mode absorbs radiation in the infra-red region, both in the gas phase and when the CO molecule is adsorbed at a surface. The vibrational frequency of this mode is sensitive to the bonding site of the adsorbed molecule. It is also dependent on the local physical and chemical environment of the CO, which may be perturbed by the presence of either other CO molecules or co-adsorbates. Hence RAIRS is a suitable probe of these inter-molecular interactions, which will be discussed in more detail in sections 1.3 and 1.4. The technique has a higher resolution than electron energy loss spectroscopy (EELS), another vibrational spectroscopy and hence is more suitable for measurement of small changes in vibrational frequencies, of the order of 1-10 wavenumbers. The infra-red activity of the CO molecule was the second reason for its choice as the co-adsorbate

with potassium.

Throughout the experiments a well studied and throughly characterised single metal crystal surface, Pt(110)-(1 x 2) was used. Initial experiments focussed on the adsorption of CO on this surface at temperatures of 300K and 100K. This was to establish a control with which to compare the more complicated co-adsorption system and as a test for the new RAIRS spectrometer which was constructed as part of this work.

In addition to RAIRS, the technique of temperature programmed desorption (TPD) was used to estimate desorption energies of CO from the surface. Low energy electron diffraction (LEED) was used to characterise the clean surface and various adsorbate overlayer structures, of both potassium and CO.

1.2 Previous Studies of CO/Pt(110)-(1 x 2) at 300K

A number of studies of the CO/Pt(110) adsorption system have been carried out previously by a number of different research groups using a variety of experimental techniques [8-20]. A brief summary of the work carried out prior to this study is as follows. The clean Pt(110) surface when prepared in UHV by argon ion bombardment, chemical treatment and high temperature annealing does not show the same surface structure which

is expected by a simple termination of the bulk. This has been established by low energy electron diffraction (LEED) studies. The surface produced is referred to as the Pt(110)-(1 x 2) reconstruction [8]. Preparation of a metastable surface in UHV conditions with the LEED pattern corresponding to bulk termination, the (1 x 1) pattern, has also been reported [17].

Adsorption of CO at 300K on the Pt(110)-(1 x 2) surface results in a lifting of the reconstruction at a coverage of θ_{CO}=0.5, giving the (1 x 1) LEED pattern [8,9]. However adsorption of CO whilst the crystal cools from 600K to 300K results in a different LEED pattern with systematic absences of certain diffraction beams. This pattern has been identified as the Pt(110)-(2 x 1)p1g1 pattern [8]. The appearance of this pattern has been ascribed to the tilting of the C-O molecular axis away from the surface normal, resulting in a breaking of the symmetry of the surface unit cell and the formation of glide planes [8,9]. The existence of tilted CO molecules at high coverages has been confirmed by two angle resolved ultra-violet photoelectron spectroscopy (ARUPS) studies [13,18], one of which reports that the C-O bond axis is tilted away from the surface normal at low coverages, starting at coverages θ_{CO}=0.2 [13].

Temperature programmed desorption (TPD) experiments have been carried out by a number of groups [8-10,15,16], the consensus of results suggest that two desorption states are observed, the higher temperature state appears at all CO coverages and remains at a constant temperature. The low temperature state appears at intermediate coverages. This feature has been attributed to strong repulsive forces between CO molecules [10]. An alternative model [12] has been proposed, in which some CO desorbs from the surface with a lifting of the reconstruction and some desorbs without lifting the reconstruction. These models will be discussed further in chapter four.

The adsorption system has also been studied with vibrational spectroscopy, both EELS and RAIRS [12]. The conclusions are that CO is exclusively bonded in on-top positions on the Pt(110) surface; the bridged bonded species of CO is not found at all when CO is adsorbed at 300K. The higher resolution of RAIRS has been used to measure C-O stretching frequency for the linearly bound CO molecules. A doublet adsorption band is observed at coverages of $\theta_{CO}<0.3$ and a singleton absorption band at higher coverages.

The interpretation of these results was as follows, at coverages of $\theta_{CO}<0.1$, CO exists as isolated

molecules on the surface, whilst in the coverage range $0.1<\theta_{CO}<0.3$, a mixture of isolated CO molecules and CO adsorbed in islands occurs. The frequency of the CO stretch in the islands is greater than that of the isolated species because of dipole-dipole coupling between neighbouring CO molecules. At higher coverages the island CO species predominates, as the islands spread over the surface, and the absorption band becomes a singlet [12]. The formation of island species implies attractive intermolecular forces in order to form the islands of CO.

A new study of this adsorption system has been carried out using RAIRS, TPD and LEED with the twin objectives of testing the new RAIRS spectrometer and further characterisation of this interesting adsorption system.

1.3 Previous Studies of CO/Pt(110)-(1 x 2) at 100K

The adsorption of CO on the Pt(110)-(1 x 2) surface at temperatures below 250K has been the subject of several previous studies [17,19,20] and these have revealed that there are significant differences between CO adsorption at low temperatures and that at room temperature, in that the (1 x 2) reconstruction is not lifted and a metastable c(8 x 4) LEED pattern has been

reported by some groups [10,17,20], but not observed by others [19]. The absolute coverage of CO on the surface is increased slightly at low temperatures compared to 300K [20]. Vibrational spectroscopy studies using EELS, indicate the presence of a bridge bonded species of CO as well as the predominant linear bonded CO species [19] and from consideration of the relative intensities of the absorption bands and an estimate of the dynamic dipole moment of the linear and bridge bonded species, the bridge bonded species has been estimated to consist of 30% of all the adsorbed CO.

During this work the first RAIRS study of the CO/Pt(110)-(1 x 2) adsorption system at 100K was carried out.

1.4 Co-adsorption of potassium and CO on platinum.

Many studies of co-adsorption of alkali metals with simple adsorbates, such as CO, on single crystal metal surfaces have been made in an attempt to understand the surface processes which give rise to promotion [21]. A variety of surface techniques have been used to characterise the co-adsorption systems, notably TPD, EELS, and photoemission spectroscopy. The most thoroughly studied systems are those of CO and potassium on transition metal surfaces. The general effects of

alkali metal co-adsorption are to increase the desorption temperature of CO from the surface and a consequent increase in the desorption energy of CO and a weakening of the C-O bond, manifested in the large downward shift of the C-O stretching frequencies observed by EELS and RAIRS [21]. In some co-adsorption systems the dissociation of CO is promoted [22]. In many of these studies a relatively high coverage of the alkali metal is placed on the surface of the metal. Most of the metal surfaces studied have been the relatively simple geometries such as the (111) face of face centred cubic metals such as copper and platinum or the (001) face of hexagonal close packed metals such as ruthenium.

1.5 Range of interaction between potassium and CO

The question as to the range and nature of the interaction between the co-adsorbates is also open, whether a local interaction between those CO molecules adsorbed at nearest neighbour sites to the alkali metal or a longer range interaction in which the dopant may affect CO molecules adsorbed at more remote lattice sites.

Short range interactions which have been suggested generally involve a change in the molecular bonding of

CO to the metal surface. The most commonly used model for CO-metal bonding is that due to Blyholder [23], in which bonding occurs via 5σ donation to the metal together with metal- d to CO $2\pi^*$ backdonation. The latter orbital is antibonding in character, thus increased occupation causes a weakening of the C-O bond.

One short range co-adsorbate interaction which has been suggested on the basis of ESDIAD [24] and metastable quenching spectroscopy [25] studies by Arias and co-workers is that the alkali metal induces a tilting in the CO molecules at nearest neighbour sites, but does not change the orientation of CO adsorbed at other sites. This tilting model, when extended to its logical conclusion, leads to the possibility of side on bonding of CO to the surface at nearest neighbour sites to the alkali metal, several instances of which have been reported [26,27]

Another model giving rise to a short range interaction which has been reported on the basis of photoemission studies is the re-hybridisation of the CO-metal bond from sp type hybridisation (the 5σ bond) to sp^2 hybridisation [28-30].

A change in the CO-metal bonding in which the 1π CO molecular orbital becomes the main bonding orbital in preference to the Blyholder model of bonding has also

been considered [31,32]. The presence of potassium is reported to cause a downward shift in the energy of the 1π bonding orbital, which is strongly bonding towards CO. This weakens the C-O bond leading to reduced vibrational frequencies [33,34]. This modified type of bonding is analogous to that in CO-metal π cluster compounds [35]. The range of the interaction between potassium and CO in this bonding model is uncertain.

The formation of ionic CO-potassium complexes of with the general formula $K_2(CO)_n$ on the Cu(110) surface has also been suggested on the basis of the similarity between the absorption band due to the C-O stretch which is shifted downwards on co-adsorption, as measured by HREELS (high resolution EELS) and infra-red spectra of the solid salts [36].

A number of studies have suggested that there may be a longer ranged CO-potassium interaction on certain metal surfaces [27,37-42] either associated with the effects of the interaction of the electric field generated by the partially ionised alkali metal species with the co-adsorbed CO or with the perturbation of the surface electronic structure of the metal.

Holloway and Norskov [43] have suggested that the electrostatic potential associated with the adsorbed species (such as potassium) cause a downward shift in

the molecular CO levels relative to the Fermi surface, including the partially occupied $2\pi^*$ levels. The occupancy of the antibonding level is increased and the C-O bond weakened, resulting in a downward shift in C-O stretching frequency. The increased occupation of the $2\pi^*$ levels has been reported for the CO/K/Ni(111) adsorption system at a potassium coverage of Θ_K=0.34 [26]. A later extension of this approach by Lang, Norskov and Holloway [44], in which the electric fields generated by a variety of electropositive and electronegative adsorbates (representing alkali metal promotors and poisons respectively) on a jellium surface indicated that these effects would be strongest over distances of the order of one metal lattice parameter.

Muller and Bagus [48] have suggested that the reduction in frequency of the C-O stretch under the influence of electropositive adsorbates such as potassium is a consequence of the direct interaction of the electric field induced by the presence of the adsorbate with the electric dipole of the C-O molecule; this is a vibrational Stark effect. This is similar to the electrostatic interaction proposed by Norskov and Holloway but does not require the perturbation of the occupancy of the CO molecular orbitals. In addition Efrima and Metiu [45] have calculated that for molecules

such as CO adsorbed at metal surfaces, downwards shifts in the C-O stretching frequency of the order of 10-20 cm^{-1} may occur purely due to interaction with the electric fields associated with the metal surface, without any enhancement due to electropositive adsorbates.

Feibelmann and Hamann [46,47] have calculated the perturbation of the one-electron density of states at the surface of rhodium, due to a variety of adsorbates, such as sulphur, phosphorus and lithium. Their results show that this perturbation extends over distances greater than one metal lattice constant. The nature of the changes in the metal surface electronic states suggest that interaction between adsorbates would involve changes in the metal-CO bonding and hence in the occupancy of the molecular orbitals. A change in the occupation of the $2\pi^*$ antibonding orbital would weaken the C-O bond and hence reduce the C-O stretching frequency.

The models for long ranged interactions between alkali metal atom and CO are thus divided into two classes, those which perturb the $2\pi^*$ orbital occupation and the Stark effect interaction, which does not. The use of RAIRS to investigate changes in occupation of the $2\pi^*$ orbital will be discussed in chapter four, for the

case of CO adsorbed on the "clean" Pt(110)-(1 x 2) surface and in chapter six for case of CO and potassium co-adsorption on Pt(110)-(1 x 2).

The study reported here of co-adsorption of potassium and CO on the Pt(110)-(1 x 2) surface, was carried out in the low potassium coverage limit as this a more realistic model of real heterogeneous catalysts, where small quantities of potassium are added as promotors.

Experimental techniques: theory

2.1 Interaction of infra-red radiation with matter

In order to excite an intra-molecular vibrational mode, interaction with a photon of radiation with the appropriate wavelength is necessary. In general this will be in the infra-red portion of the electromagnetic spectrum with wavelengths in the range 10^{-6} to 10^{-3} metres.

In the gas phase a molecule containing N atoms possesses 3N degrees of freedom. Of these degrees of freedom, three are translational and three are rotational for non-linear molecules; linear molecules have only two rotational degrees of freedom. This leaves 3N-6 and 3N-5 vibrational degrees of freedom for non-linear and linear molecules respectively. Following adsorption the translational and rotational degrees of freedom become frustrated and may be converted into vibrational modes.

The excitation of any vibrational mode is dependent upon the interaction of the incident infra-red radiation with the electric dipole of the molecule. The transition probability of a vibrational excitation from initial state i to final state f is P_{if} where

$$P_{if} = M^2_f \qquad (2.1)$$

where M_{if} is known as the transition moment and is defined as:

$$M_{if} = \langle \Psi_f | \hat{\mu} | \Psi_i \rangle \qquad (2.2)$$

where Ψ_i and Ψ_f are the vibrational eigenfunctions of the initial and final states and $\hat{\mu}$ is the electric dipole moment operator of the molecule [49]. To obtain a finite transition probability, equation (2.2) must be non-zero. The dipole moment operator can be resolved into the three components in cartesian space yielding:

$$M_{(x)if} = \langle \Psi_f | \hat{\mu}_x | \Psi_i \rangle \qquad (2.3)$$

$$M_{(y)if} = \langle \Psi_f | \hat{\mu}_y | \Psi_i \rangle \qquad (2.4)$$

$$M_{(z)if} = \langle \Psi_f | \hat{\mu}_z | \Psi_i \rangle \qquad (2.5)$$

To determine which, if any, of equations (2.3) to (2.5) are non-zero requires the application of group theory and symmetry arguments [50]. The criterion for a non-zero value is that the product of the symmetry representations of Ψ_i , Ψ_f and $\hat{\mu}$ must contain the totally symmetric representation. In general for vibrational spectroscopy the initial level is v=0 (the ground state) which has the totally symmetric representation, and the final level is v=1. In this case the representation of the final state must belong to the same representation as any of $\hat{\mu}_x$, $\hat{\mu}_y$ or $\hat{\mu}_z$. This means

that only vibrational modes which transform with x, y or z are infra-red active. This is the general selection rule in infra-red spectroscopy; it is modified by the presence of a metal substrate when the molecule is in an adsorbed state and vibrational excitation occurs.

2.2 Interaction of radiation with metal substrates

Having considered the interaction of the infra-red radiation with the molecule, it is now necessary to consider the effect of the metal substrate on the absorption of radiation. The adsorption system may be considered as a three phase system, where the first layer is a vacuum, the second is the adsorbate and the third the metal substrate. Using classical electrodynamics, the ratio of reflected intensity to incident radiation may be calculated. It is useful to first consider a simple two phase system of vacuum and metal substrate as this demonstrates many of the essential features of the interaction between reflected radiation and the metal substrate.

2.3 Two and three phase reflection models

The two phase reflection model is shown in Figure 2.3.1. for the two different cases of plane polarised

FIGURE 2.3.1a

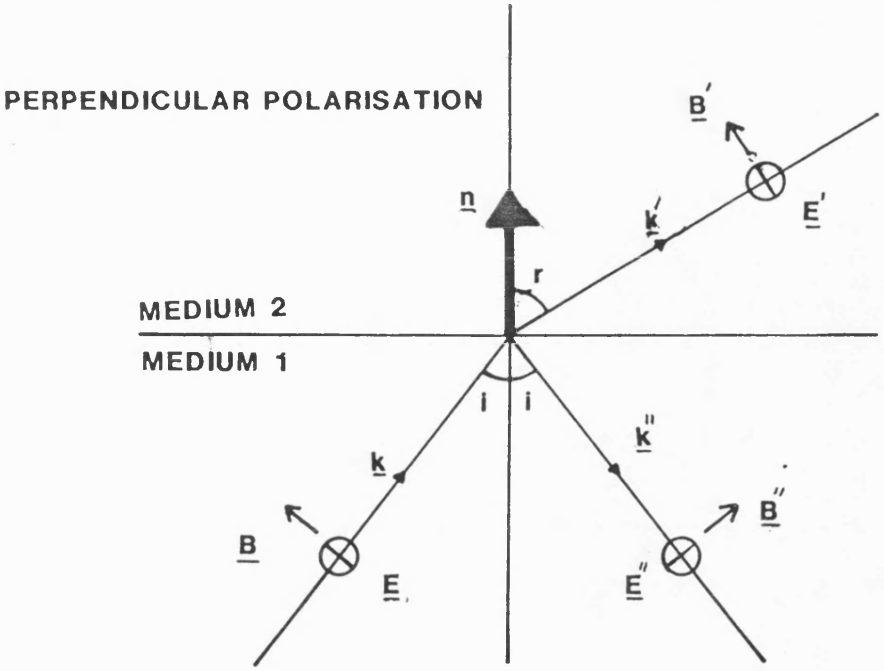

FIGURE 2.3.1b

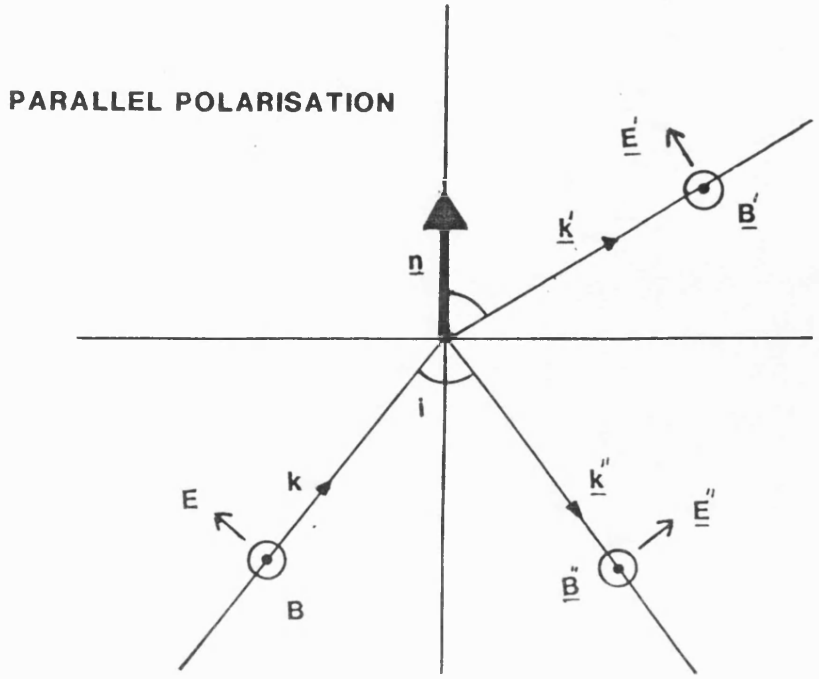

radiation.

The electric fields $\underline{E}$ are assumed to obey the wave equation:

$$\underline{E} = E_o \exp [j(\underline{k}.\underline{r} - wt)] \qquad (2.6)$$

where $\underline{k}$ is the wavevector, $\underline{r}$ the propagation direction, w the angular frequency and t time. The constant j is the square root of minus one. The plane of incidence is defined by $\underline{k}$ and $\underline{n}$, which is a unit vector normal to the surface. In general there may be reflection of the incident wave $\underline{E}$, denoted by $\underline{E}$" and also refraction, denoted by $\underline{E}$'. For linearly polarised incident radiation, there are two possible situations, the plane of polarisation of the electric field vector $\underline{E}$ may be either in the plane of incidence (p-polarisation) or perpendicular to the plane of incidence (s-polarisation). As a consequence of Maxwell's equations, the boundary conditions for such a system are that the components of $\underline{E}$ and $\underline{B}$ (the magnetic induction field) parallel to the incident plane are conserved across the boundary between vacuum and metal, as are the perpendicular components of the fields $\underline{D}$ (the electric displacement field) and $\underline{H}$, the magnetic intensity [51]. This leads to the four boundary condition equations [52]:

$$[\varepsilon \underline{E}_o + \varepsilon \underline{E}_o'' - \varepsilon' \underline{E}_o'].\underline{n} = 0 \qquad (2.7)$$

$$[\underline{k} \times \underline{E}_o + \underline{k}'' \times \underline{E}_o'' - \underline{k} \times \underline{E}_o''].\underline{n} = 0 \qquad (2.8)$$

$$[\underline{E}_o + \underline{E}_o'' - \underline{E}_o'].\underline{n} = 0 \qquad (2.9)$$

$$[(\underline{k} \times \underline{E}_o + \underline{k}'' \times \underline{E}_o'') = (\underline{k}' \times \underline{E}_o)].\underline{n} \qquad (2.10)$$

where ε and ε' are the dielectric constants of the two media. This treatment of the electromagnetic fields requires the magnetic permeabilities of both media to be unity, an approximation true for optical and near optical frequencies.

In the case of the plane of polarisation in the incident plane ('p' polarisation), there are no components of $\underline{E}$ parallel to the surface, so equation (2.7) is zero. From equation (2.9):

$$E_o'' + E_o = E_o' \qquad (2.11)$$

and from equation (2.10):

$$\surd\varepsilon(E_o - E_o'')\cos(i) = \surd\varepsilon' E_o' \cos(r) \qquad (2.12)$$

By eliminating E_o' from equations (2.11) and (2.12), it is possible to obtain the ratio of the magnitudes of the reflected electric field to the incident one. These are known as the Fresnel equations.

$$\frac{E_o''}{E_o} = \frac{\surd\varepsilon \cos(i) - \surd\varepsilon' \cos(r)}{\surd\varepsilon \cos(i) + \surd\varepsilon' \cos(r)} \qquad (2.13)$$

In the case of ς-polarisation the boundary conditions give:

$$E_o\cos(i) - E_o''\cos(i) = E_o'\cos(r) \qquad (2.14)$$

and:

$$\sqrt{\varepsilon}(E_o + E_o'') = \sqrt{\varepsilon'}E_o' \qquad (2.15)$$

and again, eliminating E_o'

$$\frac{E_o''}{E_o} = \frac{\varepsilon'\cos(i) - \sqrt{(\varepsilon\varepsilon')}\cos(r)}{\varepsilon'\cos(i) + \sqrt{(\varepsilon\varepsilon')}\cos(r)} \qquad (2.16)$$

The angle of refraction, r, may be eliminated using Snell's law:

$$\varepsilon \sin(i) = \varepsilon' \sin(r) \qquad (2.17)$$

Equations (2.13) and (2.16) are valid for complex dielectric constants, which take account of absorption by the material. The complex dielectric constant, ε, is defined as:

$$\varepsilon = n - jk \qquad (2.18)$$

The intensity of radiation is proportional to the square of the modulus of the electric field vector, so the quantity of interest in a reflection absorption experiment is the reflectivity ratio R defined as [53]:

$$R = (E_o''/E_o)^2 \qquad (2.19)$$

In the two phase model with medium 1 as a vacuum ($\varepsilon_1=1$) and medium two as the metal ($\varepsilon_2=n-jk$) and providing that $n^2 + k^2 >> 1$, a criterion which is satisfied in the infra-red region, the values of R for the s-polarised and p-polarised cases respectively are [54]:

$$R_p = \frac{(n - \sec(i))^2 + k^2}{(n + \sec(i))^2 + k^2} \qquad (2.20)$$

$$R_s = \frac{(n - \cos(i)) + k^2}{(n + \cos(i)) + k^2} \qquad (2.21)$$

The phase changes on reflection for the two types of polarisation are d_s and d_p with:

$$d_p - d_s = \arctan\left[\frac{2\,k\,\tan(i)\sin(i)}{(\tan^2(i)-(n^2+k^2)}\right] \qquad (2.22)$$

The value of the phase shift for the s-polarisation is approximately 180 degrees for all incident angles [55].

Now consider the total electric field at the point of reflection at the surface, which is the field experienced by an adsorbed molecule. If the amplitude of the incident wave is given by $E^i\sin(\theta)$, where θ is the arbitrary phase, then the electric field at the point of intersection with the surface due to the incident and reflected wave is:

$$E = E^i\sin(\theta) + \surd R\,\sin(\theta+d) \qquad (2.23)$$

where d is the phase shift on reflection and R is the reflectivity ratio defined in (2.18). For s-polarised light, this is:

$$E_s = E^i\sin(\theta) + \sqrt{R_s}\,\sin(\theta+d_s) \qquad (2.24)$$

For a highly reflective metal, with n=3 and k=30 [55], the value of R_s defined in equation (2.21) is approximately unity at all incident angles, and since d_s has a value of approximately 180 degrees at all incident angles, the incident and reflected waves have the same amplitudes, but a phase difference of 180 degrees. This leads to destructive interference and so the electric field at the surface due to s-polarised light is negligible.

For p-polarised light, there are components of the electric field parallel to the surface and perpendicular to the surface:

$$E_p^{perp} = E_p\sin(i)[\sin(\theta)+\sqrt{R_p}\sin(\theta+d_p)] \qquad (2.25)$$

and

$$E_p^{para} = E_p\cos(i)[\sin(\theta)-\sqrt{R_p}\sin(\theta+d_p)] \qquad (2.26)$$

At low angles of incidence, the parallel component is small since the value of R_p is approximately one and the phase change, calculated from equation (2.22) is also

small, thus the incident and reflected waves are of the same magnitude, but opposed in direction, thereby interfering destructively. For the perpendicular component, although the incoming and outgoing waves constructively interfere, there is only a small component resolved in that direction. At larger angles of incidence, the perpendicular component becomes enhanced over the parallel component, with a value of the order of $2E_p$, but eventually is diminished by the increasing change of phase with incident angle, as a consequence of equation (2.22), causing destructive interference. The value of E_p^{perp} falls to zero at grazing incidence angles.

It can be concluded that the enhanced electric field due to reflection at the surface is mostly due to the perpendicular component of the p-polarised radiation. This is a statement of the surface selection rule; only dipole oscillators perpendicular to the surface interact strongly with the incident radiation, the parallel components of the radiation are screened out by the metal. Thus we have an additional surface selection rule for vibrational excitation by infra-red radiation in addition to the general selection rule for gas phase molecules discussed in section 2.1.

The intensity of an absorption band is proportional

to $(E_p^{perp})^2$. The area of the surface intersected by a parallel beam of radiation, a measure of the number of molecules which the beam can interact with, is inversely proportional to cos(i). The intensity of an absorption band will therefore depend on the product $(E_p^{perp})^2 sec(i)$.

This function is plotted in Figure 2.3.2 for a strongly reflecting metal (n=3, k=30). It is sharply peaked at high incident angles and falls away rapidly as the incidence angle decreases, emphasising the need to perform the RAIRS experiment at angles of at least 85 degrees.

The additional complications of the three phase model (Figure 2.3.3) was treated by Francis and Ellison [56], and developed subsequently by Greenler [57,58] and by McIntyre and Aspnes [59] using slightly differing approaches, the former analysis is in the same terms as that described above for the two phase model. Layer one is assumed to be a vacuum, with a dielectric constant of unity and both the substrate and the absorbing layer are assigned the complex dielectric constants e_2 and e_3 respectively so that the reflection coefficients analogous to equations (2.20) and (2.21) are correspondingly more complicated. The essential facts derived from the two phase model, that grazing incident

FIGURE 2.3.2

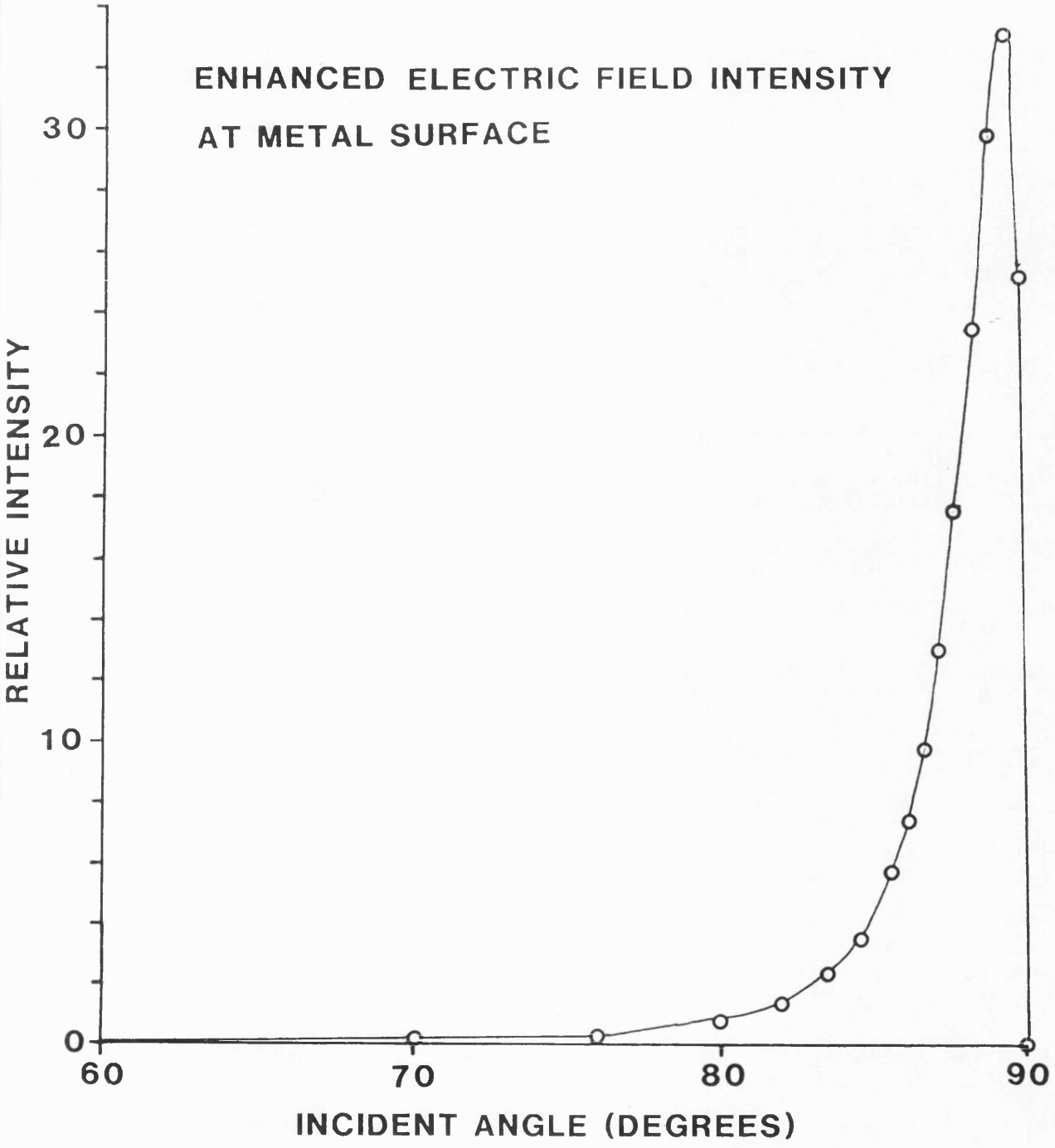
ENHANCED ELECTRIC FIELD INTENSITY
AT METAL SURFACE
RELATIVE INTENSITY
30
20
10
0
60
70
80
90
INCIDENT ANGLE (DEGREES)

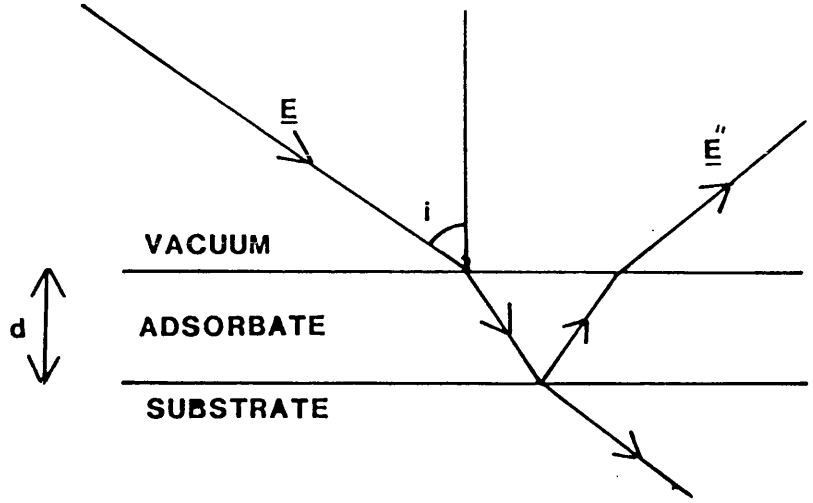

FIGURE 2.3.3 THREE PHASE REFLECTION MODEL

angles are required and that only the perpendicular component of p-polarised light interacts strongly with the adsorbed molecules are still true.

To simplify the form of the reflection coefficients, McIntyre and Aspnes [59] have modelled an adsorbed layer of thickness d and assuming that the incident radiation was of wavelength λ, employed a linear approximation in d/λ assuming $d/\lambda << 1$.. This is valid for infra-red wavelengths $\approx 10^{-6}$ m and thin adsorbed layers ≈ 0.1 nm. If the reflectivity in the absence of the adsorbate is R_o and the reflectivity in the presence of the adsorbate is R, the the relative reflectivity change on adsorption is

$$A = (R_o - R)/R_o \qquad (2.27)$$

and the expression derived for s-polarised incident radiation is:

$$A_s = (8\pi d/\lambda)\cos(i)\, \mathrm{Im}[(\varepsilon_2-\varepsilon_3)/(1-\varepsilon_2)] \qquad (2.28)$$

and for p-polarised radiation:

$$A_p = (8\pi d/\lambda)\cos(i)\, \mathrm{Im}[Z(\varepsilon_2-\varepsilon_3)/(1-\varepsilon_2)] \qquad (2.29)$$

where:

$$Z = \frac{1-(1/\varepsilon_2\varepsilon_3)(\varepsilon_3+\varepsilon_2)\sin^2(i)}{1-(1/\varepsilon_3)(1+\varepsilon_3)\sin^2(i)} \qquad (2.30)$$

The expression given by equation (2.29) has been simplified by Ibach [60] for the case of $\varepsilon_3 >> \varepsilon_2$ and $\cos^2(i) >> |1/\varepsilon_3|$ to give:

$$A_p = (8\pi d/\lambda)\sin(i)\tan(i)\ \mathrm{Im}\ (1/\varepsilon_2) \qquad (2.31)$$

In the case of a highly reflecting metal such as copper, $\varepsilon_2 = 3-30j$, and for a moderate absorber such as CO, $\varepsilon_3 = 1.3-0.3j$ [61,62]. Assuming an adsorbate layer 0.3nm thick and a wavelength of 2100 cm^{-1}, then by substitution of these values into equations (2.29) and (2.31), the values of $A_s = 1.47 \times 10^{-6}$ and $A_p = 3.0 \times 10^{-3}$ are obtained, demonstrating that the p-polarised radiation provides a significant reflectivity change whilst that of s-polarised light is negligible.

Using the three phase model Greenler has demonstrated that the RAIRS spectra of a moderate absorber on a highly reflecting metal is equivalent to that obtained in a transmission IR experiment [61].

2.4 Optimum number of reflections

The metal surfaces considered in the models have complex dielectric constants and so absorb a certain amount of the incident radiation. Greenler [62,63] has calculated the optimum number of reflections to obtain a maximum change in reflectivity for a number of metals.

The model used has the adsorbate layer 0.3 nm thick with dielectric parameters n_2=1.3 and k_2=0.3, simulating a layer of CO. For highly reflective metals such as gold, copper and silver there is an appreciable advantage in using multiple reflections. For the transition metals, which absorb more radiation, the optimum number of reflections is smaller. For platinum with dielectric constants of n_3=3.0 and k_3=20 (valid at a frequency of 2100 cm^{-1}), the optimum number of reflections lies between 2 and 6, depending on the incident angle. However 62% of the total absorption signal is obtained after the first reflection so that the experimental advantages of the single reflection experiment, with simplified optical arrangements outweighs the loss of some intensity in the absorption band.

2.5 Temperature programmed desorption experiments

Temperature programmed desorption, sometimes known as flash desorption, is the removal of adsorbed species from a surface by thermal excitation caused by the heating of the substrate; it is a dynamic process and can be described in terms of kinetics.

For a particular chemical species, the rate of desorption per unit surface area, N(t), for desorption kinetics of order n can be given by the Polanyi-Wigner

type equation:

$$N(t) = - dc/dt = k_n c^n \exp(-E_d/RT) \qquad (2.32)$$

where c is the number of molecules per unit area, k_n is the nth order rate constant and E_d the energy of desorption. Under the conditions found in ultra-high vacuum systems, with very high pumping speeds, it has been shown that the rate of desorption is proportional to the pressure rise in the system caused by the desorption of the adsorbate from the substrate [64].

For a rise in temperature T from an initial temperature T_o with a linear heating rate ß:

$$T = T_o + ßt \qquad (2.33)$$

equation (2.32) can now be solved to give:

$$E_d/RT_p^2 = (nk_n c_p^{n-1}/ß)\exp(-E_d/RT_p) \qquad (2.34)$$

where T_p is the temperature at which the maximum rate of desorption (the maximum pressure) occurs.

For first order reaction kinetics, equation (2.34) becomes:

$$E_d/RT_p^2 = (k_1/ß)\exp(-E_d/RT_p) \qquad (2.35)$$

The temperature at the maximum desorption rate is now independent of the initial coverage of the adsorbate.

The pre-exponential factor k_1 can be evaluated in terms of transition state theory [65]. Assuming that the transition state is a 2-dimensional ideal gas and a mobile adlayer, k_1 has a value of $\approx 10^{13}$ sec^{-1}. The value of k_1 as 10^{13} sec^{-1} is widely used in the literature as the basis for calculating the desorption energy E_d for first order desorption kinetics. For values of k_1/β in the range 10^8 to 10^{13}, Redhead [64] has shown that equation (2.35) can be approximated to:

$$E_d/RT = \ln(k_1T_p/\beta) - 3.64 \qquad (2.36)$$

For second order desorption kinetics, T_p is coverage dependent and decreases with increasing initial coverage [66]. The shape of the pressure versus temperature profile for first order desorption kinetics is obtained by integration of equation (2.32); Redhead [64] has shown that a single slightly asymmetric peak is produced, with a slight tail on the low temperature side.

For desorption spectra which show multiple desorption peaks, the obvious explanation is that there is a superposition of several different states with different desorption energies. However Goymour and King [67] and Adams [68] have shown that the appearance of secondary desorption peaks may be due to adsorbate-

adsorbate interactions, which appear at intermediate coverages.

2.6 Low Energy Electron Diffraction

Low energy electron diffraction (LEED) has been used extensively in recent years to examine surface structures [69]. In the energy range 30-500 eV, the electron has a de Broglie wavelength comparable to the lattice spacing of many crystals. The penetration depth of the electrons in this energy range is limited to a few interatomic spacings [70], so that the diffraction process may be treated as being from a two-dimensional lattice array at the surface.

If the real space net has lattice vectors $\underline{a}_1$ and $\underline{a}_2$, then there are reciprocal lattice vectors $\underline{a}_1^*$ and $\underline{a}_2^*$ such that:

$$\underline{a}_1.\underline{a}_1^* = \underline{a}_2.\underline{a}_2^* = 1 \qquad (2.37)$$

and:

$$\underline{a}_1.\underline{a}_2^* = \underline{a}_1^*.\underline{a}_2 = 0 \qquad (2.38)$$

If the incident and emergent beams have unit wave vectors $\underline{s}$ and $\underline{s}'$ then the diffraction from the lattice satisfies the Laue conditions:

$$\underline{a}_1.(\underline{s} - \underline{s}') = h\lambda \qquad (2.39)$$

and

$$\underline{a}_2.(\underline{s} - \underline{s}') = k\lambda \qquad (2.40)$$

which have solutions when:

$$(\underline{s} - \underline{s}') = \lambda(h\underline{a}_1^* + k\underline{a}_2^*) \qquad (2.41)$$

The surface structure may have lattice vectors which differ from the substrate lattice vectors; this occurs if the surface is reconstructed from that expected from a termination of the bulk material or from the structure of an adsorbed overlayer. If the surface lattice vectors are $\underline{b}_1$ and $\underline{b}_2$, then they can be described in terms of the substrate lattice vectors:

$$\underline{b}_1 = m_{11}\underline{a}_1 + m_{12}\underline{a}_2 \qquad (2.42)$$

and:

$$\underline{b}_2 = m_{21}\underline{a}_1 + m_{22}\underline{a}_2 \qquad (2.43)$$

or in matrix form by:

$$\underline{b} = \underline{m}.\underline{a} \qquad (2.44)$$

There will then be reciprocal lattice vectors $\underline{b}_1^*$ and $\underline{b}_2^*$ so that:

$$\underline{b}^* = \underline{m}^*.\underline{a}^* \qquad (2.45)$$

where:

$$\underline{\mathbf{m}}^{*} = \begin{pmatrix} m^{*}_{11} & m^{*}_{12} \\ m^{*}_{21} & m^{*}_{22} \end{pmatrix} \tag{2.46}$$

Using matrix algebra:

$$\underline{\mathbf{m}} = (1/\det(\underline{\mathbf{m}}^{*})) \begin{pmatrix} m^{*}_{22} & -m^{*}_{21} \\ -m^{*}_{12} & m^{*}_{11} \end{pmatrix} \tag{2.47}$$

where $\det(\underline{\mathbf{m}}^{*})$ is the determinant of matrix $\underline{\mathbf{m}}^{*}$.
The labelling of the diffraction beams defined by the indices h,k in equation (2.41) is given by the reciprocal lattice vector elements contained in equation (2.47).

A notation to describe surface structures which differ from the bulk substrate has been described by Woods [71]. If the vectors $\underline{b}_1$ and $\underline{b}_2$ are related to the lattice vectors $\underline{a}_1$ and $\underline{a}_2$ by:

$$|\underline{b}_1| = m|\underline{a}_1| \tag{2.48}$$

and:

$$|\underline{b}_2| = n|\underline{a}_2| \tag{2.49}$$

and the angle between $\underline{b}_1$ and $\underline{b}_2$ is the same as that between $\underline{a}_1$ and $\underline{a}_2$ then the surface may be described as:

$$(m \times n)R\Theta \tag{2.50}$$

where Θ is the angle through which the surface lattice vectors are rotated from the substrate lattice

vectors.

For a Pt(110) surface cleaned and annealed in UHV, there is a surface reconstruction to the (1 x 2) form in Wood's notation. From equations (2.48) and (2.49) this leads to $|b_1|=2|a_1|$ and $|b_2|=|a_2|$. Matrix m* can then be calculated to determine the sizes of the reciprocal surface lattice vectors $\underline{b}_1^*$ and $\underline{b}_2^*$ giving:

$$\underline{b}_1^* = 1/2 \quad \underline{a}_1^* \tag{2.51}$$

$$\underline{b}_2^* = \underline{a}_2^* \tag{2.52}$$

This means that there are extra beams in the direction defined by the reciprocal lattice vector $\underline{a}_1^*$, half way between those beams present for the unreconstructed surface; using the notation of equations (2.39) and (2.40) these are referred to as the [h/2,k] spots, whilst those of the (1 x 1) surface would be [h,k].

As well as the positioning of atoms (or molecules when considering adsorbed layers), the orientation of species in the unit cell must also be considered. The existence of a glide plane symmetry operator may cause the systematic absence of certain diffraction beams [72,73]. The glide plane may be present owing to a surface reconstruction [74,75] or due to the overlayer geometry [76]. The symmetry notation refers to the

space group of the surface layer [77]; for a two dimensional net there are seventeen possible space groups. Another case of an overlayer with glide plane symmetry is that of CO on Pt(110)-(1 x 2) formed under certain conditions, in this case the overlayer is referred to as the (2 x 1)p1g1 overlayer [9,12,73].

Experimental

3.1 The Vacuum System

A two level stainless steel ultra high vacuum system was constructed for and used throughout this work. The system had two chambers with a gate valve (CVT Ltd.) between them to allow independent operations in each chamber. The sample, a platinum single crystal, was mounted on the end of a sample manipulator which was mounted on top of the upper chamber (see figure 3.1.1). Both vacuum chambers were normally maintained in ultra-high vacuum (UHV), with a base pressure of 1 x 10^{-10} mbar. The presence of the gate valve between the two chambers was an advantage in that the sample could be removed from the vacuum system using the upper chamber as an air-lock so that the lower chamber could be maintained in UHV.

The lower chamber (figure 3.1.2) contained the following facilities: low energy electron diffraction (LEED), a quadrupole mass spectrometer (Vacuum Science Workshop, Vacuum Analyst), titanium sublimation pump, ion gauge, argon ion bombardment gun (Ion Tech Ltd) and a potassium deposition source (SAES Getters). The LEED equipment was an Omicron Vacuumphysik four grid system with back view optics. The alkali metal source consisted

FIGURE 3.1.1

UHV SYSTEM

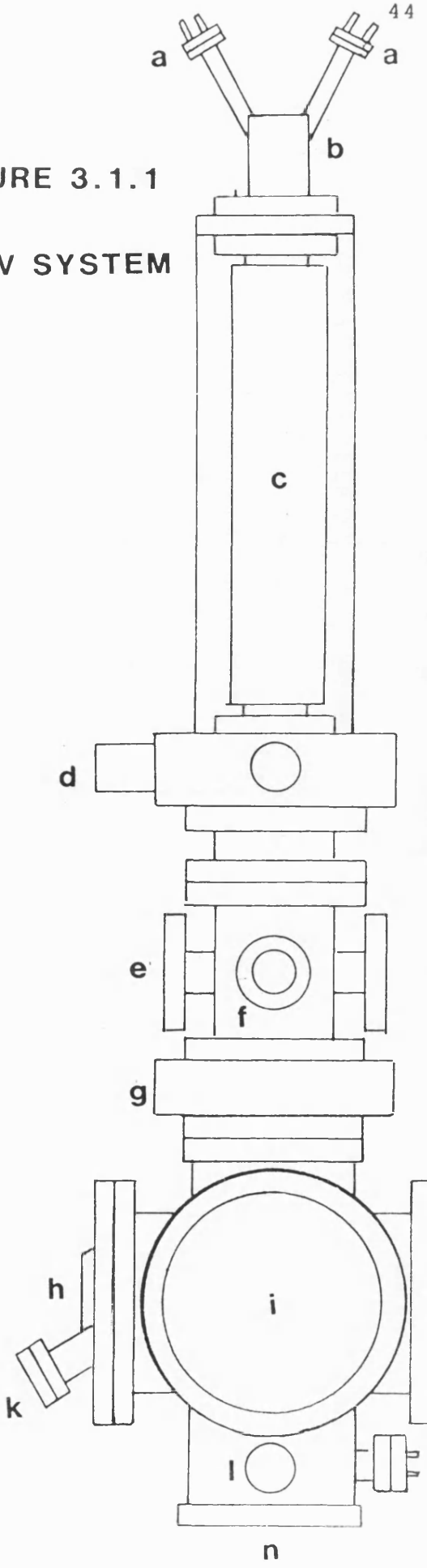

a ELECTRICAL FEEDTHROUGHS

b DIFFERENTIALLY PUMPED ROTARY FEEDTHROUGH

c BELLOWS

d X-Y MOVEMENT STAGE

e IR LEVEL

f VIEWPORT

g GATE VALVE

h VIEWPORT

i LEED

j ION GUN

k ALKALI METAL SOURCE

l ION GAUGE

m Ti SUBLIMATION PUMP

n ION PUMP

FIGURE 3.1.2 LOWER UHV CHAMBER

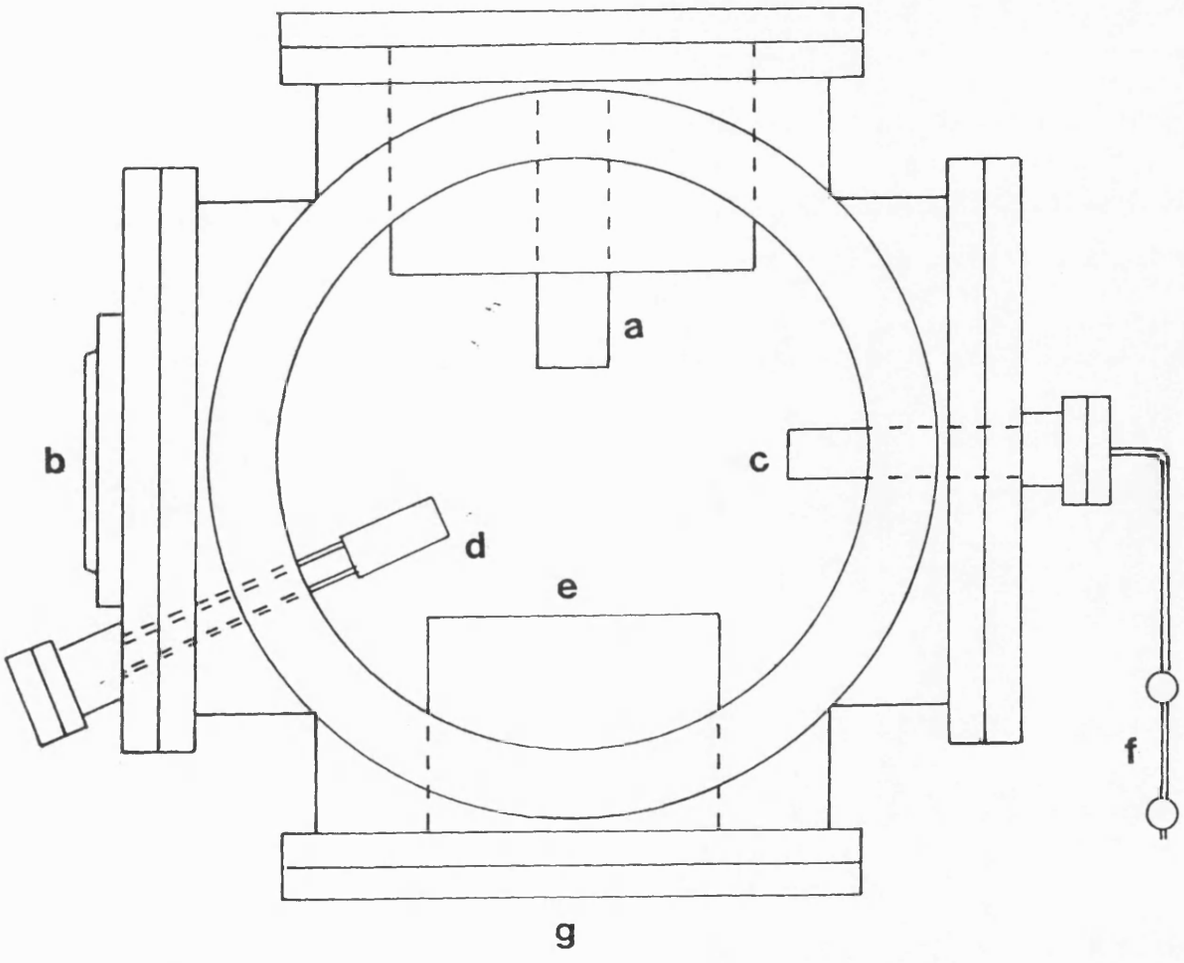

a MASS SPECTROMETER IONISER

b VIEWPORT

c ION GUN

d ALKALI METAL SOURCE

e LEED OPTICS

f ARGON SUPPLY

g LEED VIEWPORT

of two dispensers (SAES Getters) mounted on a feedthrough and surrounded by a cylindrical nickel foil shield to prevent alkali metal deposition on the LEED optics or the mass spectrometer ioniser. The mass spectrometer ioniser was mounted on a re-entrant flange to allow positioning within a few centimetres of the sample in direct line of sight, in order to maximise the pressure signal measured during thermal desorption experiments. The chamber was pumped continuously by an ion pump (pumping capacity 80 l/s, Varian Associates).

The upper level (figure 3.1.3) consisted of a chamber with gas dosing facilities, a Pirani pressure gauge head (Vacuum Generators Ltd.) and sodium chloride windows mounted in conflat flanges to allow infra-red radiation to pass through the upper chamber.

Attached to this chamber were the IR source, mirror boxes and monochromator. All of these components were also mounted in stainless steel vacuum chambers. These chambers were pumped independently of the rest of the system using a 25 l/s ion pump (Leisk Engineering) mounted beneath the monochromator and were maintained in high vacuum. In addition to these three independently pumped vacuum chambers there was also a backing line and gas dosing facility. This was pumped by a turbomolecular pump (Balzers Gmbh) and backed by a

FIGURE 3.1.3

UPPER UHV CHAMBER

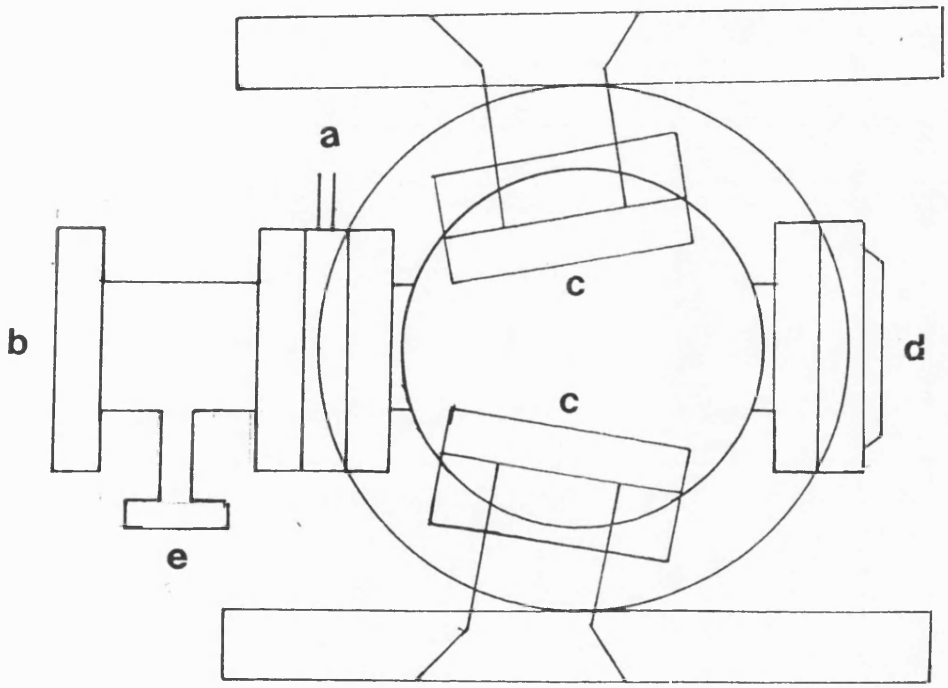

a GAS DOSING LINE

b TO BACKING LINE

c NaCl WINDOWS

d VIEWPORT

e PIRANI GAUGE HEAD

rotary pump. This line could be independently connected to upper chamber, lower chamber or IR optics chambers to provide a rapid pumpdown from atmospheric pressure. The gas dosing line had up to three gas bottles attached via leak valves and could be sealed from the backing line. Gases in this line could be dosed into the upper (IR) chamber. Both the backing and dosing lines were maintained in UHV.

3.2 The Manipulator and Sample Mounting

Transfer of the sample between the two levels of the vacuum chamber was by means of a sample manipulator (Leisk Engineering), which was mounted on top of the upper chamber. The manipulator had 30 cm travel in the vertical direction (z axis) and was also movable in x and y axes and in rotation. The manipulator also had facilities for resistive heating of the sample and for cooling the sample using liquid nitrogen.

Mounting the sample in a mechanically durable manner, in order to survive frequent transfers between the two levels of the vacuum system and to provide both cooling and heating facilities proved to be a difficult task. In all mounting designs, the platinum single crystal was supported between two tungsten filaments spot-welded to the crystal. The thickness of the

filaments was optimised at 0.25 mm, this being consistent with a relatively low (25 amp) current to resistively heat the crystal to 1300K and a sturdy mounting with a long lifetime between mechanical failure. A type K (chromel-alumel) thermocouple was spot welded directly to the top of the crystal.

The original manipulator design (Figure 3.2.1) provided for liquid nitrogen to be circulated through a stainless steel tube, which was separated into two halves by a ceramic tube to provide electrical isolation between the two sides. Resistive heating could be performed by applying a potential across the two cooling tubes. The cooling arrangements proved unsatisfactory and this design was only suitable for operation at room temperature and above.

The manipulator was redesigned to act as a cold finger, allowing direct cooling using a reservoir of liquid nitrogen. This required a differentially pumped rotary feedthrough mounted at the top of the manipulator. The initial design for sample mounting is shown in Figure 3.2.2. Electrical isolation of the sample was provided by the two glass beads which separated the two halves of the tungsten mounting pins. With this arrangement, cooling from room temperature to 140K was possible, although the rate of cooling was

FIGURE 3.2.1 ORIGINAL SAMPLE MOUNTING DESIGN

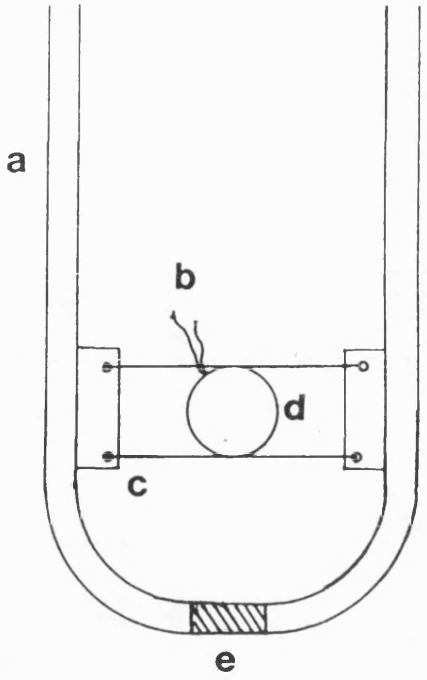

a STAINLESS STEEL PIPES

b THERMOCOUPLE

c TUNGSTEN FILAMENTS

d Pt CRYSTAL

e CERAMIC INSULATOR TUBE

FIGURE 3.2.2

SECOND SAMPLE MOUNTING DESIGN

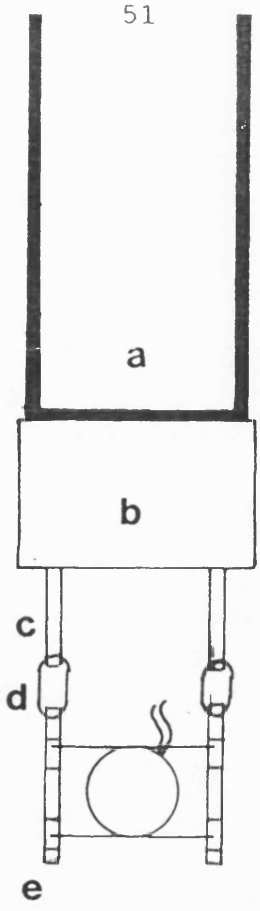

a LIQUID NITROGEN RESERVOIR

b COPPER BLOCK

c TUNGSTEN PIN

d GLASS BEAD

e ELECTRICAL CONNECTORS

FIGURE 3.2.3

FINAL SAMPLE MOUNTING DESIGN

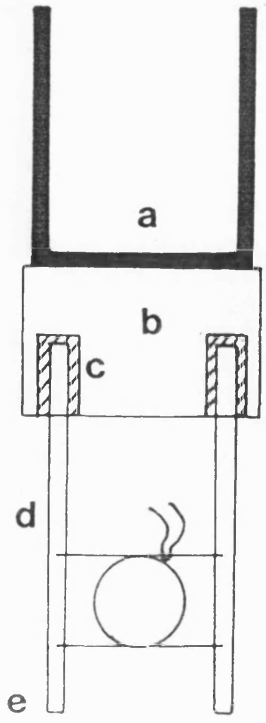

a LIQUID NITROGEN RESERVOIR

b COPPER BLOCK

c ELECTRICAL INSULATORS

d TUNGSTEN PINS

e ELECTRICAL CONNECTORS

rather slow. The glass beads proved to be vulnerable to fracture especially during temperature programmed desorption measurements where the temperature was typically increased from 140K to 600K at heating rates of 4-6 K/s. An alternative arrangement with one tungsten pin electrically isolated and passing the current through the system ground was more effective in obtaining low temperatures and speed of cooling, but retained the disadvantage of a glass bead and lead to problems with temperature measurements from the thermocouple, where the A.C. heating potential superimposed on the D.C voltage produced by the thermocouple, making temperature acquisition impossible.

The final sample mounting design used insulators mounted within the copper block at the base of the cold finger and proved to be very successful (fig 3.2.3). Temperatures of 100K were easily attainable within a few minutes of cooling and resistive heating to 1300K was possible. Connection of the copper conductors to the tungsten mounting pins was initially by means of stainless steel barrel connectors, but in later work connections were hard soldered which proved to be much more durable.

3.3 Obtaining ultra-high vacuum conditions

In order to obtain base pressures of less than 1 x 10^{-10} mbar, it was necessary to bake the vacuum chambers to 450K. Heating of the lower chamber was by means of resistive heaters placed within an insulating shroud. The upper chamber and sample manipulator were baked independently using heating tape. Thermostatic temperature control was only available for the lower chamber. The temperature at various points on the upper vacuum chamber and manipulator was monitored by using thermocouples. In particular it was necessary to carefully regulate the temperature close to the gate valve between the two main vacuum chambers and the rotary feedthrough at the top of the manipulator, since both contained teflon or other plastic components which would deteriorate if heated too much.

3.4 The Infra-red Spectrometer

A variety of designs for monochromation of infra-red radiation have been developed [78]. The usual design for a dispersive RAIRS monochromator is the Czerny-Turner monochromator [79] where the radiation passes through an entrance slit onto a concave mirror, onto a blazed diffraction grating and then focussed on

an exit slit via a second concave mirror. This was the design used in the present work.

The optical path and components are illustrated in Figure 3.4.1. Radiation produced by the infra-red source passes through a mirror box and into the upper vacuum chamber through a sodium chloride window, where it is reflected at grazing incidence. The reflected radiation passed through a second mirror box and was focussed on the entrance slit of the monochromator. It then passed through the Czerny-Turner monochromator components, the two concave mirrors and blazed diffraction grating and was focussed onto the exit slit and thereafter onto the infra-red detector. A wheel with a selection of infra-red filters was placed in front of the infra-red detector. The filter-wheel could be rotated whilst the system was under vacuum, using a rotary feed-through drive.

In the Czerny-Turner design, the frequency of radiation which falls on the detector depends on the angle at which radiation is incident on the diffraction grating. To scan over a range of frequencies it was thus necessary to rotate the grating. A mechanism to convert linear motion from a suitable linear motion drive (Burleigh instruments) was installed beneath the grating. Position measurement was provided by a

FIGURE 3.4.1 RAIRS SPECTROMETER OPTICS

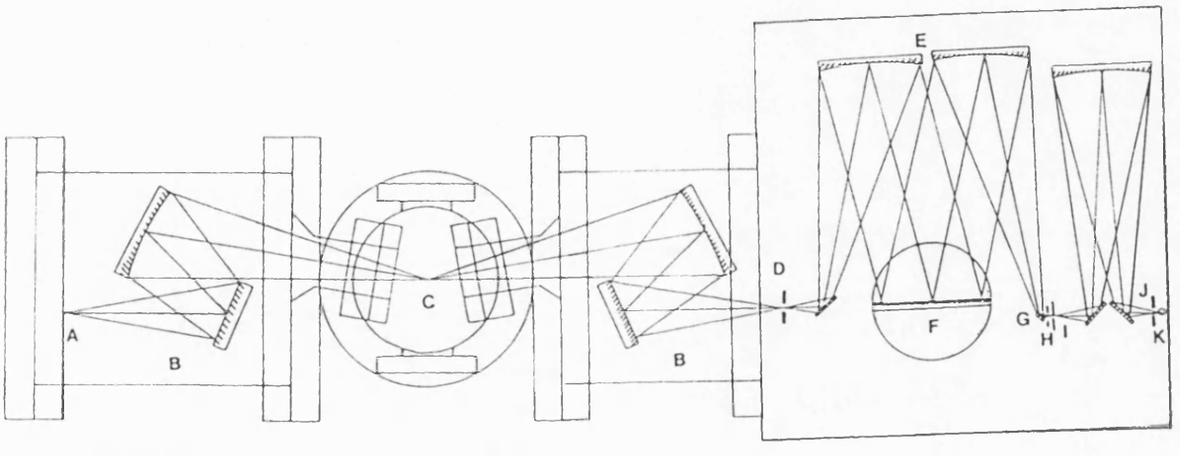

A IR SOURCE
B MIRROR BOX
C SAMPLE
D VARIABLE APERTURE SLIT
E CONCAVE MIRRORS
F DIFFRACTION GRATING
G VIBRATING MIRROR
H RADIATION CHOPPER
I VARIABLE APERTURE SLIT
J FILTER
K IR DETECTOR

Heidenhein optical encoder, capable of measuring positions to tenths of microns, thus allowing angular resolution of 0.3 seconds of arc. A feedback circuit between the linear motion drive and encoder ensured that position of the diffraction grating was held constant once the drive was stationary, which significantly reduced the effects of external vibration.

Both entrance and exit slits were mounted on mechanisms which allowed four slits of different widths to be moved into the optical path in order to change the resolution of the monochromator. Using the two narrowest slits, a resolution of 5 cm^{-1} was possible.

The IR source was a tungsten ribbon clamped in a water cooled holder and resistively heated using a stabilised voltage power supply. Development work using a variety of different mounting arrangements and source geometries, including tungsten filaments, ribbons and folded ribbons showed that a ribbon 2 mm long and 0.025 mm thick provided a satisfactory source.

3.5 Modulation Techniques

In order to separate the signal of the absorption bands under study from the signal received at the detector, a variety of modulation techniques, using phase sensitive detection have been developed. The

measured signal contains noise components from a variety of sources:

(1) Background radiation from within the optics

(2) Drifts due to fluctuations in source intensity

(3) Drifts due to variations in detector sensitivity

(4) Movement of the sample

The use of modulation with phase sensitive detection, using a lock-in amplifier (E.G.&G., model 5205) is designed to eliminate noise at frequencies away from the modulation frequency.

The monochromator used in these studies had facilities for two types of modulation. The first and simplest modulation technique was intensity modulation, in which the radiation was chopped by means of an obstruction periodically placed in the optical path. Demodulation of the measured signal yielded the total intensity. In the present work, the radiation chopper used (Edinburgh Instruments Ltd.) was of the oscillating vane type, which had the advantage of being constructed from materials which were ultra-high vacuum compatible. It was mounted just in front of the second slit in the monochromator (Figure 3.4.1).

The other modulation technique used in this study was that of wavelength modulation [80]. This technique, first applied to RAIRS by Pritchard and co-workers

[81,82] is a differential one, where radiation is swept across the second slit in the Czerny-Turner monochromator. This was carried by means of a vibrating mirror (General Scanning Inc.). The demodulated signal yields the differential of intensity with respect to wavelength if the phase sensitive detection is carried out at the oscillation frequency (F mode), or the second differential with respect to wavelength if carried out at twice the frequency (2F mode). Thus it has similarities to Auger electron spectroscopy, where small Auger loss peaks are distinguished from a large background signal by measuring a differential spectrum.

The advantages of wavelength modulation are that the absorption spectrum is obtained by numerical integration, which smooths out noise and that slowly varying noise factors such as drifts in detector or infra-red source are minimised (see Figure 3.5.1). However the technique is not well suited to picking up broad absorption bands. It was found that using a large oscillation amplitude for the vibrating mirror artificially broadened the absorption bands and could also induce components in the demodulated signal due to higher order differentials of intensity with respect to wavelength. The latter effect was used in the alignment of the optics.

FIGURE 3.5.1 WAVELENGTH MODULATED SPECTRUM

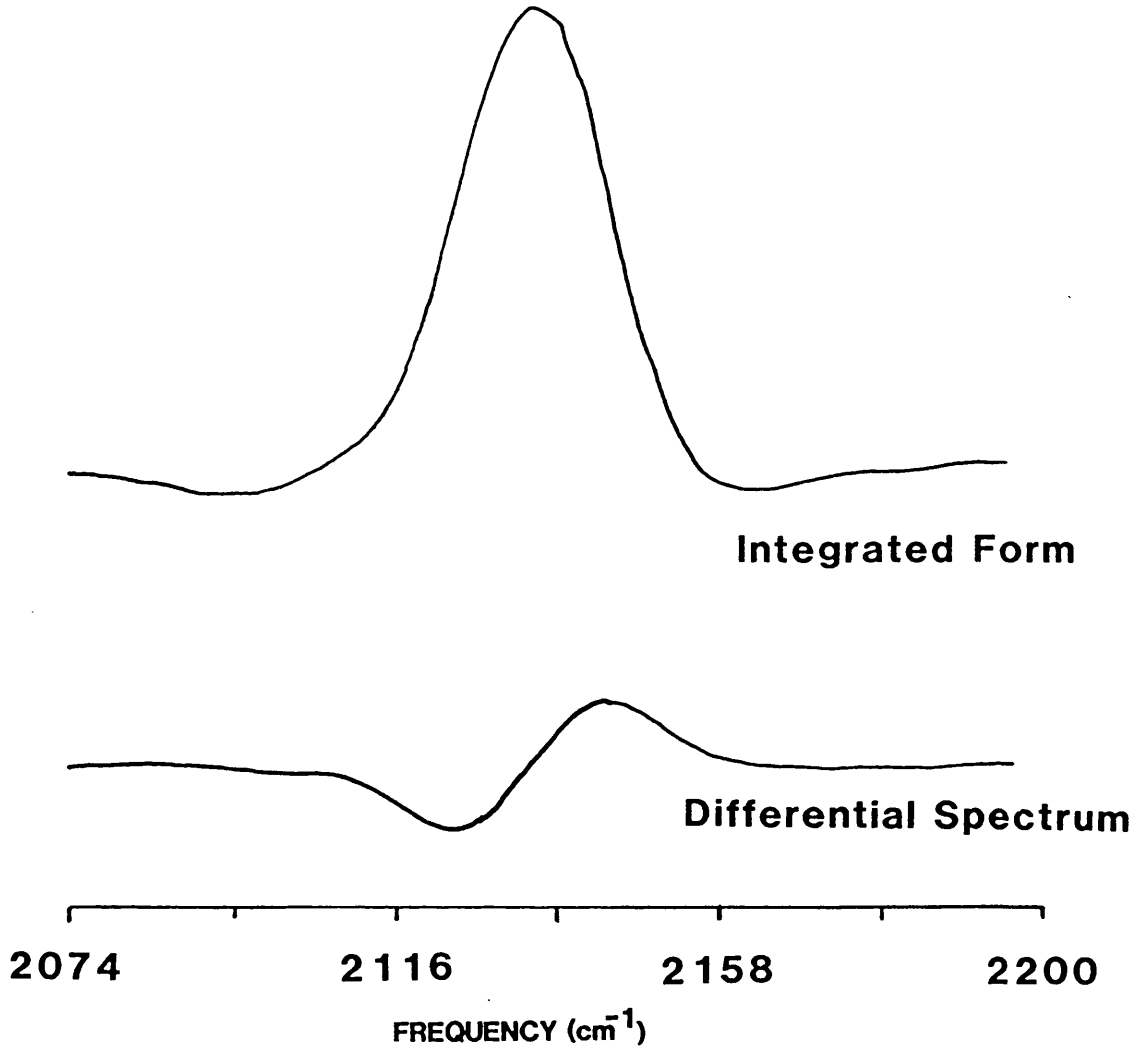

The vibrating mirror was mounted just before the second slit, in such a position that when stationary, the radiation reflected directly onto the slit. This was necessary when using the intensity modulation technique.

In practise it was found that the performance of the radiation chopper was unsatisfactory, the two chopping vanes either hit each other, thus not providing a sinusoidal modulation, or failed to chop all of the incoming radiation, thereby reducing the signal. This may have been due to operating the device in a vacuum. The moving vanes in the chopper were positioned in close proximity and in atmosphere a layer of gas would be trapped between them whilst they vibrated, keeping them apart; this cushion of air is absent in vacuum allowing transverse oscillations to occur and the vanes to collide.

Most spectra were obtained by using wavelength modulation in F mode, yielding the differential of intensity with respect to wavelength. This technique proved satisfactory until the IR detector was changed. The changing in the internal electrical connections following this caused a tendency for the vibrating mirror driving signal to interfere with the signals from the optical encoder at higher mirror oscillation amplitudes. Reduction of the oscillation amplitude

halted this problem.

3.6 Infra-red detectors

During the course of this work two different infra-red detectors were used. The first was an indium antimonide (InSb) photo-diode operating in photovoltaic mode and the other a Mercury Cadmium Telluride (MCT) photo-diode operating in photo-conductive mode.

The InSb detector has the advantage of a high detectivity (a measure of the response to incident IR radiation) but had a low frequency cut-off of 1880 cm^{-1}. It is suitable for measurements in the range 1880 cm^{-1} to 3300 cm^{-1}, which included the C-O stretch for molecules adsorbed in on-top sites and also for characteristic absorption bands for adsorbed hydrocarbons. The MCT detector has a somewhat lower detectivity, but a greatly enhanced frequency range of 800 cm^{-1} to 4000 cm^{-1}.

Both detectors required cooling to 77K and so were mounted on a copper rod attached to a dewar to allow cooling with liquid nitrogen. Electrical connections were made as short as possible to a feedthrough and the appropriate pre-amplifier connected directly to the feedthrough in order to minimise noise pick-up. In operation the MCT detector (photo-conductive pre-

amplifier, Renishaw Scientific Ltd.) proved to be much less susceptible to long term drifts, possibly due to the different design of pre-amplifier used. In particular the InSb detector (photovoltaic pre-amplifier, Laser Monitoring Systems Ltd.) was very vulnerable to drift when the ambient temperature in the laboratory was high, for instance when an adjacent UHV apparatus was being baked.

3.7 Alignment of Infra-red Optics

The other movable optical component in the IR spectrometer, apart from the diffraction grating and variable aperture slits, was the platinum single crystal. This required careful alignment before starting to measure with the spectrometer.

The procedure adopted was to move the diffraction grating to the position corresponding to 2000 cm^{-1} and monitor the output from the infra-red pre-amplifier on an oscilloscope (and simultaneously on the lock-in amplifier in 2F mode). The vibrating mirror was used with an oscillation amplitude corresponding to a sinusoidal signal of 3 volts peak to peak from the external output of the vibrating mirror controller. This large oscillation amplitude was sufficient to make breakthrough of the second differential of intensity

with respect to wavelength signal dominate the demodulated signal, so that the signal was proportional to total intensity. The sinusoidal trace on the oscilloscope was then maximised in intensity using the x and y positioning controls on the manipulator, with fine adjustments made whilst monitoring the lock-in amplifier output, and made symmetrical by altering the position of the sample in rotation. A signal which was not symmetrical produced differential absorption spectra with asymmetric positive and negative excursions, which could not be numerically integrated to give a flat baseline.

This technique was developed because of the problems encountered with the radiation chopper, (see section 3.5). A simpler alignment technique, using intensity modulation and so measuring signal intensity directly would have been preferable, but was impossible owing to the inability of the chopper to modulate sufficient of the radiation in the monochromator.

3.8 Computer Control

The computer used to control both the RAIRS experiments and TPD measurements was a PDP11-03 (Digital Equipment Corporation) running the RT-11 operating system. Interfaces installed with this system included

twin digital to analogue (DA) output lines, eight analogue to digital (AD) input lines and four RS232 serial communications lines. One serial line was conFigured to operate the computer terminal (Selanar Hirez-100), a dual mode terminal capable of acting as both a normal alphanumeric terminal (conforming to the VT-100 standard) and as a high resolution graphics terminal (using the Tektronix 4014 standard). In graphics mode the terminal was capable of displaying 1024 by 780 points and both VT100 and TEK 4014 modes could be displayed simultaneously on screen. Switching between terminal modes was possible under appropriate software control.

The programming language used to write the main control programs was FORTRAN, a compiled high level language, producing compact and time efficient code. The size of the code proved to be very important, as the computer has a very limited memory space (64 kilobytes) available. Standard FORTRAN does not contain control routines for AD input, DA output, serial communications or control of graphics, which require operations on specific memory locations on the PDP11. Moreover FORTRAN is not suitable for writing such routines. The RT11 operating system allows such control routines to be written in the MACRO-11 assembly language in such a way

that they may be called from FORTRAN main programs.

The software written to drive the spectrometer during experiments was:

(a) The main control program for controlling the spectrometer, manipulation, display and storage of data, IR.FOR, and associated subroutines, written in FORTRAN (Appendix One).

(b) Serial communications with and control of the lock-in amplifier, LIA.MAC, written in assembly language (Appendix Two).

(c) Serial communications with and control of the linear motion drive, LMD.MAC, written in assembly language (Appendix Three).

(d) Control of the digital to analogue output lines to allow control over the mass number set on the mass spectrometer, DACONV.MAC written in assembly language (Appendix Four).

(e) Control of the analogue to digital input lines to acquire temperature and pressure readings during TPD measurements ADCONV.MAC, written in assembly language (Appendix Five).

(f) Control of the Rikadenki digital plotter to allow

the plotting of images displayed on screen. These routines were available in three varieties, depending on the size of paper being drawn on. All routines (PLOTA3.MAC, PLOTA4.MAC, PLOTA5.MAC) were written in assembly language except for the graph axis plotting routine (RAXIS.FOR) which was written in FORTRAN (Appendix Six).

(g) Screen handling routines for the VT100 terminal mode, allowing text to be positioned anywhere on screen and highlighted by using bold or reverse video display.

(h) Graphics handling routines for plotting of points, drawing of lines and positioning of text on the graphics screen when in TEK 4014 graphics mode.

Most of the code for tasks (g) and (h) was written in assembly language (GRAPH.MAC) although some routines, such as the graph axis plotting (TAXIS.FOR) were written in FORTRAN (Appendix Seven).

The control program for TPD measurements and for control of mass scans on the mass spectrometer has been described elsewhere [83], although a heavily modified version was used for most of the TPD experiments. The modifications were to speed up acquisition, hard copy plotting routines, improved screen display routines and numerical integration routines.

The mode of operation of the infra-red spectrometer control program was determined by hardware constraints. Both the lock-in amplifier and the linear motion drive control units contained on-board microprocessors and communicated with the PDP-11/03 using RS232 serial communications lines. These were relatively slow, the time taken for communication between computer and lock-in amplifier and the command being executed was approximately 40 milliseconds, whilst the time for the linear motion drive was considerably slower, at 100 milliseconds. To measure a spectrum required the motion drive to rotate the diffraction grating, to scan across a range of frequencies and sample the output from the lock-in amplifier at various frequencies. One possible method of doing this was to rotate the diffraction grating continuously whilst the computer interrogated the linear motion drive for position (and hence frequency) and for output signal from the lock-in amplifier. However unless the diffraction grating moved very slowly, there was always a disparity between measured position and signal strength due solely to the difference in time at which the data was acquired. Moreover, using this technique, the time constant of the lock-in amplifier (which determined the response time of the lock-in amplifier to changes in signal) had to be

reduced to being considerably less than the time taken between output sampling from the lock-in amplifier. This did not produce favourable signal to noise ratios.

The alternative approach, which was the one adopted, was to move the diffraction grating in a series of discrete steps, stopping between steps to determine position and signal strength (see Figure 3.8.1).

The control program was broken up into a large number of subroutines in order to make modification both simpler and quicker and consisted of three main elements:

(1) The main program, IR.FOR, written in FORTRAN to set up the data storage arrays and then monitor the terminal keyboard for incoming commands.

(2) A number of subroutines, also written in FORTRAN, which were called from the main program following a command, to execute that command.

(3) A number of assembly language subroutines,called from FORTRAN code in either the main program or subroutines which controlled the graphics, on screen display and formatting, communications with the lock-in amplifier and linear motion drive, and with the digital plotter.

FIGURE 3.8.1

RAIRS DATA ACQUISITION PROGRAMME

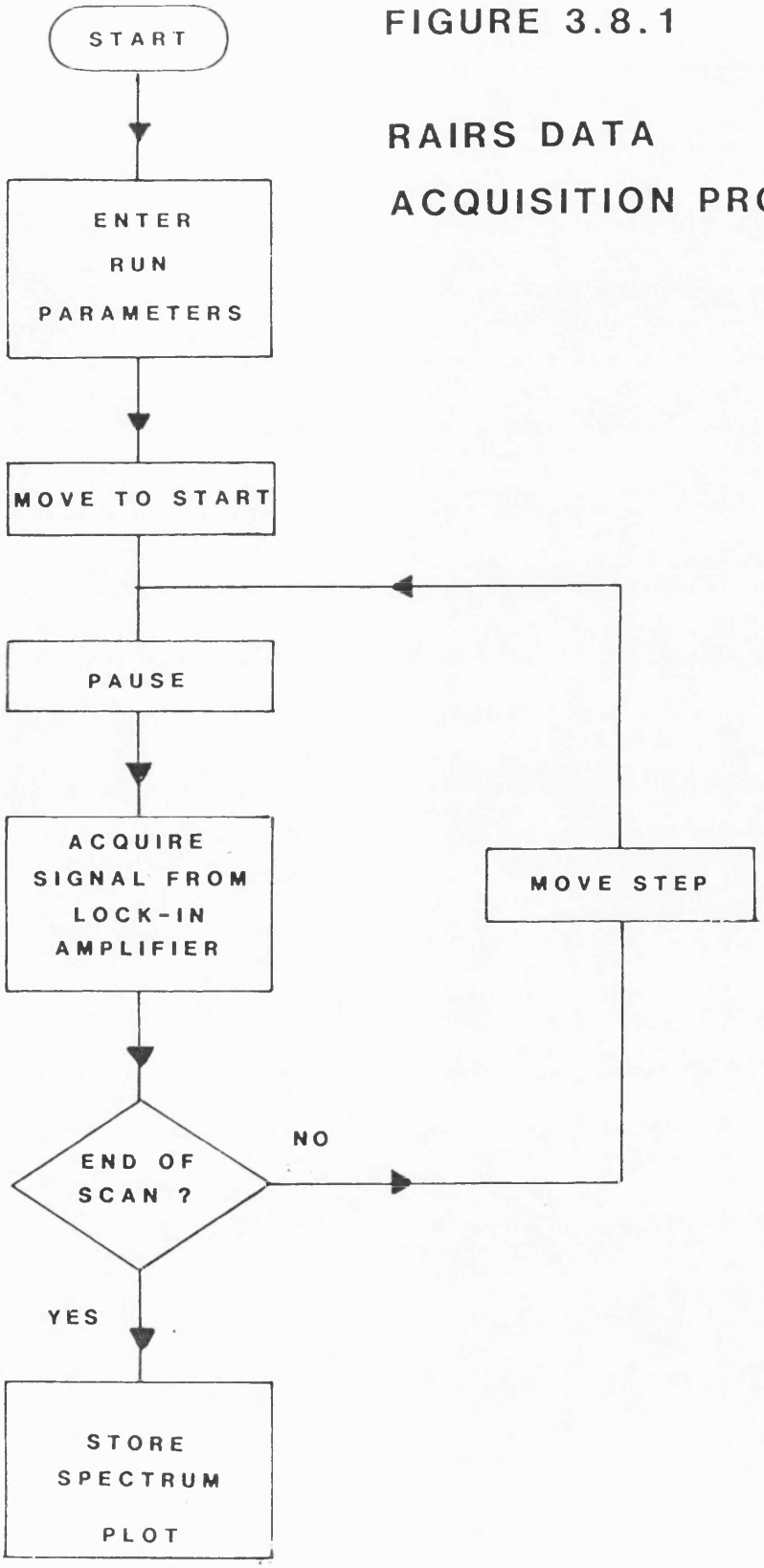

The tasks which the control program had to perform were to maintain certain control parameters which defined what frequency range was scanned, how the amplified signal was acquired from the lock-in amplifier, how it was displayed on the screen and how the data was saved onto computer disk.

The lock-in amplifier parameters which the program controlled were the sensitivity scale of the output, the voltage offset, the instrumental timeconstant, the rolloff value (another time constant) and the times ten expand feature. Unfortunately owing to limitations of computer memory it was not possible to include automatic ranging and set-up routines, so that the values of these parameters had to be set up manually on the lock-in amplifier. The values of the parameters were displayed at the bottom of the screen.

The second group of control parameters required were the frequency range to be scanned and the speed of scanning. The scan range was defined by the starting frequency, the finishing frequency and the step width, the distance between points in the scan. The values of these parameters, together with the number of points in the spectrum were displayed at the bottom of the screen.

A third group of parameters controlled the display of spectra on the screen. These were the y-axis

magnification factor and the y-axis offset of the displayed spectrum from the bottom of the screen.

The final set of parameters necessary were the filename, the file number and the (optional) file title. The RT11 operating system saves data files onto disc with identifiers consisting of six characters (the filename) with a three character suffix (incorporating the filenumber).

The program recognised two data types. The first, the baseline spectrum was displayed on the screen exactly as acquired. The filenumber of this type of file was always zero and the data file suffix was always IBS (infra-red baseline spectrum). The second data type, the subtraction spectrum was acquired and stored exactly as for the baseline type, except in the manner in which it was displayed on the screen, where it was subtracted from the current baseline spectrum. Spectrum files were saved to disk with the data file suffix Inn, where nn was the current filenumber.

A list of all of the commands recognised by IR.FOR and a brief description of their function is given in Appendix Eight.

3.9 Calibration of the RAIRS Spectrometer

The frequency of radiation which was focussed on the detector depended on the angle at which radiation was incident upon the diffraction grating. This in term depended on the rotational position of the grating. Since the drive mechanism was based on a linear motion drive, a calibration of linear position of the drive with respect to frequency was required. This was carried out by placing a 0.044mm thick polystyrene reference film (Perkin-Elmer Ltd., part number 0457-51) in front of the NaCl window on the radiation source side. Polystyrene has a large number of characteristic absorption bands over a wide frequency range and the frequencies of these bands have been determined accurately (84).

In principle, the simplest calibration method would have been to operate the monochromator in intensity modulation mode, recording intensity versus frequency. Problems with the radiation chopper made this impossible. The wavelength modulation technique was used, with the lock-in amplifier locking in on twice the modulation frequency (2F mode). The recorded signal was thus the second differential of intensity with respect to frequency, i.e proportional to intensity. This

technique was easily able to measure the strong polystyrene absorption bands. Once the bands had been measured, with known linear positions, frequencies could be assigned either from the standard reference document [84] or later by comparing the spectra obtained with those spectra obtained from the same reference film measured on a Perkin-Elmer 963 spectrophotometer. Spectra measured in 2F mode, as pseudo-integral spectra are shown in Figure 3.9.1 for the MCT detector and Figure 3.9.2 for the InSb detector and are displayed in the format produced by the FORTRAN plotting routines. The wavenumber scale on Figures 3.9.1 and 3.9.2 is due to the previous calibration data. Data was saved in the data files with the linear position of the diffraction grating in order to remain independent of calibration changes. It was thus easy to determine peak positions in terms of linear position and relate these to the known frequencies of the polystyrene absorption bands.

FIGURE 3.9.1

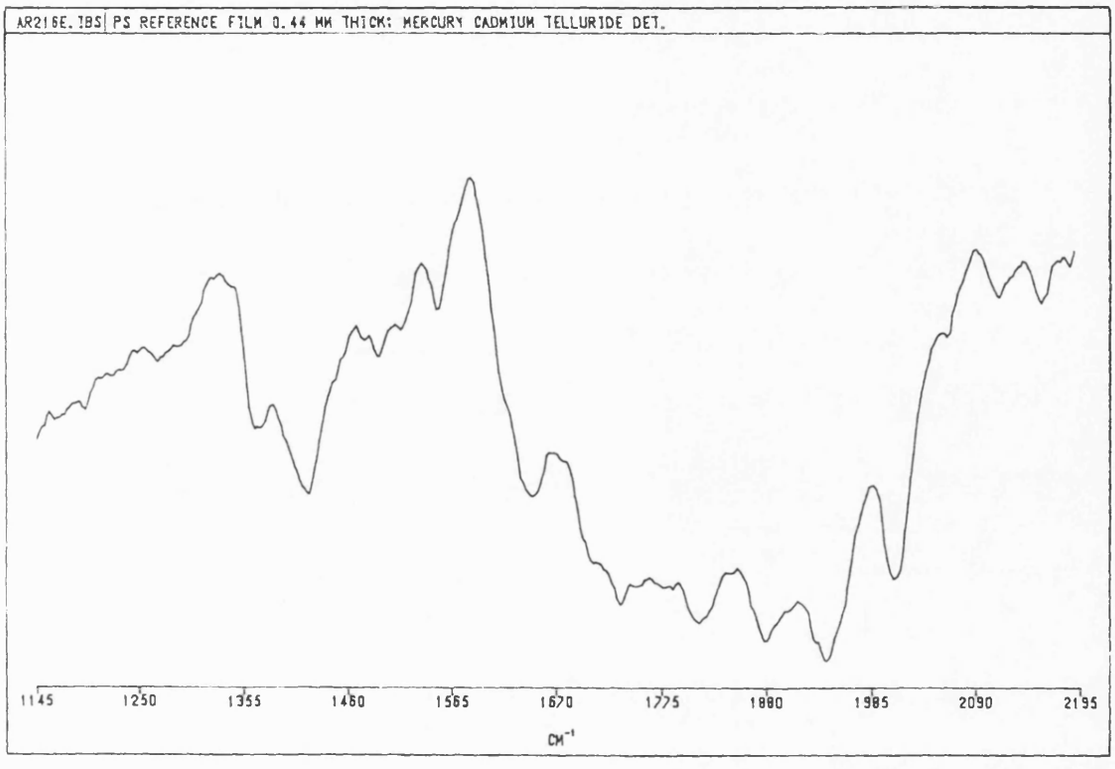
AR216E.IBS PS REFERENCE FILM 0.44 MM THICK: MERCURY CADMIUM TELLURIDE DET.
1145
1250
1355
1460
1565
1670
1775
1880
1985
2090
2195
CM-1

FIGURE 3.9.2

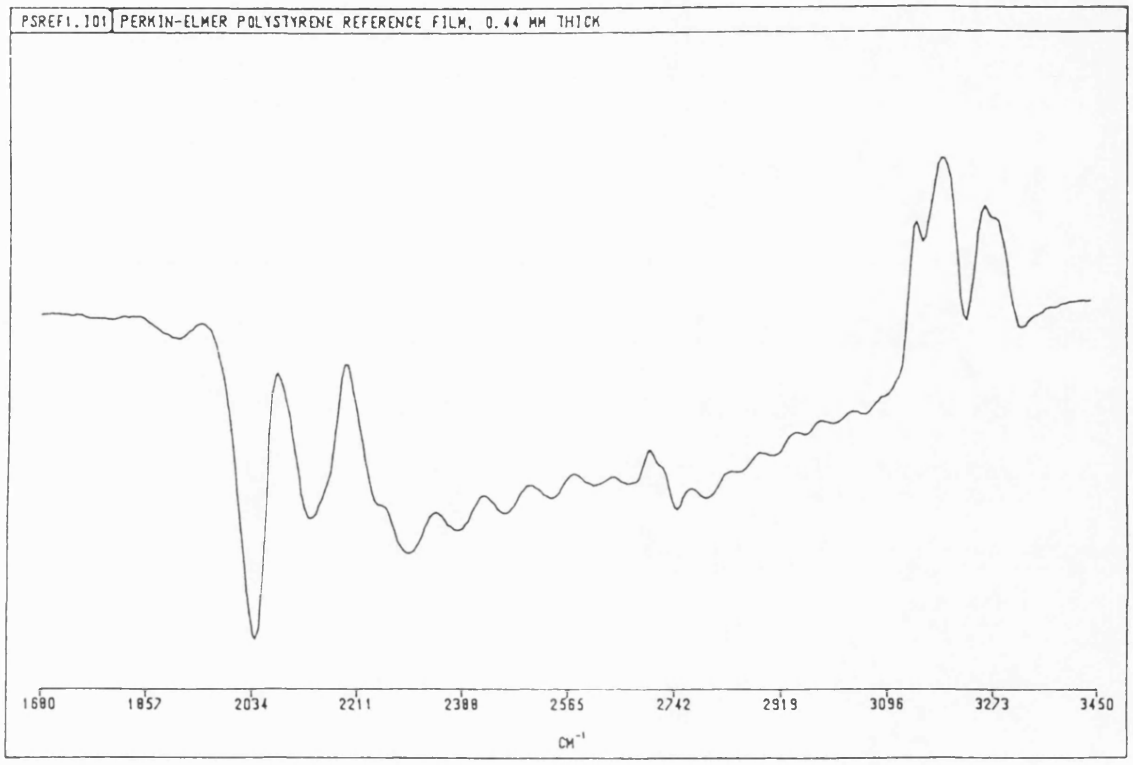
PSREF1.101 PERKIN-ELMER POLYSTYRENE REFERENCE FILM, 0.44 MM THICK
1680
1857
2034
2211
2388
2565
2742
2919
3096
3273
3450
CM-1

3.10 Sample Cleaning Techniques

There have been several alternative procedures for preparation of Pt(110) crystals mostly using cycles of argon ion bombardment and treatment with oxygen at various temperatures and pressures [8,15,17]. King and co-workers [12] have used a technique of repeated argon ion bombardment and heat treatment and foregoing oxygen treatment on the grounds that formation of persistent subsurface oxides is possible [17]. This was the procedure adopted initially during this work, but experience with oxygen treatments demonstrated that the preparation time of a clean surface was considerably shortened by incorporating oxygen treatments into the cleaning process.

In the absence of a quantitative analytical technique to determine surface contaminants, such as Auger Electron Spectroscopy (AES), the cleanliness and order of the surface was determined by four criteria:

(1) The ability to produce well defined TPD spectra for the adsorption of CO which are similar to those reported elsewhere [8,12,15]

(2) The appearance of a well defined (1 x 2) LEED pattern for the clean surface and a lifting of the

reconstruction to give a (1 x 1) pattern following the adsorption of CO.

(3) The ability to produce the (2 x 1) p1g1 pattern in LEED by cooling the sample from 550K in 1 x 10^{-7} mbar of CO.

(4) The position, shape, intensity and coverage dependent frequency shift of the linear C-O stretching frequency.

The last criterion was only used after extensive experience with CO adsorption upon the platinum surface, but was considered the most sensitive test of surface cleanliness.

The cleaning process was as follows, bombardment with argon ions for approximately eight hours at 1000K, followed by annealing to 1300K at pressures of 1 x 10^{-10} mbar for several minutes. The sample was then treated with oxygen at 800K. Oxygen was admitted to the backing line at a pressure of 5 x 10^{-7} mbar. The gas stream was then diverted through the IR chamber for 15 minutes. During this process the lower chamber was sealed off from the IR chamber. After this treatment the oxygen was pumped off and the sample was flashed to 1300K in ultra high vacuum to remove any adsorbed oxygen [85]. This treatment normally resulted in the surface meeting

all of the cleanliness criteria, a second cycle of such treatment rarely being necessary. The pressures and temperature associated with the oxygen treatment are similar to those found by Salmeron and Somorjai [86] to remove surface carbon deposits without producing subsurface oxygen species.

A contaminated surface showed a marked tendency to deteriorate during repeated CO adsorption-desorption cycles, probably due to carbon deposition on the surface. Treatment with oxygen using the conditions referred to earlier normally restored the surface to a 'clean' condition, but subsequent CO adsorption desorption cycles usually caused further deterioration, in which case argon ion bombardment was necessary.

Surfaces which gave satisfactory CO TPD results, but were poorly ordered in LEED, tended not to form the (2 x 1) p1g1 LEED structure when cooled in CO. Annealing the crystal to 1300K for several minutes often produced better defined LEED patterns, although occasionally bombardment followed by annealing to 1300K proved necessary to produce satisfactory ordering.

3.11 Temperature Programmed Desorption Experiments

TPD experiments could be carried out in both the upper (IR) and lower chambers. The advantage of

carrying out such experiments in the upper chamber was that the gas dosing corresponded directly to that done during IR experiments. The disadvantage was that the mass spectrometer was in the lower chamber and so the pressure changes were small. In the lower chamber, the sample was able to face the mass spectrometer with line of sight to the ioniser at a distance of a few centimetres. The mass spectrometer signal was greatly enhanced, but the exposures of, for example CO, to produce equivalent TPD spectra were greater by an order of magnitude than the exposure in the IR chamber. The technique finally adopted was to dose the gas in the upper chamber and move the sample down to the lower chamber for desorption measurements.

Using the program QMS.FOR, the computer digitised a preset number of pressure temperature data pairs, performed signal averaging, displayed the resulting TPD spectrum and stored the results for future use. The program was a modification of that described by Hallam [83]. To ensure accurate recording of temperatures during the experiment, the amplification variables used within the program were adjusted by standardisation against an equivalent thermocouple standing in iced water. The sample heating was supplied by a low voltage A.C. power supply capable of producing a current of 25

amps, which was switched on and off manually. This supply was sufficient to produce heating rates of 4-6 K/s when used in conjunction with the final sample mounting design. The exposure of gas dosed into the system was measured by monitoring the pressure in the system from the mass spectrometer against time, recording the data on an X-T plotter.

3.12 Mass Spectrometry Experiments

The mass spectrometer control software, operating in a different mode could also scan a range of mass numbers, within limits of 1 to 100 atomic mass units. The control program ramped a potential from a DA output channel, through an amplifier with a gain of ten and into the external control input line on the mass spectrometer. The mass number which was set was proportional to the applied potential. The program then recorded the partial pressure at the set mass number from the mass spectrometer external output fed into an AD input line. The program allowed for the mass scan range to be set, as well as the increment at which masses were stepped up. Signal averaging was by two methods, firstly taking the mean value of a number of pressure readings at the same mass number and then by averaging a number of complete mass range scans.

This experimental facility was mainly used to check the residual gases in the vacuum system.

3.13 RAIRS Experiments

The RAIRS measurements conducted during these studies all followed essentially the same procedure. In all cases the infra-red source was allowed to run for at least 40 minutes before commencing any measurements in order to reach an equilibrium operating temperature. Since the source acted as a black-body emitter of radiation, any temperature fluctuation would change the intensity of radiation emitted at any given frequency.

In adsorption experiments where only one adsorbate was being studied, the platinum crystal was moved to the upper chamber and cleaned with the oxygen and annealing treatment described in section 3.10. In co-adsorption experiments (potassium/CO), one of the adsorbates would be pre-adsorbed on the clean surface. The crystal was then cooled to the appropriate temperature, normally room temperature or 100K. Once the temperature was stable the alignment of the sample into the correct reflection geometry was carried out (see section 3.9). The temperature of the sample had to be constant during this process, as changes in temperature caused intensity changes either due to emission of radiation or due to

small movements of the crystal caused by thermal expansion or contraction of the tungsten support filaments.

A baseline spectrum was then measured over the appropriate frequency range and stored, immediately followed by a second spectrum. In the ideal case, the two were identical, giving a perfectly flat subtraction on screen. Normally several baseline/subtraction spectrum pairs had to be measured before this occurred.

Once a stable operating regime had been established, quantities of gas could be dosed onto the platinum crystal and further absorption spectra measured. Two alternative gas dosing techniques were used. The first was to admit discrete doses of gas and measure absorption spectra between doses. This had the advantage that accurate determination of the exposure of the gas was possible. However discrete dosing required the manipulation of three valves on the vacuum system.

Experience demonstrated that the quality of spectra deteriorated substantially after several doses due to the disturbance to the system causing the the sample to move. The second technique, which was the preferred method was to continuously admit gas into the upper chamber at a low pressure (typically 2×10^{-10} mbar for

CO) whilst measuring RAIRS spectra. To aid this technique, a special automatic running routine for the control program was developed, which measured a spectrum, saved the data to disk and then repeated the process indefinitely, until terminated by a command from the keyboard. The results from these experiments consisted of a series of spectra taken at different times during the adsorption process.

With either dosing technique, the exposure of gas to the sample was measured by recording the partial pressure of the gas in the chamber versus time on an X-T chart recorder. The pressure reading was taken from the external output of the quadrupole mass spectrometer. With the continuous dosing technique it was necessary to record the starting and finishing times of each spectrum on the chart recorder trace. Since the frequency range was normally chosen so that any infra-red absorption bands appeared in the middle of the range, the mid-point between the start and finish times was normally taken as the point in time at which gas exposure was calculated.

3.14 Low Energy Electron Diffraction Experiments

The Omicron Vacuumphysik LEED system was mounted in the lower chamber. The system has four grid electron

optics with a back view screen. The advantage of the back view screen is that the diffraction pattern is not obscured by the sample holder as would occur in a traditional LEED arrangement.

LEED experiments were carried out with the single crystal moved as close as possible to the electron optics. It was necessary to switch off the ion gauge and mass spectrometer before performing LEED, as the light from the filaments obscured the LEED patterns formed on the phosphor screen. Experiments could be carried out at room temperature, although the clearest patterns were normally obtained with the crystal cooled to 100K, where the diffraction beams were sharper and the background intensity reduced. Photographs of the patterns could be taken using a standard SLR camera (Olympus OM-10) attached to a stand clamped to the vacuum system.

Adsorption of CO on Pt(110)-(1 x 2) at 300K

4.1 Introduction

The adsorption of CO on the Pt(110)-(1 x 2) at 300K has been the subject of several previous studies by a variety of experimental techniques [8,9,13-18,20]. The present study was undertaken in order to thoroughly characterise the adsorption system before moving on to study more complex co-adsorption systems such as CO/potassium/Pt(110)-(1 x 2) and to test the newly commissioned RAIRS spectrometer.

In addition, the same experimental techniques were used to examine the differences between this adsorption system and the (2 x 1)p1g1 overlayer formed by cooling the crystal from 600K to 300K under 2 x 10^{-7} mbar of CO [8,9,12].

4.2 Coverage Determination

The absolute coverage determination of CO on both (1 x 2) and (2 x 1)p1g1 CO overlayers has been measured [20]. At saturation for CO adsorption at 100K, the coverage is θ_{CO}=1.0, relative to the unreconstructed (1 x 1) surface. The CO coverage for adsorption at 300K is slightly lower, θ_{CO}=0.89. A series of TPD spectra were measured with varying exposures to CO. Since the

quadrupole mass spectrometer measures partial pressures quantitatively, the area beneath the TPD spectrum is proportional to the number of CO molecules desorbed from the surface and this is proportional to coverage. Assuming that saturation coverage for adsorption of CO at 300K corresponded approximately to full coverage of the surface (θ_{CO}=1.0), the variation of coverage as a function of exposure was calculated (see Figure 4.2.1).

FIGURE 4.2.1

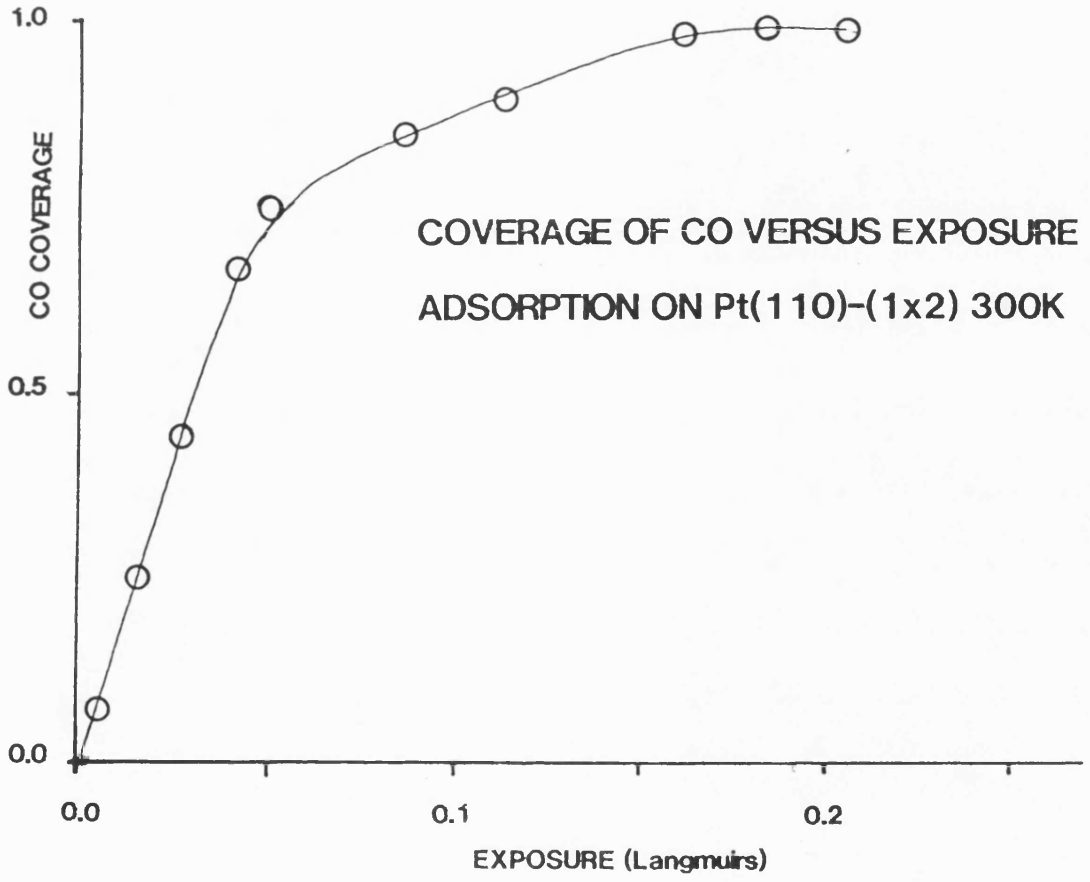
1.0
0.5
0.0
CO COVERAGE
COVERAGE OF CO VERSUS EXPOSURE
ADSORPTION ON Pt(110)-(1x2) 300K
0.0
0.1
0.2
EXPOSURE (Langmuirs)

4.3 Temperature Programmed Desorption Results

Having determined the coverage versus exposure function the TPD spectra may now be plotted in terms of CO coverage (Figure 4.3.1). A single symmetrical desorption peak is observed at all CO coverages below θ_{CO}=0.5. The desorption temperature of 540K remains constant with varying coverage, indicating first order type desorption kinetics. At CO coverages of θ_{CO}>0.5 a low temperature shoulder grows out from the main peak, forming a distinct secondary peak at saturation coverages, θ_{CO}=1.0. These results are similar to those obtained in most previous studies [8,9], the only exception being those TPD spectra reported by McCabe and Schmidt [16].

The desorption spectrum from a CO overlayer exhibiting the (2 x 1)p1g1 LEED structure is shown in Figure 4.3.2. The areas beneath this TPD spectrum and that of a saturation coverage of CO adsorbed at 300K are comparable, suggesting that both overlayers have the same coverage. The subtle difference between the two desorption spectra, with the low temperature feature much less pronounced in the p1g1 overlayer has been noted elsewhere [8,9].

FIGURE 4.3.1

CO DESORPTION SPECTRA FROM Pt(110)-(1x2)

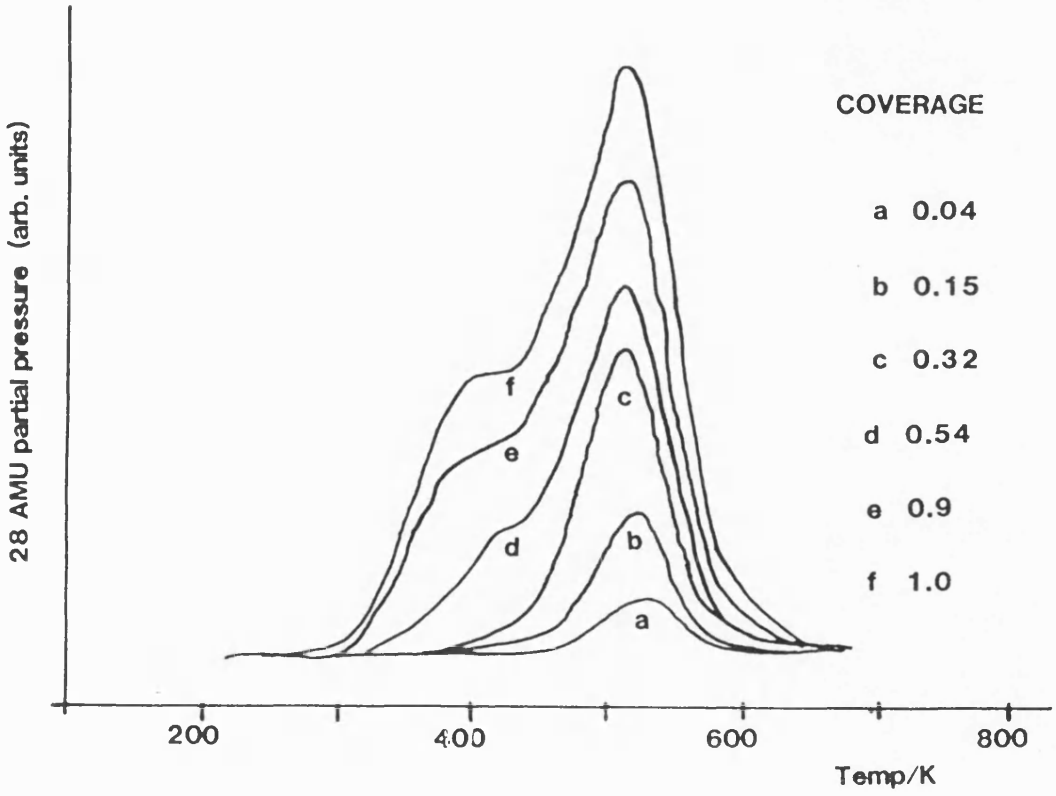

FIGURE 4.3.2

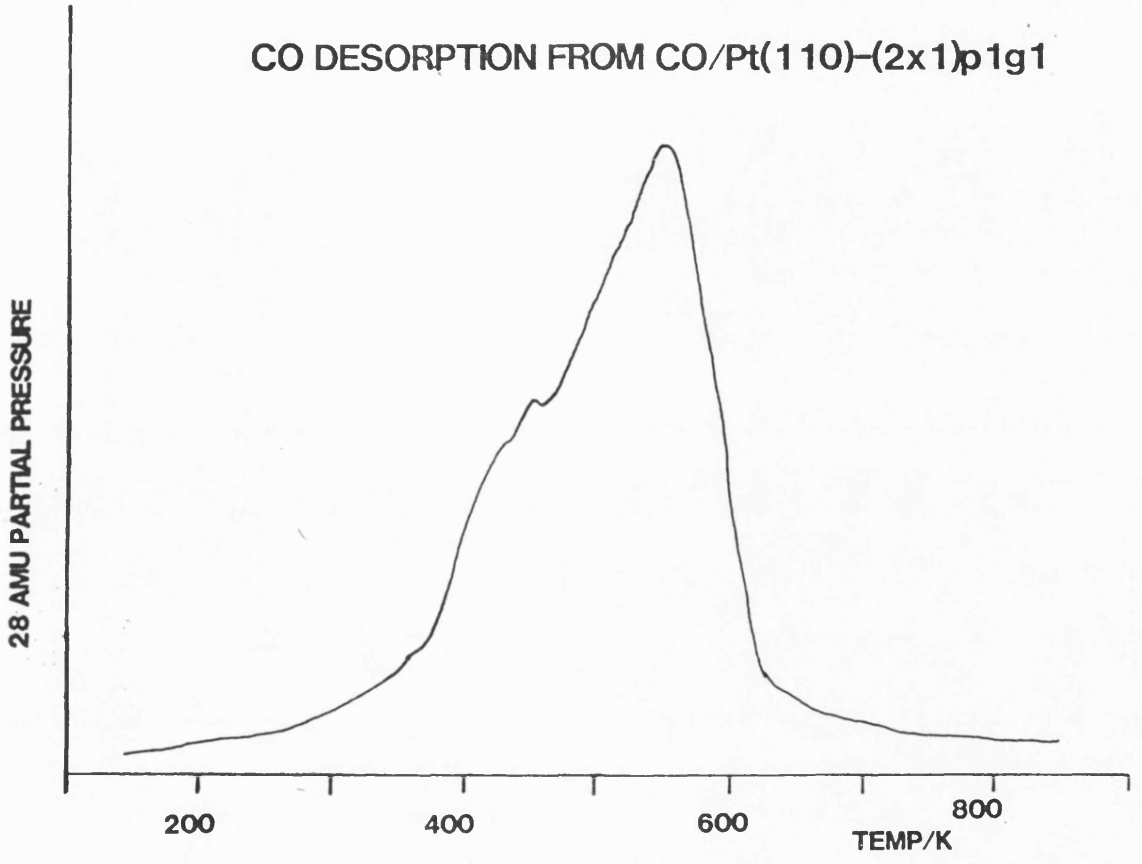
CO DESORPTION FROM CO/Pt(110)-(2x1)p1g1
28 AMU PARTIAL PRESSURE
200
400
600
800
TEMP/K

The desorption energy of CO from the surface was calculated using equation (2.36) and assuming a pre-exponential factor of 10^{13} sec^{-1}. The heating rate was 4 K/sec. The desorption energy of the high temperature state was calculated as 140 kJ/mol and that of the lower state 108 kJ/mol. These compare to the values obtained from the results of Hofmann and co-workers of 145 kJ/mol and 108 kJ/mol [9] and those of Comrie and Lambert [8] of 129 kJ/mol and 105 kJ/mol for the upper and lower desorption states respectively.

4.4 Low Energy Electron Diffraction patterns

The clean surface exhibited the (1 x 2) reconstruction pattern observed in earlier studies. Following CO adsorption at 300K, the reconstruction was lifted. The coverage of CO required to observe the formation of the (1 x 1) pattern was Θ_{CO}=0.5. This is in accord with previous observations [9]. Annealing a CO overlayer formed at 300K with saturation coverage to 350K did not result in the (2 x 1) p1g1 LEED structure being observed as had been reported by Jackman and co-workers [20].

The p1g1 overlayer exhibited the characteristic pattern with the [1/2,0] fractional order diffraction beams absent [8,9,72,73]. A real space model [12]

corresponding to the p1g1 overlayer is depicted in Figure 4.4.1. The systematic absence of the fractional order spots is thought to be due to the formation of a glide line symmetry element caused by the tilting of the C-O molecular axis away from the surface normal. The azimuthal tilt away from the [001] direction is deliberately exaggerated in Figure 4.4.1. This tilt in azimuth has been reported in one ARUPS study [13], but reported to be negligible in another [18]. This would change the symmetry group of the overlayer from p1g1 to p2mg. The glide line symmetry element which results in missing diffraction beams is present in both representations.

FIGURE 4.4.1 CO/Pt(110)-(2x1)p1g1

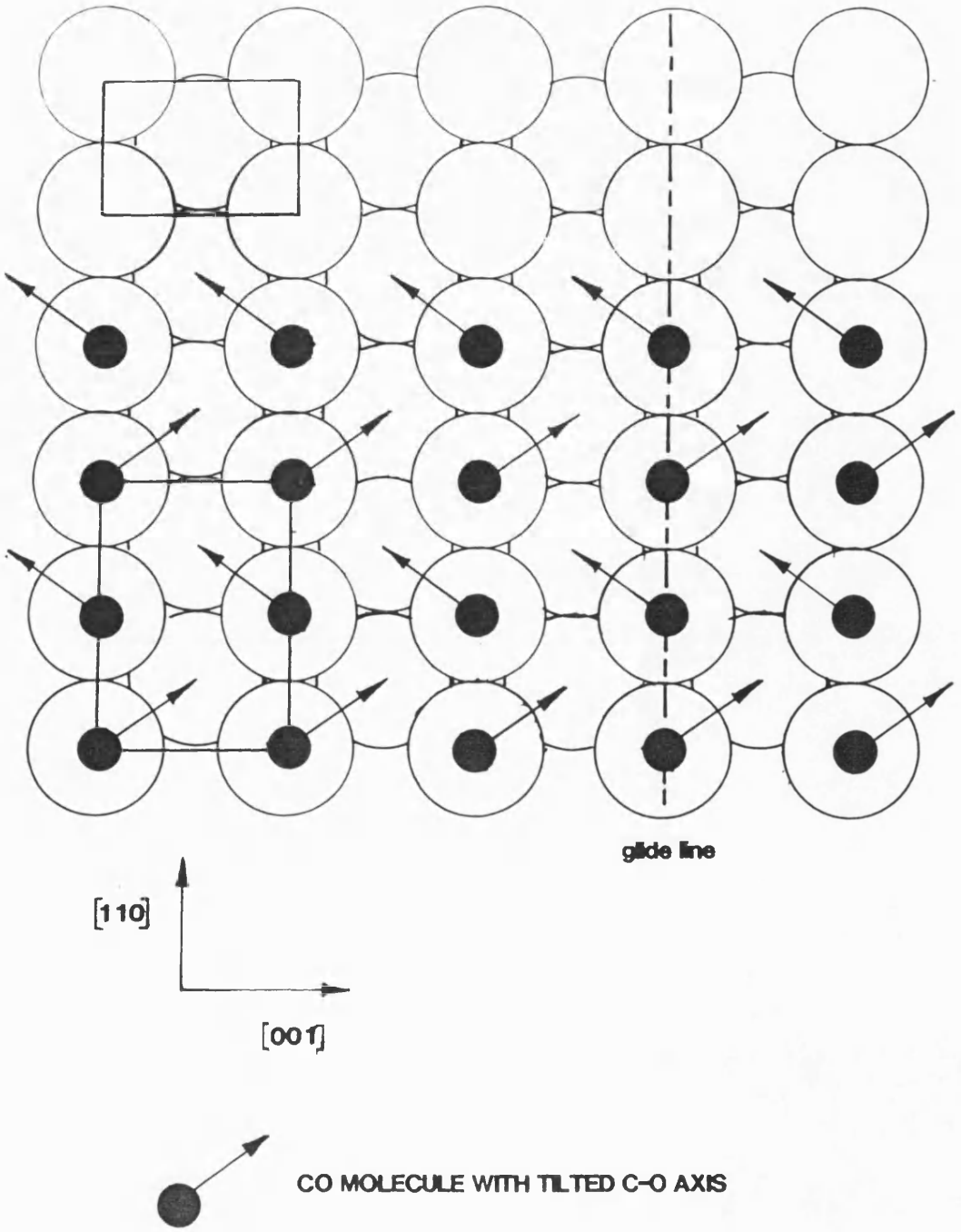

4.5 RAIRS Spectra

A series of RAIRS spectra for CO adsorption at 300K are shown in Figure 4.5.1. There is a single absorption band at all coverages, shifting from 2085 cm^{-1} at low coverage to 2130 cm^{-1} at θ_{CO}=1.0. These results were obtained using the InSb detector, a repetition of the experiment using the MCT detector failed to find any other absorption bands at lower frequencies. The observed frequency range is characteristic of CO adsorbed exclusively in on-top bonding sites. The full width at half maximum (FWHM) of the band is relatively constant over all coverages, at 18 cm^{-1}. This value is large in relation to the FWHM of linear CO absorption bands reported on other faces of platinum [87,88] and on other metals [89].

The absorption band due to the (2 x 1)p1g1 overlayer and the band formed by saturation coverage of CO adsorbed at 300K are very similar. The (2 x 1)p1g1 band is shifted downwards in frequency by 2 cm^{-1} and the FWHM slightly reduced to 16 cm^{-1} compared to 18 cm^{-1} for the absorption band of a saturation coverage of CO adsorbed at 300K.

FIGURE 4.5.1 RAIRS SPECTRA CO/Pt(110)–(1x2) 300K

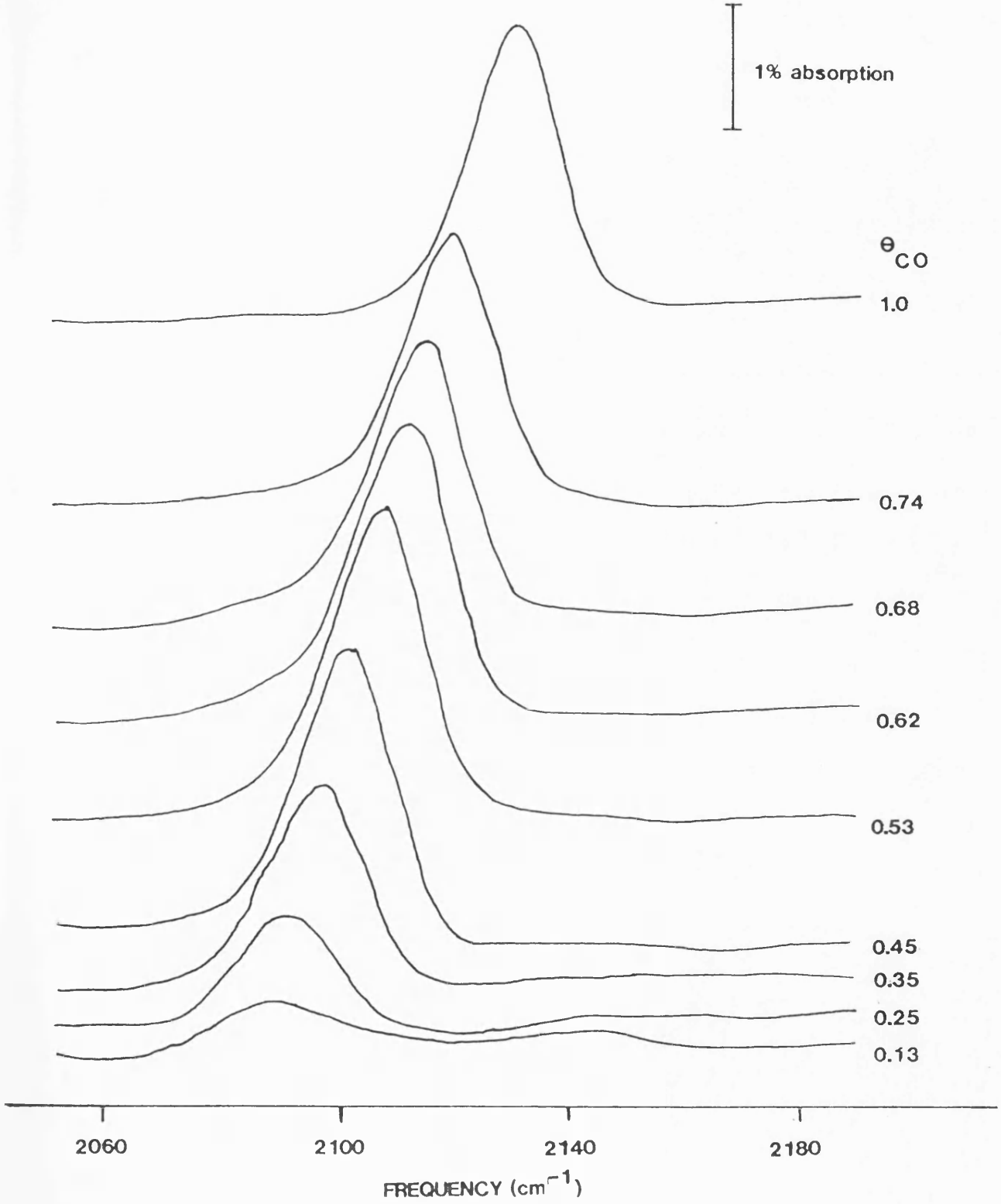

It is suggested that the slight narrowing of the absorption band of the p1g1 overlayer reflects a slight increase in the order of the adsorbed layer, but the large FWHM of the absorption bands in both overlayers reflects the degree of surface disorder caused by the imperfect lifting of the reconstruction and is hence inhomogeneous in nature.

4.6 RAIRS results from previous studies

The RAIRS results presented here for adsorption of CO at 300K differ significantly from those measured in the only other RAIRS study [12], where a doublet is observed at coverages of $\theta_{CO}<0.3$ and a singleton absorption band at higher coverages. The FWHM of the singleton band is reported as 12 cm^{-1}, although no baselines are visible on the spectra, which have a non-Gaussian shape. The FWHM value quoted may be an underestimate of the true value. The frequency range of the absorption bands also indicated that CO was bound in on-top adsorption sites.

The interpretation of the doublet absorption band at low coverage was as follows: at coverages $\theta_{CO}<0.1$, CO exists as isolated molecules on the surface, whilst at intermediate coverages ($0.1<\theta_{CO}<0.3$) a mixture of isolated CO and CO adsorbed in islands occurs. The

frequency of the CO stretch in the islands is greater than that of the isolated species because of dipole-dipole coupling between neighbouring CO molecules.

As discussed in section 1.2, the doublet structure has been interpreted as being due to the formation of islands of CO together with the existence of singleton CO molecules exhibiting lower C-O stretch frequencies at low coverages. This implies attractive intermolecular forces especially at low coverages in order to form the island species.

In contrast, the results presented here demonstrate that island formation with equilibrium with singleton CO molecules to produce a doublet does not occur, since symmetric absorption bands with a constant FWHM are present over the whole coverage range. It is also interesting to note that the authors of the previous study comment that that their criterion for a clean surface was the formation of a satisfactory TPD spectrum and that they were unable to verify the existence of a p1g1 overlayer on the crystal during RAIRS experiments because LEED facilities were not available. Thus only one of the first three of the cleanliness criteria discussed in section 3.9 was fulfilled. Experience with the platinum crystal used in these experiments suggests that it is the least sensitive criterion for surface

cleanliness and order.

Recent studies of CO adsorbed at vicinal Pt(111) surfaces [90,91] have indicated that CO adsorption at step or other defect sites causes a lowering of the C-O stretching frequency by several wavenumbers and that CO preferentially adsorbs at such sites. This would provide an alternative explanation to the appearance of the doublet species, if the platinum crystal used in the earlier study had a significant concentration of surface defects.

4.7 Coverage Dependent Frequency Shift

In Figure 4.7.1 the central frequency of the single RAIRS absorption band is plotted against coverage of CO. The frequency of the band shifts continuously upwards in a linear relationship with coverage. The extrapolated frequency at the zero coverage level is 2085 cm^{-1}. This is interpreted as the frequency of an isolated CO molecule adsorbed on the Pt(110)-(1 x 2) surface.

The continuous shift in the CO stretching frequency with increasing coverage for CO adsorbed on metals has been observed for both metal particles on supporting materials, such as silica [92], and on well characterised single crystal metal surfaces, including platinum [93]. The nature of this increase in the

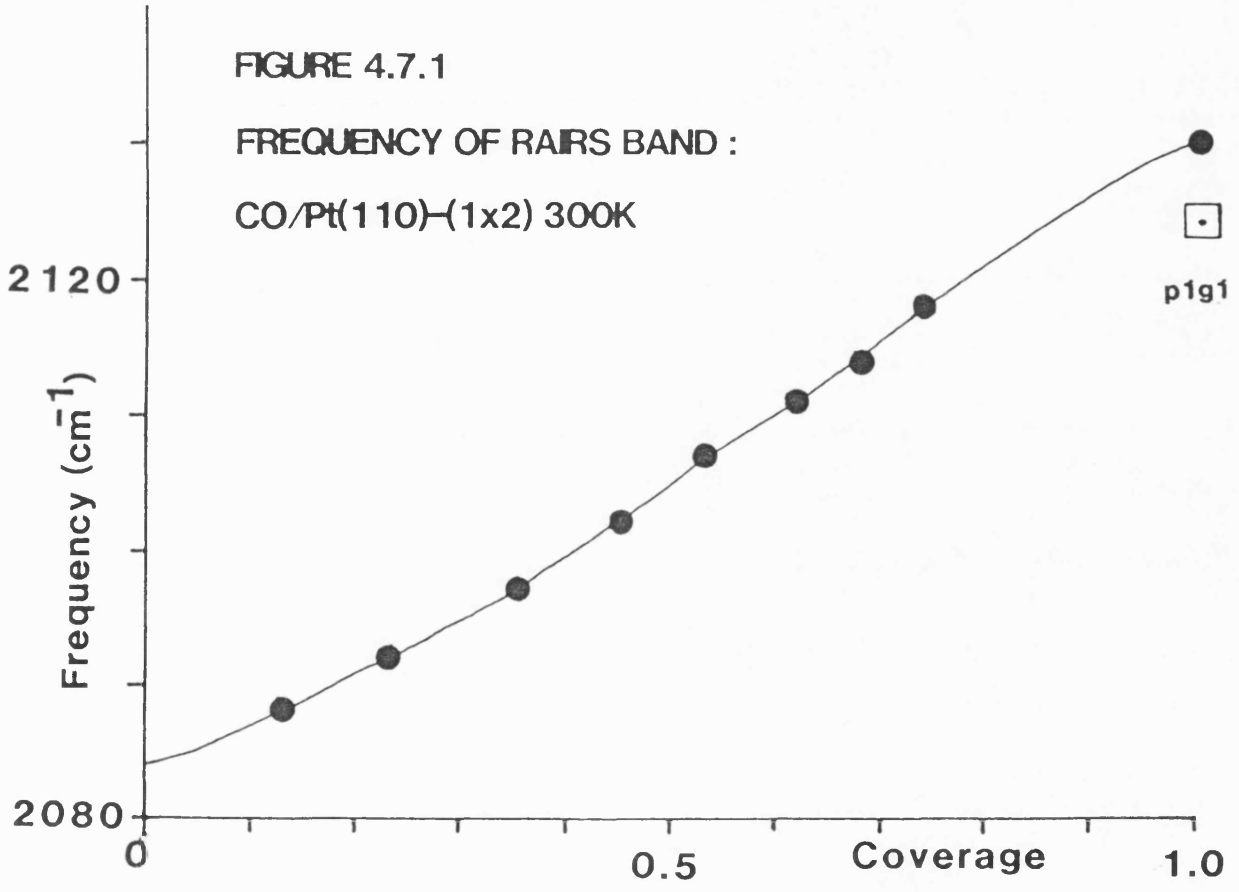
FIGURE 4.7.1
FREQUENCY OF RAIRS BAND :
CO/Pt(110)-(1x2) 300K
2120
2080
Frequency (cm-1)
0
0.5
Coverage
1.0
p1g1

vibrational frequency of the adsorbed species with increasing coverage has been described by several models.

Hammaker, Eischens and Francis [94] have suggested that the upward frequency shift is due to the interaction between neighbouring electrical dipolar oscillators, modifying the electric field experienced by each adsorbed molecule. This model was extended by Mahan and Lucas [95] to include interactions between a dipole and the image dipoles of nearby adsorbed molecules. They also considered the dielectric effect of the adsorbed layer, which tends to screen the electric fields experienced by the molecules. This is known as depolarisation. The expression which they derived for the frequency shift is:

$$(\nu_i/\nu_o)^2 = 1 + \Theta a_\nu S/(1+\Theta a_E S) \qquad (4.1)$$

where ν_i is the shifted frequency at coverage Θ, ν_o is the singleton frequency of the oscillator (the frequency in the zero-coverage limit). S is the dipole sum, containing contributions from both the direct dipole-dipole interactions and the dipole-image-dipole interactions and is dependent on the geometrical arrangement of the adsorbate. The parameters a_ν and a_E are the vibrational and electronic polarisabilities

of the CO molecule respectively.

Using this equation, and assuming gas phase values for the polarisabilities, Mahan and Lucas concluded that the dipole-dipole interaction was too small to account for all of the coverage dependent shift [95].

An extension to the dipole coupling theory was made by Scheffler [96] who also included the effect on the dipole oscillators of their own image charge and by Persson and Ryberg [97] who used the coherent potential approximation to derive essentially the same relationship between frequency shift and coverage. A similar approach has also been made by Ibach and Mills [98] who pointed out that gas phase values for the polarisabilities were inappropriate in the adsorbed state and used empirical values from experimental evidence to model the frequency shifts.

The influence of dipole-dipole interactions on intensity of absorption bands has also been reported [97,98] and will be discussed in detail later.

Another model which would account for the upward frequency shift with increasing coverage is that proposed by Moskovits and Hulse [99], which is that of vibrational coupling between adsorbed molecules due to through-metal electron interactions.

A further mechanism which may contribute to the

frequency shift is the chemical shift. This is due to the perturbation of the occupancy of the CO-metal bonding orbitals. Using the simple Blyholder model of CO-metal bonding [23], where backbonding to the $2\pi^*$ antibonding orbitals occurs, the effect of increasing the coverage is to increase competition for back-donation of electrons from the metal. As coverage increases, there is less back-donation leading to a strengthening of the C-O bond and and consequently an increase in the C-O stretching frequency. The Blyholder bonding model is inadequate to describe chemical shifts which are downwards in frequency, which have been measured on copper surfaces although more sophisticated bonding schemes have been proposed to describe this phenomena [100].

An upward frequency shift may also be induced by the direct interaction between an applied electric field and the dipole moment of the adsorbed molecules [45,101]. This will also be discussed in more detail later in relation to the co-adsorption of CO with potassium on Pt(110)-(1 x 2).

4.8 Separation of Dipole-Dipole and Chemical Shifts

In their derivation for dipole-dipole coupling interactions, Hammaker and co-workers [94] have pointed out that vibrational coupling between adsorbed molecules is only significant where the oscillation frequencies are similar. In contrast the chemical or static effects will not be affected by a difference in frequencies as they depend on the bonding of the adsorbates or the electrostatic fields. By using adsorbates with different vibrational frequencies but of identical chemical nature, a decoupling of the dipole-dipole induced shift from the chemical shift occurs. This method was demonstrated by Crossley and King [87,88] who used mixtures of ^{12}CO and ^{13}CO in investigating the origin of shifts in CO stretching frequency when adsorbed upon the Pt(111) surface.

The vibrational spectra of varying mixtures of the two isotopes are recorded at various coverages. The vibrational frequencies of the two bands are than plotted against isotopic composition at a constant coverage. Extrapolation of the vibrational frequency of one isotope to its dilution limit (a composition of 0%), leads to the vibrational frequency of a single molecule of that isotope totally surrounded by molecules of the

other isotope. Under these conditions there is complete vibrational decoupling. However any chemical shift induced by the surrounding molecules will still be present.

Hence by determination of the singleton oscillation frequency for a molecule of the isotope (the zero coverage limit for the pure isotope), the chemical (or static) contribution to the shift may be calculated. The difference between this frequency and the vibrational frequency of the molecule in the pure isotope case gives the dipole-dipole contribution.

This process can then be repeated at varying coverages to obtain the relative contributions of chemical (or static) and dipole-dipole shifts over the whole coverage range.

The RAIRS spectra of the pure ^{13}CO are shown in Figure 4.8.1. There is a reduction of ≈ 50 cm^{-1} in the C-O stretching frequency compared to that of ^{12}CO.

A series of RAIRS spectra measured following adsorption of mixtures of ^{12}CO and ^{13}CO in varying proportions (at 300K) are shown in Figures 4.8.2 to 4.8.6. Note extensive intensity borrowing from the lower to the higher absorption band, which may suppress the lower frequency band completely, even though the two isotopes are present in similar proportions.

FIGURE 4.8.1 PURE 13-CO

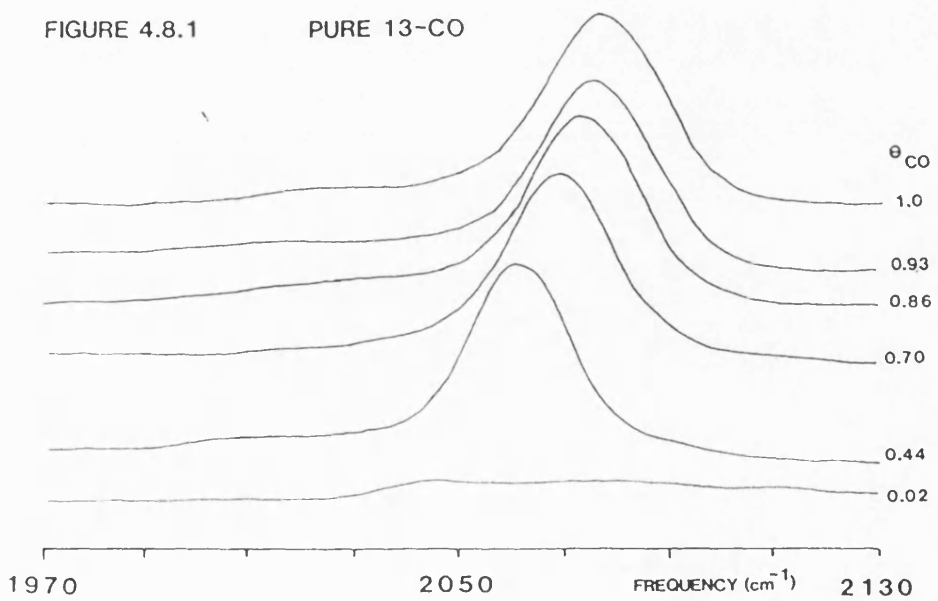

FIGURE 4.8.2 ISOTOPE MIXTURE

55% 13-CO 45% 12-CO

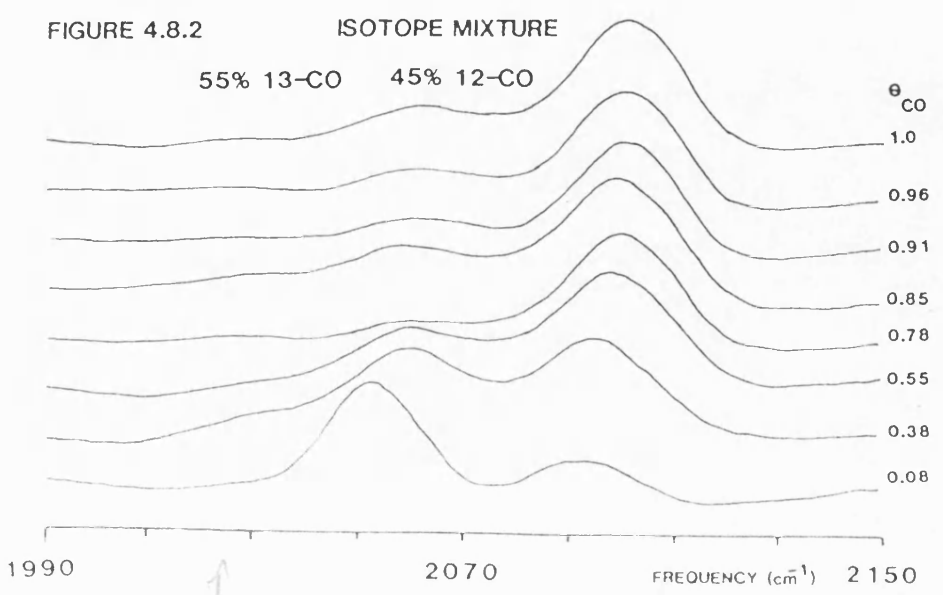

FIGURE 4.8.3 ISOTOPE MIXTURE

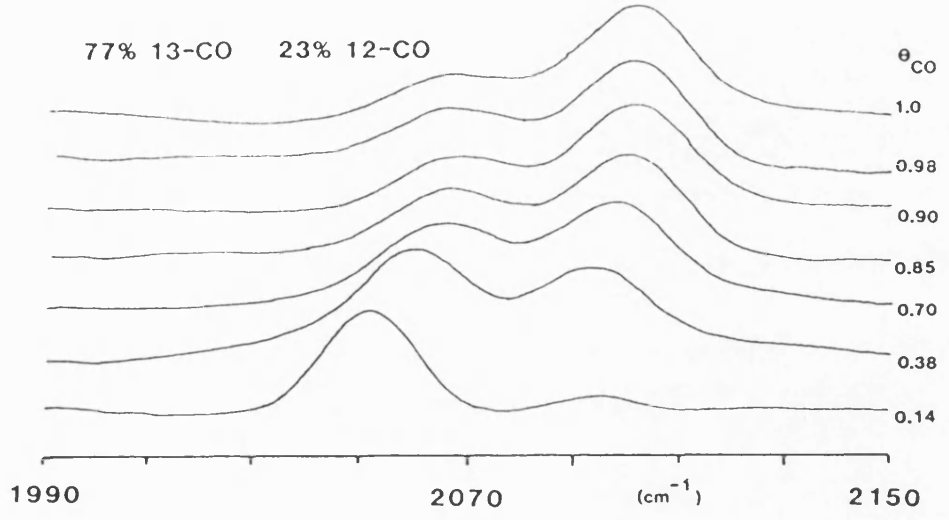

FIGURE 4.8.4

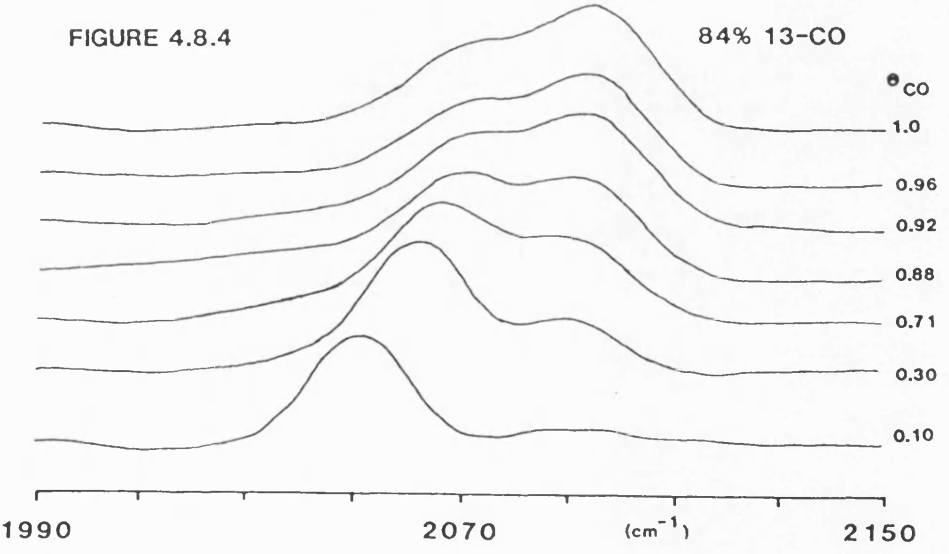

FIGURE 4.8.5 ISOTOPE MIXTURE

40% 13-CO 60% 12-CO

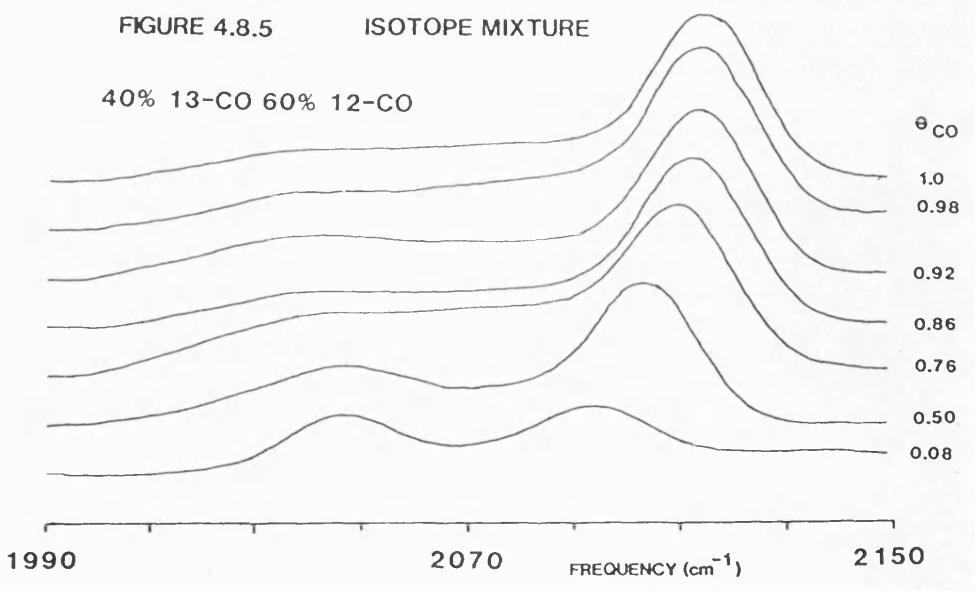

FIGURE 4.8.6

70% 13-CO 30% 12-CO

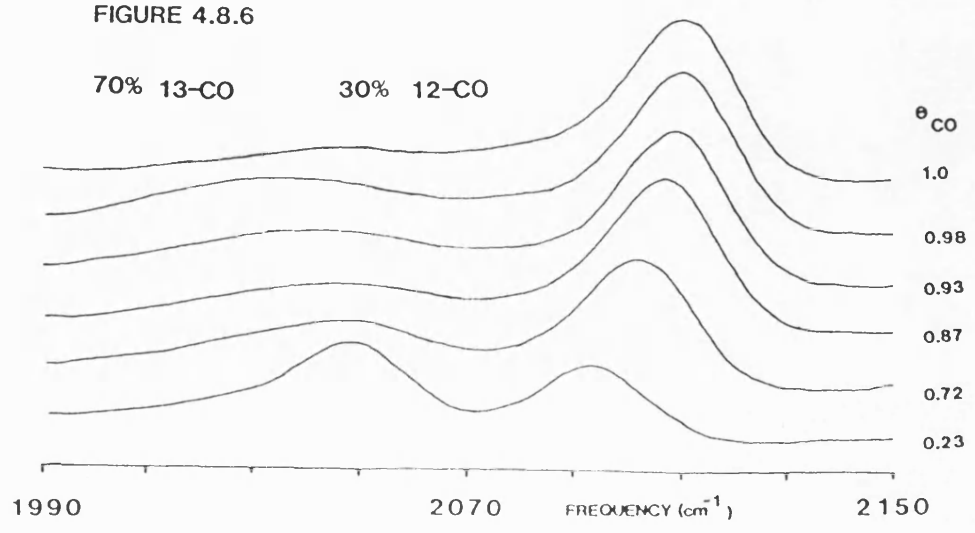

Treating the results of these experiments as described above, the frequency shifts due to dipole-dipole interactions and that due to chemical (or static) effects as a function of coverage are shown in Figure 4.8.7. Within the limits of experimental error, there is no contribution to the coverage dependent shift from chemical (or static) effects; dipole-dipole interactions are wholly responsible for the shift. Similar results have been obtained for the CO/Pt(100) [87] system and for CO/Pt(111) [88], where total dipole-dipole shifts of 35 cm^{-1} are observed. This indicates that the presence of chemical shift is ruled by the chemical nature of the adsorption system but not the adsorption geometry of the surface. However a recent RAIRS study using Fourier-Transform techniques has indicated that a chemical shift of -8 cm^{-1} is induced for CO/Pt(111), with a dipole-dipole shift of +20 cm^{-1} [102] and the explanation for this discrepancy from the present work and that previously reported is that the surfaces exhibiting no chemical shift are dominated by adsorption at defect sites. The balance of experimental evidence suggests that there is no chemical shift present on any platinum surface at any coverage of CO.

FIGURE 4.8.7

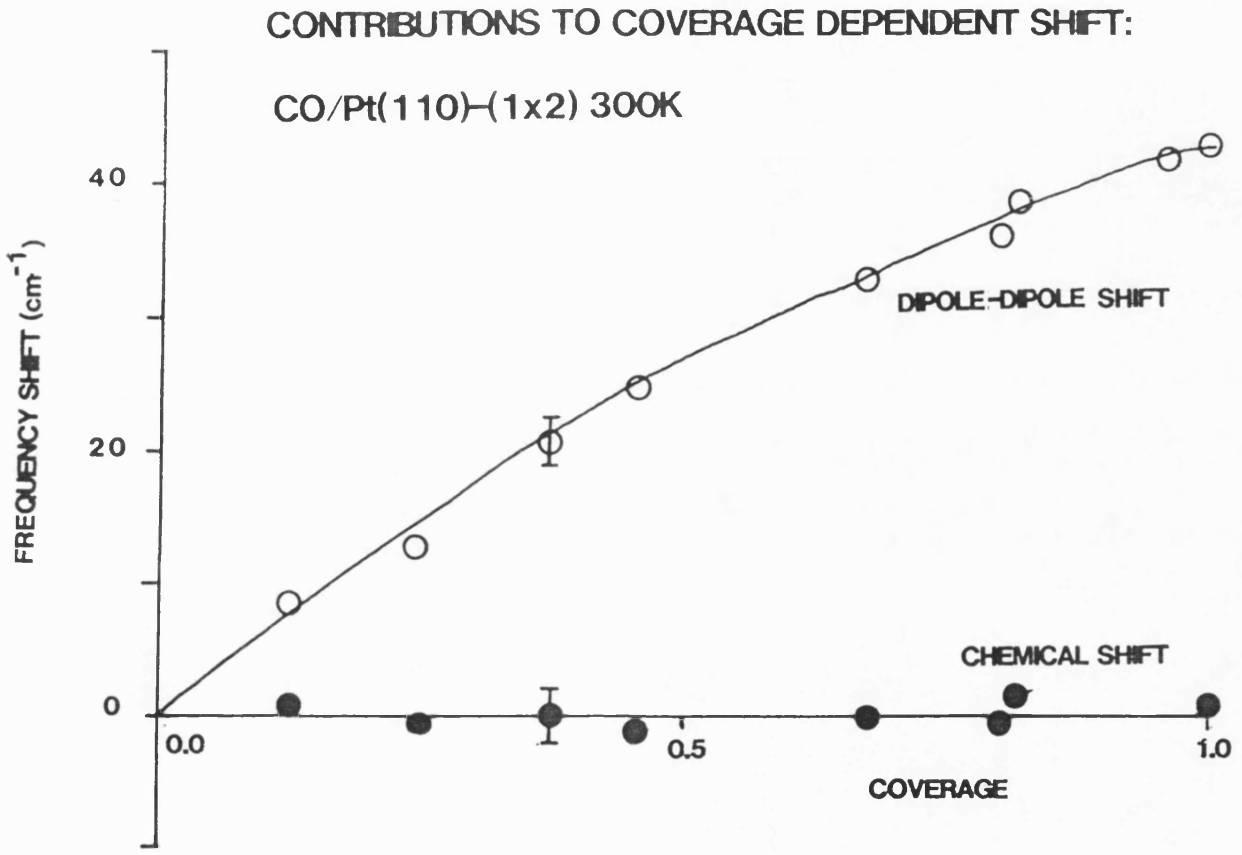
CONTRIBUTIONS TO COVERAGE DEPENDENT SHIFT:
CO/Pt(110)-(1x2) 300K
FREQUENCY SHIFT (cm-1)
40
20
0
0.0
0.5
1.0
COVERAGE
DIPOLE-DIPOLE SHIFT
CHEMICAL SHIFT

4.9 Absorption Intensity Variation with Coverage

The variation of integrated intensity of the single IR absorption band with coverage of CO is plotted in Figure 4.9.1. The value of the integrated intensity was calculated by numerical evaluation of the area beneath the absorption peak. The integrated intensity is linear with coverage in the range $0.0<\theta_{CO}<0.5$. At higher coverages the value of the integrated intensity declines slightly. Thus even though more CO is being adsorbed at the surface, there is a decrease in the amount of infra-red radiation being absorbed. This unusual variation of integrated intensity with coverage has also been observed for the case of CO adsorbed on Ru(001) at temperatures between 80K and 300K [103]. This adsorption system will be discussed briefly in order to highlight certain other similarities with the CO/Pt(110)-(1 x 2) system.

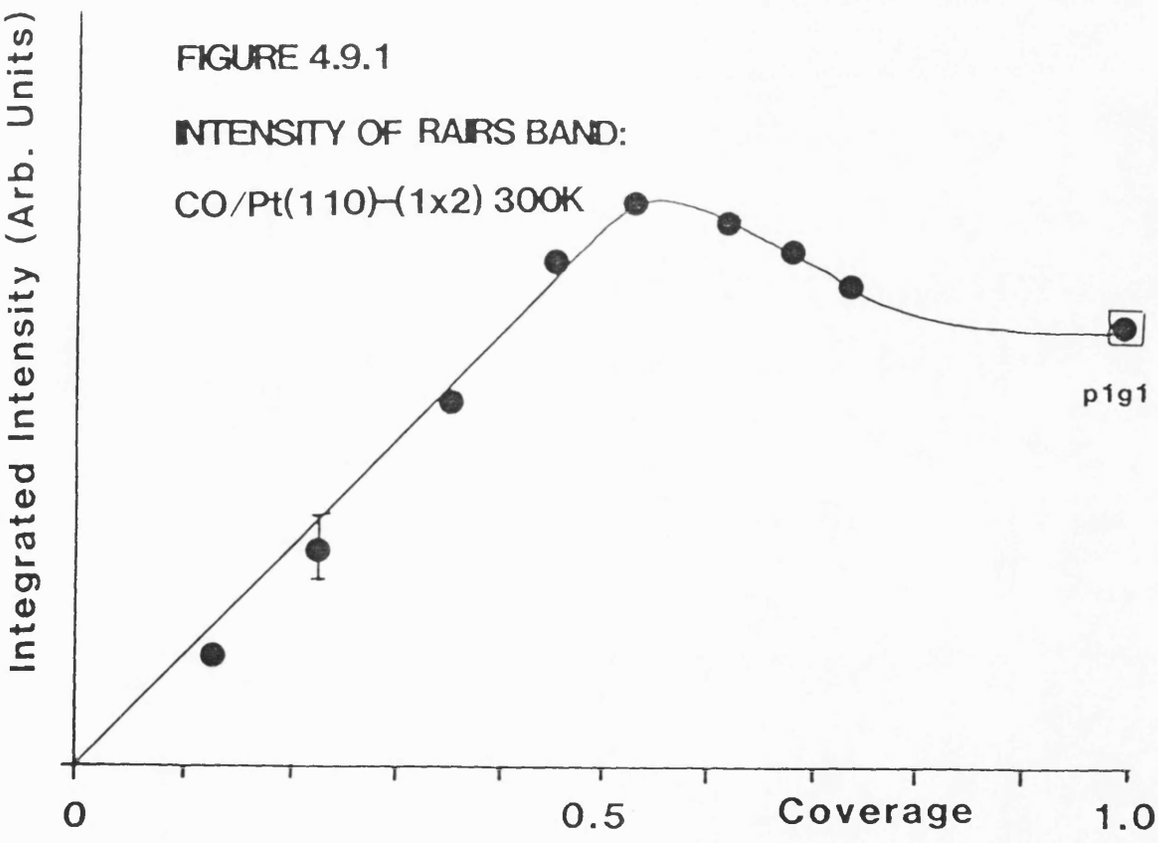
FIGURE 4.9.1
INTENSITY OF RAIRS BAND:
CO/Pt(110)-(1x2) 300K
Integrated Intensity (Arb. Units)
p1g1
0
0.5
Coverage
1.0

4.10 The CO/Ru(001) adsorption system

The TPD spectra for varying coverages of CO adsorbed on Ru(001) at 300K have been measured [104]. A single desorption peak at constant desorption temperature is observed for all coverages of $\theta_{CO}<0.33$, with a low temperature feature appearing at higher coverages. The saturation coverage of CO on the Ru(001) surface has been determined as $\theta_{CO}=0.68$ [105].

The following LEED patterns are observed: at a coverage of $\theta_{CO}=0.33$ and at 300K, a $(\sqrt{3} \times \sqrt{3})R30°$ pattern is visible, whilst at higher coverages in the range $0.51<\theta_{CO}<0.58$ and at 200K, a $(2\sqrt{3} \times 2\sqrt{3})R30°$ pattern is observed [105,106]. Vibrational spectroscopy studies using EELS [107] and RAIRS [103] show a single absorption band at all coverages of CO, in the range 1990-2070 cm^{-1}. This is characteristic of CO bonded in on-top adsorption sites. The integrated intensity of the RAIRS absorption band reaches a maximum at $\theta_{CO}=0.33$ and declines thereafter [103].

4.11 Modelling Absorption Intensity versus Coverage

The dipole-dipole interaction model discussed in in section 4.7 has also been used to describe the intensity of an infra-red absorption band as a function

of coverage. Both Ibach and Mills [98] and Persson and Ryberg [97] have used this approach to model the characteristic properties of the CO/Ru(001) adsorption system. Using the latter authors formalism:

$$(v_i/v_o)^2 = 1 + k_v\theta/(1+k_e\theta) \qquad (4.2)$$

and:

$$I_{int} \approx k_v\theta/(1+k_e\theta)^2 \qquad (4.3)$$

where k_e and k_v are constants containing the dipole sum and the electronic and vibrational polarisabilities of CO respectively (see section 4.7)

The value of I_{int} is dependent upon the value of the electronic polarisability contained in $k_e\theta$ and this term becomes more significant at high coverages. Given sufficiently large values for the value of $k_e\theta$, the value of I_{int} may reach a maximum and decline thereafter.

On the assumption that the intensity reaches a maximum turning point at a critical coverage of θ_M, then differentiation of equation (4.3) leads to the solution:

$$k_e = \theta_M^{-1} \qquad (4.4)$$

and by substitution into equation (4.2):

$$I_{int} \approx \theta/(1 + \theta/\theta_M)^2 \qquad (4.5)$$

We can now model the intensity profiles at varying coverages by assuming a value for θ_M. Using the experimentally determined value of θ_M=0.5 for the CO/Pt(110)-(1 x 2) adsorption system and substituting into equation (4.5), the normalised integrated intensity can be calculated. The results are displayed in Figure 4.11.1 and compared to the experimentally determined values. The theoretical prediction differs significantly in that the intensity is non-linear up to the critical coverage of θ_M=0.5 and then declines slowly. The experimentally determined intensity declines much more rapidly after the critical coverage.

The analogous situation for CO/Ru(001), with the maximum coverage at θ_{CO}=0.33 is plotted in Figure 4.11.2 and compared to the experimental results. Here the agreement with the intensity of the absorption band is rather better, as has been reported previously [97,98].

FIGURE 4.11.1

CO/Pt(110)-(1x2) RAIRS BAND INTENSITY

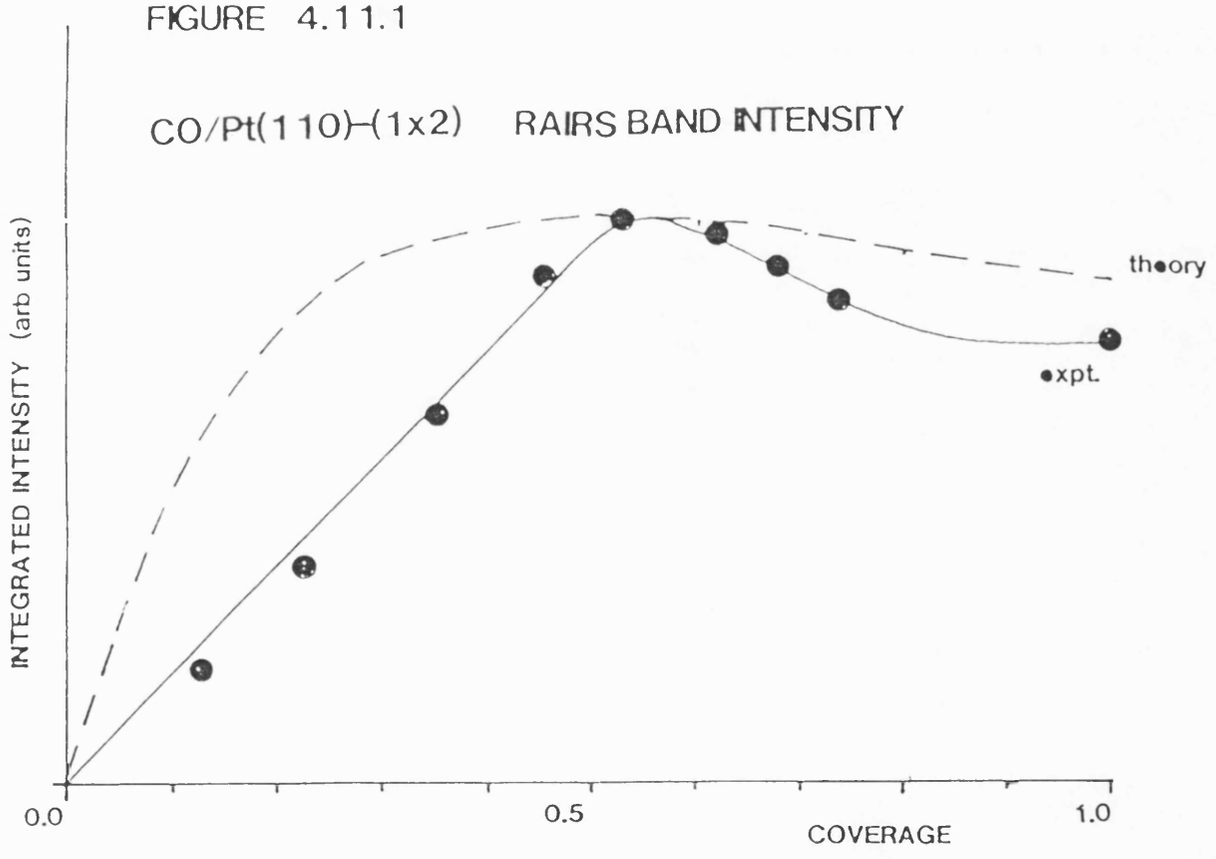

FIGURE 4.11.2

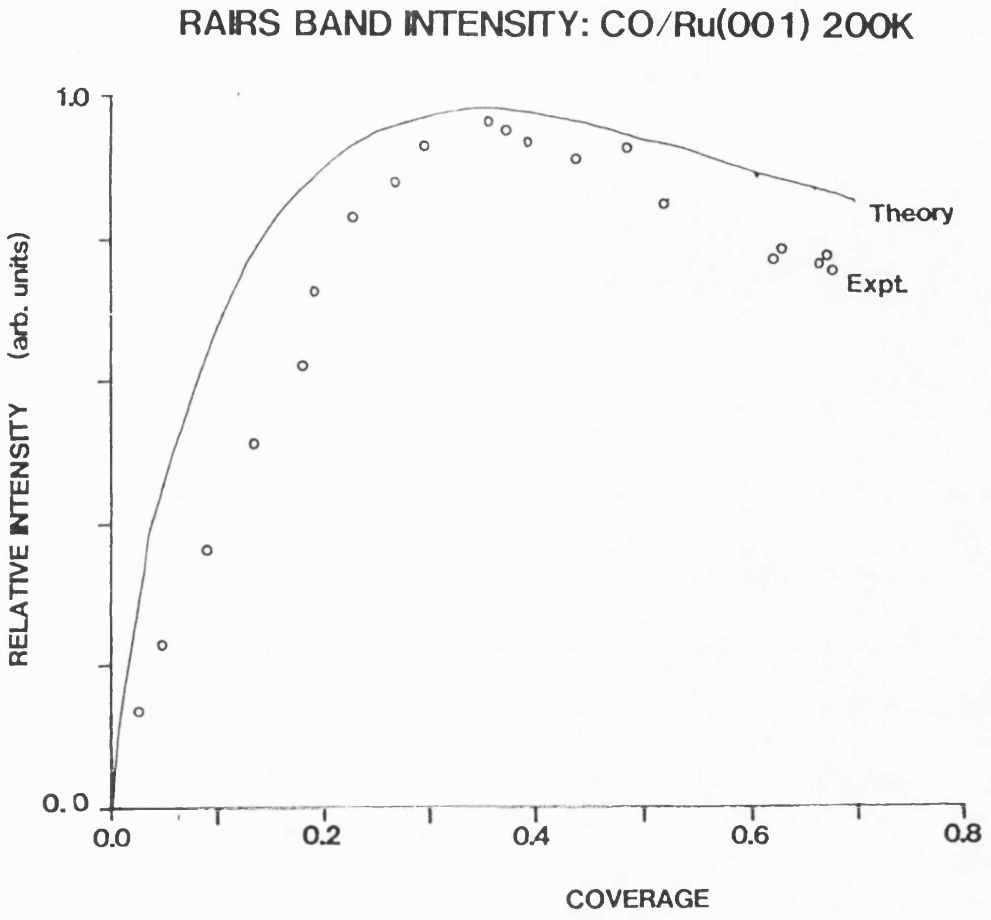
RAIRS BAND INTENSITY: CO/Ru(001) 200K
1.0
0.0
RELATIVE INTENSITY (arb. units)
Theory
Expt.
0.0
0.2
0.4
0.6
0.8
COVERAGE

It is also possible to predict the coverage dependent frequency shift from equation (4.2) using the value for k_* determined from the intensity maximum:

$$(\nu_i/\nu_o)^2 = 1 + k_\nu\theta/(1 + \theta/\theta_M) \qquad (4.6)$$

The values of ν_o can be determined from experimental results and by substituting the value of ν_i at the critical coverage θ_M, equation (4.6) may be solved for k_ν.

For the CO/Pt(110)-(1 x 2) system, the value of ν_o can be determined by extrapolation from Figure 4.7.1 and is 2085 cm^{-1}. The value of ν_i at θ_{CO}=0.5 is 2105 cm^{-1}. The predicted frequencies from the model are plotted in Figure 4.11.3 and are compared with the experimental values from Figure 4.7.1. The dipole-dipole induced shift predicted by the theory is too small at higher coverages and is non-linear, in contrast to the large shifts found experimentally and the linearity of the frequency shift with coverage.

A similar calculation for the CO/Ru(001) system with values of ν_o of 1984 cm^{-1} and ν_i (θ_{CO}=0.33) as 2021.5 cm^{-1}, [104] is plotted in Figure 4.11.4. As in the case of the CO/Pt(110) system, the predicted dipole-dipole shifts are too small in comparison with the experimental results.

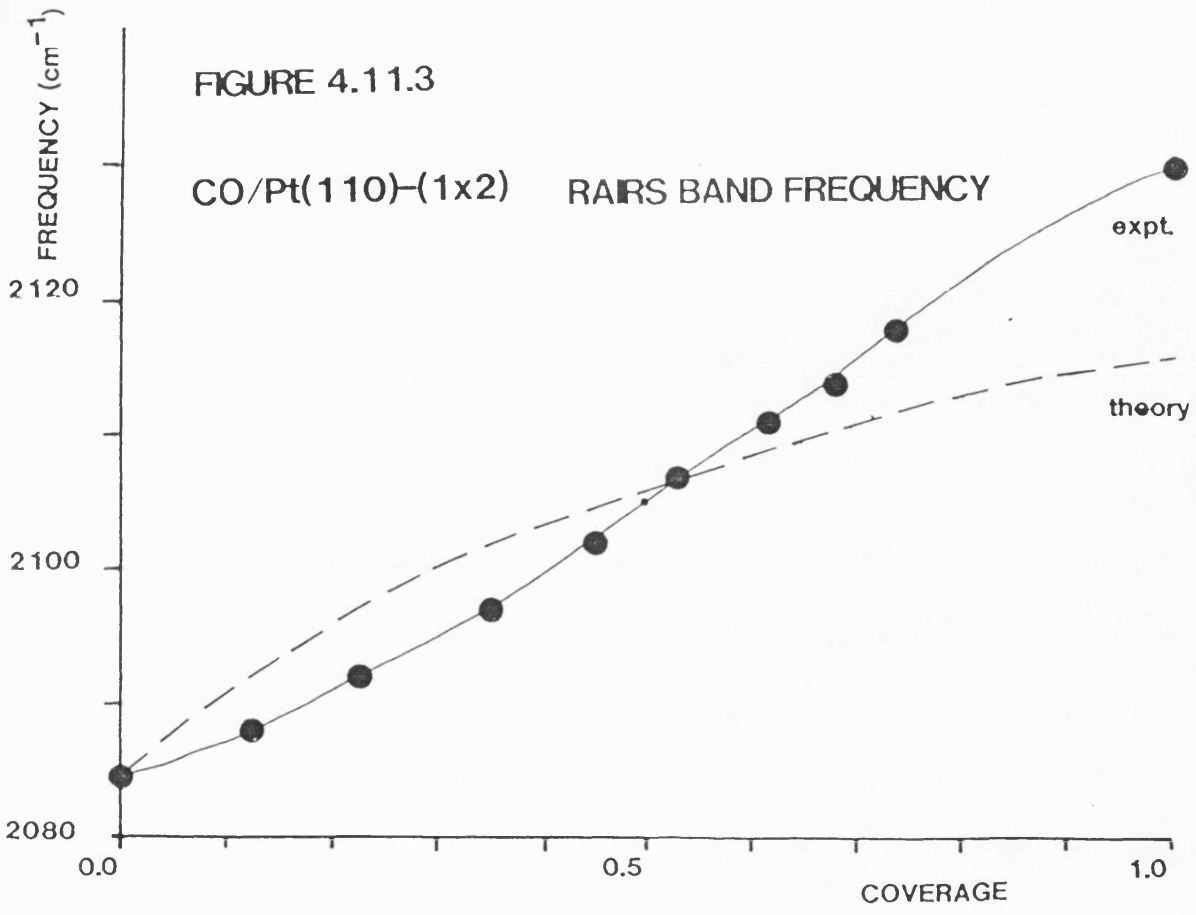
FIGURE 4.11.3
CO/Pt(110)-(1x2) RAIRS BAND FREQUENCY
FREQUENCY (cm^{-1})
2120
2100
2080
0.0
0.5
1.0
COVERAGE
expt.
theory

FIGURE 4.11.4

COVERAGE DEPENDENT FREQUENCY SHIFT CO/Ru(001)

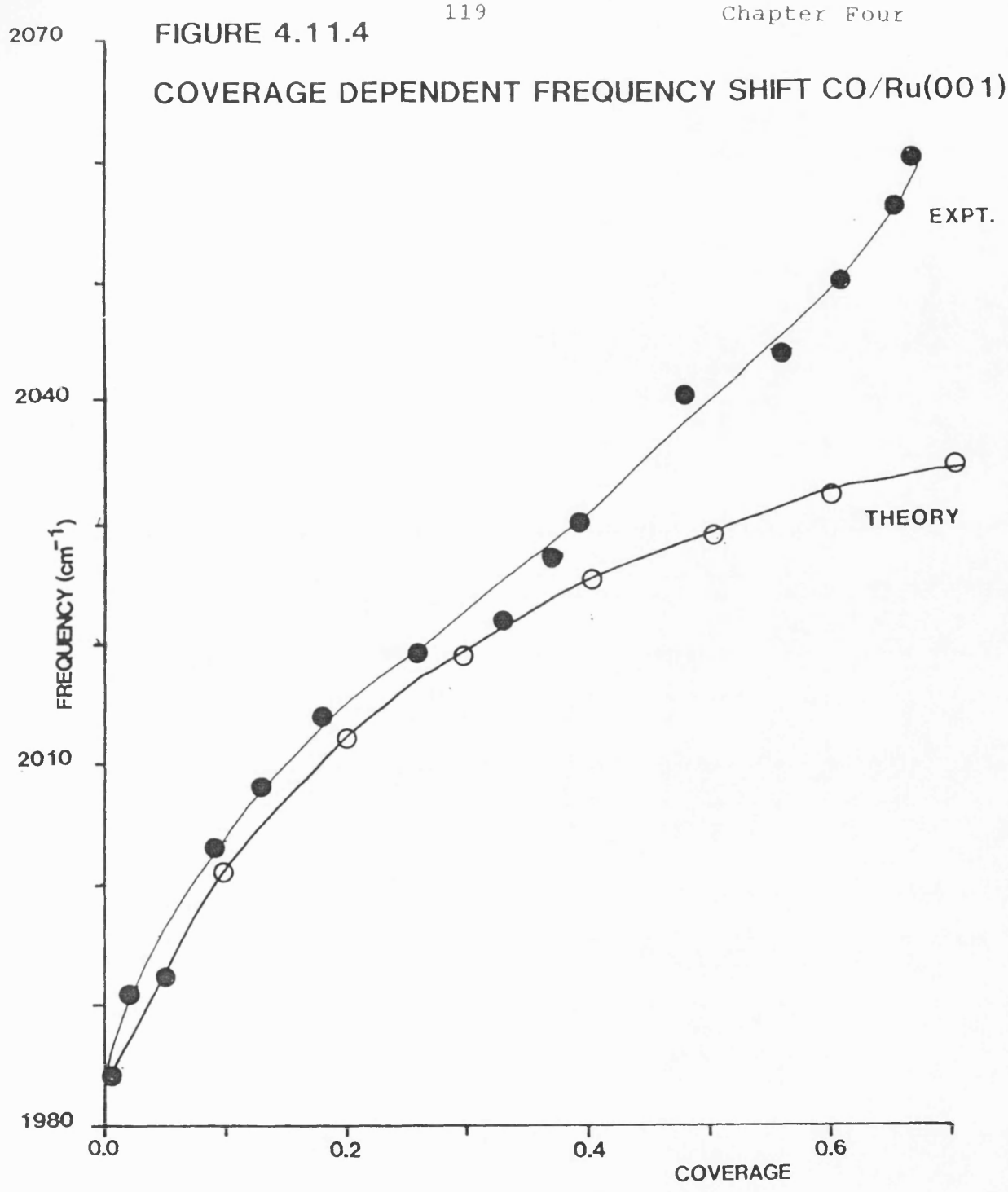

This treatment of dipole-dipole interactions requires some experimental data, primarily a knowledge of the coverage dependent frequency shift and the components of that shift, dipole-dipole interactions or chemical (and static effects). For Pt(110) this has been established by the present work as wholly due to dipole-dipole interactions. There is no data available for isotope mixture experiments on CO/Ru(001), the very large coverage dependent shift of 74 cm^{-1} [103] suggests that there may be a chemical (or static) contribution as well as a dipole-dipole contribution.

From the failure of the dipole-dipole interaction model to calculate the coverage dependent frequency shift correctly, it may be concluded that the unusual intensity versus coverage function determined by experiment cannot be modelled by the relatively simple depolarisation theory. Possible modifications to the depolarisation model including coverage dependent values for the polarisabilities have recently been discussed by Ueba [108].

4.12 The Molecular tilting model

As the depolarisation effects have been shown to be insufficient to cause the abrupt change in intensity at a coverage of θ_{CO}=0.5 for CO/Pt(110)-(1 x 2), another

mechanism must now be considered.

The maximum in integrated intensity for both CO/Pt(110)-(1 x 2) and CO/Ru(100) absorption systems is reached at the coverage where the low temperature desorption feature appears in the CO TPD spectra. These features have been attributed to the onset of strong lateral repulsion forces between CO molecules [9,15,109]. For the CO/Pt(110)-(1 x 2) system an alternative desorption-reconstruction process has also been proposed [12], in which the high temperature feature is due to desorption from the surface followed by the reconstruction of the surface to (1 x 2). The low temperature peak is due to desorption from the (1 x 1) surface without reconstruction.

From the results obtained in this study, it is suggested that there are strong lateral interactions between the CO molecules on the surface, leading to the characteristic twin peaks in the TPD spectra. The onset of these repulsive interactions between the CO molecules causes the tilting of the C-O molecular axis away from the surface normal [109]. This reduces the vertical component of the dynamic dipole moment and hence reduces the infra-red absorption cross section of the adsorbed CO molecules. If the cross-section is reduced sufficiently, the integrated intensity will fall with

increasing coverage.

The existence of tilted CO on the Pt(110) surface has already been demonstrated, from ARUPS results [13,18] and from the appearance of the (2 x 1)p1g1 LEED structure under certain absorption conditions [1,2]. The tilting of CO in this case leads to the formation of glide plane symmetry elements and hence missing reflexes in the diffraction pattern [72,73]. A similar LEED structure would not be apparent for Ru(001) since the formation of tilted overlayers does not necessarily lead to the formation of glide plane symmetry elements on the hexagonal close packed surface.

There is also a considerable body of evidence that molecular tilting occurs on another similar adsorption system, CO/Ni(110). Electron stimulated desorption ion angular distribution (ESDIAD) studies have indicated that CO molecules tilt at 19 degrees to the surface normal [110]. In addition Lee and co-workers [111] have concluded, on the basis of ESDIAD, metastable quenching spectroscopy and TPD measurements that CO undergoes a reversible transition between an upright absorption geometry and a tilted phase at the critical coverage of θ_{CO}=0.65. Of particular relevance to this study is the appearance of a low temperature TPD feature at the critical coverage. This is also attributed to strong

lateral repulsion between CO molecules.

Ban and co-workers [112] have carried out calculations using extended Huckel molecular orbital theory, for CO adsorption on the (110) faces of nickel and platinum clusters. They conclude that CO molecules adsorbed along the ridges in the [110] direction alternately tilt in opposite directions to each other in order to relieve repulsive interactions. This tilting is similar to the model proposed to account for the appearance of the (2 x 1) p1g1 LEED structure on Pt(110). They also point out that the distances between adjacent CO molecules on the (110) surface of transition metals are considerably less than those found between CO ligands in stable organometallic complexes, or in three-dimensional crystals of CO or CO_2. Intermolecular interactions would be expected to be greater in the close packed layers found on the metal surfaces.

4.13 Molecular tilting model for CO/Pt(110)-(1 x 2)

The proposed model for CO adsorption at 300K on the Pt(110)-(1 x 2) surface [109] is that up to coverages of $\Theta_{CO}=0.5$, the CO occupies on-top adsorption sites and the C-O bond axis is oriented parallel to the surface normal. The integrated intensity of the RAIRS spectra is linear with coverage up to the critical coverage. At

a coverage of $\theta_{CO}=0.5$, every other adsorption site in the close packed rows of the surface may be considered to be occupied and repulsive interactions at such distances may be considered to be small. At higher coverages, $\theta_{CO}>0.5$, further CO adsorption requires the filling of adjacent adsorption sites in the close packed rows. The repulsive interactions between the close packed CO molecule now cause the appearance of a low temperature desorption feature and also the tilting of the C-O molecular axis away from the surface normal. The tilting effect is non-linear with coverage; at intermediate coverages since adsorption of one extra molecule of CO in a site between two CO molecules adsorbed in the upright geometry causes all three to tilt, so that one extra molecule at the surface causes a reduction of surface normal dynamic dipole moment in three CO molecules. The total infra-red cross-section decreases and there is an abrupt change in the integrated intensity of the absorption band at the critical and greater coverages.

It should be noted that this model is at odds with the ARUPS results of King and co-workers [12,13], which indicate the appearance of the tilted CO molecules in islands at coverages $\theta_{CO}=0.2$. As the evidence here does not suggest the formation of islands of CO, it is

difficult to explain why CO should tilt at such low coverages when intermolecular forces should be minimal. The differences between the RAIRS results obtained in this and the previous study of this adsorption system have already been discussed in section 4.6.

4.14 Molecular tilting model for CO/Ru(001)

Having developed an adsorption model for CO/Pt(110)-(1 x 2) based on molecular tilting at a critical coverage, the next step is to develop an analogous model for the CO/Ru(001) system at high coverages of CO.

Williams and Weinberg have suggested a real space model [106] to account for the $(\sqrt{3}$ x $\sqrt{3})$R30° LEED pattern observed at coverages of θ_{CO}=0.33 and this is depicted in Figure 4.14.1. All CO molecules are adsorbed in on-top adsorption sites, in accord with the RAIRS results.

Real space models to account for the LEED pattern described as $(2\sqrt{3}$ x $2\sqrt{3})$R30° observed at higher CO coverages have also been proposed. One explanation of the LEED pattern is that the CO overlayer forms an expanded hexagonal packing arrangement [105,106] (see Figure 4.14.2). This is unsatisfactory since the layer is incommensurate with the ruthenium surface net and

FIGURE 4.14.1

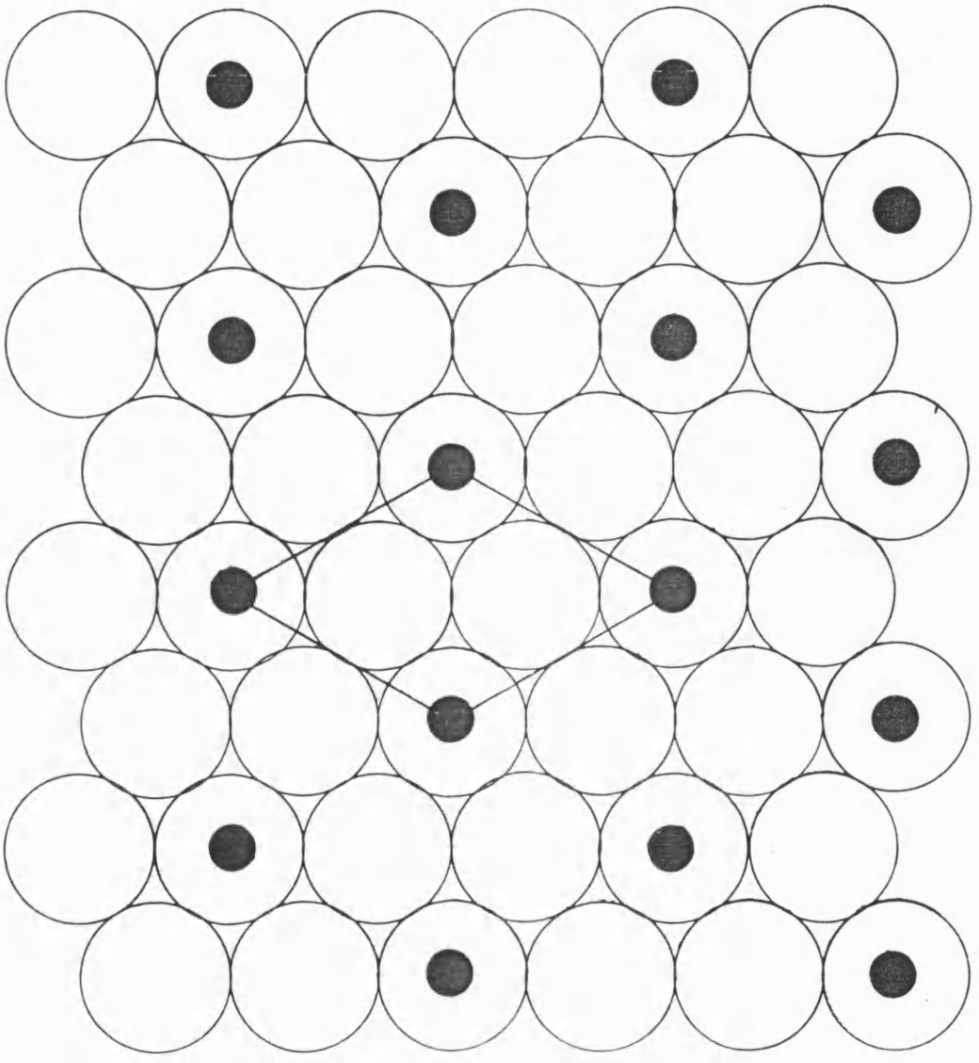

REAL SPACE MODEL FOR CO/Ru(001) ($\sqrt{3}$ x $\sqrt{3}$)R30

FIGURE 4.14.2

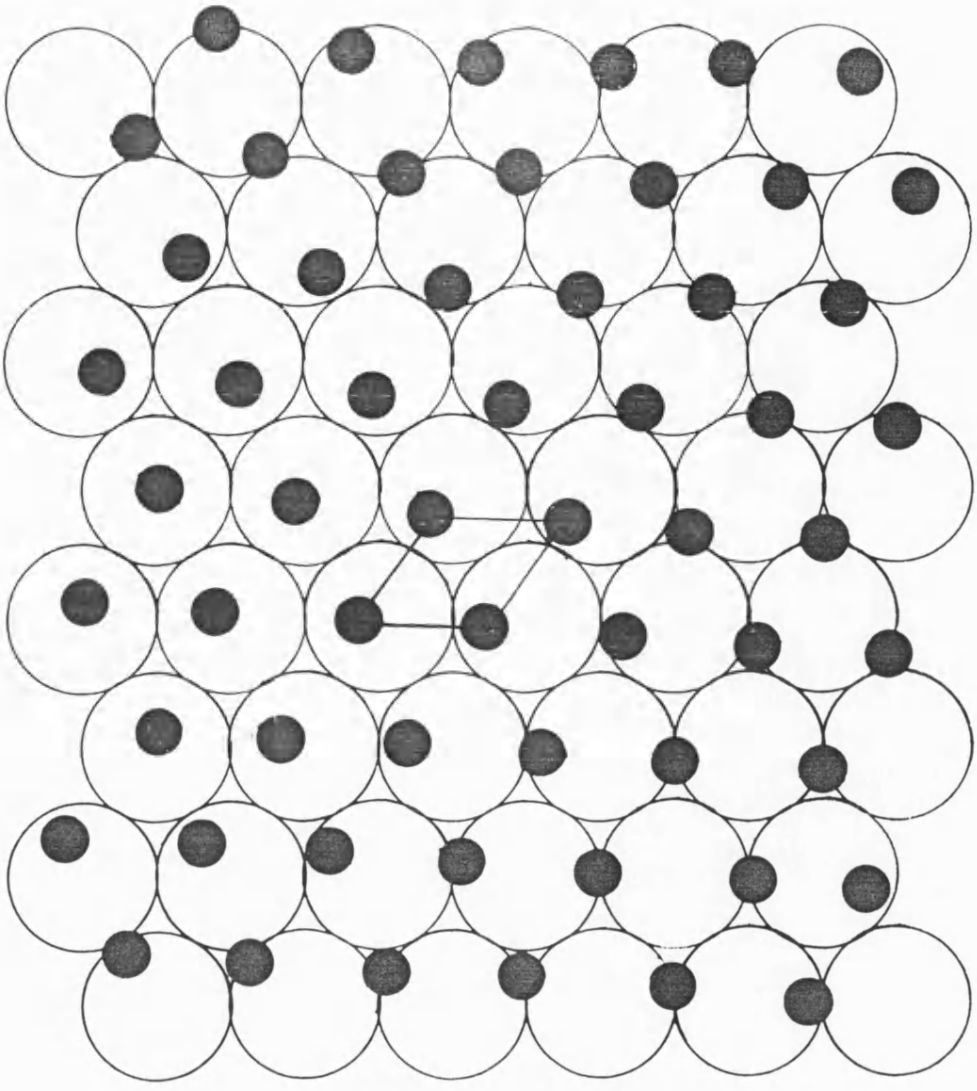

EXPANDED HCP STRUCTURE FOR CO/Ru(001) (2$\sqrt{3}$ x 2$\sqrt{3}$)R30

hence some of the CO molecules must be adsorbed at non-linear sites, in contradiction to the RAIRS measurements, which indicate on-top bonding at all coverages. It has been proposed that re-hybridisation of metal orbitals at the ruthenium surface results in a homogeneous bonding environment for CO despite adsorption in non-linear sites [103].

Laser simulation of diffraction patterns by Biberian and Van Hove [113] has demonstrated that the LEED pattern which had previously been interpreted as $(2\sqrt{3} \times 2\sqrt{3})R30°$ may be due to a $(2\sqrt{3} \times \sqrt{3})R30°$ overlayer with three domains oriented at 120 degrees to each other. They have proposed a real space model with an appropriate unit cell to account for this structure (Figure 4.14.3). This model satisfies the LEED evidence and the RAIRS frequency evidence, as every CO is in an on-top site, but does not account for the intensity variation of the RAIRS absorption band with coverage. It also does not have a geometry related to that of the low coverage model (see Figure 4.14.1); a considerable re-organisation of the adsorbed layer would be required to produce this structure.

FIGURE 4.14.3

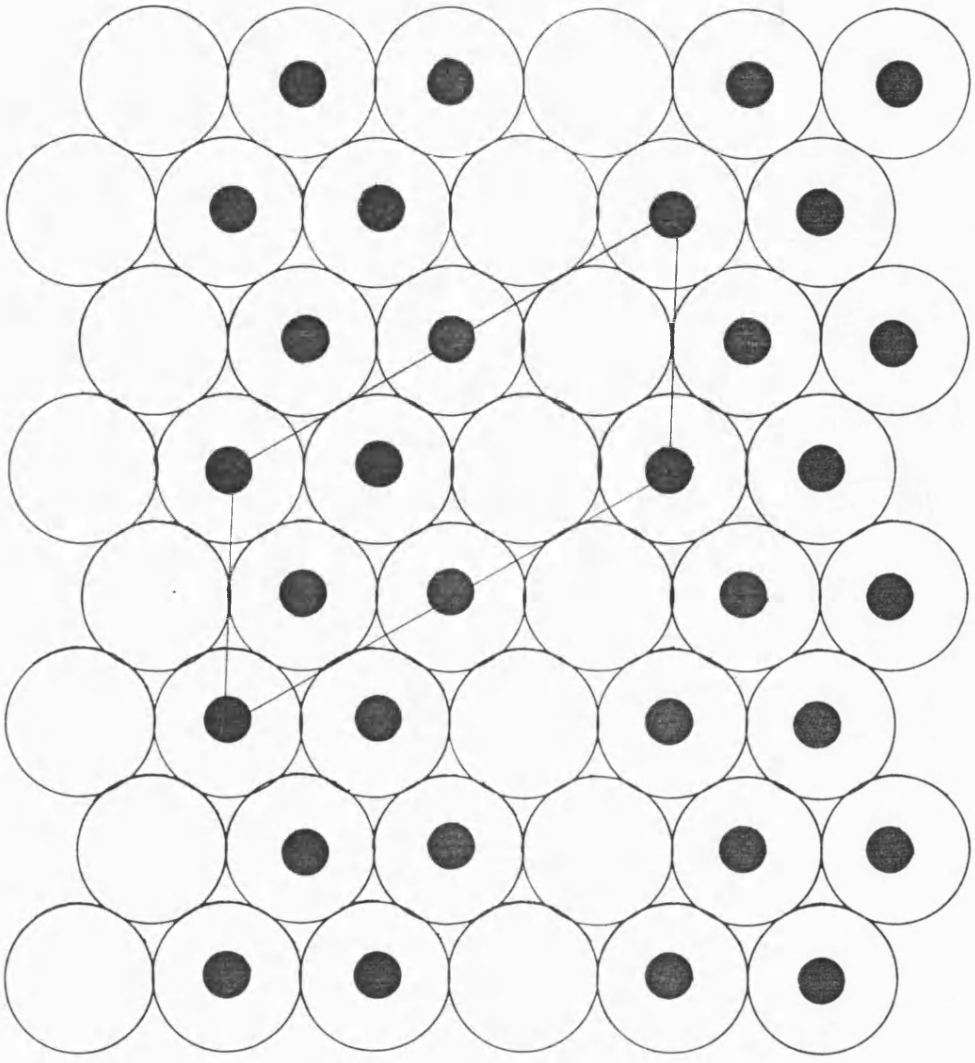

REAL SPACE MODEL FOR CO/Ru(001) ($2\sqrt{3}$ x $\sqrt{3}$)R30

From the experimental evidence and by analogy to the CO/Pt(110)-(1 x 1) adsorption model discussed previously, the following real space model, incorporating molecular tilting, to describe the adsorption of CO on Ru(001) at high coverages is now proposed [114]. The basis of this model is an overlayer which would normally exhibit the ($\sqrt{3}$ x $\sqrt{3}$)R30° LEED structure, except that the symmetry of the unit cell is broken by the tilting of the C-O molecular axis to produce the ($2\sqrt{3}$ x $\sqrt{3}$)R30° structure. Two equivalent overlayer structures which satisfy this model are depicted in Figure 4.14.4. Three domains of each structure are possible, oriented at 120 degrees to each other. These models satisfy the LEED and RAIRS evidence since all adsorption is in on-top sites and is based on the structure of the low coverage model (Figure 4.14.1) with further CO adsorption at random sites. A large re-organisation of the adlayer is not necessary.

The model of CO adsorption is now similar to that of Pt(110)-(1 x 2), the CO is adsorbed at on-top sites with the C-O molecular axis oriented along the surface normal up to coverages of θ_{CO}=0.33. Further adsorption leads to repulsive interactions between the CO molecules causing tilting away from the surface normal. The saturation coverage of the tilting model is θ_{CO}=0.66,

FIGURE 4.14.4

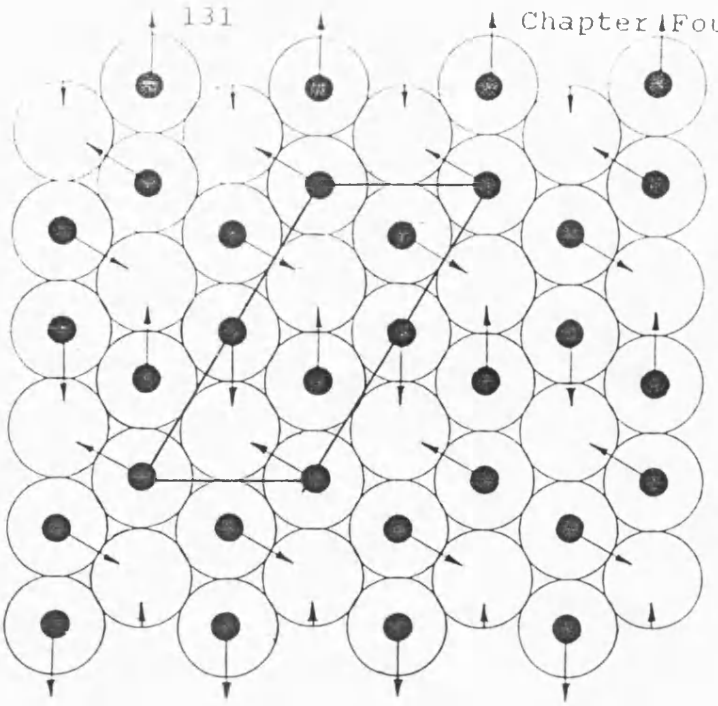

ALTERNATIVE MODELS FOR CO/Ru(001) ADSORPTION INCORPORATING MOLECULAR TILT

$(2\sqrt{3}x\sqrt{3})R30$ STRUCTURE

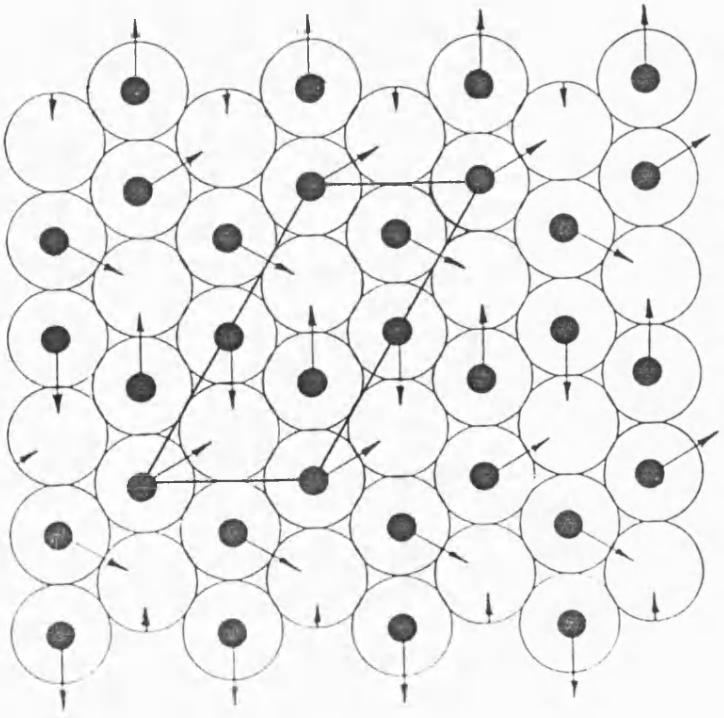

in comparison with the experimentally derived value of θ_{CO}=0.69. The unoccupied ruthenium surface atoms are protected from further adsorption due to the tilting of two adjacent CO molecules over them.

4.15 Evidence for tilting of CO on Ru(001)

Evidence from ESDIAD [112] indicates that CO adsorbed at high coverages is tilted at 5 degrees to the surface normal with no preferred azimuthal direction. The overlayer models proposed here have equal numbers of CO molecules oriented in the six equivalent directions associated with the hexagonal symmetry of the surface.

ARUPS studies of CO/Ru(001) are contradictory, with one study indicating no molecular tilting away from the surface normal [115] and the other indicating a tilt of the C-O molecular axis away from the surface normal of 10 degrees or less [105].

The molecular axis tilt angles in the case of Pt(110)-(1 x 2) have been measured to be 26 degrees with a rotation away from the [001] direction [6] or as 20 degrees oriented in the [001] direction [18]. The distance between CO molecules in the [001] direction of the Pt(110) surface is considerably greater than that between the tilted CO pairs in the proposed model, so that it might be expected that the angle of tilt away

from the surface normal would be less for CO on Ru(001) than for CO on Pt(110).

Adsorption of CO on Pt(110)-(1 x 2) at 100K

5.1 Introduction

The adsorption of CO on the Pt(110)-(1 x 2) surface at temperatures below 250K has been the subject of previous studies [10,17,19,20]. There are significant differences reported between CO adsorption at low temperatures and that at room temperature, in that the (1 x 2) reconstruction is not lifted and a metastable c(8 x 4) LEED pattern has been reported by some groups [10,17,20], but not observed by others [19]. HREELS results indicate the presence of a bridge bonded species of CO as well as the predominant linear bonded CO species [19].

Using nuclear microanalysis, Jackman and co-workers have reported that the saturation coverage of CO on Pt(110) is 0.92×10^{15} molecules/cm^2, corresponding to full coverage, with one CO molecule per surface platinum atom. For adsorption at 300K, the saturation coverage is 8.1×10^{14} molecules/cm^2, corresponding to $\theta_{CO}=0.89$.

5.2 Experimental Results

When CO was adsorbed at 100K, the reconstruction of the surface was not lifted. The LEED pattern remained of the (1 x 2) form and showed no differences from that of

the clean surface. This is in accord with the observations of Hofmann and co-workers [19]. No signs of the metastable c(8 x 4) LEED pattern reported by Jackman and co-workers [10] and Ferrer and Bonzel [17] was observed during this work.

TPD spectra taken following adsorption of CO at 100K showed no difference from those obtained following adsorption at at 300K. This is a reflection of the fact that the lifting of the reconstruction appears to take place in the temperature range 280-340K [19], which is lower than the desorption temperature of CO at experimentally accessible heating rates.

The RAIRS spectra for adsorption of CO at 100K are shown in Figure 5.2.1. The single absorption band is in the frequency range of on-top (linear) CO adsorption, as for the CO/Pt(110)-(1 x 2) (300K) adsorption system. This work was carried out using the InSb detector, which has a cut-off frequency of 1880 cm^{-1} making the detection of the band assigned to CO in bridge-bonded sites at 1855 cm^{-1} reported by Hofmann and co-workers [19] impossible to detect. As in the case of CO adsorption at 300K, there is a single symmetrical absorption band which moves upwards in frequency with increasing exposure of CO.

FIGURE 5.2.1

RAIRS SPECTRA : CO/Pt(110)-(1x2) 100K

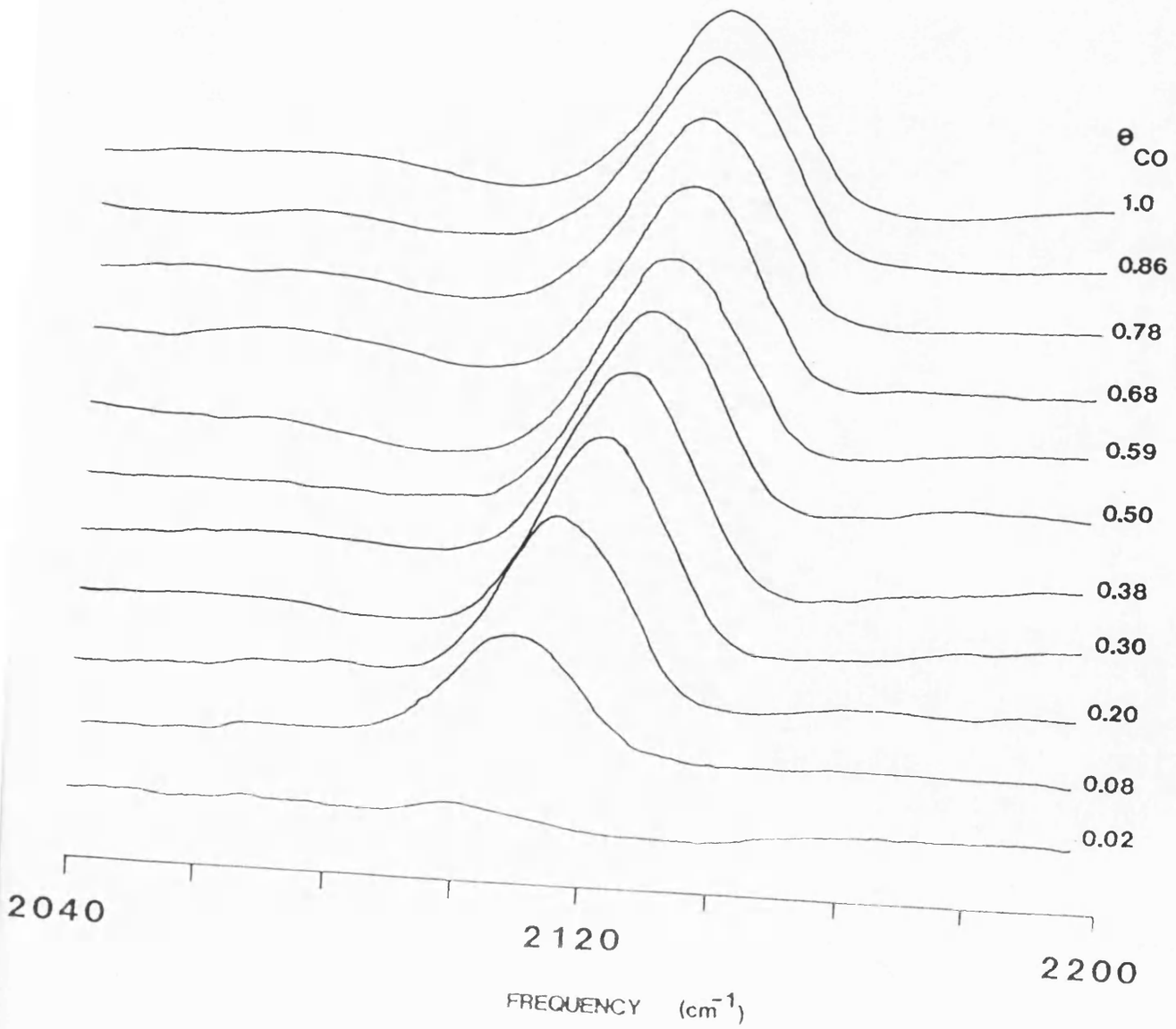

Immediately following the adsorption of CO at 100K, the surface was flashed to desorb the CO and then another adsorption sequence carried out, this time at 300K, using exactly the same spectrometer parameters in order to make a direct comparison between the absorption bands at the two temperatures. The (1 x 2) surface reconstruction was lifted.

The variation of the C-O stretching frequency with θ_{CO} following adsorption at temperatures of 100K and 300K is displayed in Figure 5.2.3. The frequency of the absorption band at 100K is consistently several wavenumbers greater than that of the band at 300K for a given CO exposure. However the overall frequency shift with increasing coverage is similar. The saturation coverage frequency is 2129 cm^{-1} for adsorption at 300K and 2135 cm^{-1} at 100K.

The integrated intensity versus CO coverage for the absorption bands at 100K and 300K are compared in Figure 5.2.4. Both bands show a maximum in the integrated absorption intensity at a coverage $\theta_{CO}=0.5$. The numerical values of the integrated intensity are similar at all coverages.

FIGURE 5.2.2

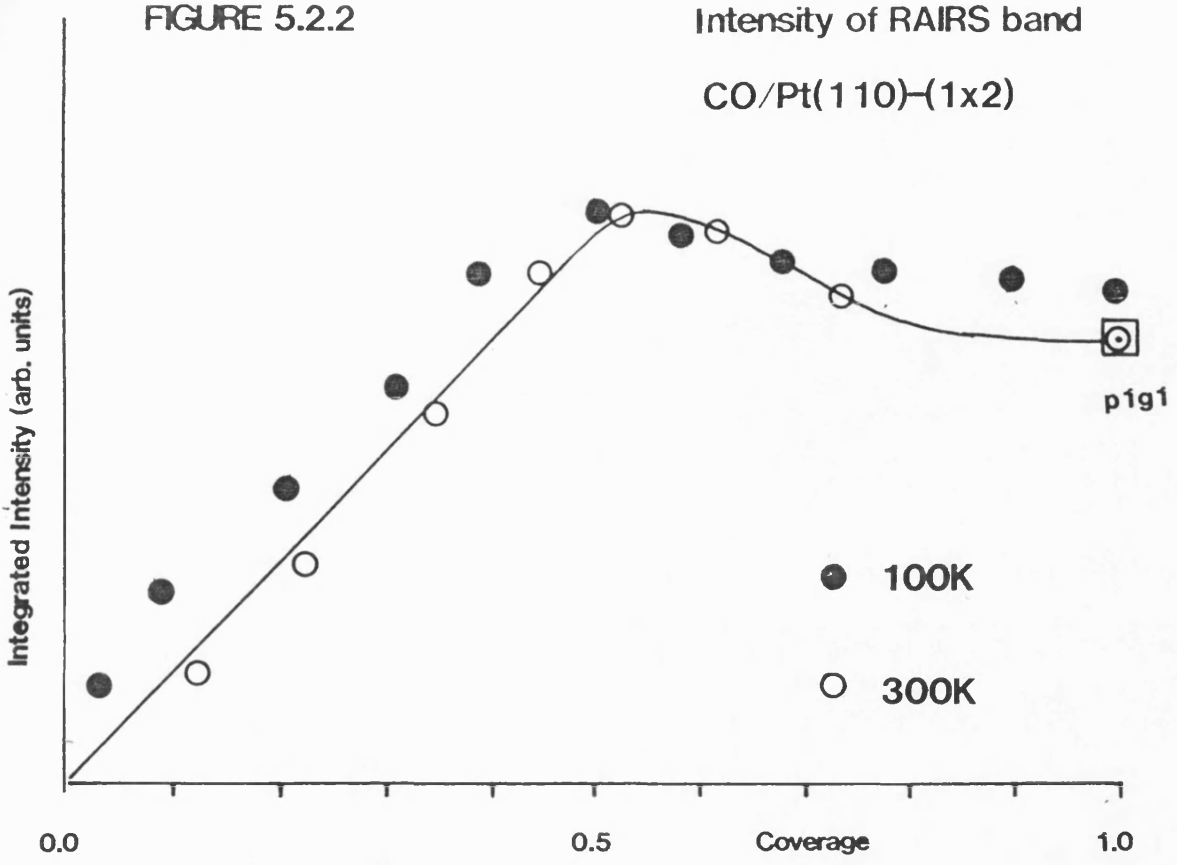

FIGURE 5.2.3

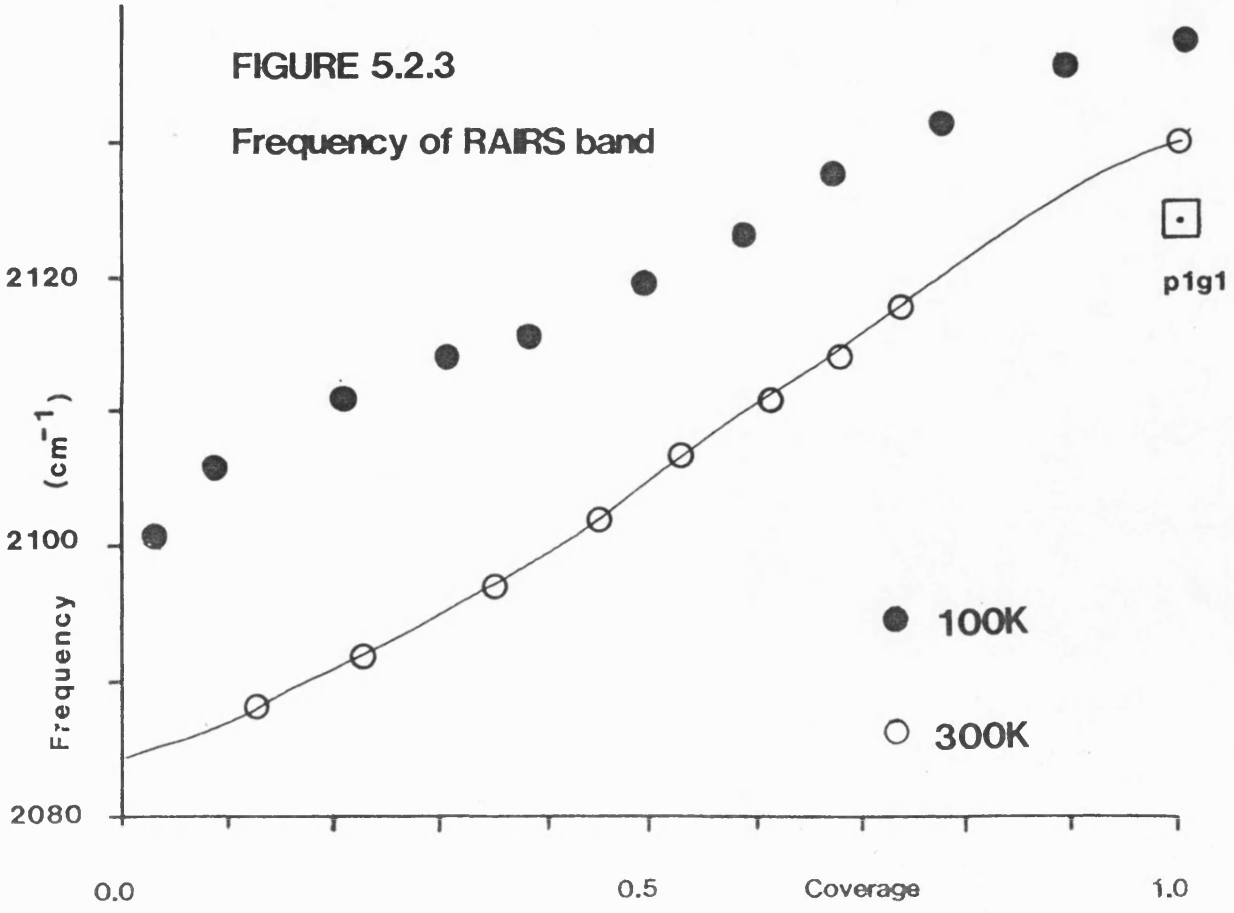

THE BRITISH LIBRARY DOCUMENT SUPPLY CENTRE
Boston Spa, Wetherby, West Yorkshire LS23 7BQ

PhD Thesis by _____

We have given the above thesis the Document Supply Centre identification number:

DX 81149

In your notification to Aslib please show this number, so that it can be included in their published Index to Theses with Abstracts.

Theses Office

5.3 Discussion

In order to determine a satisfactory adsorption model for CO/Pt(110)-(1 x 2) at 100K, further information is desirable. In particular, the development of the bridge-bonding CO absorption band, if present, with CO coverage would be very useful, in order to determine the ratio between bridge and linear bonded species. Hofmann and co-workers have suggested from HREELS vibrational studies [19] that the linear band predominates up to a coverage of 0.2, when a bridge band appears with a relative intensity of 1:8 of that of the linear band. They have also estimated that the ratio of the dynamic dipole moments of the two species is 2.5:1 in favour of the bridged species, and hence that approximately 30% of adsorbed CO at 160K is in the bridged rather than the linear adsorption site. However a RAIRS study of CO adsorbed on Pt(111) has concluded that the dynamic dipole moments of the bridged and linear species are similar [116]. The problems of using EELS intensity measurements to give meaningful relationships between the ratios of adsorbed species has been discussed by Baro and Ibach [117]. This suggests that the estimate of 30% of the adsorbed CO being adsorbed at bridging sites is an overestimate.

Examination of the behaviour of the linear CO absorption band in Figures 5.2.2 and 5.2.3 shows that there is a marked similarity in both frequency and integrated intensity variation with CO exposure at 100K and 300K. The major difference between the absorption bands is the consistently higher frequency for a given coverage for the lower temperature band.

Persson and co-workers [118,119] have recently suggested that the linewidth and position of IR absorption peaks in adsorption systems showing significant dipole-dipole interactions and anharmonic coupling to a low frequency frustrated translational mode, is temperature dependent. In the case of CO adsorbed on Ru(001) at a coverage of θ_{CO}=0.33, they have reported a broadening of the linear bonded C-O stretching band by 2cm^{-1} as the temperature is raised from 100K to 400K. The frequency at a constant coverage decreases slightly with temperature; the zero-coverage limit of the frequency of the C-O stretching mode decreases by 9 cm^{-1} as temperature increases from 100K to 400K.

In the case of CO adsorbed on Pt(110)-(1 x 2), the nature of the adsorption system with the reconstruction of the surface leading to uncertainty of the equivalence of the adsorption sites and the large FWHM of the

absorption bands, ascribed to inhomogeneous broadening due to the disorder of the surface, means that the system is not the most suitable to carry out detailed studies of temperature dependent effects.

A comparison of the RAIRS spectra measured for CO adsorption at 100K and 300K reveals a slight increase in FWHM at 100K, the FWHM is $\approx$20 cm^{-1} at this temperature and $\approx$18 cm^{-1} at 300K. However the temperature dependent frequency shift of the linear CO band is $\approx$10 cm^{-1} at saturation coverage, with the lower temperature band being at higher frequency, a shift of the same magnitude and direction as predicted by Persson and co-workers.

Since it has already been demonstrated that the coverage dependent frequency shift for CO adsorption at 300K is dominated by dipole-dipole interaction, the similarity in coverage dependent frequency shift at 100K suggests that the surface geometry and hence the distance between adsorbed CO molecules is similar on the (1 x 1) and the reconstructed (1 x 2) surface.

It is suggested that given the similarity between the RAIRS absorption bands for CO adsorption at 100K and 300K, the coverage and packing of CO molecules at the platinum surface must also be similar. This is despite the lifting of the (1 x 2) reconstruction at 300K which is not observed for adsorption at 100K. The striking

similarities between the absorption bands also demonstrates that the lifting of the reconstruction following adsorption at 300K, which occurs at a coverage of θ_{CO}=0.5 is not responsible for the change in the integrated intensity of the absorption band which also occurs at this coverage. It is now necessary to consider the proposed real-space models for the reconstructed Pt(110)-(1 x 2) surface in order to find a surface geometry which exhibits some similarity to the (1 x 1) surface present following adsorption at 300K.

Several models have been proposed for the (1 x 2) reconstruction of platinum [121]. Jackman and co-workers have suggested on the basis of Rutherford back-scattering results [20] that the most plausible models are the so-called "missing row" model (Figure 5.3.1) and the "rumpled" model. In the former model, alternate close packed rows of surface platinum atoms running in the [110] direction are absent from the surface. In the latter model there is an alternate vertical relaxation of the close packed rows of surface atoms.

Another model, the "sawtooth" reconstruction has been proposed by Bonzel and Ferrer [11], which involves the displacement of an entire [110] row by one lattice constant parallel to [001] (Figure 5.3.2). This produces microfacets of (111) surface three atoms wide. This

FIGURE 5.3.1

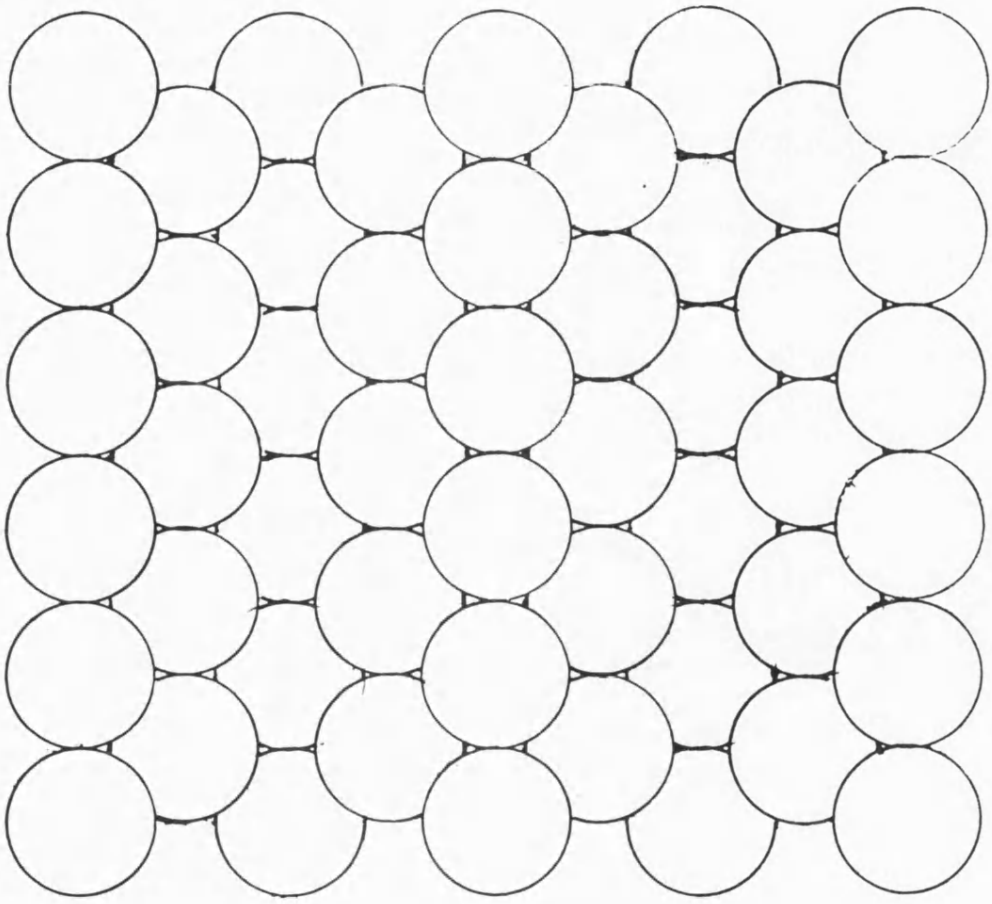

MISSING ROW MODEL FOR (1x2) RECONSTRUCTION OF Pt(110)

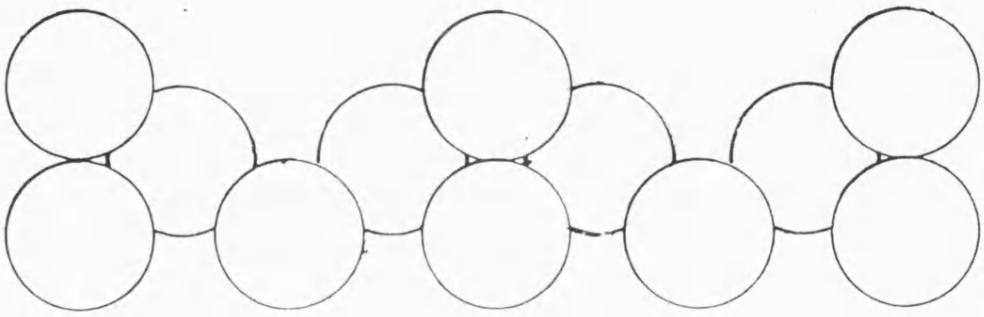

FIGURE 5.3.2

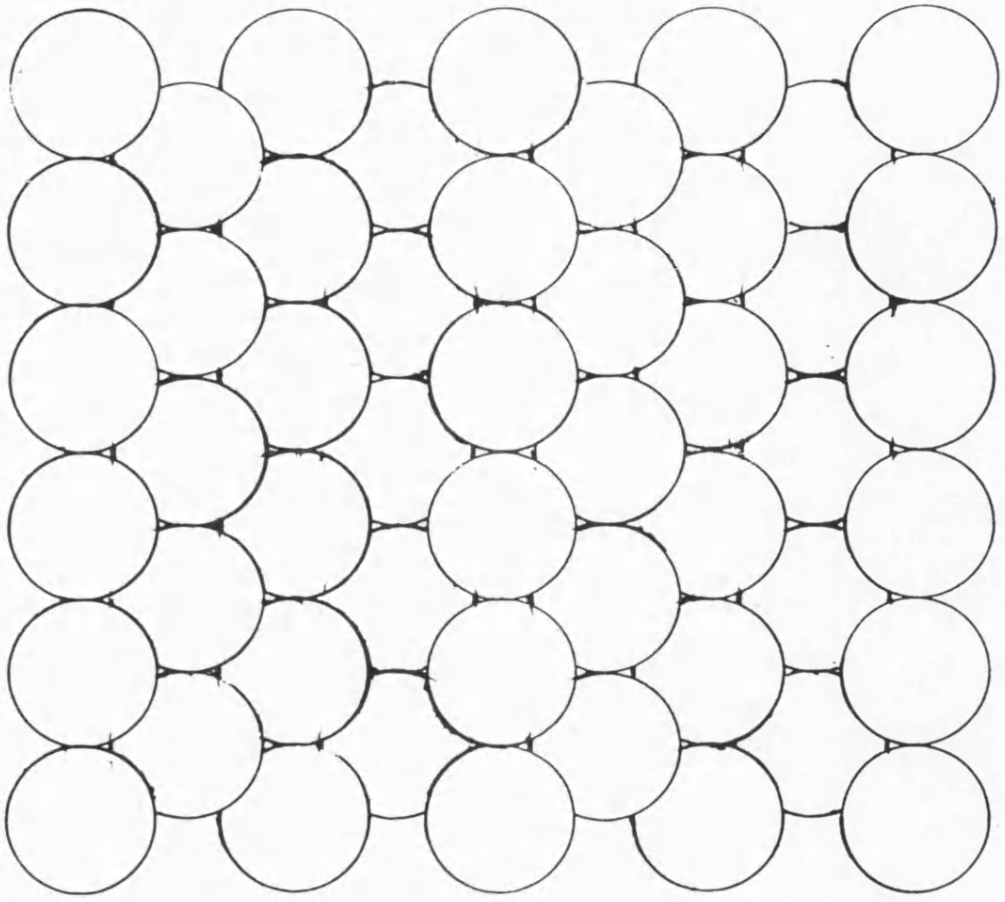

SAWTOOTH MODEL FOR (1x2) RECONSTRUCTION OF Pt(110)

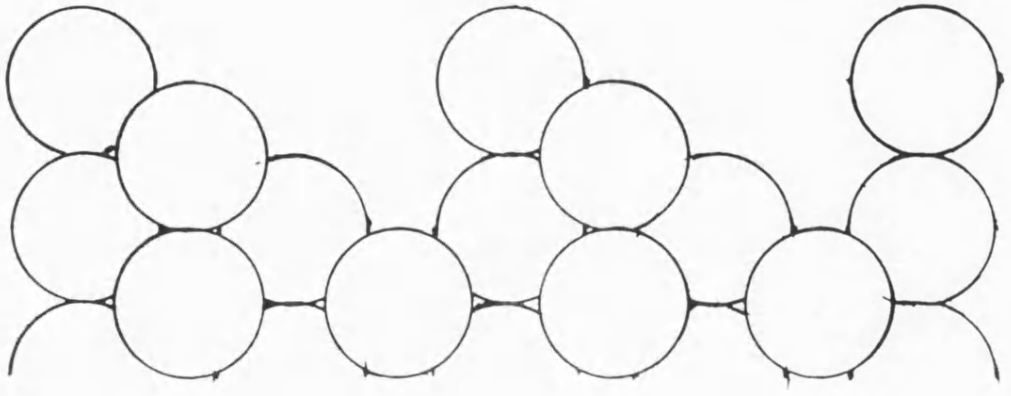

model does not require a large mass transport of platinum atoms which had been one of the main objections to the missing row model. However Campuzano and co-workers [120] have demonstrated that a large mass transport of platinum surface atoms is unnecessary for the missing row reconstruction, as terrace defects at the surface allows the reconstruction to take place easily. A recent LEED I(V) intensity analysis for the similar Ir(110)-(1 x 2) surface [122] has also concluded that a missing row model, with some relaxation in the first three surface layers is the best model to to describe the experimental data set.

The surface geometry which leads to the (1 x 2) LEED structure obtained following adsorption of CO at 100K is not necessarily the same as that which leads to the (1 x 2) LEED structure of the clean reconstructed surface. Hofmann and co-workers [19] and Jackman and co-workers [20] have suggested that there is a metastable intermediate state between the clean surface (1 x 2) reconstruction and the (1 x 1) surface evident following adsorption of CO at 300K. The appearance of the metastable c(8 x 4) LEED structure in certain experiments would tend to support this.

The results obtained in this study indicate that the CO is adsorbed largely at the same sites as on the

(1 x 1) surface and that there are a similar number of adsorption sites at both the (1 x 2) surface and the (1 x 1) surface. The most viable model for the CO/Pt(110)-(1 x 2) surface is the rumpled surface model, which has essentially the same adsorption sites as the (1 x 1) surface but with alternate rows of close packed platinum atoms at different heights above the surface. This would lead to a reduction in CO-CO repulsive interactions, along the [001] direction, but no significant change in the [110] direction. Thus the nearest-neighbour CO interactions remain very similar and so does the coverage dependent frequency shift due to dipole-dipole coupling. Using this model of the reconstruction, the absorption band produced by linearly bonded CO, will possess similar characteristics to that found at 300K, despite the fact that the reconstruction is not observed to be lifted.

The weaknesses with this particular surface geometry are:

(1) Ion scattering results [20] indicate that vertical surface displacements are less than 0.007 nm and it is unclear whether such a small displacement is sufficient to produce intense half order diffraction beams in LEED.

(2) The HREELS results in an earlier study [19] also

show a proportion of bridge-bonded CO and the authors comment that the spectra are dissimilar to those obtained at 300K when the reconstruction is lifted. The RAIRS results obtained here are diametrically opposed to this view, there is great deal of similarity between the adsorption at 100K and that at 300K.

(3) The rumpled surface model suggested, does not contain any available sites for the bridge bonded species.

In the present work, the coverage dependent shift of the linear bound CO is very similar at both 100K and 300K. It is suggested that this is due to similar coverages of the linear bound CO species being present on the platinum surface at both 100K and 300K. The absolute saturation coverages of CO on the Pt(110) surface are similar at both temperatures, implying that the predominant CO species on the (1 x 2) surface following adsorption at 100K is the linear bonded form and the bridge bonded species forms only a minor portion of the total CO coverage. The increase in absolute coverage of CO at low temperature, reported by Jackman and co-workers, is ascribed to the appearance of the bridge bonded species which was not detected by this study, but reported in EELS. The estimate that 30% of

the adsorbed CO is in bridge bonding sites appears to be an overestimate.

It should be noted that the presence of a small quantity of bridged CO is not incompatible with defects in the rumpled model. The FWHM of the low temperature band is $\approx 20\ cm^{-1}$ compared to $\approx 18\ cm^{-1}$ for the same band at 300K. This may be due to inhomogeneous broadening of the absorption band due to surface disorder, in which case the CO/Pt(110)-(1 x 2) phase is more disordered than the CO/Pt(110)-(1 x 1). The bridged CO species may then adsorb at the defect areas. If the crystal is warmed up, the surface transforms to the (1 x 1) phase as the rumpling of the surface vanishes ,the linear CO band becomes sharper and the bridging species disappears; the surface becomes less defective, so fewer bridging CO sites are available.

ARUPS results [19] indicate that at saturation coverage the CO molecular axis is tilted away from the surface normal. The ARUPS spectra obtained from CO adsorbed at 100K were not identical to those produced by the (2 x 1)p1g1 overlayer. The CO bond axis is calculated as being tilted between 15-20° from the surface normal and oriented along the [001] direction. This is similar to the orientation determined for the CO/Pt(110)-(1 x 1) and CO/Pt(110)(2 x 1)p1g1 systems

[12,13,18].

Both the missing row and saw-tooth models would require CO adsorption on sites not equivalent to that of the (1 x 2) surface, either within the missing row itself or on the (111) facets produced by the sawtooth reconstruction in order to produce a coverage of CO equivalent to that on the CO/Pt(110)-(1 x 1) and CO/Pt(110)(2 x 1)p1g1 overlayers.

The proposed real space model for CO adsorbed on the Pt(110)-(1 x 2) surface at 100K is that the clean surface shows a (1 x 2) reconstruction which becomes a (1 x 2) rumpled surface model on adsorption of CO at temperatures less than 250K. There is no visible change in the LEED pattern. Warming the surface causes a smoothing out of the rumpled surface and leads to the lifting of the reconstruction. CO is mainly adsorbed in linear sites at all coverages for both the CO/Pt(110)-(1 x 2) phase and the CO/Pt(110)-(1 x 1) phase.

The proposed adsorption model requires further investigation, in particular determination of the sticking probability of CO on the Pt(110) surface at 100K and a RAIRS measurement to determine whether a bridged CO band is present at low temperatures. If such a band is present then a measurement of the relative

intensities could be used to recalculate the ratio of the bridge bonded to linear bonded CO species, given the relative dipole moments of the two species [116].

Co-adsorption of potassium and CO on Pt(110)-(1x2) at 300K

6.1 Introduction

The co-adsorption of potassium with CO on the Pt(110)-(1 x 2) surface at 300K was studied, focussing particularly on the low potassium coverage limit, as this is more appropriate to the quantity of alkali metals present as promotors in catalysis. During the study, potassium was pre-adsorbed onto the clean platinum surface and then CO adsorbed onto the doped surface.

6.2 Low Energy Electron Diffraction Studies

Potassium was gradually deposited onto the surface from the source and LEED patterns observed. Due to the geometry of the potassium source and LEED optics it was not possible to deposit potassium whilst making LEED observations.

Deposition of small quantities of potassium onto the platinum surface resulted in no observable change from the (1 x 2) pattern of the reconstructed surface. Further deposition of potassium lead to a streaked pattern appearing running in the [001] direction and approximately two thirds of the distance between the

[n,0] and [n,1] reflexes. This streaking became more pronounced as deposition continued. Eventually the streaking pattern gave way to a pattern with a high background intensity, where the only diffraction beams visible were those of a (1 x 2) pattern corresponding to the original clean surface net, and then only at high electron energies. This was attributed to a high coverage of potassium on the platinum surface. The original (1 x 2) pattern, could be restored by briefly heating the crystal to 1300K. Thermal desorption measurements made during the heating process failed to detect any potassium desorption. The (1 x 2) pattern produced following the annealing process appeared better ordered than the original pattern, with a lower background intensity and sharper diffraction spots.

Forming the strongly streaked pattern at intermediate exposures of potassium, followed by annealing the crystal to 550K and cooling to 300K resulted in the formation of a (3/2 x 2) pattern superimposed on the (1 x 2) pattern due to the platinum surface. This was taken to be an overlayer structure due to the potassium. The (3/2 x 2) LEED pattern structure was still strongly streaked in the [001] direction, but well ordered in the [110] direction.

6.3 Real Space Model for the (3/2 x 2) LEED Pattern

The following real space model for the (3/2 x 2) pattern is proposed: potassium atoms adsorb into the troughs of the (1 x 2) surface. A possible overlayer structure is shown in Figure 6.3.1, assuming a missing row model for the reconstructed surface. The distance between the neighbouring potassium atoms in the troughs is 1.5 times the platinum-platinum distance in the [110] direction. Taking the bulk platinum lattice parameter of 0.39 nm [112], the platinum-platinum distance in the [110] direction is 0.28 nm. Hence from the LEED evidence there is a potassium-potassium distance of 0.42 nm. This value is less than the atomic diameter of potassium, 0.462 nm [123], and implies that the adsorbed potassium species is partially ionised (the diameter of K^+ is 0.266 nm [124]). This also explains the streaking in the [001] direction and the high ordering in the [110] direction: electrostatic repulsions between adjacent potassium ions in the troughs of the surface cause a relatively highly ordered structure. However the potassium ions sit within the surface and are partially screened from ions in the neighbouring troughs by the intervening platinum atoms in the top surface layer. Thus there is less repulsion between rows of potassium

FIGURE 6.3.1

(3/2x2) POTASSIUM OVERLAYER ON Pt(110)-(1x2)

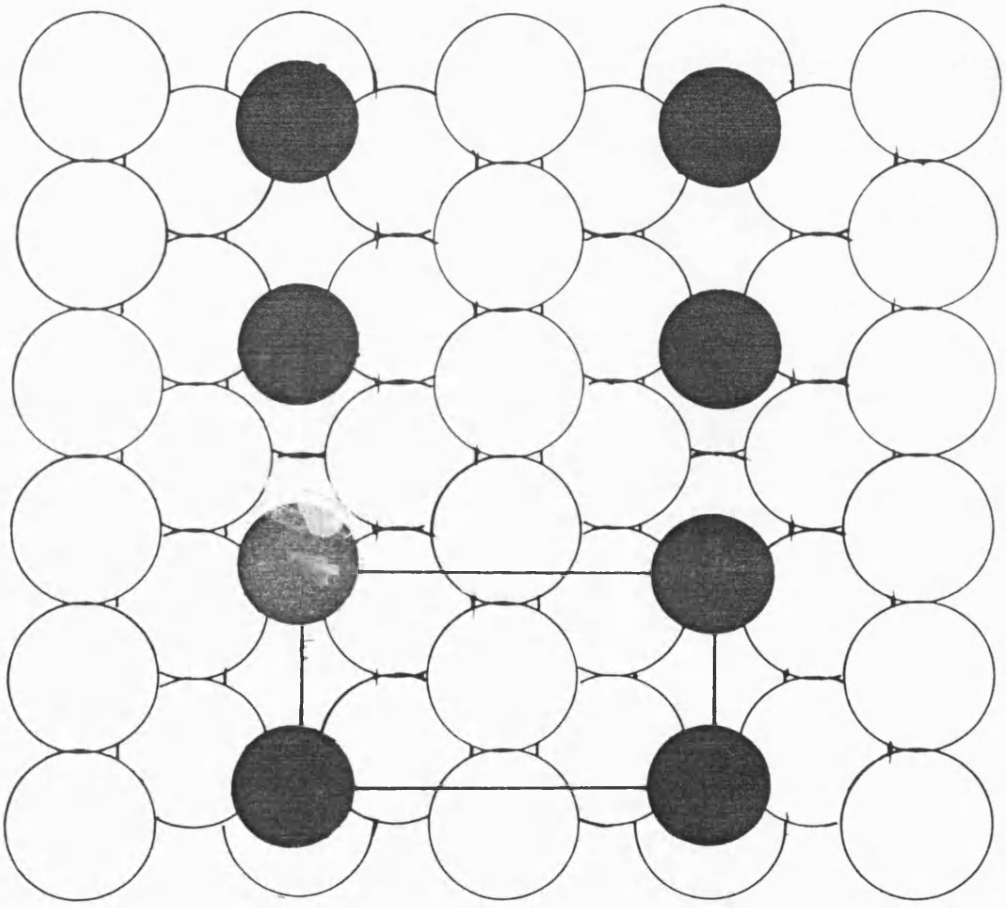

ion and less ordering in the [001] direction. The fact that warming the adsorbed layer produces more highly ordered LEED structures shows that the inter-row electrostatic interactions are not negligible.

6.4 Potassium coverage determination

The potassium coverages during co-adsorption experiments were estimated using the real space model described above, which has an ideal potassium coverage of θ_K=0.33 relative to the Pt(110)-(1 x 1) surface. The time taken to deposit this quantity of potassium at a constant source heating current was known, so subsequent coverages were calculated on the assumption that coverage was proportional to the deposition time.

6.5 Desorption experiments: CO/K co-adsorption

TPD spectra for CO adsorbed on doped platinum surfaces, with varying coverages of potassium are shown in Figure 6.5.1. The exposure of CO used for each desorption spectra was constant and was sufficient to produce saturation coverage (θ_{CO}=1.0) on the clean Pt(110)-(1 x2) surface.

At low potassium coverages, the desorption spectra are similar to that of the clean surface, with a broadening of the high temperature desorption state to

FIGURE 6.5.1

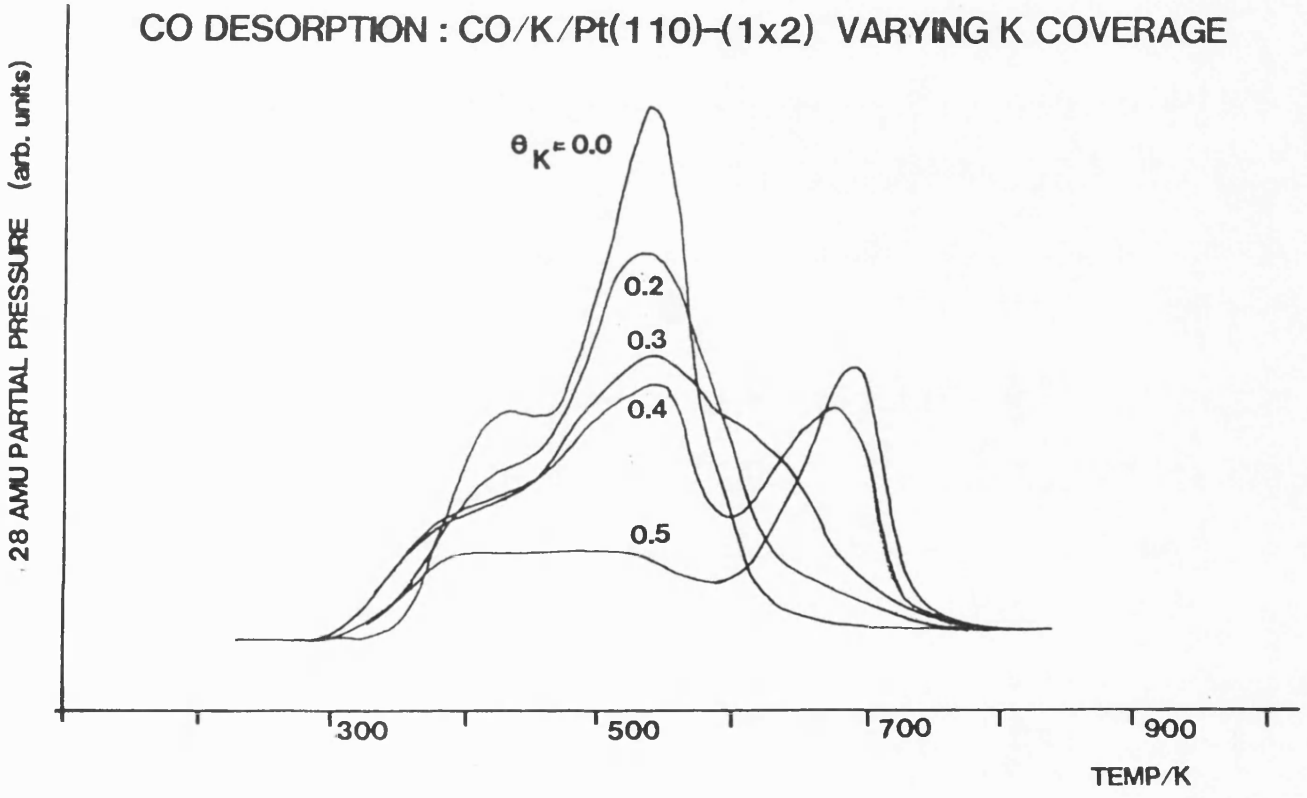
CO DESORPTION : CO/K/Pt(110)–(1x2) VARYING K COVERAGE
28 AMU PARTIAL PRESSURE (arb. units)
θK= 0.0
0.2
0.3
0.4
0.5
300
500
700
900
TEMP/K

higher temperatures occurring. At medium and high potassium coverages this broadening becomes resolved into a separate desorption state, with the low temperature feature from the clean surface becoming less pronounced. At high potassium coverages there is a residual low temperature feature and the high temperature feature also decreases in size.

These results show a marked similarity to those found for CO/Pt(111) [37,38], where the residual low temperature feature (corresponding CO adsorbed onto a "clean" surface) has been determined as being from the sides and rear face of the platinum crystal and from the crystal support.

These results suggest that a strongly perturbed CO species is present on the surface at intermediate coverages of potassium, with either an increased desorption energy compared to CO adsorbed on the clean surface or a reduced pre-exponential factor in equation 2.36. The sticking probability of CO on potassium appears to be considerably less than that on platinum.

This study was focussed on the low potassium coverage limit, where the difference in the desorption spectra from the clean surface are only apparent at low CO coverages. In Figure 6.5.2, the CO desorption spectra from the platinum surface with a potassium coverage of

FIGURE 6.5.2 CO DESORPTION FROM K/Pt(110)-(1x2)

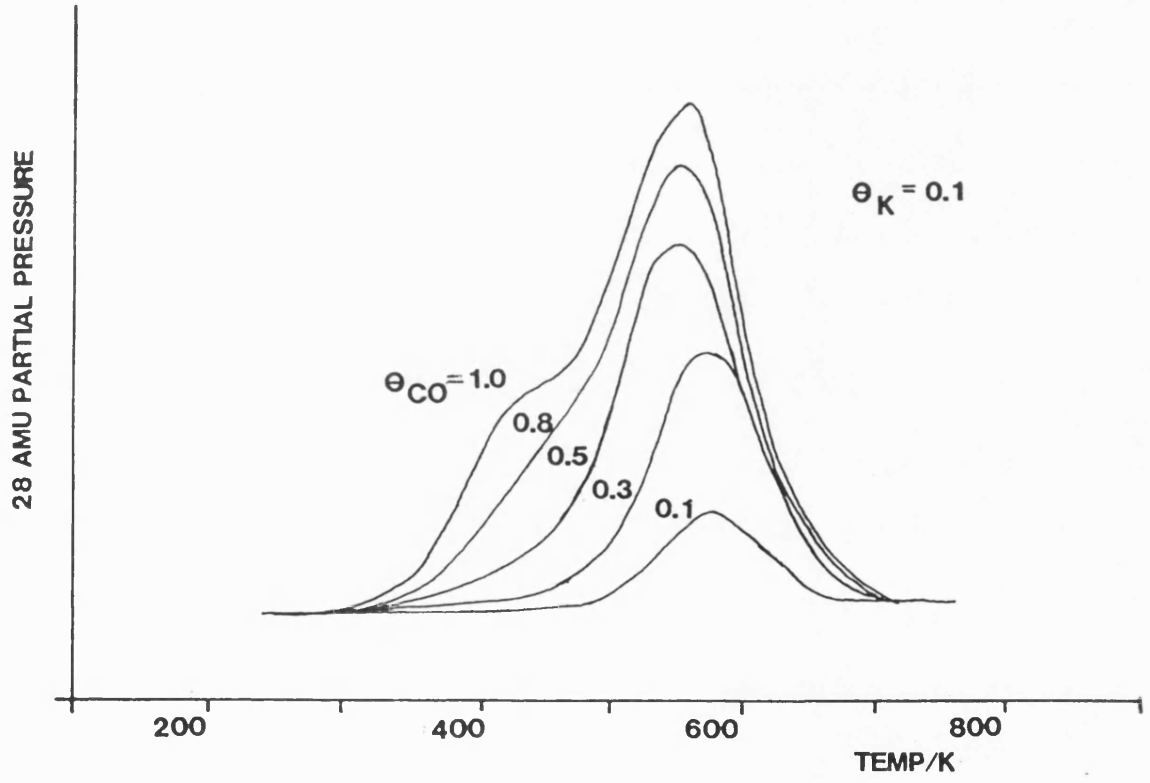

θ_K=0.1 at varying coverages of CO are plotted. The singleton desorption peak shifts from 540K on the clean surface to 570K on the doped surface. Assuming that the pre-exponential factor in equation 2.36 is 10^{13} sec^{-1}, with a heating rate of 4 K/sec, this leads to a desorption energy of 148 kJ/mol. This compares with the desorption energy of CO from the clean surface of 140 kJ/mol calculated in section 4.3. The apparently strengthened CO-platinum bond is only observed at low CO coverages, at high coverages of CO the desorption energy is that associated with CO adsorbed on the clean surface.

6.6 RAIRS spectra: CO/K/Pt(110) θ_K=0.05

At a potassium coverage of θ_K=0.05, the RAIRS spectra, shown in Figure 6.6.1, exhibit a doublet structure. At low CO coverages a low frequency band is observed first, with a higher frequency band becoming dominant at higher CO coverages. The position of the high frequency band is within the frequency range associated with CO on the clean platinum surface. The low frequency band is relatively constant at intermediate and high CO exposures, at 2025 cm^{-1}, but is shifted down at lower CO exposures.

FIGURE 6.6.1 RAIRS SPECTRA CO/K/Pt(110)-(1x2)

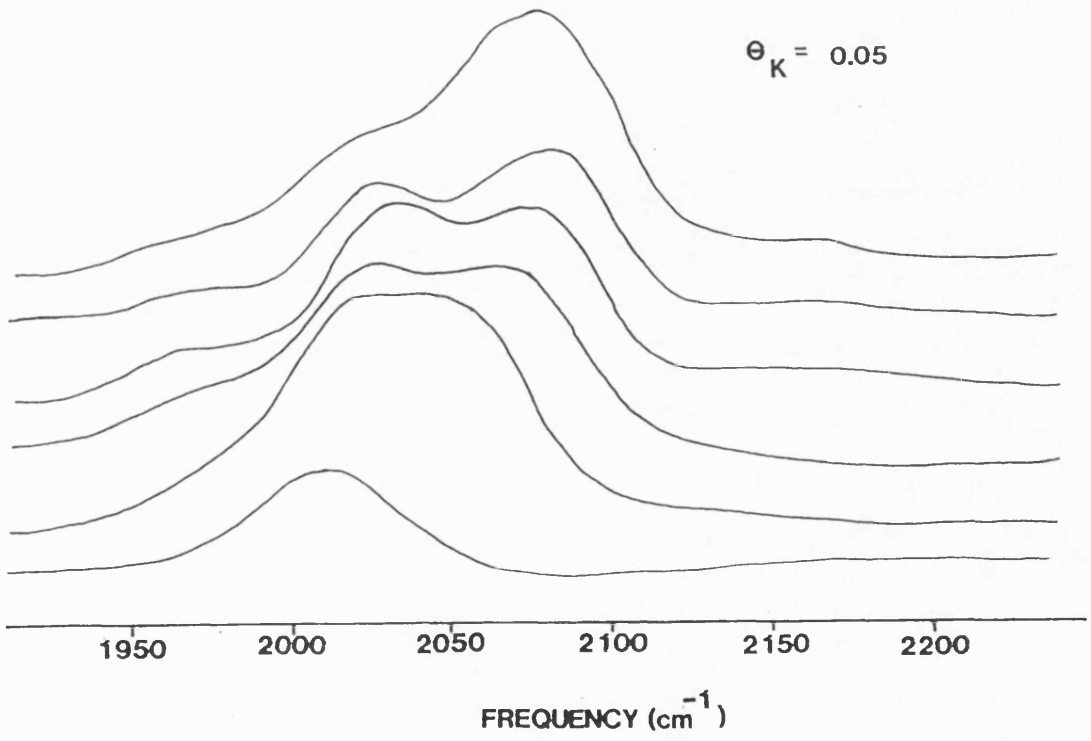

6.7 Adsorption model for CO/K/Pt(110) at θ_K=0.05

These RAIRS results have been interpreted as follows [125]: at this low coverage of potassium, areas of the platinum surface exist which are free from the influence of the potassium adspecies. CO adsorbs preferentially into islands associated with the adsorbed potassium and so is perturbed by the presence of the dopant. This manifests itself as a low frequency IR absorption band, which indicates a weaker C-O bond, and also as a higher CO desorption temperature.

Subsequent CO adsorption occurs at sites which are not affected by the presence of potassium on the surface and so an absorption band characteristic of the C-O stretch on a clean platinum surface appears at higher CO coverages.

6.8 RAIRS spectra for CO/K/Pt(110) at θ_K=0.10

At the higher potassium coverage of θ_K=0.10, a singleton infra-red absorption band is observed (see Figure 6.8.1). This band shifts upwards in frequency with coverage of CO over the range 1980-2030 cm^{-1}. It has a FWHM of 40 cm^{-1}, considerably broader than the FWHM of the absorption band of CO on the clean platinum surface. The frequency shift with coverage is plotted in Figure 6.8.2, with the frequency shift of the clean

FIGURE 6.8.1 RAIRS SPECTRA : CO/K/Pt(110)-(1x2)

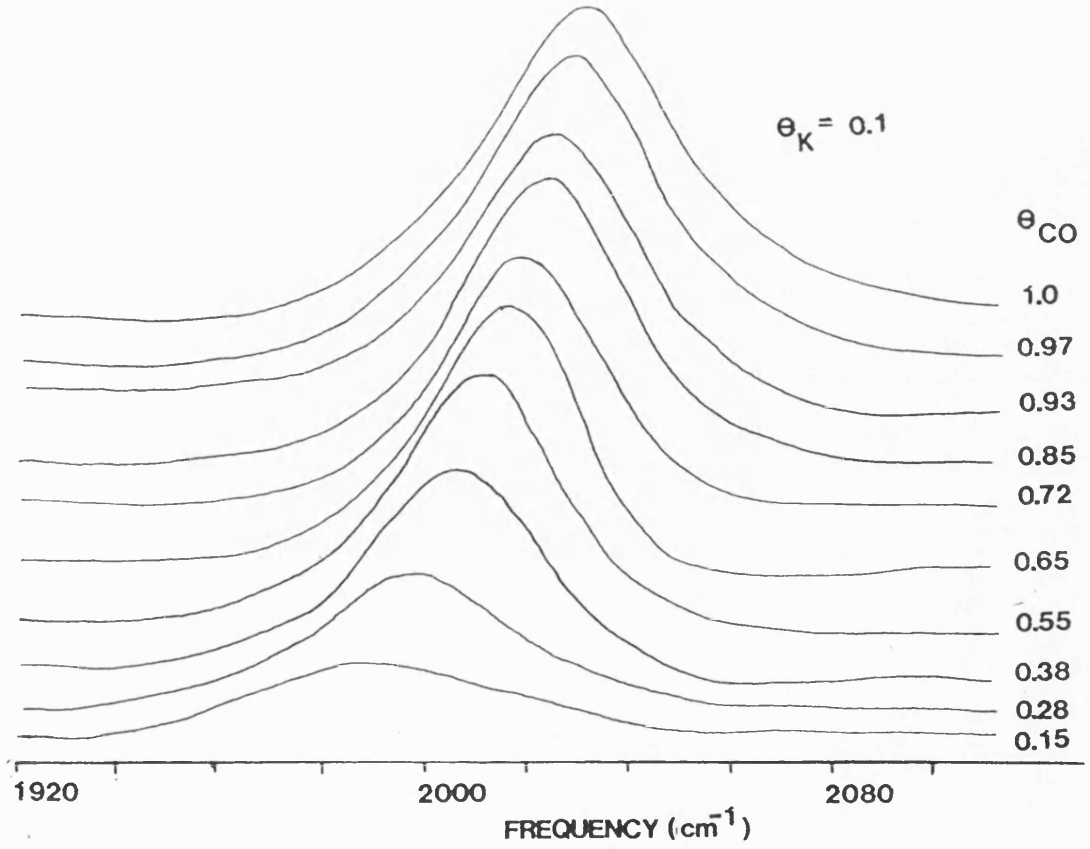

FIGURE 6.8.2 COVERAGE DEPENDENT FREQUENCY SHIFTS FOR CO/Pt(110)-(1 x2) 300K

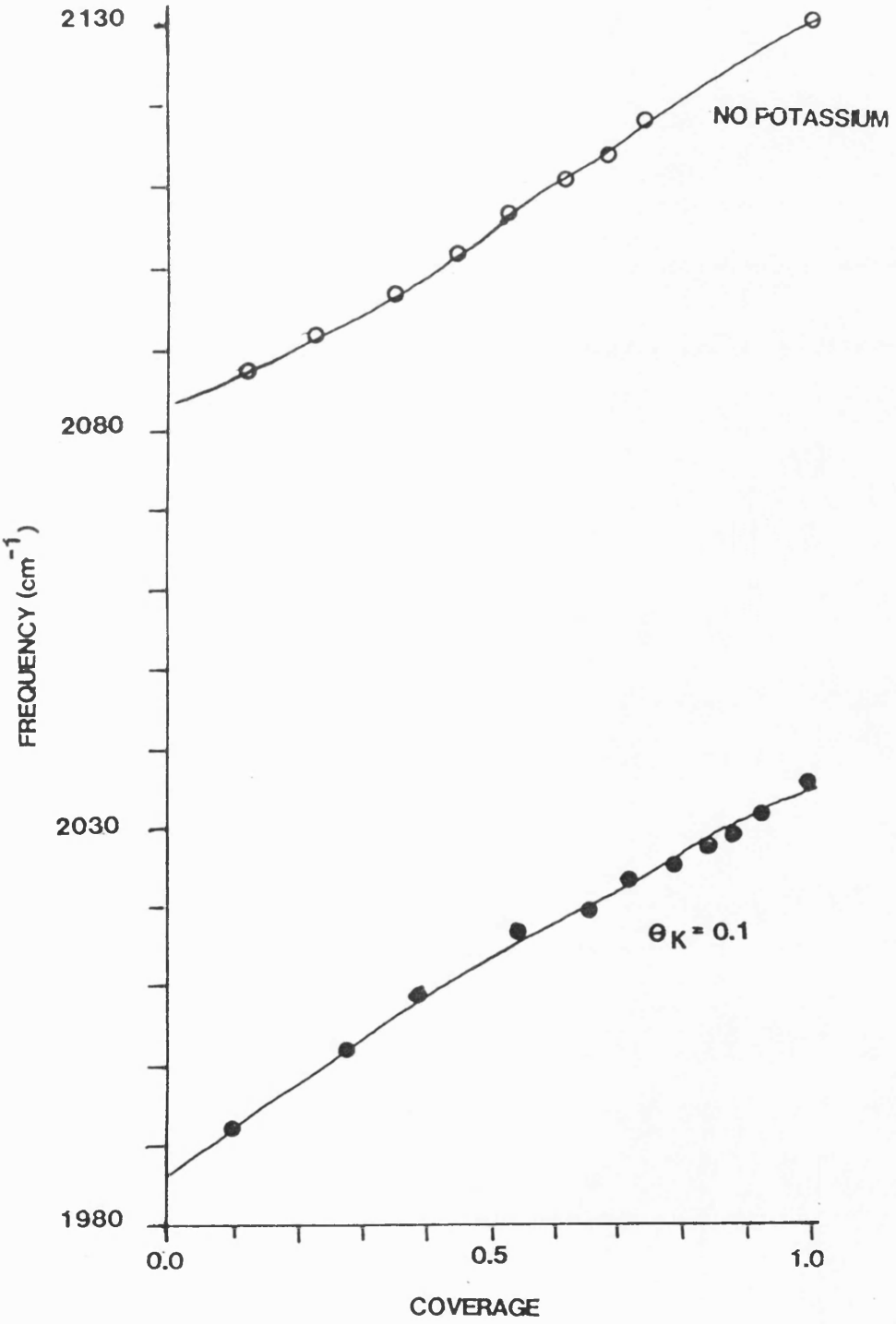

surface absorption band plotted as a comparison. The coverage dependent shifts are identical despite the differences in the singleton frequency.

The RAIRS spectra of CO remained identical even after desorption of CO from the doped surface and then re-adsorption at 300K. This was interpreted as meaning that potassium was not desorbed from the surface at temperatures of 600K, the desorption temperature of CO. This made possible a series of $^{13}CO/^{12}CO$ isotope mixture experiments, similar to those described in section 4.7, with constant coverage of potassium, Θ_K=0.1. The results, shown in Figure 6.8.3, demonstrate that the coverage dependent shift in the CO stretching frequency is entirely due to dipole-dipole interactions, just as for the clean platinum surface. There was no chemical (or static) shift induced by the presence of the potassium.

The variation of integrated intensity of the absorption band with CO coverage is plotted in Figure 6.8.4.

FIGURE 6.8.3

CONTRIBUTION TO COVERAGE DEPENDENT SHIFT

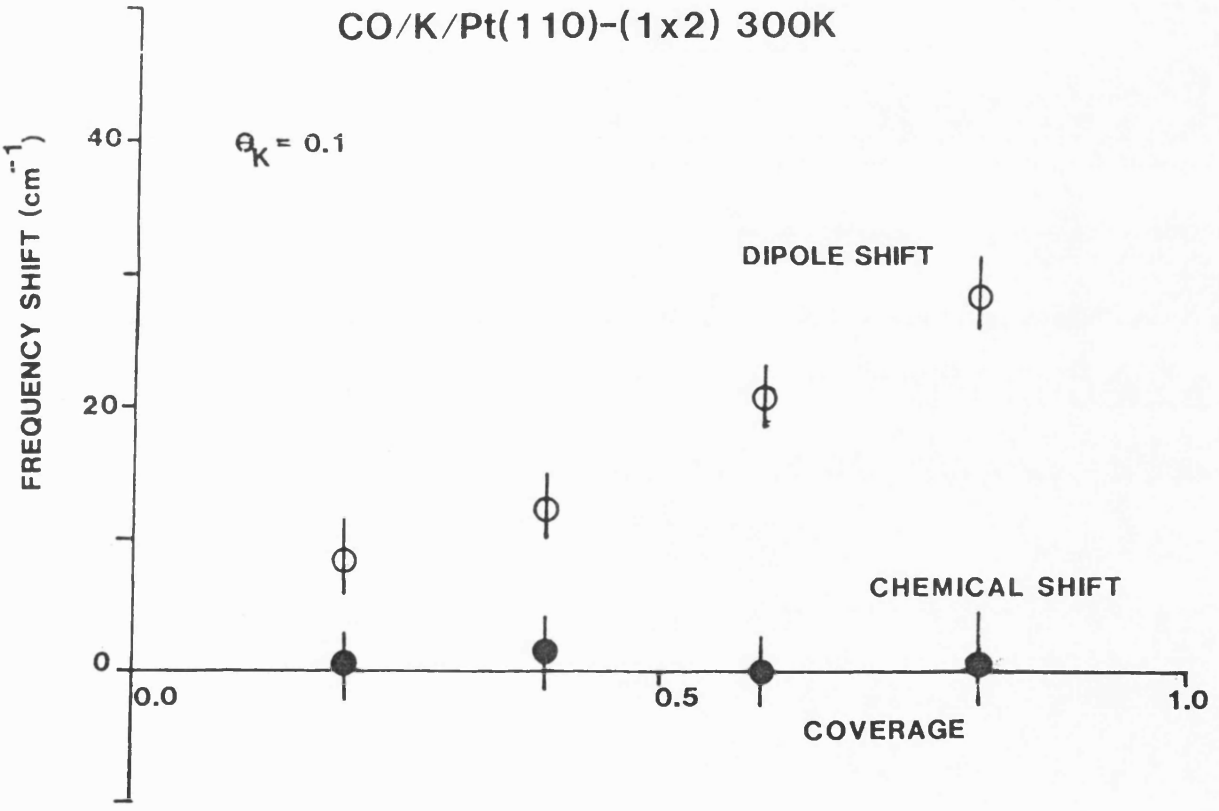

FIGURE 6.8.4 INTENSITY OF RAIRS BAND

CO/K/Pt110)-(1x2) 300K

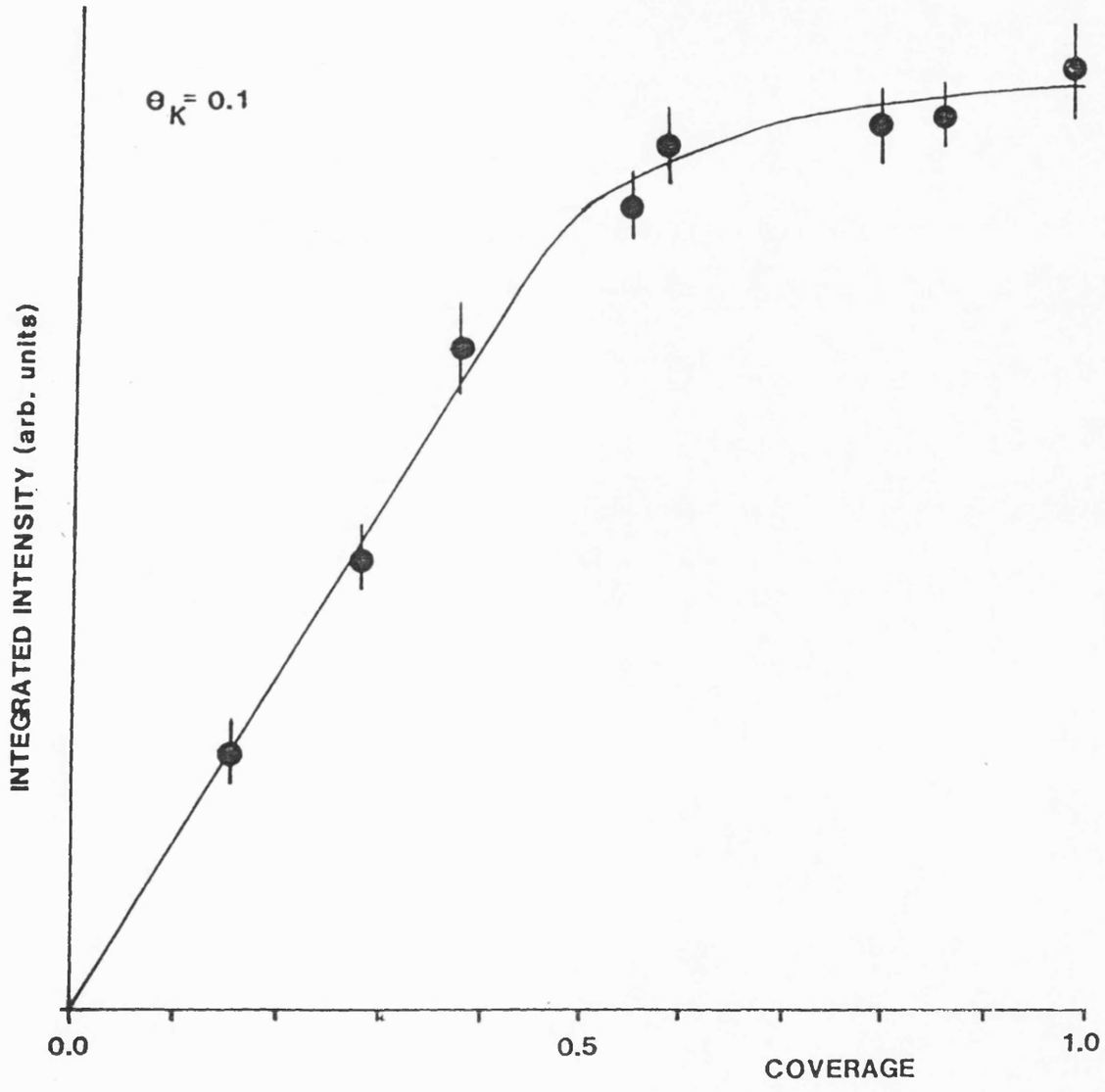

6.9 Adsorption model for CO/K/Pt(110) at θ_K=0.10

The infra-red absorption band has the same integrated intensity and frequency shift behaviour as functions of coverage as the absorption band for CO on the clean surface. However the singleton frequency of the band is shifted down by approximately 100 cm^{-1}, and the band has an FWHM of 40 cm^{-1} compared with 18 cm^{-1} for the band on the clean surface.

In comparison with the θ_K=0.05 case, there is now sufficient potassium present to spread out over the entire surface, due to the electrostatic repulsion of the charged potassium adspecies. The entire CO adsorbate layer is now influenced by the presence of potassium and a single absorption band is observed, which has many of the characteristics of the CO absorption band on the clean surface. We must now consider various CO bonding models and various models for the potassium/CO interaction to determine which model most appropriately conforms with these results.

6.10 Origin of Chemical Shifts: CO-metal bonding

The origin of the chemical shift component of the coverage dependent shift has been discussed in section 4.7 and is essentially due to a perturbation in the

occupation of the $2\pi^*$ antibonding orbitals of the CO. The Blyholder bonding model [23] is able to account for the upward frequency shifts found on palladium [126], ruthenium [127] and nickel [128].

However on copper surfaces, the total coverage dependent shift is small or negative [130-132]. Isotope mixture experiments have determined that this is due to a cancellation between the positive shift due to dipole-dipole interactions and a negative chemical shift [100,132]. The Blyholder model cannot account for the negative chemical shift.

One possible explanation of this negative chemical shift has been proposed by Hollins and Pritchard [133], who suggest that since the 5σ bond is slightly anti-bonding with respect to the C-O bond, an increased coverage of CO causes a weakening of the chemisorption bond and hence lowers the C-O stretch frequency. This model is open to criticism in that the metal-carbon bond is weakened; experimental evidence from EELS for N_2 on ruthenium [133] suggests that this is not the case as the Ru-N vibrational frequency increases with increasing nitrogen coverage.

A modification of the Blyholder bonding model has been proposed by Woodruff and co-workers [100]. In this case the $2\pi^*$ antibonding orbital is split into two

components, $2\pi_a$, which is antibonding with respect to the metal-CO bond and lies well above the Fermi level and $2\pi_b$ which is bonding and lies close to the Fermi level. Overlap of the $2\pi^*$ orbitals with increased CO coverage cause a broadening of the $2\pi_b$ band. If the band lies above the Fermi level, then it becomes more occupied and the C-O bond becomes weaker. This corresponds to the weak chemisorption case such as CO/Cu, where the chemical shift is increasingly negative with coverage. If the $2\pi_b$ level lies below the Fermi level, then band broadening causes a loss of occupation; back-donation is weakened and the C-O stretch frequency increases. This gives the positive chemical shifts associated with the strong CO chemisorption case.

A similar model has recently been proposed by Ueba [108] who has accounted for the competitive effects of band broadening due to orbital overlap and depolarisation effects caused by the adlayer on the adsorbate density of states.

The chemical shift is thus thought to be dependent on the relative occupancy of the $2\pi^*$ level. On clean platinum surfaces [88,109] there is no evidence of a coverage dependent chemical shift; platinum is thought to be an intermediate case between strong and weak chemisorption systems.

The experimental results from the isotope mixture experiments suggest that since there is no induced chemical shift from the presence of the potassium co-adsorbate, the occupation of the $2\pi^*$ antibonding orbital is not perturbed.

6.11 Origin of long range potassium-CO interactions

Holloway and Norskov [43] have suggested that the electrostatic potential associated with the adsorbed species (such as potassium) causes a downwards shift in the molecular CO levels relative to the Fermi surface, including the partially occupied $2\pi^*$ antibonding levels. The occupation of the antibonding level is increased and the C-O bond weakened, resulting in a downward shift in C-O stretching frequency. The basis for their calculations is to use the effective medium theory [134] to determine adsorbate-adsorbate interaction energies:

$$\delta E = \int_a \delta\phi_o^{(-a)}(\underline{r}) n_a(\underline{r}) d\underline{r} + \delta\left[\int_{-\infty}^{\epsilon_f} n_a(\varepsilon)\varepsilon d\varepsilon\right] \qquad (6.1)$$

This assumes that the influence of adsorbate A_1 on the nearby adsorbate A_2 is first order near to A_1 and vice versa. The first term is the direct electrostatic interaction with $\delta\phi_o$ as the electrostatic potential

induced by A_2 and $\pi_a(r)$ the charge density induced by A_1. The second term is the difference in the sum of one-electron density of states with and without A_2 present, with $n_a(e)$ the A_1 induced density of states. The Fermi energy is e_F. This term contains the direct orbital overlap and indirect electronic adsorbate interactions.

Further work by Lang, Norskov and Holloway using this approach, in which the electric fields generated by a variety of electropositive and electronegative adsorbates (modelling alkali metals promotors and poisons such as sulphur respectively) on a jellium surface indicated that these effects would be strongest over distances of the order of one metal lattice parameter [44]. This required evaluation of the first term in equation 6.1.

Feibelmann and Hamann [46,47] have calculated the perturbation of the one-electron density of states at the metal surface due to a variety of electropositive and electronegative adsorbates. This is evaluation of the interactions due to the second term in equation 6.1. Their results show that the perturbation in $n_a(e)$ is over distances greater than one metal lattice constant. The nature of the changes in the metal surface electronic states suggest that interaction between

adsorbates would involve changes in the occupancy of the molecular orbitals.

Muller and Bagus [48] have suggested that the reduction in frequency of the C-O stretch under the influence of electropositive adsorbates such as potassium is due to the direct interaction of the electric field induced by the presence of the adsorbate with the electric dipole of the C-O molecule (a vibrational Stark effect). This is similar to the interaction proposed by Norskov and Holloway, being electrostatic in nature, but does not require the perturbation of the occupancy of the CO molecular orbitals.

Efrima and Metiu [45] have investigated the interaction of the electric field associated with a metal surface with an adsorbed molecule. They have calculated that for a molecule such as CO a downwards shift of ≈10-20 cm^{-1} for interaction with the electric field due to a clean metal surface, without any enhancement due to electropositive adsorbates.

6.12 Long range interaction between K and CO on Pt(110)

The bonding schemes for CO on metals discussed above indicate that any chemical shift to the CO stretching frequency is induced as a result of a change

of occupancy of the antibonding $2\pi^*$ orbital. In the case of CO/K/Pt(110), isotope mixture experiments indicate that the presence of potassium does not induce any chemical shift to the CO stretch, despite the overall downward shift of the singleton C-O stretching frequency of 100 cm^{-1}. Thus it is concluded that the most likely mechanism to account for the significant perturbation of the C-O stretch is the direct interaction between the electric field associated with the potassium with the electric dipole of the CO molecule, as proposed by Muller and Bagus. This physical effect accounts for the overall downward shift in frequency, but as no changes of a chemical nature are involved, preserves the essential features of the CO/Pt(110) adsorption system, such as the coverage dependent frequency shift due to dipole-dipole coupling and the unusual integrated intensity variation with coverage [109].

6.13 Comparison with CO/K/Ni(111)

The results obtained in this study of the CO/K/Pt(110) adsorption system differ significantly from those obtained recently for the CO/K/Ni(111) system [42] by Yates and co-workers. In the latter work, whilst the singleton frequency of the C-O stretch decreased

continuously with increasing potassium coverage, there was a simultaneous increase in the magnitude of the coverage dependent frequency shift. The conclusions drawn from these results are very similar to those drawn in the present work; that the dominant long range interaction is that of the vibrational Stark effect, which extends over several metal lattice parameters and that CO molecules aggregate around a potassium kernel species. The increase in the coverage dependent shift is accounted for in the following way: at low CO coverages, adsorption takes place at sites close to the potassium kernel (see Figure 6.13.1). The CO is significantly perturbed by the action of the local electric field and consequently has a very low C-O stretching frequency (type 1 CO in Figure 6.13.1). Subsequent CO adsorption takes place at sites further from the potassium (type 2 in Figure 6.13.1), where the electric field is weaker due to both decay with distance and by the screening of the intervening CO molecules in the type 1 layer. Thse CO molecules have a higher C-O stretching frequency than those of type 1. Extensive intensity borrowing from the lower frequency band to the higher results in the virtual extinction of the lower band, associated with type 1 CO molecules. Thus the coverage dependent shift appears to be extremely large.

FIGURE 6.13.1 CO/K/Ni(111) $\theta_K = 0.02$

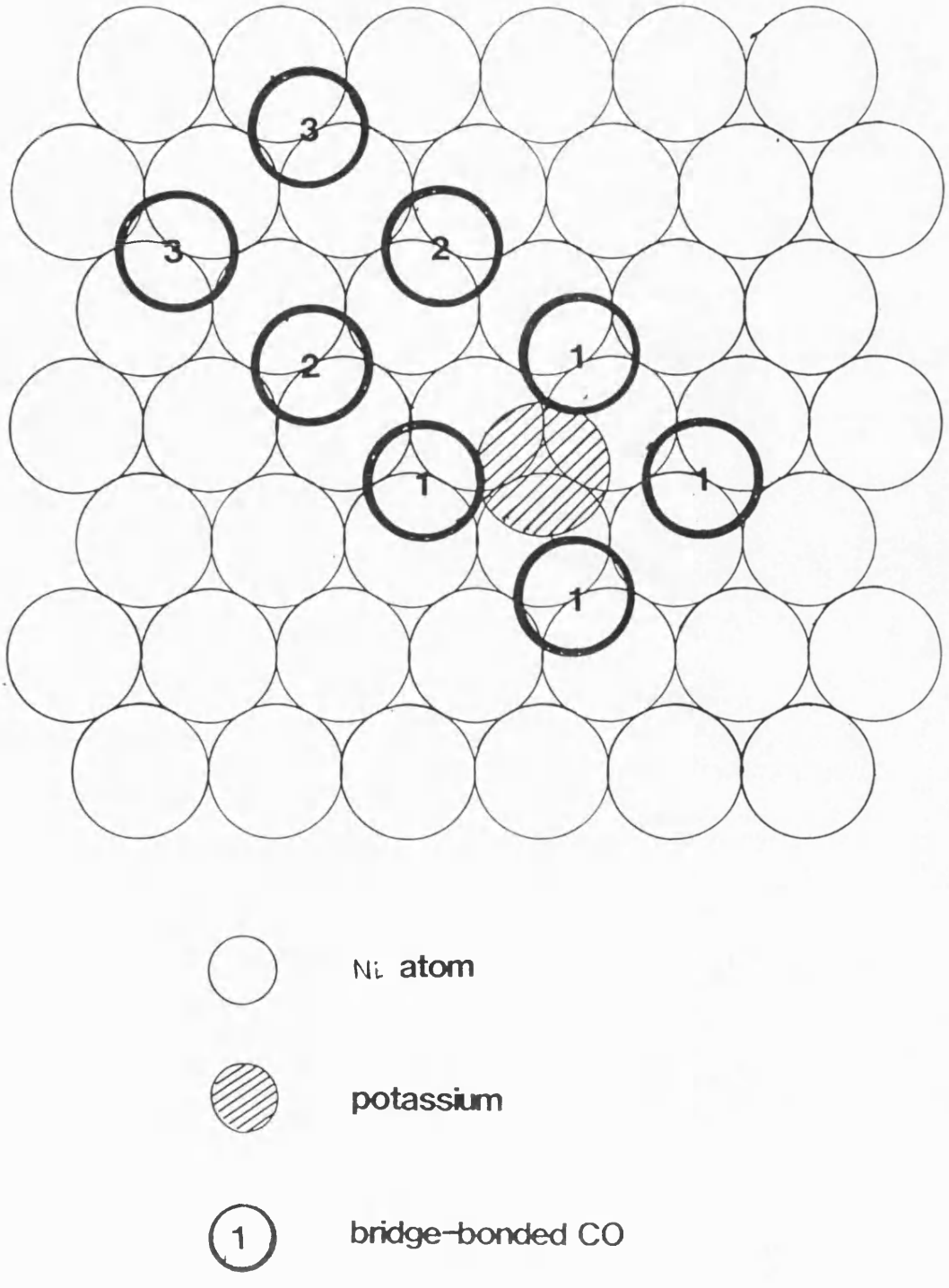

This process can continue with type 3 CO molecules, shifting the absorption band to a still higher frequency, until full coverage is reached. Each potassium ion has approximately 25 CO molecules associated with it in the island. The IR absorption bands are characterised by low frequency tails which might be indicative of such a model.

This model is similar to that proposed in section 6.7 to explain the existence of the doublet absorption band visible in the case of CO/K/Pt(110) with θ_K=0.05 except that in that case the bands associated with perturbed and relatively unperturbed CO are clearly visible as separate entities, intensity borrowing is not sufficient to extinguish the lower band.

It should also be noted that this potassium kernel model should result in an eventual decrease in the coverage dependent frequency shift, as the CO islands become sufficiently close together for the CO molecules at the edges to be affected by several different potassium ions, which is the interpretation given to the RAIRS spectra obtained for CO/K/Pt(110) in the higher potassium coverage regime (θ_K=0.1), where only a singleton species is visible. This is not observed for the CO/K/Ni(111) system, where the coverage dependent frequency shift appears to increase with increasing

potassium coverage up to a coverage of θ_K=0.16. It is unfortunate that no isotope mixture experiments have been carried out on CO/K/Ni(111) to determine if any of the observed coverage dependent frequency shift was of a chemical nature, i.e. perturbation of the occupancy of the $2\pi^*$ antibonding orbitals, which has been reported for the high potassium coverage limit for CO/K/Ni(111) [25].

The assignment of such large CO coverage dependent shifts on CO/K/Ni(111) which increase with potassium coverage, depends on the interpretation that there is one absorption band which shifts continuously with coverage. In the case of high potassium precoverage (θ_K=0.16) this is not necessarily the case as there appears to be a coverage insensitive band at 1434 cm^{-1} at low CO coverages. Yates and co-workers have suggested that this may be due to the formation of a potassium-CO ionic complex [42]; the frequency is similar to that reported for potassium deltate, $K_2[CO_3]$, 1445 cm^{-1}.

If the RAIRS spectra are interpreted as being a two band system then the first band is due to the complex formation and the second, which is CO coverage dependent, is due to CO further afield from the potassium kernel. The coverage dependent frequency shift of this CO species is then very similar for the

situations with potassium coverages of θ_K=0.06 and θ_K=0.16, although the singleton frequency in the higher coverage case is shifted down by ≈80-100 cm^{-1}. This is very similar to the results obtained in the present study of CO adsorption on K/Pt(110)-(1 x 2), suggesting the electrostatic interaction previously proposed, although there is still the ambiguity in the Ni(111) absorption system because contribution by chemical shifts have not been established.

6.14 Simple electrostatic interaction model

Yates and co-workers [42] have proposed that the electrostatic interaction between a charged potassium species and an adsorbed CO molecule can be modelled in terms of an array of simple electric dipoles (the potassium species) lying in an infinite conducting plane.

If the potassium species is represented by a point charge q at distance a above the infinite conduction plane, then the system can be represented as the field due to a dipole moment of 2qa lying in the plane (see Figure 6.14.1).

FIGURE 6.14.1

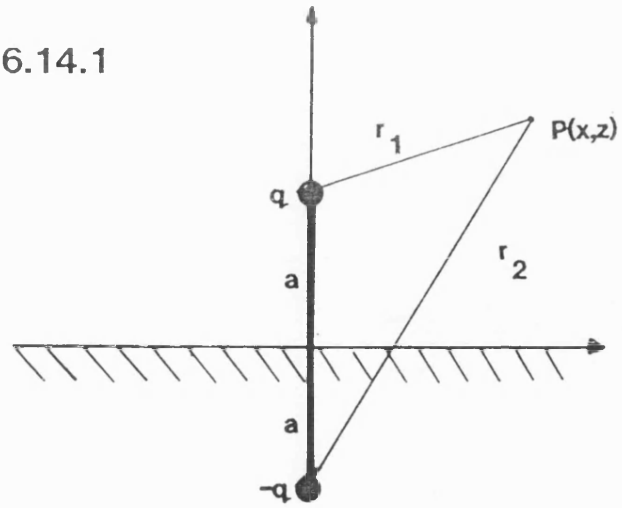

CHARGE OVER A CONDUCTING SURFACE AND IMAGE CHARGE

The potential V at a point P is then given by:

$$V = \frac{q}{4\pi\varepsilon\varepsilon_0}(1/r_1 - 1/r_2) \qquad (6.2)$$

and if the point P has cartesian coordinates x and z then

$$V = \frac{q}{4\pi\varepsilon\varepsilon_0}([(z-a)^2-x^2]^{-1/2} - [(z-a)^2-x^2]^{-1/2}) \qquad (6.3)$$

The component of the electric field in the z-direction is the differential of the z-component of this quantity:

$$E_z = \frac{q}{4\pi\varepsilon\varepsilon_0}\left(\frac{(z-a)}{[(z-a)^2+x^2]^{3/2}} - \frac{(z+a)}{[(z+a)^2+x^2]^{3/2}}\right) \qquad (6.4)$$

where z is the height above the conduction plane.

By choosing suitable values for a,z,x and q the charge on the potassium ion, Yates and co-workers were able to calculate an E_z value of 2.21×10^{-9} V/m at a distance of 0.36 nm from the potassium species, for the CO/K(θ_K=0.02)/Ni(111) adsorption system. The distance was chosen as the closest available CO adsorption site to the potassium. They then used the experimentally measured Stark tuning rate for Ni(100) [136,137] to determine the Stark shift due to the field E_z, -29 cm^{-1}. This was substantially lower than the experimentally observed value of -80 cm^{-1}. This model has been adapted

for the Pt(110)-(1 x 1) surface used in this work in order to to model the CO/K/Pt(110) adsorption system.

6.15 Modelling the CO/K/Pt(110) adsorption system

The model described above was adapted for the Pt(110) surface as follows: the infinite conduction plane was taken to run through the centre of the top row of platinum atoms at the surface, which was assumed to be ideal (1 x 1) (i.e. no reconstruction). The K^+ ions are assumed to have a charge of -e coulombs and so have an ionic radius of 0.133 nm. They sit in four-fold sites at the surface. The CO molecules are assumed to be adsorbed parallel to the surface normal, in on-top adsorption sites and with a C-O bond length of 0.115 nm and a Pt-C bond length of 0.198 nm [112]. Using these values and adsorption geometry, the height of the potassium charge above the conduction plane was calculated as 0.126 nm (parameter a in equation 6.4) and the height of the centre of mass of the C-O molecule was 0.264 nm (the parameter z). The values of the field E_z were then evaluated using equation 6.4 at varying distances from a single electric dipole, to simulate the formation of a single CO island with a potassium kernel.

The experimental Stark shift for Pt(111) has been determined by Lambert as 1.0×10^{-6} $cm^{-1}/V.cm^{-1}$ [138], so

that the shift in vibrational frequency due to the electric field was calculated, and is plotted against distance from the potassium ion in Figure 6.15.1. The field extends over ranges corresponding to several metal lattice parameters. In equation 6.4 the variables a,x,z are all of comparable size and therefore it should be expected that the values of the electric field would be rather sensitive to changes in the height of the potassium ion above the surface and the height of the centre of mass of the C-O molecule. In fact the magnitude of the Stark shift is rather insensitive to the height of the dipole above the surface (parameter a), but is much more sensitive to the height of the centre of mass of the CO molecule above the conduction plane (parameter z). The Stark shift for a CO molecule with a z parameter value of 0.244 nm above the surface is plotted in Figure 6.15.1 as a comparison with the upright CO. The height of the centre of mass above the conduction plane would certainly change for tilted CO molecules. This parameter is also highly dependent on the choice of the level of the conduction plane.

FIGURE 6.15.1

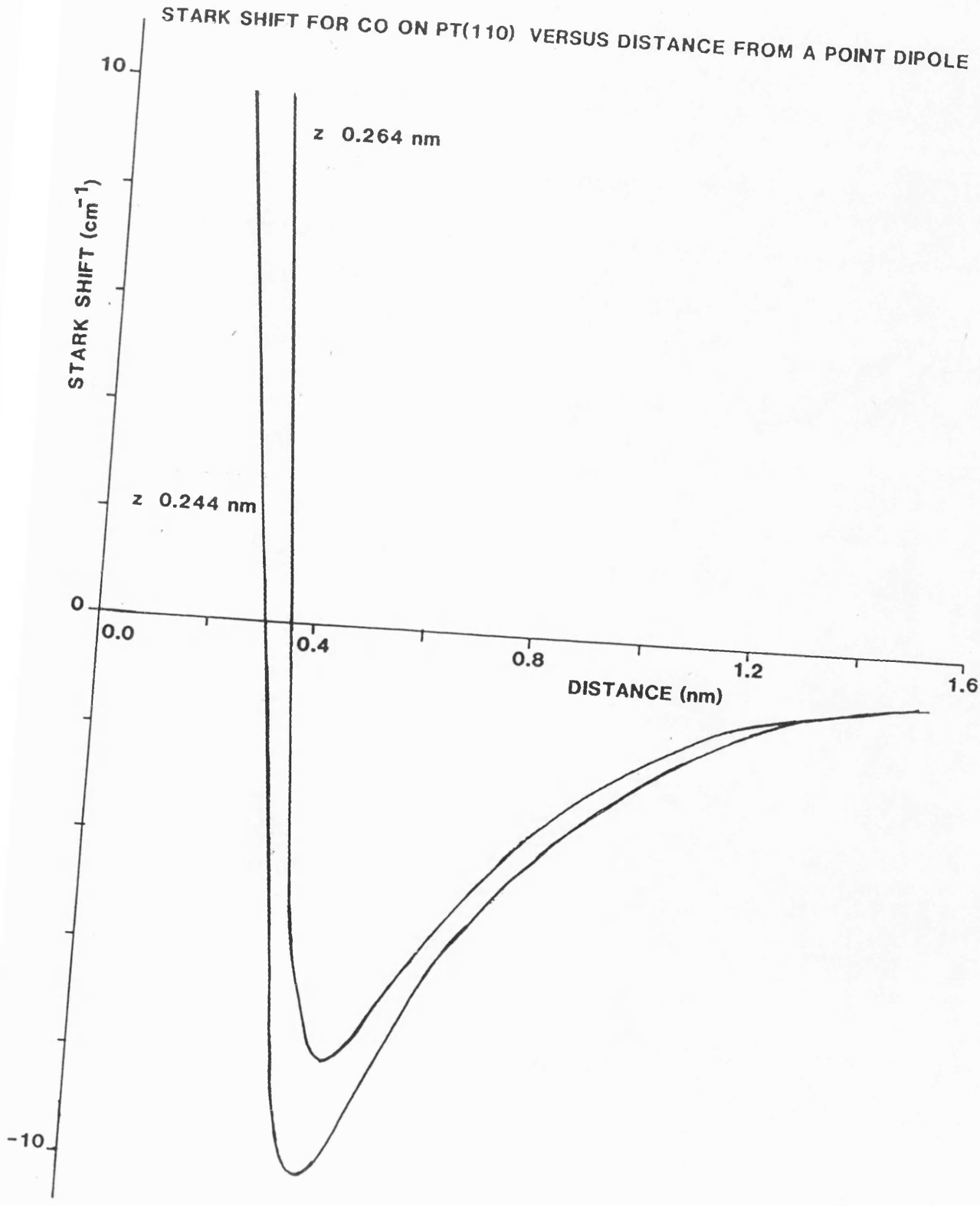
STARK SHIFT FOR CO ON PT(110) VERSUS DISTANCE FROM A POINT DIPOLE
10
0
-10
STARK SHIFT (cm^{-1})
z 0.264 nm
z 0.244 nm
0.0
0.4
0.8
1.2
1.6
DISTANCE (nm)

This model was then adapted to place a moderate coverage of potassium on the platinum surface. This is shown in Figure 6.15.2, where a net of K^+ ions are evenly spread over the surface, corresponding to a potassium coverage of Θ_K=0.083. In the model it is assumed that the four platinum atoms making up the 4-fold potassium adsorption site are blocked to CO adsorption. There are now three non-equivalent CO adsorption sites. The Stark shifts for each site has been calculated using equation 6.4, and summing over the electrostatic contributions of the nearest 16 potassium ions, assuming full coverage of CO on all available adsorption sites. The screening of the electrostatic potential by CO molecules is accounted for as in the model for CO/K/Ni(111), by using the relative dielectric constant 1.41 (the value for nitrogen) for the adsorbed layer.

For type 1 sites, there is screening by nearby CO from all potassium ions except for the closest pair; the calculated Stark shift is -22.3 cm^{-1}. For type 2 sites, all potassium ions are screened and the calculated Stark shift is -15.7 cm^{-1}. Type 3 sites are screened from all potassium ions except the closest and the calculated shift is -18.7 cm^{-1}.

FIGURE 6.15.2

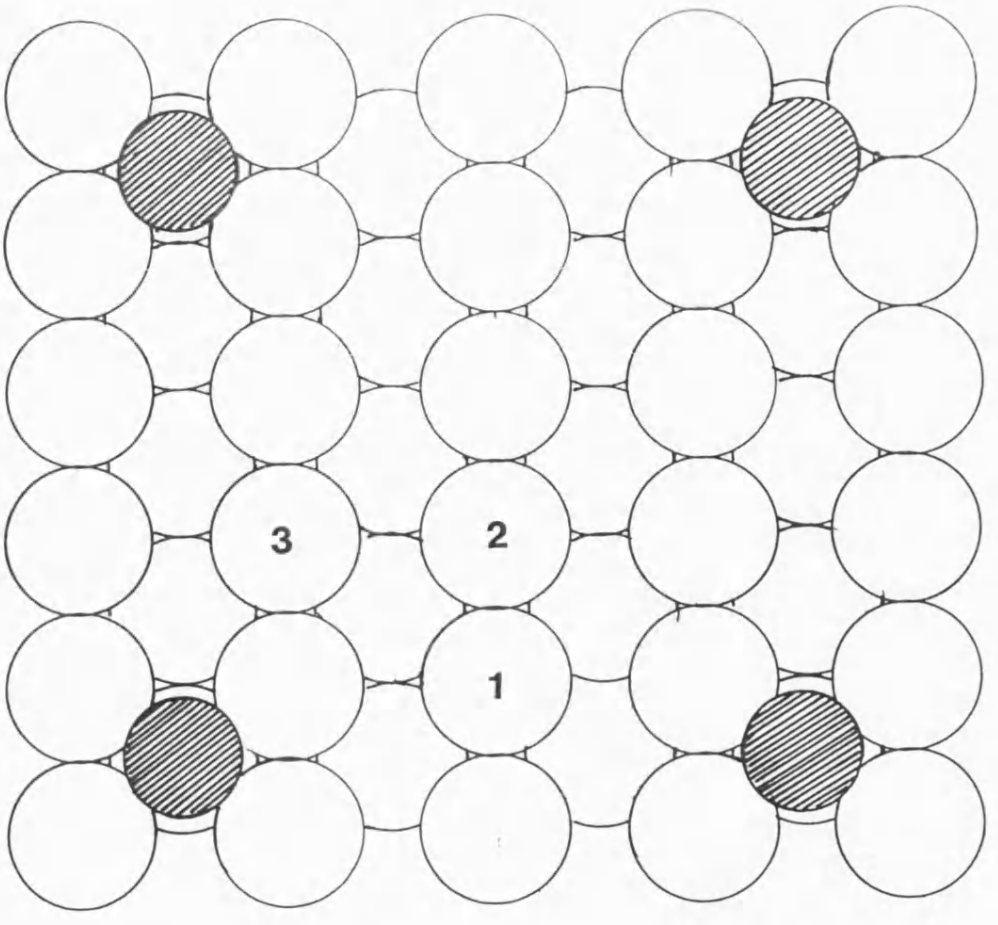

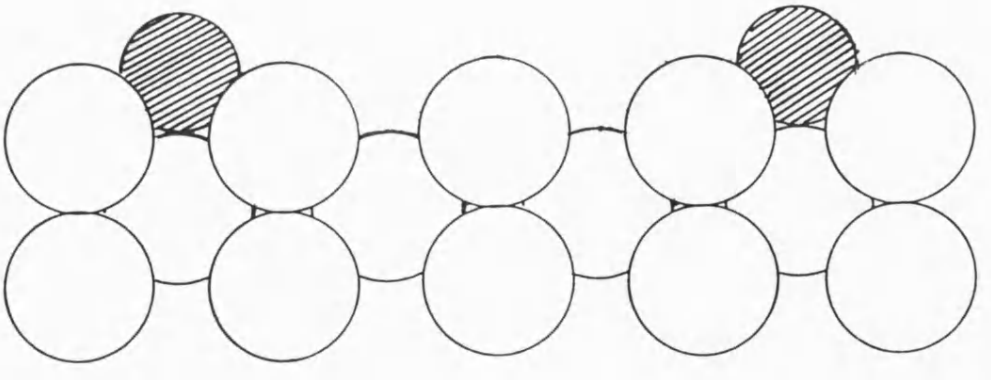

POTASSIUM OVERLAYER ON Pt(110)-(1x1):

NON-IDENTICAL CO ADSORPTION SITES

The model predicts Stark shifts of the order of 20 cm^{-1}, which is rather less than the experimentally deduced shift of -100 cm^{-1} for a similar coverage of potassium. However it does show a qualitative similarity to the experimentally observed RAIRS spectra, with an overall downward shift in C-O stretching frequency. Moreover the broadening of the RAIRS absorption band induced by the presence of potassium may be explained by the inhomogeneities in the electric field over different adsorption sites; the adsorbed CO molecules experience an electric field of a similar magnitude but not identical at all points on the surface. Hence the Stark shift is not the same for all adsorbed CO molecules.

There are several weaknesses in such a simple model:

(1) The calculations are sensitive to the parameters for bond lengths and adsorption geometry and to the choice of the position of the conduction plane.

(2) CO molecules are assumed to be adsorbed with the molecular axis parallel to the surface normal. However given the conclusions of chapter 4 and in preceding sections of this chapter, the CO molecule is probably tilted at higher coverages.

(3) Another result of the tilting of the C-O molecular axis from the surface normal is that the components of the electric field in the x and y directions would interact with the C-O dipole; this model only calculates the Stark shift due to interaction with the electric field normal to the surface.

(4) The experimentally observed Stark tuning rates are not necessarily due solely to the applied electric field. Bauschenlicher [139] has suggested that only one third of the experimentally measured Stark tuning rate is due to direct electric field-oscillator interactions.

Even with these reservations, this simple model qualitatively demonstrates the effects of applied electric fields to the vibrational frequency of adsorbates and shows that such interactions may extend over ranges corresponding to several metal lattice parameters.

6.16 CO induced reconstruction of Pt(110)-(1 x 2)

The coverage dependent frequency shift and the coverage dependent intensity of the CO absorption band on the K/Pt(110)-(1 x 2) surface are very similar to those measured on the clean Pt(110)-(1 x 2) surface. This suggests that the reconstruction of the surface is

a continuous process rather than a sudden phase change occurring at θ_{CO}=0.5. If a sudden change in the surface geometry occurred at a critical coverage of CO,in the presence of potassium, it would be expected that the position of the potassium relative to the co-adsorbed CO would also change. For example assuming a missing row model for the (1 x 2) surface, with potassium adsorbed in the missing rows, the lifting of the reconstruction to the (1 x 1) formation must force the potassium out of the troughs in the surface and hence change the potassium-CO distances. Thus the interaction between CO and potassium should also show an abrupt change at that critical coverage; either the onset of a large Stark shift, if the electrostatic interaction model applies, or the onset of a chemical shift contribution to the coverage dependent frequency shift if the electronic perturbation model applies. As there is no such abrupt change in comparison to the characteristics of the clean Pt(110)-(1 x 2) surface, it is suggested that the reconstruction is lifted locally by adsorbed CO and that this process is largely complete at a coverage θ_{CO}=0.5.

Conclusions

7.1 Adsorption of CO on Pt(110)-(1 x2) at 300K

The adsorption of CO on the reconstructed Pt(110)-(1 x 2) surface at 300K was studied using LEED, TPD measurements and RAIRS. The (1 x 2) LEED pattern is transformed to a (1 x 1) pattern on adsorption of CO at a coverage of θ_{CO}=0.5, when CO is adsorbed at 300K. If the clean reconstructed platinum surface is cooled in 5.0 x 10^{-7} mbar of CO from 600K down to 300K, a LEED pattern with systematic absences of the [1/2,0] diffraction beams is observed. This has been observed previously and is identified as the (2 x 1) p1g1 overlayer, formed by the existence of glide line symmetry elements in the CO overlayer due to the tilting of the C-O molecular axis away from the surface normal.

TPD studies show a single desorption peak at coverages of θ_{CO}<0.5, with a desorption energy of 140 kJ.mol^{-1}, assuming a first order process. At higher coverages, a secondary low temperature desorption peak appears corresponding to a desorption energy of 108 kJ.mol^{-1}. This feature is attributed to strong lateral interactions between CO molecules which occur at high coverages.

The RAIRS spectra of CO adsorbed on the surface

shows a single absorption band in the frequency range attributed to CO bonded in a linear configuration. The band shows a coverage dependent shift which is linear with coverage. The FWHM of the band is constant at all CO coverages at ≈18 cm^{-1}. Isotope experiments using mixtures of ^{12}CO and ^{13}CO demonstrate that this shift is wholly due to dipole-dipole coupling between CO molecules; there is no evidence of any contribution to the shift from chemical or static influences.

The integrated intensity of the absorption band due to the CO stretching mode shows an unusual dependence upon CO coverage, reaching a maximum at a coverage of θ_{CO}=0.5 and declining slightly thereafter.

The (2 x 1)p1g1 overlayer exhibits a TPD which has a less well defined low temperature desorption state. The coverage of the layer is equivalent to that of the saturated layer formed by adsorption at 300K. The RAIRS spectrum of the (2 x 1) p1g1 adlayer is slightly narrower at 16 cm^{-1}.

It is suggested that the large FWHM of both absorption bands is due to inhomogeneous broadening associated with inherent disorder caused by the lifting of the surface reconstruction.

A new model of CO adsorption on the Pt(110)-(1 x 2) surface at 300K is proposed in order to explain the

RAIRS and TPD observations. CO bonds in a linear configuration on on-top sites at all coverages. Up to a coverage of θ_{CO}=0.5, the C-O bond axis is normal to the surface and so intensity rises linearly with coverage. At higher CO coverages, the CO begins to be closely packed on the surface and strong lateral repulsions between the CO molecules cause the tilting of the C-O bond axis away from the surface normal. The onset of these repulsive interactions is visible in TPD spectra, where a low temperature feature appears. Tilting of the C-O molecular axis forms the glide line symmetry element responsible for the appearance of the (2 x 1)p1g1 overlayer under certain circumstances. The (2 x 1)p1g1 structure is not observed at 300K because the inherent disorder in the overlayer due to the lifting of the reconstruction. The tilting of the C-O molecular axis away from the surface normal causes a reduction of the normal component of the dynamic dipole moment and hence a reduction in the infra-red absorption cross-section of the adsorbed molecule and a reduction in the integrated intensity of the absorption band.

7.2 Adsorption of CO on Ru(001); new real space model

Investigations by RAIRS, TPD and LEED on the CO/Pt(110)-(1 x 2) adsorption system reveals striking

similarities with those on CO/Ru(001). A new real space model is proposed to explain CO adsorption on Ru(001) at coverages $0.33<\theta_{CO}<0.66$ in the light of the tilting model proposed for CO/Pt(110)-(1 x 2). This model consists of three domains of tilted CO in a $(2\sqrt{3}$ x $\sqrt{3})R30°$ structure, which have been reported to give a LEED pattern equivalent to a $(2\sqrt{3}$ x $2\sqrt{3})R30°$ pattern.

7.3 Adsorption of CO on Pt(110)-(1 x 2) at 100K

Adsorption of CO on Pt(110)-(1 x 2) at 100K does not lift the surface reconstruction. The RAIRS absorption band observed is extremely similar to that obtained for CO adsorption at 300K in magnitude of coverage dependent shift, intensity versus coverage behaviour and magnitude of intensity. It is concluded that the real space model for adsorption of CO on the Pt(110)-(1 x 2) surface which fits these observations best is that of the rumpled surface, where alternate close packed layers in the [110] direction relax upwards and downwards along the surface normal.

7.4 Co-adsorption of potassium and CO on Pt(110)-(1 x2)

The adsorption of CO on a Pt(110)-(1 x 2) surface doped with small coverages of potassium was studied using RAIRS, LEED and TPD.

Following a potassium precoverage of θ_K=0.10 the TPD spectra show a noticeable difference from that of CO adsorbed on the clean Pt(110)-(1 x 2) surface only at coverages $\theta_{CO}\approx$0.1, where the desorption peak temperature increases from 540K to 570K. At higher CO coverages, there is no observable differences between CO desorption at a clean surface and that at the doped surface.

RAIRS measurements for CO adsorption taken at potassium pre-coverages of θ_K=0.05 show a doublet absorption feature; at low exposures to CO there is a low frequency component, with a high frequency component appearing at higher exposures. The high frequency component has a frequency similar to that of CO on the clean surface. This is interpreted as being due to a long range interaction between potassium and CO on the surface. At low coverages CO preferentially adsorbs close to potassium ions. The interaction between the potassium and CO weakens the C-O stretch and produces a low frequency absorption band. As the CO coverage increases, the CO adsorbs at sites further way from the potassium kernel and so is relatively unperturbed. This results in the high frequency absorption band, similar in frequency to CO adsorbed on a clean surface appearing at large CO exposures.

At Θ_K=0.10, the RAIRS spectra show a single absorption band in the range 1985 cm^{-1} to 2035 cm^{-1} with a constant FWHM of 40 cm^{-1} at all coverages. The magnitude of the coverage dependent shift is identical to that of CO on the clean surface. The integrated intensity as a function of coverage also exhibits the same characteristics as the absorption band on the clean surface, From these observations it is apparent that the band observed is very similar to that of CO on the clean surface, with an overall downward shift of 100 cm^{-1} and a considerable increase in FWHM, from 18 cm^{-1} to 40 cm^{-1} from the clean surface to the doped one. Isotope mixture experiments performed upon the doped surface show that all of the coverage dependent shift is due to dipole-dipole interaction. There is no chemical shift induced by the presence of the potassium, despite the weakening of the C-O bond. This implies that the occupation of the $2\pi^*$ antibonding orbitals is not perturbed by the presence of potassium.

It is suggested that the nature of the interaction between the CO and potassium is that of a direct interaction between the C-O vibrational mode and the electric field induced by the presence of the partially ionised potassium at the surface i.e. the vibrational Stark effect.

A simple electrostatic model has been applied to the CO/K/Pt(110) system in order to determine the magnitude of Stark shifts upon CO molecules. The calculated Stark shifts obtained with this model are ≈25% of the observed ones; the model does reproduce qualitatively the broadening of the absorption band due to relative inhomogeneities of the applied electric field over different adsorption sites.

7.5 CO induced phase transition on Pt(110)-(1 x 2)

The lifting of the (1 x 2) reconstruction of the surface by adsorption of CO is visible in LEED at a coverage of Θ_{CO}=0.5. However it has not been clear whether this process occurs over the whole surface only at this critical coverage, or occurs locally on the surface with the process being completed at this coverage.

The RAIRS spectra obtained during this study all show similar characteristics in the size of the coverage dependent frequency shift and in the variation of the integrated intensity of the absorption band with coverage . These features occur for CO adsorption at 300K, at 100K and in the presence of low coverages of potassium. It may be concluded that the break in intensity of the absorption band at Θ_{CO}=0.5, measured

at 300K, is not due to the lifting of the reconstruction of the surface, reported to occur at the same coverage, since for CO adsorption at 100K the surface reconstruction is not lifted but the change in intensity is still present.

The similarity between the CO stretch absorption bands measured on the potassium-precovered platinum surface and on the clean surface suggest that no major surface restructuring occurs at a critical coverage, since this would be expected to change the position of potassium adatoms relative to the adsorbed CO molecules and hence change the potassium-CO interactions. The experimental evidence does not suggest a major change in the geometry of the adsorption system at θ_{CO}=0.5. Hence it is concluded that the (1 x 2) reconstruction is lifted locally by the adsorption of CO. This also accounts for the high degree of disorder on the surface, producing the broad C-O absorption band.

APPENDIX ONE

Master control program, IR.FOR, and associated FORTRAN subroutines to operate the RAIRS spectrometer, store spectra and plot them onto the Hirez-100 terminal and to the RY-101 digital plotter.

```
      PROGRAM IR
C
C     DATA AQUISITION PROGRAM FOR IR SPECTRA
C
C     ANDREW ROBINSON              AUGUST 12TH 1986
C
C
      DOUBLE PRECISION DNAME
      BYTE BTITLE(64),BFILE(6),BKEY(64),BDOT,BT,
     +BCOM(4),B
      COMMON/C/IBASE(400),IBDAY,IBMONT,IBYEAR,BSTART,
     +BFIN,BWIDTH,BSTEP,IBSPD,BSENS,BTIME,BOFFS,IBDAT,
     +BYSCAL,IBSPNO,IBYOFF,IBUF,ISPEC(400),ISDAY,ISMONT,
     +ISYEAR,START,SFIN,SWIDTH,STEP,ISPD,SENS,STIME,
     +SOFFS,ISDAT,SYSCAL,ISPNO,ISYOFF,IZ,DNAME,BFILE,
     +IFILE,ARG,IROLL,BTITLE,ID(9,2),IEXPB,IEXPS
C
C STARTING AND DEFAULT VALUES FOR BASELINE AND SPECTRUM
      CALL CLS
      IFILE=0      !CURRENT FILE NUMBER (SET TO BASELINE)
      BT='T'
      BDOT='.'
      ISDAT=101
      IBDAT=101
C
C
C
      CALL CURSOR(4,20)
      WRITE(7,81)
81    FORMAT(1X,
     +'RAIRS DATA AQUISITION AND DISPLAY PROGRAM')
      CALL CURSOR(6,20)
      WRITE(7,82)
82    FORMAT(1X,
     +'VERSION 1.11              JANUARY 29TH 1987')
C     IS DATE SET FROM RT 11 ?
      CALL DATE(IBDAY,IBMONT,IBYEAR)
      IF(IBDAY.NE.0) GOTO 904    !IF YES GOTO 904
909   CALL CURSOR(20,21)
      WRITE(7,901)
901   FORMAT(1X,'PLEASE SET THE DATE ')
      CALL CURSOR(22,31)
      WRITE(7,902)
902   FORMAT(1X,'FORMAT IS DD/MM/YY')
      READ(5,903,ERR=909) IBDAY,IBMONT,IBYEAR
```



```
      IF(IBDAY.EQ.0) GOTO 909
      CALL CLS
904   ISDAY=IBDAY
      ISMONT=IBMONT
      ISYEAR=IBYEAR
903   FORMAT(I2,1X,I2,1X,I2)
      ENCODE(6,950,DNAME)
950   FORMAT('SETUP1')
      CALL CURSOR(12,20)
      CALL RVIDEO
      WRITE(7,84)
84    FORMAT(1X,
     +'(I)NITIALISE MONOCHROMATOR OR (R)ESTART ? ')
      CALL CLEAR
83    CALL CURSOR(12,63)
      READ(5,86) B
86    FORMAT(A1)
      IF(B.EQ.73) GOTO 88      !INITIALISE
      IF(B.EQ.82) GOTO 89      !SKIP THE INITIALISATION
      GOTO 83
88    CALL CURSOR(13,20)
      CALL RVIDEO
      WRITE(7,85)
85    FORMAT(1X,
     +'MONOCHROMATOR NOW RUNNING BACK TO REVERSE LIMITS')
      CALL CLEAR
      IFILE=0
C     LOCKS KEYBOARD DURING MONOCHROMATOR MOTION
      CALL LOCK
      CALL IWCOM('R:')    !GIVE INCHWORM REVERSE COMMAND
      CALL GTREVL         !GOTO REVERSE LIMITS
      CALL UNLOCK
      ENCODE(6,1,BFILE) DNAME
1     FORMAT(A6)
      CALL CURSOR(12,20)
      CALL RVIDEO
      WRITE(7,*) 'READING SETUP FILE           '
      CALL CLEAR
      CALL FREAD
      ARG=1.
      CALL PTRANS
      IFILE=0
      CALL GTSTRT
      GOTO 10
C     CORE COMMAND MENU
```

```
C
C       ERROR TRAP SECTION
C
89      CALL FREAD
        ARG=1.
        CALL PTRANS
        IFILE=0
        GOTO 10
 7      CALL CURSOR(23,9)
        GOTO 12
 10     CALL PDISP()              !DISPLAY PARAMETERS
 11     CALL CURSOR(22,0)
        WRITE(7,*)
     - 'COMMAND>                                          '
        CALL CURSOR(22,9)
 12     READ(5,900,ERR=7) BCOM,ARG
900     FORMAT(4A1,F7.1)
        JDEX=INDEX('    STA=FIN=STE=SPE=SEN=TIM=OFF=BASE
     +RUN REA=SCRESAVEFIL=NAMEYSC= AUTOTITL CLB TRA MAR=
     +CLM PRM GOTOEXP YOF=INT GSTAGFINROL=READQUITPLOT
     +IPLODPLOKEY=DISPEXIT',BCOM)/4+1
        CALL CURSOR(3,1)
        WRITE(7,*) '
     +          '
        GOTO(200,210,220,230,240,250,260,270,275,280,
     +290,300,310,330,340,350,360,370,380,400,410,420,
     +450,460,470,480,500,510,530,540,550,560,570,580,
     +590,600) JDEX
C
C       END OF CENTRAL CORE
C
200     GOTO 11                       !IF NO COMMAND ENTERED
210     CALL CSTART
        CALL CURSOR(21,1)
        WRITE(7,*) '       '
        CALL CURSOR(21,1)
        IF(IFILE.EQ.0) GOTO 215      !BASELINE
        W=FREQ(START)
        WRITE(7,211) W
211     FORMAT(1X,F7.1)
C       CHANGE NUMBER OF POINTS
        CALL CPOINT(START,SFIN,STEP,ISDAT)
        GOTO 11
215     W=FREQ(BSTART)
        WRITE(7,211) W
```



```
        CALL CPOINT(BSTART,BFIN,BSTEP,IBDAT)    !AND AGAIN
        GOTO 11
220     CALL CFIN
        CALL CURSOR(21,9)
        WRITE(7,*) '       '
        CALL CURSOR(21,9)
        IF(IFILE.EQ.0) GOTO 225
        W=FREQ(SFIN)
        WRITE(7,221) W
221     FORMAT(1X,F7.1)
        CALL CPOINT(START,SFIN,STEP,ISDAT)
        GOTO 11
225     W=FREQ(BFIN)
        WRITE(7,211) W
        CALL CPOINT(BSTART,BFIN,BSTEP,IBDAT)
        GOTO 11
230     CALL CSTEP
        CALL CURSOR(21,17)
        WRITE(7,*) '       '
        IF(IFILE.EQ.0) GOTO 235
        CALL CURSOR(21,17)
        W=FREQ(START)-FREQ(SFIN)
        W=W*STEP/(SFIN-START)
        WRITE(7,231) W
231     FORMAT(1X,F7.1)
        CALL CPOINT(START,SFIN,STEP,ISDAT)
        GOTO 11
235     CALL CURSOR(21,17)
        W=FREQ(BSTART)-FREQ(BFIN)
        W=W*BSTEP/(BFIN-BSTART)
        WRITE(7,231) W
        CALL CPOINT(BSTART,BFIN,BSTEP,IBDAT)
        GOTO 11
240     CALL CSPEED
        CALL CURSOR(21,26)
        WRITE(7,*) '    '
        CALL CURSOR(21,26)
        IF(IFILE.EQ.0) GOTO 242
        WRITE(7,241) ISPD
241     FORMAT(1X,I3)
        GOTO 11
242     WRITE(7,241) IBSPD
        GOTO 11
250     CALL CSENS          !CHANGE LIA SENSITIVITY
        GOTO 11
```

```
C
260     CALL CTIME          !CHANGE LIA TIME CONSTANT
        GOTO 11
C
270     CALL COFFS          !CHANGE LIA OFFSET
        GOTO 11
C
275     IF(IFILE.EQ.0) GOTO 439  !RUNS BASELINE SPECTRUM
        ARG=0.
        CALL PTRANS      !DISPLAYED PARAMETERS TO BASELINE
        IFILE=0
        ARG=0.
        CALL CFILNO      !FILE NUMBER ALWAYS 0 FOR BASELINE
439     CALL RVIDEO
        CALL CURSOR(22,9)
        WRITE(7,281)
        CALL CLEAR
        CALL LOCK
        CALL GTSTRT      !GOTO START OF GRATING POSITION
        CALL UNLOCK
        CALL PDISP
        CALL CURSOR(22,9)
        CALL RVIDEO
        WRITE(7,282)
        CALL CLEAR
C       SETS DYNAMIC RESERVE ON LIA TO NORMAL
        CALL ALTER1('R:',1)
        CALL BASE                !RUNS THE BASELINE SPECTRUM
        CALL ALTER1('X:',0)      !TURNS EXPAND OFF
        IF(IZ.EQ.1) GOTO 11
        CALL PSCREE
        CALL CURSOR(2,1)
        CALL RVIDEO
        WRITE(7,276)
276     FORMAT(1X,'SAVE BASELINE FILE ?  Y/N ')
        CALL CLEAR
277     CALL CURSOR(2,27)
        READ(5,440) B
440     FORMAT(A1)
        IF(B.EQ.89)      GOTO 279        !WRITE THE FILE
        IF(B.EQ.78)      GOTO 278        !DON'T WRITE IT
        GOTO 277
279     CALL FSAVE                       !SAVES THE FILE
278     CALL CURSOR(3,1)
        WRITE(7,*) '
```



```
        CALL CURSOR(23,9)
        GOTO 11
280     IFILE=IFILE+1              !INCREMENT FILE NUMBER
        ARG=FLOAT(IFILE)
        CALL PTRANS
        CALL PDISP
        CALL RVIDEO
        CALL CURSOR(22,9)
        WRITE(7,281)
281     FORMAT(1X,'MOVING TO STARTING POSITION')
        CALL CLEAR
        CALL LOCK
        ARG=0.
        CALL GTSTRT
        CALL UNLOCK
        CALL CURSOR(22,9)
        CALL RVIDEO
        WRITE(7,282)
282     FORMAT(1X,'NOW RUNNING - CTRL Z TO ABORT')
        CALL CLEAR
C       SETS DYNAMIC RESERVE ON LIA TO NORMAL
        CALL ALTER1('R:',1)
        CALL RUN
        CALL ALTER1('X:',0)              !TURNS EXPAND OFF
        IF(IZ.EQ.1) IFILE=IFILE-1        !IF ABORTED
C       IZ SET IF CTRL Z PRESSED IN RUN MODE
        IF(IZ.EQ.1) GOTO 11
        CALL PSCREE
        CALL CURSOR(2,1)
        CALL RVIDEO
        WRITE(7,283)
283     FORMAT(1X,'SAVE SPECTRUM FILE ?  Y/N ')
        CALL CLEAR
        CALL CURSOR(2,27)
284     READ(5,440) B
        IF(B.EQ.89)      GOTO 286        !WRITE THE FILE
        IF(B.EQ.78)      GOTO 285
        GOTO 284
286     CALL FSAVE
285     CALL CURSOR(3,1)
        WRITE(7,*) '
        CALL CURSOR(23,9)
        GOTO 11
290     CALL CFILNO          !CHANGES FILE NUMBER TO ARG
        CALL FREAD           !READS FILE WITH THAT NUMBER
```

```
      CALL PDISP
      CALL CURSOR(23,9)
      CALL PSCREE
      CALL CURSOR(23,9)
      GOTO 11
300   CALL CURSOR(23,9)
      CALL PSCREE
      CALL CURSOR(23,9)
      GOTO 11
C
310   CALL FSAVE      !SAVES FILE WITH CURRENT FILE NUMBER
      GOTO 11
320   CALL CFILNO
      IF(IFILE.NE.0) CALL CPOINT(START,SFIN,STEP,ISDAT)
      IF(IFILE.EQ.0) CALL CPOINT(BSTART,BFIN,BSTEP,IBDAT)
      GOTO 11
330   CALL CNAME              !CHANGE NAME OF FILE
      GOTO 11
340   CALL CYSCAL             !CHANGE SCREEN Y SCALE
      CALL CURSOR(23,9)
      CALL PSCREE
      CALL CURSOR(23,9)
      GOTO 11
350   NRUN=INT(ARG)           !AUTO RUN ROUTINE
      IRUN=0
      IF(NRUN.EQ.0) NRUN=99
351   IFILE=IFILE+1
      IRUN=IRUN+1
      ARG=FLOAT(IFILE)
      IF(IRUN.EQ.1) CALL PTRANS
      CALL PDISP
      CALL CURSOR(22,9)
      CALL RVIDEO
      WRITE(7,353)
353   FORMAT(1X,'RUNNING BACK FOR NEXT SCAN')
      CALL CLEAR
      CALL LOCK
      ARG=0.
      CALL GTSTRT
      CALL UNLOCK
      CALL CURSOR(22,9)
      CALL RVIDEO
      WRITE(7,352)
352   FORMAT(1X,'AUTO RUN - CTRL Z TO ABORT')
      CALL CLEAR
```



```
C     SET DYNAMIC RESERVE ON LIA TO NORMAL
      CALL ALTER1('R:',1)
      CALL RUN
      CALL ALTER1('X:',0)      !TURNS EXPAND OFF
      IF(IZ.EQ.1) GOTO 11      !IZ SET IF CTRL Z PRESSED
      CALL FSAVE
      IF(IFILE.LT.NRUN) GOTO 351
      CALL PSCREE
      GOTO 11
360   CALL CTITLE
      GOTO 11
370   DO 60 I=1,400
      IBASE(I)=0
60    CONTINUE
      GOTO 11
380   CALL PTRANS
      CALL PDISP
      GOTO 11
400   CALL MARKER
      CALL PMARKR
      GOTO 11
410   DO 411 I=1,9            !CLEAR THE MARKER POINTS
      ID(I,1)=0
      ID(I,2)=0
411   CONTINUE
      GOTO 11
420   CALL PMARKR             !PRINTS MARKERS ON SCREEN
      GOTO 11
450   CALL RVIDEO
      CALL CURSOR(22,9)
      WRITE(7,451)
451   FORMAT(1X,'MOVING TO START POSITION')
      CALL CLEAR
      CALL LOCK
      CALL GTSTRT
      CALL UNLOCK
      GOTO 11
460   CALL STAT1('X:',N)              !IS EXPAND ON ?
      CALL CURSOR(21,78)
      IF(N.EQ.1) GOTO 462             !NO
      WRITE(7,461)
461   FORMAT(1X,'EXP')
      IEXP=1
      IF(IFILE.EQ.0) IEXPB=1
      IF(IFILE.GT.0) IEXPS=1
```

```
      GOTO 464
462   WRITE(7,463)
463   FORMAT(1X,'    ')
      IF(IFILE.EQ.0) IEXPB=0
      IF(IFILE.GT.0) IEXPS=0
      IEXP=0
464   CALL ALTER1('X:',IEXP)          !CHANGE IF NECESSARY
      CALL CURSOR(23,9)
      GOTO 11
470   CALL CYOFF
      CALL PSCREE
      GOTO 11
480   CALL IRINT                  !INTEGRATION SUBROUTINES
      CALL CURSOR(23,9)
      GOTO 11
500   IF(IFILE.EQ.0) ARG=FREQ(BSTART) !MOVES TO START
      IF(IFILE.GT.0) ARG=FREQ(START)
      CALL RVIDEO
      CALL CURSOR(22,9)
      WRITE(7,501)
501   FORMAT(1X,'MOVING TO START ')
      CALL CLEAR
      CALL LOCK
      CALL GTSTRT
      CALL UNLOCK
      GOTO 11
510   IF(IFILE.EQ.0) ARG=FREQ(BFIN)
      IF(IFILE.GT.0) ARG=FREQ(SFIN)
C     MOVES END OF SPECTRUM
      CALL RVIDEO
      CALL CURSOR(22,9)
      WRITE(7,511)
511   FORMAT(1X,'MOVING TO FINISH')
      CALL CLEAR
      CALL LOCK
      CALL GTSTRT
      CALL UNLOCK
      GOTO 11
520   CALL CROLL                  !CHANGES ROLLOFF ON LIA
      GOTO 11
530   CALL FREAD                  !READS FILE
      CALL PDISP
      CALL CURSOR(23,9)
      CALL PSCREE
      CALL CURSOR(23,9)
```



```
      GOTO 11
540   CALL CLS          !QUIT(SAME AS EXIT,BUT LEAVES
      CALL TSETUP       !EXPAND ON) USED IF THE INCHWORM
      CALL CLG          !AND ENCODER ARE OFF
      CALL TEND
      GOTO 999                        !STOP
550   IF((ARG.GT.0.).AND.(ARG.LT.4.)) GOTO 559
C     STRAIGHT TO PLOT ROUTINE
C     NB DOES NOT PLOT INTEGRATED SPECTRA
      CALL BOLD
      CALL CURSOR(6,1)
      WRITE(7,*) 'OPTIONS'
      CALL CURSOR(8,1)
      WRITE(7,553)
553   FORMAT(1X,'GRAPH WITH AXES              1.')
      WRITE(7,554)
554   FORMAT(1X,'GRAPH WITHOUT AXES           2.')
      WRITE(7,555)
555   FORMAT(1X,'MARKERS ONLY                 3.')
      CALL CLEAR
      CALL CURSOR(22,0)
      WRITE(7,558)
558   FORMAT(1X,'OPTION >',$)
      READ(5,551) ARG
551   FORMAT(F5.2)
      CALL CURSOR(6,1)
      DO 556 I=1,6
      WRITE(7,552)
556   CONTINUE
552   FORMAT(1X,
     +'                                                ')
      ARG=FLOAT(INT(ARG))
      IF(ARG.GT.3) GOTO 11      !ILLEGAL VALUE;ABORT
      IF(ARG.EQ.0.) GOTO 550    !BACK TO MENU
559   CALL GPLOT
      GOTO 11
560   IBUF=1                    !SETS IBUF=1 INTEGRATE MODE
      CALL CURSOR(20,78)
      WRITE(7,*) 'INT'
      GOTO 11
570   IBUF=0              !SETS IBUF FOR DIFFERENTIAL MODE
      CALL CURSOR(20,78)
      WRITE(7,*) 'DIF'
      GOTO 11
580   I=INT(ARG)              !PROGRAM USER KEYS F11 TO F20
```

```
      IF((I.LE.0).OR.(I.GT.10)) GOTO 11 !KEY OUT OF RANGE
      CALL CURSOR(2,1)
      CALL RVIDEO
      WRITE(7,582) I
582   FORMAT(1X,
     +'DEFINE FN KEY SHIFT F',I1,'     USE  ! AS RETURN')
      CALL CLEAR
      CALL CURSOR(22,0)
      WRITE(7,583) I
583   FORMAT(1X,
     +'KEY F',I1,' >                                  ')
      CALL CURSOR(22,9)
      READ(5,581) BKEY
581   FORMAT(64A1)
      I=I+9            !WE ARE USING FN KEYS 10 TO 19
      CALL KEY(I,BKEY)
      GOTO 10
590   GOTO 10
600   CALL ALTER1('X:',0)        !TURNS EXPAND OFF
      CALL CLS                   !CLEARS TEXT
      CALL TSETUP
      CALL CLG                   !CLEARS GRAPHICS
      CALL TEND
999   STOP
```

Subroutines for IR.FOR follow:

To save space the common block has been removed from the beginning of each subroutine except CPOINT which does not require the common block. The functions FREQ and POSIT also do not require alteration. The common block is:

```
      COMMON/C/IBASE(400),IBDAY,IBMONT,IBYEAR,BSTART,
     +BFIN,BWIDTH,BSTEP,IBSPD,BSENS,BTIME,BOFFS,IBDAT,
     +BYSCAL,IBSPNO,IBYOFF,IBUF,ISPEC(400),ISDAY,ISMONT,
     +ISYEAR,START,SFIN,SWIDTH,STEP,ISPD,SENS,STIME,
     +SOFFS,ISDAT,SYSCAL,ISPNO,ISYOFF,IZ,DNAME,BFILE,
     +IFILE,ARG,IROLL,BTITLE,ID(9,2),IEXPB,IEXPS


      SUBROUTINE BASE
      DOUBLE PRECISION DNAME
      BYTE BTITLE(64),BFILE(6),BKEY(64),BDOT,BT,
     +BCOM(4),B
C
```



```
      IF(IFILE.NE.0) GOTO 298
      CALL CFILNO
      IXOFF=37
      IYOFF=180
      IZ=0
      IBST=INT(FREQ(BSTART))
      INC=INT(FREQ(BSFIN)-FREQ(BSTART))/10
      BPIX=950./(FLOAT(IBDAT))
      RATIO=BSENS/SENS
      ARG=BTIME
      CALL CTIME
      ARG=BSENS
      CALL CSENS
      ARG=BOFFS
      CALL COFFS
      ARG=FLOAT(IBSPD)
      CALL CSPEED
      ARG=BSTEP*(FREQ(BFIN)-FREQ(BSTART))/(BSTART-BFIN)
      CALL CSTEP
      CALL ALTER1('X:',IEXPS)
      CALL CPOINT(BSTART,BFIN,BSTEP,IBDAT)
      T0=SECNDS(0.)
3     T1=SECNDS(T0)
      IF(T1.LE.4.) GOTO 3
      CALL CURSOR(23,9)
      CALL TSETUP
      CALL CLG
      CALL TAXIS(IXOFF,180,950,0,95,IBST,INC)
      CALL HOME
      CALL TMOVE(IXOFF,IYOFF)
      IEND=ISDAT-1
      IBASE(0)=0
      CALL STAT1('Q1:',IBASE(0))
      IY=INT((RATIO*IBASE(0))+IYOFF+IBYOFF
      IF(IY.GT.779) IY=779
      IF(IY.LT.180) IY=180
      CALL TMOVE(IXOFF,IY)
      DO 249 J=1,IEND
      CALL IWCOM('F:')
288   CALL IWSTAT(IS,IPOS,IPOS2)
      IF(IS.NE.132) GOTO 700
      CALL IWCOM('@R:')
700   IF(IS.NE.232) GOTO 288
      IBASE(J)=0
      DO 4 L=1,1000
```

```
4       CONTINUE
        CALL STAT1('Q1:',IBASE(J))
        IX=INT(J*BPIX)+IXOFF
        IY=INT((RATIO*IBASE(J)BYSCAL)+IYOFF+IBYOFF
        IF(IY.GT.779) IY=779
        IF(IY.LT.180) IY=180
        CALL TDRAW(IX,IY)
        IFLAG=ITTINR()
        IF(IFLAG.EQ.26) GOTO 770  !ABORT IF  CTRL Z ENTERED
249     CONTINUE
        GOTO 771
770     IZ=1
771     CALL TEND
261     RETURN
        END

        SUBROUTINE CFILNO
        DOUBLE PRECISION DNAME
        BYTE BTITLE(64),BFILE(6),BKEY(64),BDOT,BT,
     +BCOM(4),B
C
        IF (ARG.LT.0.) GOTO 147
        IF (ARG.GT.99.) GOTO 147
        IFILE=INT(ARG)
        IF(IFILE.GT.0)  ISPNO=IFILE
        IBSPNO=0
        CALL CURSOR(1,9)
        WRITE(7,*) '  '
        CALL CURSOR(1,9)
        IF(IFILE.EQ.0) WRITE(7,144)
144     FORMAT(1X,'BS')
        IF((IFILE.NE.0).AND.(IFILE.LT.10))
     +WRITE(7,145) IFILE
145     FORMAT(1X,'0',I1)
        IF(IFILE.GE.10) WRITE(7,146) IFILE
146     FORMAT(1X,I2)
        GOTO 149
147     CALL CURSOR(2,1)
        CALL RVIDEO
        WRITE(7,148)
148     FORMAT(1X,'ERROR - FILE NUMBER OUT OF RANGE')
        CALL CLEAR
149     RETURN
        END
```



```
        SUBROUTINE CLBASE
        DOUBLE PRECISION DNAME
        BYTE BTITLE(64),BFILE(6),BKEY(64),BDOT,BT,
     +BCOM(4),B
C       CLEARS THE BASELINE ARRAY
C
C       (DOES NOT AFFECT BASELINE ATTRIBUTES)
C
        DO 101 I=0,400
        IBASE(I)=0
101     CONTINUE
        RETURN
        END
        SUBROUTINE COFFS
        DOUBLE PRECISION DNAME
        BYTE BTITLE(64),BFILE(6),BKEY(64),BDOT,BT,
     +BCOM(4),B
        IF (ARG.EQ.0.) N2=0
        IF (ARG.GT.0.) N2=1
        IF (ARG.LT.0.) N2=2
        IF (ARG.LT.0.) ARG=-ARG
        IF (IFILE.EQ.0) GOTO 114          !BASELINE
        IF (ARG.LE.SENS) GOTO 111         !IF OFFSET<SENS
        CALL CURSOR(2,1)
        CALL RVIDEO
        WRITE(7,110)
110     FORMAT(1X,
     +'WARNING - OFFSET GREATER THAN SENSITIVITY')
        CALL CLEAR
        GOTO 116
111     SOFFS=ARG
        CALL CURSOR(21,50)
        WRITE(7,112)
112     FORMAT(1X,'          ')
        IF(N2.EQ.2) SOFFS=-SOFFS
        CALL CURSOR(21,51)
        WRITE(7,113) SOFFS
113     FORMAT(1X,G10.3)
        IOFFS=INT((ARG/SENS)*1000.)
C
        CALL ALTER2('O:',IOFFS,N2)
C
        GOTO 116
114     IF(ARG.LE.BSENS) GOTO 115
        CALL CURSOR(2,1)
```

```
      CALL RVIDEO
      WRITE(7,110)
      CALL CLEAR
      GOTO 116
115   BOFFS=ARG
      CALL CURSOR(21,50)
      WRITE(7,117)
117   FORMAT(1X,'          ')
      IOFFS=INT((ARG/BSENS)*1000.)
      IF(N2.EQ.2) BOFFS=-BOFFS
      CALL CURSOR(21,51)
      WRITE(7,118) BOFFS
118   FORMAT(1X,G10.3)
C
      CALL ALTER2('O:',IOFFS,N2)
116   RETURN
      END

      SUBROUTINE CPOINT(START,FINISH,STEP,IPTS)
      IPTS=INT((FINISH-START)/STEP)+1
      IF(IPTS.LE.400) GOTO 93
      CALL CURSOR(2,1)
      CALL RVIDEO
      WRITE(7,92)
92    FORMAT(1X,
     +'WARNING -MORE THAN 400 POINTS IN THIS SPECTRUM')
      CALL CLEAR
      GOTO 95
93    CALL CURSOR(21,74)
      WRITE(7,90)
90    FORMAT(1X,'   ')
      CALL CURSOR(21,74)
      WRITE(7,91) IPTS
91    FORMAT(1X,I3)
95    RETURN
      END

      SUBROUTINE CROLL
      DOUBLE PRECISION DNAME
      BYTE BTITLE(64),BFILE(6),BKEY(64),BDOT,BT,
C
      IF(ARG.EQ.0) GOTO 100
      IF(ARG.EQ.6.) IROLL=6
      IF(ARG.EQ.12.) IROLL=12
      GOTO 110
```



```
100   CALL CURSOR(2,1)
      CALL RVIDEO
      WRITE(7,101) IROLL
101   FORMAT(1X,'ROLL-OFF SET AT ',I2,' DB/OCTAVE')
      CALL CLEAR
110   RETURN
      END

      SUBROUTINE CSTEP
      DOUBLE PRECISION DNAME
      BYTE BTITLE(64),BFILE(6),BKEY(64),BDOT,BT,
     +BCOM(4),B
C
      IF(ARG.LE.0.) GOTO 76
      WSPEC=FREQ(START)-FREQ(SFIN)
      WBASE=FREQ(BSTART)-FREQ(BFIN)
      IF((ARG.GT.WSPEC).AND.(IFILE.NE.0)) GOTO 73
      IF((ARG.GT.WBASE).AND.(IFILE.EQ.0)) GOTO 73
      IF(IFILE.EQ.0) BSTEP=(BFIN-BSTART)*ARG/WBASE
      IF(IFILE.GT.0) STEP=(SFIN-START)*ARG/WSPEC
      GOTO 75
73    CALL CURSOR(2,1)
      CALL RVIDEO
      WRITE(7,74)
74    FORMAT(1X,'VALUE GIVEN GREATER THAN SPECTRUM WIDTH')
      CALL CLEAR
      GOTO 76
75    CALL CPOINT(BSTART,BFIN,BSTEP,IBDAT) !NO. OF POINTS
      CALL CPOINT(START,SFIN,STEP,ISDAT)   !NO. OF POINTS
      IF(IFILE.EQ.0) GOTO 701
      IS=10*INT(STEP)
      GOTO 702
701   IS=10*INT(BSTEP)
702   CALL IWSEND('T:',IS)
76    RETURN
      END

      SUBROUTINE CTIME
      DOUBLE PRECISION DNAME
      BYTE BTITLE(64),BFILE(6),BKEY(64),BDOT,BT,
     +BCOM(4),B
C
      IF(ARG.GT.100.) ARG=100.
      IF(ARG.LT.0.001) GOTO 127
C     TIMECONSTANT LESS THAN 1 MILLISECOND
```

```
      RMAX=100.
      RMIN=30.
      DUMMY=0.
      NTC=0
      I=0
      TC=0.
121   IF((ARG.LE.RMAX).AND.(ARG.GT.RMIN)) TC=RMAX
      IF((ARG.LE.RMAX).AND.(ARG.GT.RMIN)) NTC=I
      DUMMY=RMAX
      RMAX=RMIN
      RMIN=DUMMY/10.
      I=I+1
      IF(I.EQ.10) GOTO 122
      GOTO 121
C
C     LIA COMMAND T NTC,IROLL
C      (IROLL IS 6 OR 12 DB/OCTAVE )
C
122   IF(IROLL.EQ.6) J=1
      IF(IROLL.EQ.12) J=0
      CALL ALTER2('T:',NTC,J)
      IF (IFILE.EQ.0) GOTO 125
      STIME=TC
      CALL CURSOR(21,40)
      WRITE(7,123)
123   FORMAT(1X,'        ')
      CALL CURSOR(21,40)
      WRITE(7,124) STIME
124   FORMAT(1X,G9.2)
      GOTO 126
125   BTIME=TC
      CALL CURSOR(21,40)
      WRITE(7,123)
      CALL CURSOR(21,40)
      WRITE(7,124) BTIME
      GOTO 126
127   CALL CURSOR(2,1)
      WRITE(7,128)
128   FORMAT(1X,
     +'ERROR - TIMECONSTANT LESS THAN 1 MILLISECOND')
126   RETURN
      END

      SUBROUTINE CTITLE
      DOUBLE PRECISION DNAME
```



```
      BYTE BTITLE(64),BFILE(6),BKEY(64),BDOT,BT,
     +BCOM(4),B
C
      DO 10 J=1,64
      BTITLE(J)=32
10    CONTINUE
      CALL CURSOR(2,1)
      CALL RVIDEO
      WRITE(7,*) '>'
      CALL CLEAR
      CALL CURSOR(2,66)
      CALL RVIDEO
      WRITE(7,*) '<'
      CALL CLEAR
      CALL CURSOR(2,2)
      READ(5,100) BTITLE
100   FORMAT(64A1)
      CALL CURSOR(1,13)
      WRITE(7,*) '
     +                '
      CALL CURSOR(1,13)
      WRITE(7,101) BTITLE
101   FORMAT(1X,64A1)
      CALL CURSOR(2,1)
      WRITE(7,*) '

     +                '
      RETURN
      END

      SUBROUTINE CYOFF
      DOUBLE PRECISION DNAME
      BYTE BTITLE(64),BFILE(6),BKEY(64),BDOT,BT,
     +BCOM(4),B
C
      IF(ARG.GT.768) GOTO 101
      IF(IFILE.EQ.0) IBYOFF=INT(ARG)
      IF(IFILE.GT.0) ISYOFF=INT(ARG)
      CALL CURSOR(21,68)
      WRITE(7,*) '      '
      CALL CURSOR(21,68)
      IF(IFILE.EQ.0) WRITE(7,100) IBYOFF
      IF(IFILE.GT.0) WRITE(7,100) ISYOFF
100   FORMAT(1X,I4)
101   RETURN
      END
```

```
      SUBROUTINE CYSCAL
      DOUBLE PRECISION DNAME
      BYTE BTITLE(64),BFILE(6),BKEY(64),BDOT,BT,
     +BCOM(4),B
C
      IF(ARG.LE.0.) GOTO 175
      IF(IFILE.EQ.0) GOTO 172
      SYSCAL=ARG
      CALL CURSOR(21,62)
      WRITE(7,100)
100   FORMAT(1X,'     ')
      CALL CURSOR(21,62)
      WRITE(7,101) SYSCAL
101   FORMAT(1X,F5.2)
      GOTO 175
172   BYSCAL=ARG
      CALL CURSOR(21,62)
      WRITE(7,100)
      CALL CURSOR(21,62)
      WRITE(7,101) BYSCAL
175   RETURN
      END

      SUBROUTINE FREAD
      DOUBLE PRECISION DNAME
      BYTE BTITLE(64),BFILE(6),BKEY(64),BDOT,BT,
     +BCOM(4),B
C
      BDOT='.'
      BB='B'
      BS='S'
      BI='I'
      IZERO=0
      IF(IFILE.EQ.0) GOTO 405
      IF(IFILE.LT.10) GOTO 401
      ENCODE(10,400,BNAME) DNAME,BDOT,BI,IFILE
400   FORMAT(A6,A1,A1,I2)
      GOTO 403
401   ENCODE(10,402,BNAME) DNAME,BDOT,BI,IZERO,IFILE
402   FORMAT(A6,A1,A1,I1,I1)
403   OPEN(UNIT=10,NAME=BNAME,TYPE='OLD',ERR=409)
      READ(10,500,ERR=420) BNAME
      READ(10,509,ERR=420) BTITLE
      READ(10,501,ERR=420) ISDAY,ISMONT,ISYEAR
```



```
      READ(10,502,ERR=420) START,SFIN,SWIDTH
      READ(10,503,ERR=420) STEP,ISPD
      READ(10,504,ERR=420) SENS,STIME,SOFFS
      READ(10,505,ERR=420) ISDAT,SYSCAL,ISPNO
      READ(10,508,ERR=420) ISYOFF,IEXPS
      IEND=ISDAT-1
      DO 404 I=0,IEND
      READ(10,506,ERR=420) ISPEC(I)
404   CONTINUE
      DO 440 I=1,9                    !READ MARKERS
      READ(10,507) ID(I,1),ID(I,2)
440   CONTINUE
      CLOSE(UNIT=10)
      GOTO 408
405   IFILE=0
      ENCODE(10,406,BNAME) DNAME,BDOT,BI,BB,BS
406   FORMAT(A6,A1,A1,A1,A1)
      OPEN(UNIT=10,NAME=BNAME,TYPE='OLD',ERR=409)
      READ(10,500,ERR=420) BNAME
      READ(10,509,ERR=420) BTITLE
      READ(10,501,ERR=420) IBDAY,IBMONT,IBYEAR
      READ(10,502,ERR=420) BSTART,BFIN,BWIDTH
      READ(10,503,ERR=420) BSTEP,IBSPD
      READ(10,504,ERR=420) BSENS,BTIME,BOFFS
      READ(10,505,ERR=420) IBDAT,BYSCAL,IBSPNO
      READ(10,508,ERR=420) IBYOFF,IEXPB
      IEND=IBDAT-1                    !END OF ARRAY
      DO 407 J=0,IEND
      READ(10,506,ERR=420) IBASE(J)
407   CONTINUE
      DO 430 I=1,9                    !READ MARKERS
      READ(10,507,ERR=420) ID(I,1),ID(I,2)
430   CONTINUE
      CLOSE(UNIT=10)
500   FORMAT(1X,10A1)
501   FORMAT(1X,I2,1X,I2,1X,I2)
502   FORMAT(1X,E12.6,1X,E12.6,1X,E12.6)
503   FORMAT(1X,F7.1,1X,I3)
504   FORMAT(1X,E12.6,1X,E12.6,1X,E13.6)
505   FORMAT(1X,I3,1X,F7.3,1X,I2)
506   FORMAT(1X,I5)
507   FORMAT(1X,I5,1X,I5)
508   FORMAT(1X,I5,1X,I1)
509   FORMAT(1X,64A1)
      GOTO 408
```

```
409     CALL RVIDEO
        WRITE(7,499) BNAME
499     FORMAT(1X,'ERROR OPENING FILE ',10A1)
        CALL CLEAR
        GOTO 100
420     CALL RVIDEO
        WRITE(7,421) BNAME
421     FORMAT(1X,'ERROR READING FROM FILE ',10A1)
        CALL CLEAR
        CLOSE(UNIT=10)
100     A=SECNDS(0.)
101     D=SECNDS(A)
        IF(D.LT.3.) GOTO 101
408     RETURN
        END

        FUNCTION FREQ(ARG)
        INTEGER IM(15),IW(15)
        DATA IM/12524,11950,11602,11254,10958,10645,10071
     +,9775,9549,9305,9079,8870,8383,8157,7803/IW/1940,2055
     +,2117,2180,2240,2303,2402,2487,2545,2600,2664,2722
C    +2847,2926,3075/
C       DATA IM/12694,12138,11772,11422,11088,10802,10166
C    +,9864,9625,9371,9148,8910,8417,8178/IW/1940,2055
C    +,2117,2180,2240,2303,2402,2487,2545,2600,2664,2722
C    +,2847,2926/
C       DATA CHANGED FOLLOWING RECALIBRATION 26/2/87
C       OLD DATA IN FREQ.OLD
        I=2
        IF(ARG.GT.IM(1)) GOTO 2
1       IF((ARG.GT.IM(I)).AND.(ARG.LE.IM(I-1))) GOTO 2
        I=I+1
        IF(I.NE.15) GOTO 1
2       GRAD=FLOAT(IW(I)-IW(I-1))/FLOAT(IM(I)-IM(I-1))
        FREQ=GRAD*(ARG-FLOAT(IM(I)))+IW(I)
        RETURN
        END

        SUBROUTINE FSAVE
        DOUBLE PRECISION DNAME
        BYTE BTITLE(64),BFILE(6),BKEY(64),BDOT,BT,
     +BCOM(4),B
C
        BDOT='.'
        BB='B'
```



```
        BS='S'
        BI='I'
        IZERO=0
        IF(IFILE.EQ.0) GOTO 205
        IF(IFILE.LT.10) GOTO 201
        ENCODE(10,200,BNAME) DNAME,BDOT,BI,IFILE
200     FORMAT(A6,A1,A1,I2)
        GOTO 203
201     ENCODE(10,202,BNAME) DNAME,BDOT,BI,IZERO,IFILE
202     FORMAT(A6,A1,A1,I1,I1)
203     CONTINUE
C       OPEN(UNIT=10,NAME=BNAME,TYPE='OLD',ERR=199)
C       CALL CURSOR(2,1)
C       CALL RVIDEO
C       WRITE(7,102)
C102    FORMAT(1X,
     +'FILE ALREADY EXISTS: (A)BORT OR (C)ONTINUE ')
C       CLOSE(UNIT=10)
C       CALL CLEAR
C       CALL CURSOR(3,53)
C103    I=ITTINR()
C       IF(I.EQ.65) GOTO 208     !ABORT
C       IF(I.EQ.67) GOTO 105     !CONTINUE
C       GOTO 103
105     CONTINUE
199     OPEN(UNIT=10,NAME=BNAME,TYPE='NEW',ERR=209)
        ENCODE(64,309,BSTR) BTITLE
        WRITE(10,300,ERR=220) BNAME
        WRITE(10,310,ERR=220) BSTR
        WRITE(10,301,ERR=220) ISDAY,ISMONT,ISYEAR
        WRITE(10,302,ERR=220) START,SFIN,SWIDTH
        WRITE(10,303,ERR=220) STEP,ISPD
        WRITE(10,304,ERR=220) SENS,STIME,SOFFS
        WRITE(10,305,ERR=220) ISDAT,SYSCAL,ISPNO
        WRITE(10,308,ERR=220) ISYOFF,IEXPS
        IEND=ISDAT-1
        DO 204 I=0,IEND
        WRITE(10,306,ERR=220) ISPEC(I)
204     CONTINUE
        DO 240 I=1,9                    !WRITE MARKERS
        WRITE(10,307,ERR=220) ID(I,1),ID(I,2)
240     CONTINUE
        CLOSE(UNIT=10)
        GOTO 208
205     IFILE=0
```

```
      ENCODE(10,206,BNAME) DNAME,BDOT,BI,BB,BS
206   FORMAT(A6,A1,A1,A1,A1)
405   CONTINUE
499   OPEN(UNIT=10,NAME=BNAME,TYPE='UNKNOWN',ERR=209)
      ENCODE(64,309,BSTR) BTITLE
      WRITE(10,300,ERR=220) BNAME
      WRITE(10,310,ERR=220) BSTR
      WRITE(10,301,ERR=220) IBDAY,IBMONT,IBYEAR
      WRITE(10,302,ERR=220) BSTART,BFIN,BWIDTH
      WRITE(10,303,ERR=220) BSTEP,IBSPD
      WRITE(10,304,ERR=220) BSENS,BTIME,BOFFS
      WRITE(10,305,ERR=220) IBDAT,BYSCAL,IBSPNO
      WRITE(10,308,ERR=220) IBYOFF,IEXPB
      IEND=IBDAT-1
      DO 207 J=0,IEND
      WRITE(10,306,ERR=220) IBASE(J)
207   CONTINUE
      DO 230 I=1,9                        !WRITE MARKERS
      WRITE(10,307,ERR=220) ID(I,1),ID(I,2)
230   CONTINUE
      CLOSE(UNIT=10)
300   FORMAT(1X,10A1)
301   FORMAT(1X,I2,1X,I2,1X,I2)
302   FORMAT(1X,E12.6,1X,E12.6,1X,E12.6)
303   FORMAT(1X,F7.1,1X,I3)
304   FORMAT(1X,E12.6,1X,E12.6,1X,E13.6)
305   FORMAT(1X,I3,1X,F7.2,1X,I2)
306   FORMAT(1X,I5)
307   FORMAT(1X,I5,1X,I5)
308   FORMAT(1X,I5,1X,I1)
309   FORMAT(64A1)
310   FORMAT(1X,64A1)
      GOTO 208
209   CALL CURSOR(2,1)
      CALL RVIDEO
      WRITE(7,210)
210   FORMAT(1X,'ERROR OPENING FILE ')
      CALL CLEAR
      CLOSE(UNIT=10)
      GOTO 208
220   CALL CURSOR(2,1)
      CALL RVIDEO
      WRITE(7,221)
221   FORMAT(1X,'ERROR WRITING TO FILE ')
      CALL CLEAR
```



```
      CLOSE(UNIT=10)
208   RETURN
      END

      SUBROUTINE GPLOT
      DOUBLE PRECISION DNAME
      BYTE BTITLE(64),BFILE(6),BKEY(64),BDOT,BT,
     +BCOM(4),B
      IXOFF=37
      IYOFF=80
      BDOT='.'
      BB='B'
      BS='S'
      BI='I'
      IZERO=0
      A=FREQ(BFIN)
      B=FREQ(BSTART)
      IBST=INT(A)
      INC=INT((B-A)/10.)
      D=(B-A)/10.-FLOAT(INC)
      IF(D.GT.0.5) INC=INC+1
      BPIX=950./(FLOAT(IBDAT))          !FINISH CALCULATIONS
      WFIN=FREQ(BFIN)
      W=FREQ(BSTART)-WFIN
      WPIX=W/950.
      IEND=IBDAT-1
      IF(ARG.EQ.3.) GOTO 400            !MARKERS ONLY
      IF(ARG.EQ.2.) GOTO 300            !JUST DRAW SPECTRA
C
C     DRAW THE BOX SURROUND AND AXIS
C
      IF(IFILE.EQ.0) GOTO 203           !BASELINE
      IF(IFILE.LE.9) GOTO 201           !I01 TO I09
      ENCODE(10,200,BNAME) DNAME,BDOT,BI,IFILE
C     NO. >10
200   FORMAT(A6,A1,A1,I2)
      GOTO 205                          !CONTINUE
201   ENCODE(10,202,BNAME) DNAME,BDOT,BI,IZERO,IFILE
C     NO. <10
202   FORMAT(A6,A1,A1,I1,I1)
      GOTO 205
203   ENCODE(10,204,BNAME) DNAME,BDOT,BI,BB,BS !BASELINE
204   FORMAT(A6,A1,A1,A1,A1)
205   CONTINUE
      CALL RSETUP
```

```
      CALL RMOVE(10,10)     !DRAW THE SURROUND LINES
      CALL RDRAW(10,775)
      CALL RDRAW(1013,775)
      CALL RDRAW(1013,10)
      CALL RDRAW(10,10)
      CALL RMOVE(10,750)
      CALL RDRAW(1013,750)
      CALL RMOVE(100,775)
      CALL RDRAW(100,750)
      CALL RSIZE(3)
      BTITLE(64)=0
      IF(BTITLE(1).EQ.0) GOTO 206
      CALL RPRINT(110,755,BTITLE) !PRINT TITLE
206   CALL RPRINT(20,755,BNAME)       !FILE NAME
      CALL RPRINT(504,20,'CM')
      CALL RSIZE(2)
      CALL RPRINT(520,30,'-1')
      CALL RSIZE(4)
      CALL RAXIS(37,80,950,0,95,IBST,INC)
      CALL REND
C
C     END OF BOX AND AXIS DRAWING
C
C     NOW FOR THE SPECTRA

300   IF(IFILE.GT.0) GOTO 302   !IF ITS NOT A BASELINE
      CALL RSETUP
      CALL HOME
      IX=INT((IEND-1)*BPIX)+IXOFF
      IY=INT(IBASE(1)*BYSCAL)+IYOFF+IBYOFF
      IF(IY.GT.779) IY=779
      IF(IY.LT.80) IY=80
      CALL RMOVE(IX,IY)
      DO 301 I=2,IEND
      K=IEND-I
      IX=INT(K*BPIX)+IXOFF
      IY=INT(IBASE(I)*BYSCAL)+IYOFF+IBYOFF
      IF(IY.GT.779) IY=779
      IF(IY.LT.80) IY=80
      CALL RDRAW(IX,IY)
301   CONTINUE
      CALL REND
      GOTO 500       !END OF BASELINE DRAWING
C     SPECTRUM DRAWING
C
```



```
302   IF(IBUF.EQ.1) GOTO 305      !IF INTEGRAL MODE IS ON
C
C     DIFFERENTIAL PLOT
      CALL RSETUP
      IEND=ISDAT-1
      IX=INT((IEND-1)*BPIX)+IXOFF
      IY=INT(SYSCAL*(IBASE(1)-ISPEC(1)))+IYOFF+ISYOFF
      IF(IY.GT.779) IY=779
      IF(IY.LT.80) IY=80
      CALL RMOVE(IX,IY)
      DO 303 J=2,IEND
      L=IEND-J
      IX=INT(L*BPIX)+IXOFF
      IY=INT(SYSCAL*(IBASE(J)-ISPEC(J)))+IYOFF+ISYOFF
      IF(IY.GT.779) IY=779
      IF(IY.LT.80) IY=80
      CALL RDRAW(IX,IY)
303   CONTINUE
      CALL REND
      GOTO 500                  !FINISHED
C
C     INTEGRAL PLOT
305   IEND=ISDAT-1
      ICORR=IBASE(IEND)-ISPEC(IEND)-IBASE(1)+ISPEC(1)
      CORR=FLOAT(ICORR)/FLOAT(IEND)
      SUM=0.
      DO 306 I=1,IEND
      SUM=SUM+FLOAT(IBASE(I)-ISPEC(I)-(I*CORR))
306   CONTINUE
      IMEAN=INT(SUM/FLOAT(IEND))
      ITOTAL=0
      CALL RSETUP
      DO 307,I=1,IEND
      L=IEND-I
      IX=INT(L*BPIX)+IXOFF
      ITOTAL=ITOTAL-(IMEAN-IBASE(I)+ISPEC(I)+(I*CORR))
      IY=INT(SYSCAL*FLOAT(ITOTAL))+80+ISYOFF
      IF(IY.GT.779) IY=779
      IF(IY.LT.80) IY=80
      IF(I.GT.1) GOTO 308
      CALL RMOVE(IX,IY)
      GOTO 307
308   CALL RDRAW(IX,IY)
307   CONTINUE
      CALL REND
```

```
309     GOTO 500
C       PLOT MARKERS ONLY
400     CALL RSETUP
        DO 401 I=1,9
        IF((ID(I,1).EQ.0).AND.(ID(I,2).EQ.0)) GOTO 401
        IX=INT((FLOAT(ID(I,1))-WFIN)/WPIX)+37
        IY=INT(FLOAT(ID(I,2))*20.*SYSCAL)+ISYOFF+80
        IF(IFILE.EQ.0)
     +IY=INT(FLOAT(ID(I,2))*20.*BYSCAL)+IBYOFF+80
        IF(IY.GT.779) IY=779
        CALL RMOVE(IX,IY)
        CALL RDRAW(IX,80)
        CALL RSIZE(3)
        CALL RNUM(IX-10,40,ID(I,1))
        CALL RSIZE(4)
401     CONTINUE
        CALL REND
500     RETURN
        END

        SUBROUTINE GTREVL
C       THIS SEND INCHWORM BACK TO REVERSE LIMITS AND  MOVES
C       IT FORWARD SLOWLY TO 0.1 MICRONS IN FRONT OF REV LIM
        CALL IWCOM('@RR:')
        CALL IWSEND('Q',450)
        CALL IWSEND('A',900)
        CALL IWCOM('B:')
450     CALL IWSTAT(IS,IPOS,IPOS2)
        IFLAG=ITTINR()
        IF(IFLAG.EQ.26) GOTO 451
        IF (IS.EQ.251) GOTO 451
        GOTO 450
451     CALL IWCOM('FFFFFFFFFFF:')
        DO 452 J=1,50
452     CONTINUE
        CALL IWCOM('HZS:')
        RETURN
        END

        SUBROUTINE GTSTRT
        DOUBLE PRECISION DNAME
        BYTE BTITLE(64),BFILE(6),BKEY(64),BDOT,BT,
     +BCOM(4),B
C
        IF(ARG.EQ.0.) GOTO 502
```



```
        IF ((ARG.LT.3500.).AND.(ARG.GT.1700.)) GOTO 502
        GOTO 501
502     IF (IFILE.EQ.0) STPOS=BSTART
        IF (IFILE.GT.0) STPOS=START
        IF (ARG.GT.0.)  STPOS=POSIT(ARG)
        ISTART=INT(STPOS)
        CALL IWSTAT(IS,IPOS,IPOS2)
        RPOS=FLOAT(IPOS)+(FLOAT(IPOS2)/10.)
        IGAP=ISTART-IPOS
        IF(IGAP.GT.0) GOTO 200          !GO FORWARD
        IF(IGAP.EQ.0) GOTO 500          !GO NOWHERE
C
        IF(IGAP.GT.-3200)  GOTO 400 !ONE STEP BACK WILL DO
        CALL IWCOM('R:')
        CALL IWSEND('A',900)          !RUN MODE,REVERSE SPEED
        CALL IWCOM('B:')
101     CALL IWSTAT(IS,IPOS,IPOS2)
        IF(IPOS.GT.ISTART) GOTO 101
        CALL IWCOM('HHH:')
        GOTO 300                        !STEP FORWARD
200     IF(IGAP.LT.3200) GOTO 300       !STEP FORWARD
        CALL IWCOM('R:')
        CALL IWSEND('Q',900)
        CALL IWCOM('F:')
201     CALL IWSTAT(IS,IPOS,IPOS2)
        IF(IPOS.LT.ISTART) GOTO 201
        CALL IWCOM('HHH:')
        GOTO 400                        !STEP BACK
300     CALL IWCOM('S:')
        CALL IWSEND('Q',900)
        CALL IWSTAT(IS,IPOS,IPOS2)
        RPOS=FLOAT(IPOS)+(FLOAT(IPOS2)/10.)
        IGAP=INT((STPOS-RPOS)*10.)
        CALL IWSEND('T',IGAP)
        CALL IWCOM('F:')
        GOTO 500
400     CALL IWCOM('S:')
        CALL IWSEND('A',900)
        CALL IWSTAT(IS,IPOS,IPOS2)
        RPOS=FLOAT(IPOS)+(FLOAT(IPOS2)/10.)
        IGAP=INT((RPOS-STPOS)*10.)
        CALL IWSEND('D',IGAP)
        CALL IWCOM('B:')
500     CALL IWSTAT(IS,IPOS,IPOS2)
        RPOS=FLOAT(IPOS)+FLOAT(IPOS2)/10.
```

```
501     RETURN
        END

        SUBROUTINE IRINT
        DOUBLE PRECISION DNAME
        BYTE BTITLE(64),BFILE(6),BKEY(64),BDOT,BT,
     +BCOM(4),B
        BB='B'
        BS='S'
        BI='I'
        BDOT='.'
        IZERO=0
        CALL CURSOR(2,1)
        CALL RVIDEO
        WRITE(7,1)
1       FORMAT(1X,'DEFINE EXCLUSION REGION MIN. AND MAX.')
        CALL CLEAR
        READ(5,2) IMIN,IMAX
2       FORMAT(2I)
        CALL CURSOR(3,1)
        WRITE(7,3)
3       FORMAT(1X,
     +'                                                  ')
        WRITE(7,3)
        IEND=ISDAT-1
        ICORR=IBASE(IEND)-ISPEC(IEND)-IBASE(0)+ISPEC(0)
        CORR=FLOAT(ICORR)/FLOAT(IBDAT)
        CALL CURSOR(2,1)
        CALL RVIDEO
        WRITE(7,4) CORR
4       FORMAT(1X,'SLOPE CORRECTION SET AT ',F,$)
        CALL CLEAR
        READ(5,5) FCORR
5       FORMAT(F)
        IF(FCORR.NE.0) CORR=FCORR
        SUM=0.
        IP=0
        DO 100 I=1,IEND
        POS=BSTART+FLOAT(I)*BSTEP
        WP=FREQ(POS)
        IF((WP.GT.IMIN).AND.(WP.LT.IMAX)) GOTO 100
C     IGNORE THESE POINTS
        IP=IP+1
        SUM=SUM+FLOAT(IBASE(I)-ISPEC(I)-(I*CORR))
100     CONTINUE
```



```
        IMEAN=INT(SUM/FLOAT(IP))
        CALL TSETUP
        CALL CLG
        BPIX=950./(FLOAT(IBDAT))     !FINISH CALCULATIONS
        IXOFF=37
        IYOFF=180
        BPIX=950./FLOAT(ISDAT)
        A=FREQ(BFIN)
        E=FREQ(BSTART)
        IBST=INT(A)
        INC=INT((E-A)/10.)
        D=(E-A)/10.-FLOAT(INC)
        IF(D.GT.0.5) INC=INC+1
        CALL TAXIS(IXOFF,180,950,0,95,IBST,INC)
        ITOTAL=0
        IAREA=0
        DO 103,I=1,IEND
        L=IEND-I
        IX=INT(L*BPIX)+IXOFF
        ITOTAL=ITOTAL-(IMEAN-IBASE(I)+ISPEC(I)+(I*CORR))
        IXX=IMEAN-IBASE(I)+ISPEC(I)+(I*CORR)
        IF(IXX.LT.0) IXX=-IXX
        IAREA=IAREA+IXX
        IY=INT(SYSCAL*FLOAT(ITOTAL))+180+ISYOFF
        IF(IY.GT.779) IY=779
        IF(IY.LT.180) IY=180
        IF(I.GT.1) GOTO 102
        CALL TMOVE(IX,IY)
        GOTO 103
102     CALL TDRAW(IX,IY)
103     CONTINUE
        CALL TNUM(0,200,IAREA)
        CALL TEND
        CALL CURSOR(3,1)
        CALL RVIDEO
        WRITE(7,104)
104     FORMAT(1X,
C    +' (P)LOT, (S)PECTRUM ONLY, ANY OTHER KEY TO EXIT ',$)
        CALL CLEAR
        READ(5,107) B
107     FORMAT(A1)
        CALL CURSOR(3,1)
        WRITE(7,3)
        IF((B.NE.80).AND.(B.NE.83)) GOTO 110
        CALL RSETUP
```

```
      IF(B.EQ.80) GOTO 111          !FULL PLOT
      IF(B.EQ.83) GOTO 112          !SPECTRUM ONLY
      GOTO 110                      !OTHER KEYS GOTO END
111   B=0
      IF(IFILE.EQ.0) GOTO 203       !BASELINE
      IF(IFILE.LE.9) GOTO 201       !101 TO 109
      ENCODE(11,200,BNAME) DNAME,BDOT,BI,IFILE,B !NO. >10
200   FORMAT(A6,A1,A1,I2,A1)
      GOTO 205                      !CONTINUE
201   ENCODE(11,202,BNAME) DNAME,BDOT,BI,IZERO,IFILE,B
202   FORMAT(A6,A1,A1,I1,I1,A1)
      GOTO 205
203   ENCODE(11,204,BNAME) DNAME,BDOT,BI,BB,BS,B !BASELINE
204   FORMAT(A6,A1,A1,A1,A1,A1)
205   CONTINUE
      CALL RMOVE(10,10)             !DRAW THE SURROUND LINES
      CALL RDRAW(10,775)
      CALL RDRAW(1013,775)
      CALL RDRAW(1013,10)
      CALL RDRAW(10,10)
      CALL RMOVE(10,750)
      CALL RDRAW(1013,750)
      CALL RMOVE(913,750)
      CALL RDRAW(913,775)
      CALL RMOVE(100,775)
      CALL RDRAW(100,750)
      CALL RSIZE(3)
      BTITLE(64)=0
      IF(BTITLE(1).EQ.0) GOTO 9
      CALL RPRINT(110,755,BTITLE)     !PRINT TITLE
9     CALL RPRINT(920,755,'INTEGRATION')
      CALL RPRINT(20,755,BNAME)       !FILE NAME
      CALL RAXIS(37,80,950,0,95,IBST,INC)
      CALL RSIZE(3)
      CALL RPRINT(504,20,'CM')
      CALL RSIZE(2)
      CALL RPRINT(520,30,'-1')
      CALL RSIZE(4)
      ITOTAL=0
112   DO 105,I=1,IEND
      L=IEND-I
      IX=INT(L*BPIX)+IXOFF
      ITOTAL=ITOTAL-(IMEAN-IBASE(I)+ISPEC(I)+(I*CORR))
      IY=INT(SYSCAL*FLOAT(ITOTAL))+80+ISYOFF
      IF(IY.GT.779) IY=779
```



```
      IF(IY.LT.80) IY=80
      IF(I.GT.1) GOTO 106
      CALL RMOVE(IX,IY)
      GOTO 105
106   CALL RDRAW(IX,IY)
105   CONTINUE
      CALL REND
110   RETURN
      END

      SUBROUTINE PDISP
      DOUBLE PRECISION DNAME
      BYTE BTITLE(64),BFILE(6),BKEY(64),BDOT,BT,
     +BCOM(4),B
C
      BDOT='.'
      BB='B'
      BS='S'
      BI='I'
      BZERO='0'
      CALL CLS
      CALL CURSOR(1,1)
      IF(IFILE.GT.0) GOTO 800
      WRITE(7,41) BFILE,BDOT,BI,BB,BS,BTITLE
41    FORMAT(1X,6A1,A1,A1,A1,A1,2X,64A1)
      GOTO 804
800   IF(IFILE.GT.9) GOTO 802
      WRITE(7,801) BFILE,BDOT,BI,BZERO,IFILE,BTITLE
801   FORMAT(1X,6A1,A1,A1,A1,I1,2X,64A1)
      GOTO 804
802   WRITE(7,803) BFILE,BDOT,BI,IFILE,BTITLE
803   FORMAT(1X,6A1,A1,A1,I2,2X,64A1)
804   CALL BOLD
      CALL CURSOR(20,3)
      WRITE(7,*) 'STA'
      CALL CURSOR(20,10)
      WRITE(7,*) 'FIN'
      CALL CURSOR(20,19)
      WRITE(7,*) 'STE'
      CALL CURSOR(20,26)
      WRITE(7,*) 'SPE'
      CALL CURSOR(20,33)
      WRITE(7,*) 'SEN'
      CALL CURSOR(20,41)
      WRITE(7,*) 'TIM'
```

```
      CALL CURSOR(20,52)
      WRITE(7,*) 'OFF'
      CALL CURSOR(20,62)
      WRITE(7,*) 'YSC'
      CALL CURSOR(20,69)
      WRITE(7,*) 'YOF'
      CALL CLEAR
      CALL CURSOR(20,74)
      WRITE(7,*) 'PTS'
      CALL CURSOR(20,72)
      WRITE(7,*) 'F'
      CALL CURSOR(20,65)
      WRITE(7,*) 'ALE'
      CALL CURSOR(20,55)
      WRITE(7,*) 'SET'
      CALL CURSOR(20,44)
      WRITE(7,*) 'ECON'
      CALL CURSOR(20,36)
      WRITE(7,*) 'S'
      CALL CURSOR(20,29)
      WRITE(7,*) 'ED'
      CALL CURSOR(20,22)
      WRITE(7,*) 'P'
      CALL CURSOR(20,13)
      WRITE(7,*) 'ISH'
      CALL CURSOR(20,6)
      WRITE(7,*) 'RT '
      IF (IFILE.NE.0) GOTO 48     !IF NOT A BASELINE
      WSTART=FREQ(BSTART)         !CONVERT TO WAVENUMBERS
      WFIN=FREQ(BFIN)
      WSTEP=-(WFIN-WSTART)*BSTEP/(BFIN-BSTART)
      WRITE(7,43) WSTART,WFIN,WSTEP,IBSPD,BSENS,
     +BTIME,BOFFS,BYSCAL,IBYOFF,IBDAT
42    FORMAT(
     +1X,F7.1,1X,F7.1,1X,F7.1,2X,I3,2X,G9.2,1X,G9.2,
     +1X,G10.3,F5.2,1X,I4,2X,I3)
      IF(IEXPB.EQ.0) GOTO 49
      CALL CURSOR(21,78)
      WRITE(7,*) 'EXP'
      GOTO 49                     !END
48    WSTART=FREQ(START)          !CONVERT TO WAVENUMBERS
      WFIN=FREQ(SFIN)
      WSTEP=-(WFIN-WSTART)*STEP/(SFIN-START)
      WRITE(7,43)
     +WSTART,WFIN,WSTEP,ISPD,SENS,STIME,SOFFS,SYSCAL,ISYOFF
```



```
     +,ISDAT
      IF(IBUF.EQ.0)   GOTO 49
      CALL CURSOR(20,78)
      WRITE(7,*) 'INT'
      GOTO 51
49    CALL CURSOR(20,78)
      WRITE(7,*) 'DIF'
      GOTO 51
      IF(IEXPS.EQ.0) GOTO 51
      CALL CURSOR(21,78)
      WRITE(7,*) 'EXP'
51    RETURN
      END

      FUNCTION POSIT(ARG)
      INTEGER IM(15),IW(15)
      DATA IM/12524,11950,11602,11254,10958,10645,10071
     +,9775,9549,9305,9079,8870,8383,8157,7803/IW/1940,2055
     +,2117,2180,2240,2303,2402,2487,2545,2600,2664,2722
     +,2847,2926,3075/
C     DATA IM/12694,12138,11772,11422,11088,10802,10166
C    +,9864,9625,9371,9148,8910,8417,8178/IW/1940,2055
C    +,2117,2180,2240,2303,2402,2487,2545,2600,2664,2722
C    +,2847,2926/
C     DATA CHANGED FOLLOWING RECALIBRATION 26/2/87
C     ORIGINAL DATA FOUND IN POSIT.OLD
      I=2
      IF(ARG.LT.IW(1)) GOTO 2
1     IF((ARG.LT.IW(I)).AND.(ARG.GE.IW(I-1))) GOTO 2
      I=I+1
      IF(I.NE.15) GOTO 1
2     GRAD=FLOAT(IM(I)-IM(I-1))/FLOAT(IW(I)-IW(I-1))
      POSIT=GRAD*(ARG-FLOAT(IW(I)))+FLOAT(IM(I))
      RETURN
      END

      SUBROUTINE RUN
      DOUBLE PRECISION DNAME
      BYTE BTITLE(64),BFILE(6),BKEY(64),BDOT,BT,
     +BCOM(4),B
C
      IF(IFILE.EQ.100) GOTO 298
      ARG=FLOAT(IFILE)
      CALL CFILNO
      IXOFF=37
```

```
      IYOFF=180
      IZ=0
      IF(START.NE.BSTART) GOTO 252
      IF(SFIN.NE.BFIN)    GOTO 254
      IF(STEP.NE.BSTEP) GOTO 256
      IF(IEXPB.NE.IEXPS) GOTO 258
      IBST=INT(FREQ(START))
      INC=INT(FREQ(SFIN)-FREQ(START))/10
      BPIX=950./(FLOAT(ISDAT))
      RATIO=BSENS/SENS
      ARG=STIME
      CALL CTIME
      ARG=SENS
      CALL CSENS
      ARG=SOFFS
      CALL COFFS
      ARG=FLOAT(ISPD)
      CALL CSPEED
      ARG=STEP*(FREQ(SFIN)-FREQ(START))/(START-SFIN)
      CALL CSTEP
      CALL ALTER1('X:',IEXPS)
      CALL CPOINT(START,SFIN,STEP,ISDAT)
      T0=SECNDS(0.)
3     T1=SECNDS(T0)
      IF(T1.LE.4.) GOTO 3
      CALL CURSOR(23,9)
      CALL TSETUP
      CALL CLG
      CALL TAXIS(IXOFF,180,950,0,95,IBST,INC)
      CALL HOME
      CALL TMOVE(IXOFF,IYOFF)
      IEND=ISDAT-1
      ISPEC(0)=0
      CALL STAT1('Q1:',ISPEC(0))
      IY=INT((RATIO*IBASE(0)-ISPEC(0))*SYSCAL)+IYOFF+ISYOFF
      IF(IY.GT.779) IY=779
      IF(IY.LT.180) IY=180
      CALL TMOVE(IXOFF,IY)
      DO 249 J=1,IEND
      CALL IWCOM('F:')
288   CALL IWSTAT(IS,IPOS,IPOS2)
      IF(IS.NE.132) GOTO 700
      CALL IWCOM('@R:')
700   IF(IS.NE.232) GOTO 288
      ISPEC(J)=0
```



```
      DO 4 L=1,1000
4     CONTINUE
      CALL STAT1('Q1:',ISPEC(J))
      IX=INT(J*BPIX)+IXOFF
      IY=INT((RATIO*IBASE(J)-ISPEC(J))*SYSCAL)+IYOFF+ISYOFF
      IF(IY.GT.779) IY=779
      IF(IY.LT.180) IY=180
      CALL TDRAW(IX,IY)
      IFLAG=ITTINR()
      IF(IFLAG.EQ.26) GOTO 770  !ABORT IF  CTRL Z ENTERED
249   CONTINUE
      GOTO 771
770   IZ=1
771   CALL TEND
      GOTO 261
252   CALL CURSOR(2,1)
      CALL RVIDEO
      WRITE(7,253)
253   FORMAT(1X,
     +'ERROR - SPECTRUM AND BASELINE STARTS NOT EQUAL')
      GOTO 260
254   CALL CURSOR(2,1)
      CALL RVIDEO
      WRITE(7,255)
255   FORMAT(1X,
     +'ERROR - SPECTRUM AND BASELINE END POINTS NOT EQUAL')
      GOTO 260
256   CALL CURSOR(2,1)
      CALL RVIDEO
      WRITE(7,257)
257   FORMAT(1X,
     +'ERROR - SPECTRUM AND BASELINE STEPS NOT EQUAL')
      GOTO 260
258   CALL CURSOR(2,1)
      CALL RVIDEO
      WRITE(7,259)
259   FORMAT(1X,'ERROR - EXPAND FEATURES NOT COMPATIBLE')
      GOTO 260
298   CALL CURSOR(2,1)
      CALL RVIDEO
      WRITE(7,299)
299   FORMAT(1X,'ERROR - SPECTRUM NO. GREATER THAN 99')
260   CALL CLEAR
261   RETURN
      END
```

```
      SUBROUTINE CSTART
      DOUBLE PRECISION DNAME
      BYTE BTITLE(64),BFILE(6)
C
      (IF.ARG.LT.0) GOTO 50
      (IF.ARG.GT.4727.) GOTO 53
      (IF.IFILE.EQ.0) BSTART=POSIT(ARG)
      (IF.IFILE.NE.0) START=POSIT(ARG)
      GOTO 55
50    CALL CURSOR(2,1)
      CALL RVIDEO
      WRITE(7,51)
51    FORMAT(1X,'VALUE GIVEN IS LESS THAN REVERSE LIMIT')
      CALL CLEAR
      GOTO 56
53    CALL CURSOR(2,1)
      CALL RVIDEO
      WRITE(7,54)
54    FORMAT(1X,'VALUE GIVEN IS > THAN FORWARD LIMIT')
      CALL CLEAR
      GOTO 56
55    BWIDTH=BFIN-BSTART
      SWIDTH=SFIN-START
      IF((IFILE.EQ.0).AND.(SWIDTH.GT.STEP)) GOTO 56
      IF((IFILE.NE.0).AND.(BWIDTH.GT.BSTEP)) GOTO 56
      CALL CURSOR(2,1)
      CALL RVIDEO
      WRITE(7,58)
58    FORMAT(1X,'STEP LENGTH EXCEEDS SPECTRUM WIDTH')
      CALL CLEAR
56    RETURN
      END

      SUBROUTINE CFIN
      DOUBLE PRECISION DNAME
      BYTE BTITLE(64),BFILE(6)
      (IF.ARG.LT.0) GOTO 50
      (IF.ARG.GT.4727.) GOTO 53
      (IF.IFILE.EQ.0) BFIN=POSIT(ARG)
      (IF.IFILE.NE.0) FIN=POSIT(ARG)
      GOTO 55
50    CALL CURSOR(2,1)
      CALL RVIDEO
      WRITE(7,51)
```



```
51    FORMAT(1X,'VALUE GIVEN IS LESS THAN REVERSE LIMIT')
      CALL CLEAR
      GOTO 56
53    CALL CURSOR(2,1)
      CALL RVIDEO
      WRITE(7,54)
54    FORMAT(1X,'VALUE GIVEN IS > THAN FORWARD LIMIT')
      CALL CLEAR
      GOTO 56
55    BWIDTH=BFIN-BSTART
      SWIDTH=SFIN-START
      IF((IFILE.EQ.0).AND.(SWIDTH.GT.STEP)) GOTO 56
      IF((IFILE.NE.0).AND.(BWIDTH.GT.BSTEP)) GOTO 56
      CALL CURSOR(2,1)
      CALL RVIDEO
      WRITE(7,58)
58    FORMAT(1X,'STEP LENGTH EXCEEDS SPECTRUM WIDTH')
      CALL CLEAR
56    RETURN
      END
```

APPENDIX TWO

Macro-11 assembly language subroutines, LIA.MAC, called from FORTRAN to control the lock-in amplifier.

```
        .title LOCK-IN AMPLIFIER CONTROL SYSTEM
        ;
        rcsr= 176500      ;addresses for the serial line
        rbuf= 176502      ;this is line 0 on the DLV11J
        xbuf= 176506
        xcsr= 176504
        .mcall .ttyout
        .macro susub,val
        mov £60,r4
1$:     cmp r1,val
        blt 2$
        sub val,r1
        inc r4
        br 1$
2$:     tstb xcsr
        bpl 2$
        movb r4,xbuf
3$:     TSTB XCSR
        BPL 3$
        .endm
;
stat1::   ;status request with 1 returned value
;
        mov 2(r5),r1          ;address of byte commands
1$:     tstb xcsr
        bpl 1$
        movb (r1)+,xbuf        ;transmit the byte
        cmpb (r1),£72          ;is next byte a colon
                               ;colon is the terminator
        bne 1$
2$:     tstb xcsr
        bpl 2$
        movb £15,xbuf          ;send CR
        clr r4                 ;flag for negative numbers
        clr r1                 ;r1 will hold value of response
3$:     clr r0
        inc rcsr               ;ask for response
4$:     tstb rcsr
        bpl 4$
        cmpb rbuf,£15          ;is character a CR ?
        beq 5$                 ;branch if yes
        cmpb rbuf,£55          ;is character a - sign ?
        bne 10$
        inc r4                 ;set neg flag
        br 4$                  ;get next char
10$:    mov rbuf,r0
```



```
        bic £177760,r0         ;strip all but last 4 bits
        mov r1,r2              ;use r2 as temporary store
        asl r1
        asl r1
        asl r1                 ;multiply r1 by 8 (2 cubed)
        asl r2                 ;multiply r2 by 2
        add r2,r1              ;net result is r1 times 10
        add r0,r1              ;add the last character
        br 3$
5$:     tst r4
        beq 11$
        neg r1
11$:    mov r1,@4(r5)          ;move value to arg address
        rts pc
;
stat2::   ;status request with 2 returned values
;
        mov 2(r5),r1           ;address of byte commands
1$:     tstb xcsr
        bpl 1$
        movb (r1)+,xbuf        ;transmit the byte
        cmpb (r1),£72          ;is next byte a colon
        bne 1$
2$:     tstb xcsr
        bpl 2$
        movb £15,xbuf
        clr r4                 ;negative number flag
        clr r1                 ;r1 holds value of response
3$:     clr r0                 ;r0 holds transmitted char
17$:    inc rcsr               ;ask for response
4$:     tstb rcsr
        bpl 4$
        cmpb rbuf,£54          ;is character a comma ?
        beq 5$                 ;branch if yes
        cmpb rbuf,£55          ;is number a minus sign
        bne 18$                ;no -do proccessing
        inc r4                 ;yes set flag
        br 17$                 ;get next char
18$:    movb rbuf,r0
        bic £177760,r0         ;clear all but last 4 bits
        mov r1,r2              ;use r2 as temporary store
        ash £3,r1              ;multiply r1 by 8
        ash £1,r2              ;multiply r2 by 2
        add r2,r1              ;net result is r1 times 10
        add r0,r1
        br 3$
```

```
5$:     tst r4                  ;test neg flag
        beq 19$                 ;if zero branch
        neg r1                  ;negate r1
19$:    mov r1,@4(r5)           ;move value to 1st address
        clr r4                  ;clear negative number flag
        clr r1                  ;r1 holds running total
6$:     clr r0                  ;r0 holds transmitted chars
20$:    inc rcsr                ;ask for response
7$:     tstb rcsr
        bpl 7$
        cmpb rbuf,£15           ;is character a CR ?
        beq 8$                  ;branch to end if yes
        cmpb rbuf,£55           ;is character a minus sign
        bne 21$                 ;if no branch
        inc r4                  ;if yes set flag
        br 20$
21$:    movb rbuf,r0            ;received value to r0
        bic £177760,r0          ;clear all but last 4 bits
        mov r1,r2               ;use r2 as temporary store
        ash £3,r1               ;multiply r1 by 8 (decimal)
        ash £1,r2               ;multiply r2 by 2 (decimal)
        add r2,r1               ;total r1 is now 10 x bigger
        add r0,r1               ;add last received value
        br 6$                   ;get next character
8$:     tst r4                  ;is r4 set
        beq 22$                 ;if no branch
        neg r1
22$:    mov r1,@6(r5)           ;move value to 2nd address
        rts pc
;
alter2::  ;alter request with 2 arguments
;
        clr r0
        mov @4(r5),r1           ;first arg value in r1
        mov 2(r5),r2            ;byte address in r2
1$:     movb (r2)+,r0           ;byte in r0
        cmpb r0,£72             ;is byte a colon?
        beq 3$
2$:     tstb xcsr
        bpl 2$
        movb r0,xbuf            ;transmit the byte
99$:    tstb xcsr
        bpl 99$
        br 1$
3$:     movb £40,xbuf           ;transmit the SP
4$:     tstb xcsr
```



```
        bpl 4$
        jsr pc,convrt           ;send the argument value
5$:     tstb xcsr
        bpl 5$
        movb £54,xbuf           ;send a comma
98$:    tstb xcsr
        bpl 98$
        mov @6(r5),r1           ;second arg value in r1
        jsr pc,convrt           ;transmit second arg value
6$:     tstb xcsr
        bpl 6$
        movb £15,xbuf           ;send CR
        inc rcsr                ;ask for acknowledgement
7$:     tstb rcsr
        bpl 7$
        rts pc                  ;return after acknowledgement
        ;
alter1::  ;alter request with 1 argument
;
        clr r0
        mov @4(r5),r1           ;first arg value in r1
        mov 2(r5),r2            ;byte address in r2
1$:     movb (r2)+,r0           ;byte in r0
        cmpb r0,£72             ;is byte a colon?
        beq 3$
2$:     tstb xcsr
        bpl 2$
        movb r0,xbuf            ;transmit the byte
99$:    tstb xcsr
        bpl 99$
        br 1$
3$:     movb £40,xbuf           ;transmit the SP
4$:     tstb xcsr
        bpl 4$
        jsr pc,convrt           ;send the argument value
6$:     tstb xcsr
        bpl 6$
        movb £15,xbuf           ;send CR
        inc rcsr                ;ask for acknowledgement
7$:     tstb rcsr
        bpl 7$
        rts pc                  ;return after acknowledgement
        ;
convrt::        ;
        clr r4
        cmp r1,£1750
```

```
        bge fig4
        cmp r1,£144
        bge fig3
        cmp r1,£12
        bge fig2
        br fig1
fig4:   susub £1750
fig3:   susub £144
fig2:   susub £12
fig1:   susub £1
        rts pc
        .end
```

APPENDIX THREE

Macro-11 assembly language subroutines to control the diffraction grating linear motion drive, callable from FORTRAN main programs.

MACRO-11 assembly language programme to control the linear motion drive.

```
        .title control
;
        rcsr=176520             ;I/O memory locations for
        rbuf=176522             ;channel 2 of serial line
        xcsr=176524
        xbuf=176526
;
        .mcall .ttyout
        .macro print,reg        ;printing macro
        movb reg,r0             ;to print a char print ___
        .ttyout
        .endm
;
;receiving macro will wait for next character
;to come in on channel two
;
        .macro get,a
        inc rcsr
a:      tstb rcsr
        bpl a
        .endm
;
        .macro process
;processes received numbers into decimal
        mov r2,r3
        ash £3,r2               ;r2 multiplied by 8
        asl r3                  ;r3 multiplied by 2
        add r3,r2               ;r2 10 x original value
        mov rbuf,r3             ;next ascii character to r3
        sub £60,r3              ;strip character to the no.
        add r3,r2               ;add to accumulator
        .endm
;
        .macro susub,val        ;processes a number into
                                ;the equivilent ASCII string
        mov £60,r4              ;r4 contains the ascii code
1$:     cmp r1,val              ;r1 the no.being processed
        blt 2$
        sub val,r1
;subtract val from r1 'til r1 is less than val
        inc r4                  ;r4 no. of subtractions
        br 1$
2$:     bpl 2$
        movb r4,xbuf            ;send r4
3$:     tstb xcsr
        bpl 3$
        .endm
;
iwcom:: mov 2(r5),r1            ;address of first byte in r1
1$:     cmpb (r1),£72           ;is byte a colon ?
        beq 4$                  ;branch if yes
        cmpb (r1),£52           ;is byte an asterisk ?
        bne 2$                  ;no - branch
        movb £15,xbuf           ;move a CR to xbuf
        inc r1
        br 3$
2$:     movb (r1)+,xbuf         ;send to the transmit buffer
3$:     tstb xcsr
        bpl 3$
        jsr pc,delay2           ;delay
        br 1$                   ;repeat for next byte
4$:     jsr pc,delay2           ;put a final delay in
        rts pc
;
iwstat::
;stores position and status code in variables
;fortran call is IWSTAT(ISTAT,IPOS)
;
        clr r0                  ;holds status code
        clr r1                  ;negative position flag
        clr r2                  ;position accumulator
        clr r3                  ;utility buffer
;
        movb £61,xbuf
;send 1 to ask for status and position
7$:     tstb xcsr               ;loop until it has gone
        bpl 7$
        get 9$
;receive char (control mode report)
        movb rbuf,r3
        cmpb £114,r3
;is it L (local mode -keypad only)
        bne 10$                 ;no branch
        add £100.,r0            ;status code 100
        br 12$
10$:    cmpb £122,r3
```

```
;is it R (remote mode -keypad and computer)
        bne 11$                 ;no - branch
        add £200.,r0            ;status code 200
        br 12$
11$:    cmpb £130,r3
;is it X (remote mode -computer only)
        br 12$                  ;no - branch
        add £300.,r0            ;status code 300
12$:    get 13$
;receive character 3 (system running state)
        movb rbuf,r3
        cmpb £111,r3            ;is it I (idle state)
        bne 14$                 ;no
        add £10.,r0             ;status code 10
        br 18$
14$:    cmpb £122,r3            ;is it R (running state)
        bne 15$                 ;no
        add £20.,r0             ;status code 20
        br 18$
15$:    cmpb £103,r3
;is it C (completed motion state)
        bne 16$                 ;no
        add £30.,r0             ;status code 30
        br 18$
16$:    cmpb £120,r3
;is it P (program complete state)
        bne 17$                 ;no
        add £40.,r0             ;status code 40
        br 18$
17$:    cmpb £105,r3            ;is it E (error state)
        bne 18$                 ;no
        add £50.,r0             ;status code 50
18$:    get 19$
;receive character 3 (movement mode)
        movb rbuf,r3
        cmpb £122,r3            ;is it R (run mode)
        bne 20$                 ;no
        add £1,r0               ;status code 1
        br 22$
20$:    cmpb £123,r3            ;is it S (step mode)
        bne 21$                 ;no
        add £2,r0               ;status code 2
        br 22$
21$:    cmpb £120,r3            ;is it P (program mode)
        bne 22$
```



```
        add £3,r0               ;status code 3
22$:    get 23$
;receive character 5 (device number)
        get 24$
;receive character 6 (sign of position)
        movb rbuf,r3
        cmpb £55,r3             ;is it a minus sign
        bne 25$                 ;no
        inc r1
;set the negative position flag
25$:    get 26$                 ;get first digit
        process
        get 27$                 ;get second digit
        process
        get 28$                 ;get third digit
        process
        get 29$                 ;get fourth digit
        process
        get 30$                 ;get fifth digit
        process
        get 31$                 ;get sixth digit
        process
        get 32$                 ;get seventh digit
        process
        tst r1
        beq 99$
        neg r2
99$:    mov r2,@4(r5)           ;place in ipos
        get 33$
;eighth digit is decimal point
        clr r2
;reset buffer to get decimal point value
        get 34$                 ;get last digit
        process
        mov r0,@2(r5)
;status code to first argument
        mov r2,@6(r5)
;position to second argument
        jsr pc,delay
;run the delay loop before exit
        rts pc
;
iwsend::
;send command and numerical information
        movb @2(r5),xbuf        ;send command character
```

```
36$:    tstb xcsr
        bpl 36$
        jsr pc,delay2
        mov @4(r5),r1           ;number into r1
        jsr pc,sendno
;send no. for conversion to ascii codes
        rts pc
;
iwnum::                         ;send numerical value
        mov @2(r5),r1           ;number to r1
        jsr pc,sendno
;send no. for conversion to ascii codes
        rts pc
;
delay:  mov £4000,r0
;delay loop to give iw time to react
loop:   dec r0
        tst r0

;used before returning to the controlling program
        bne loop
        rts pc
;
;
delay2:                         ;long delay loop
        mov £77777,r0
loop2:  dec r0
;used whilst transmitting commands
        tst r0
        bne loop2
        rts pc

;
;
sendno:
;subroutine to convert no. in r1 to ascii code
        clr r4
;r4 will contain ascii code of digit
        cmp r1,£23420           ;is no. >=10000 ie 5 digits
        bge fig5
        cmp r1,£1750            ;is no. >=1000 ie 4 digits
        bge fig4
        cmp r1,£144             ;is no. >=100 ie 3 digits
        bge fig3
        cmp r1,£12              ;is no. >=10 ie 2 digits
```



```
        bge fig2
        br fig1                 ;1 digit only
fig5:   susub £23420
        jsr pc,delay2
fig4:   susub £1750
        jsr pc,delay2
fig3:   susub £144
        jsr pc,delay2
fig2:   susub £12
        jsr pc,delay2
fig1:   susub £1
        jsr pc,delay2           ;delay loop
        movb £15,xbuf           ;send a carriage return
37$:    tstb xcsr
        bpl 37$
        jsr pc,delay
        rts pc
        .end
```

APPENDIX FOUR

Macro-11 assembly language routines to control the digital to analogue output lines from the PDP11-03. These routines are callable from FORTRAN main programs.

```
        ;title daconv
        ;operates the digital to analogue output board
        ;0 to 1 volt range in 10 bits
        ;i.e. the input range is 0 to 1023
        ;
        ;two channels available
        ;
        ;callable from fortran programs using
        ;CALL DACX(I) or CALL DACY(I)
        ;
        ;
        ; memory location definitions
        ;
        XCHAN= 160002
        YCHAN= 160004
        ;
DACX::  MOV     ε2(R5),XCHAN    ;I TO DACX
        RTS     PC
;
DACY::  MOV     ε2(R5),YCHAN    ;I TO DACY
        RTS     PC
        ;
        .END
```

APPENDIX FIVE

Macro-11 assembly language subroutines to control the analogue to digital input lines on the PDP11-03. The subroutines are callable from FORTRAN main programs.

```
        .title adconv
        ;
        ;does analogue to digital conversion
        ;from fortran subroutine
        ;fortran call is CALL ADCONV(IVAL,ICHAN)
        ;ival is the value of the input
        ;ichan is the input channel
        ;
        ;
        adsr = 170400          ;address of status register
        adbr = 170402          ;address of buffer register
adconv::
        clr adsr               ;clears status register
        mov ε4(r5),r0          ;value of ichan to r0
        cmp r0,#15.            ;is ichan>15 ?
        bgt 4∞                 ;if yes then return
        tst r0                 ;is ichan<0 ?
        blt 4∞                 ;if yes then return
1∞:     tst r0                 ;adds 400 octal times
        beq 2∞                 ;ichan to the stat. reg
        add#400,adsr           ;to set
        dec r0                 ;the correct input channel
        br 1∞
2∞:     inc adsr               ;start conversion
        mov adsr,r0
3∞:     tstb adsr              ;test to see if done
        bpl 3∞                 ;if bit 7=1 then not done
        mov adbr,ε2(r5)        ;move value to ival
4∞:     rts pc                 ;return to calling programme
        .end
```

APPENDIX SIX

Macro-11 assembly language subroutines to control plotting on the Rikadenki RY-101 digital plotter. This version designed to scale a full screen image from the Hirez-100 terminal onto A4 size paper.

```
        .title rplot4
        ;
        ;driver routine for Rikadenki graph plotter
        ;compatible with the tektronix plotter routines for
        ;the Hirez 100 terminals, scaled to plot on A4
        ; sized paper
        ;
        ;Version 1.04                Andrew Robinson 7/5/87
        ;
        ;NOW HAS RROTAT TO ALLOW TEXT ORIENTATION
        ;also relative move and relative draw commands
        ;and relative print and rnum commands
        ;
        .mcall .ttyout,.ttyin
        .macro print,val
        mov val,r0
        .ttyout
        .endm
        ;
rmove:: mov @2(r5),r1           ;ix argument to r1
        jsr pc,ixscal           ;scale ix for A4 size
        jsr pc,m                ;print a M
        jsr pc,octasc           ;convert to ascii chars
        jsr pc,comma
        mov @4(r5),r1           ;iy argument to r1
        jsr pc,iyscal           ;scale iy to A4 size
        jsr pc,octasc           ;convert to ascii string
        jsr pc,crlf             ;tranmit CR & LF
        rts pc                  ;back to fortran
        ;
rdraw:: mov @2(r5),r1           ;ix argument to r1
        jsr pc,ixscal           ;scale ix for A4 size
        jsr pc,d                ;print a D
        jsr pc,octasc           ;convert into ascii chars
        jsr pc,comma
        mov @4(r5),r1           ;iy argument to r1
        jsr pc,iyscal           ;scale iy to A4 size
        jsr pc,octasc           ;convert to ascii string
        jsr pc,crlf             ; CR LF
        rts pc                  ;back to fortran
        ;
rrmove::
        mov @2(r5),r1           ;ix argument to r1
        jsr pc,ixscal           ;scale ix for A4 size
        movb #122,r0
```



```
        .ttyout                 ;R does a relative move
        jsr pc,octasc           ;into ascii characters
        jsr pc,comma
        mov @4(r5),r1           ;iy argument to r1
        jsr pc,iyscal           ;scale iy to A4 size
        jsr pc,octasc           ;convert to ascii string
        jsr pc,crlf             ;transmit CRLF
        rts pc                  ;back to fortran
        ;
rrdraw::
        mov @2(r5),r1           ;ix argument to r1
        jsr pc,ixscal           ;scale ix for A4 size
        movb #111,r0
        .ttyout                 ;I does relative draw
        .ttyout
        jsr pc,octasc           ;convert to ascii chars
        jsr pc,comma
        mov @4(r5),r1           ;iy argument to r1
        jsr pc,iyscal           ;scale iy to A4 size
        jsr pc,octasc           ;convert to ascii string
        jsr pc,crlf             ;transmit CRLF
        rts pc                  ;back to fortran
        ;
rrprnt::
        ;rprint first moves to the starting location
        ;using RX,Y then prints whatever is the string
        ; after a P command
        ;RX,YPstring<CR><LF>
        mov @2(r5),r1
        jsr pc,ixscal
        movb #122,r0
        .ttyout
        jsr pc,octasc
        jsr pc,comma
        mov @4(r5),r1
        jsr pc,iyscal
        jsr pc,octasc
        mov 6(r5),r1
        jsr pc,p
1$:     movb (r1)+,r0
        .ttyout
        tstb (r1)
        bne 1$
        jsr pc,crlf
        rts pc
```

```
rrnum::
        ;rprint first moves to the starting location
        ;using MX,Y then prints the number
        ;after a P command
        ;MX,YPnum<CR><LF>
        mov @2(r5),r1
        jsr pc,ixscal
        movb £122,r0
        .ttyout
        jsr pc,octasc
        jsr pc,comma
        mov @4(r5),r1
        jsr pc,iyscal
        jsr pc,octasc
        jsr pc,p
        mov @6(r5),r1
        tst r1
        bge 1$
        print £55
        neg r1
1$:     jsr pc,octasc           ;convert no. to ascii string
        jsr pc,crlf
        rts pc
        ;
rrotat::
        ;rotates printing of text by x degrees
        mov @2(r5),r0
        cmp £0.,r0
        bne 1$
        print £121              ;Q
        print £60               ;0
        rts pc
1$:     cmp £90.,r0
        bne 2$
        print £121
        print £61               ;1
        rts pc
2$:     cmp £180.,r0
        bne 3$
        print £121
        print £62               ;2
        rts pc
3$:     cmp £270,r0
        bne 4$
        print £121
```



```
        print £63               ;3
4$:     rts pc
        ;
rcross::
        ;Rikadenki command for this is to move
        ;to point using MX,Y then to do N5 to print a cross
        mov @2(r5),r1
        jsr pc,ixscal
        jsr pc,m
        jsr pc,octasc
        jsr pc,comma
        mov @4(r5),r1
        jsr pc,iyscal
        jsr pc,octasc
        jsr pc, n5
        jsr pc,crlf
        rts pc
rprint::
        ;rprint first moves to the starting location
        ;using MX,Y then prints whatever is the string
        ;after a P command
        ;MX,YPstring<CR><LF>
        mov @2(r5),r1
        jsr pc,ixscal
        jsr pc,m
        jsr pc,octasc
        jsr pc,comma
        mov @4(r5),r1
        jsr pc,iyscal
        jsr pc,octasc
        mov 6(r5),r1
        jsr pc,p
1$:     movb (r1)+,r0
        .ttyout
        tstb (r1)
        bne 1$
        jsr pc,crlf
        rts pc
rnum::
        ;rnum first moves to the starting location
        ;using MX,Y then prints the number after a P command
        ;MX,YPnum<CR><LF>
        mov @2(r5),r1
        jsr pc,ixscal
        jsr pc,m
```

```
        jsr pc,octasc
        jsr pc,comma
        mov @4(r5),r1
        jsr pc,iyscal
        jsr pc,octasc
        jsr pc,p
        mov @6(r5),r1
        jsr pc,octasc           ;convert no. to ascii string
        jsr pc,crlf
        rts pc
        ;
rsetup::
        ;enables the auxiliary port on the terminal
        ;and sets printer controller on
        ;this diverts all text from the screen to the
        ;rikadenki plotter
        mov £list1,r1
1$:     movb (r1)+,r0
        beq 2$
        .ttyout
        br 1$
2$:     mov £list2,r1
3$:     movb (r1)+,r0
        beq 4$
        .ttyout
        br 3$
4$:     jsr pc,crlf
        jsr pc,h                ;reset the plotter
        jsr pc,crlf
        rts pc
list1:  .byte 33,133,77,65,151,0
        .even
list2:  .byte 33,133,65,151,0
        .even
;
;
rend::
        ;reset the plotter,disables the printer controller
        ;and the aux. port on the terminal, restoring all
        ;further text to the screen
        jsr pc,h
        jsr pc,crlf
        mov £list3,r1
5$:     movb (r1)+,r0
        beq 6$
```



```
        .ttyout
        br 5$
6$:     mov £list4,r1
7$:     movb (r1)+,r0
        beq 8$
        .ttyout
        br 7$
8$:     rts pc
;
list3:  .byte 33,133,64,151,0
        .even
list4:  .byte 33,133,77,64,151,0
        .even
;
rsize:: mov @2(r5),r1
        movb £123,r0            ;print an S

        .ttyout
        jsr pc,octasc           ;send number
        jsr pc,crlf             ;carriage return linefeed
        rts pc
;
ixscal: ;scales x axis to A4 size by multiplying by
        ;a factor of 18 and dividing by 8
        ;total factor = 2.66
        mov r1,r0
        .rept 21
        add r0,r1
        .endr
        .rept 3
        asr r1
        .endr
        rts pc
;
iyscal: ;scales y axis to A4 size by multiplying by 2
        asl r1
        rts pc
;
comma:                          ;prints a comma (ascii 54)
        print £54
        rts pc
;
crlf:                           ;prints carriage return (ascii 15)
        print £15               ;and linefeed (ascii 12)
        print £12
```

```
        rts pc
;
p:      print £120      ;prints P (ascii 120)
        rts pc
;
m:      print £115      ;prints M (ascii 115)
        rts pc
;
n5:     print £116      ;prints N (ascii 116)
        print £65       ;and 5 (ascii 65)
        rts pc
;
h:      print £110      ;prints H (ascii 110)
        rts pc
;
d:      print £104      ;prints D (ascii 104)
        rts pc
;
octasc:                 ;converts r1to the ascii codes
                        ;corresponding to the digits
        cmp r1,£23417   ;r1 > 9999 (decimal) ?
        bgt digit5      ;branch if yes
        cmp r1,£1747    ;r1 > 999 (decimal) ?
        bgt digit4      ;branch if yes
        cmp r1,£143     ;r1 > 99 (decimal) ?
        bgt digit3      ;branch if yes
        cmp r1,£11      ;r1 > 9 (decimal) ?
        bgt digit2      ;branch if yes
        br digit1
       ;r1 is <10       ; only one digit to be coded
digit5: mov £60,r2      ;put ascii code for 0 in r2
1$:     cmp r1,£23420
        blt 2$          ;is coding digit 5 complete ?
        sub £23420,r1   ;subtract 10000
        inc r2          ;add  1 to r2
        br 1$
2$:     print r2        ;digit 5 printed
digit4: mov £60,r2      ;ascii for 0 in r2
3$:     cmp r1,£1750
        blt 4$
        sub £1750,r1
        inc r2
        br 3$
4$:     print r2
digit3: mov £60,r2
```



```
5$:     cmp r1,£144
        blt 6$
        sub £144,r1
        inc r2
        br 5$
6$:     print r2
digit2: mov £60,r2
7$:     cmp r1,£12
        blt 8$
        sub £12,r1
        inc r2
        br 7$
8$:     print r2
digit1: add £60,r1
        print r1
        rts pc
;
        .end
```

APPENDIX SEVEN

Macro-11 assembly language subroutines to handle Tektronix 4014 graphics and ANSI X3.64 screen manipulation functions (VT-100 standard) for the Hirez-100 terminal. All routines are callable from FORTRAN main programs.

```
.TITLE  GRAPH
        ;EASY TEKTRONIX GRAPHICS SYSTEM
        ;Andrew Robinson  January 1985
        ;Version 1.13
        ;last update 12-5-86
        ;MODIFIED TNUM TO DEAL WITH  NEGATIVE NUMBERS
        ;
.MCALL .TTYOUT,.TTYIN
;
        .MACRO PRINT,VAL
        MOV VAL,R0
        .TTYOUT
        .ENDM
;
        .MACRO SUBTR,VAL ;does successive subtractions
        CLR R4
1$:     CMP R3,VAL       ;r3 less than val ?
        BLT 2$           ;yes
        SUB VAL,R3       ;subtract val from r3
        INC R4           ;times val has been subtracted
        BR 1$
2$:     ADD £60,R4       ;gives ascii code of number in r4
        PRINT R4
        .ENDM
;
TDRAW:: MOV @2(R5),R1    ;contains ix
        MOV @4(R5),R2    ;contains iy
TD:     CLR R4           ;contains flag for illegal vector
        JSR PC,CHECK     ;check for illegal vectors
        CMP £0,R4        ;flag set ?
        BGT 1$           ;yes -then return
        JSR PC,TRANS     ;translate ix,iy to tek format
1$:     RTS PC
;
TMOVE:: MOV @2(R5),R1    ;same as tdraw except
        MOV @4(R5),R2
TM:     CLR R4
        JSR PC,CHECK
        CMP £0,R4
        BGT 2$
        PRINT £35        ;prints GS
        JSR PC,TRANS
2$:     RTS PC
;
TSETUP:: JSR PC,TEKON    ;put in tek mode
```



```
        JSR PC,HOME      ;set to (0,0)
        RTS PC
;
TEND::  JSR PC,TEKOFF    ;exit from 4014 mode
        RTS PC
;
CLG::   print £33         ;prints ESC FF to clear screen
        print £14
        JSR PC,HOME      ;sets to (0,0)
        RTS PC
;
HOME::  JSR PC,GRAF      ;use graphic submode
                         ;(ESC FF switches to alpha)
        CLR R1
        CLR R2
        JSR PC,CHECK
        RTS PC
;
VIEW::  CLR R4           ;viewport command (Selanar native)
        MOV @2(R5),R1
        MOV @4(R5),R2
        JSR PC,CHECK     ;is (ix,iy) a legal coordinate ?
        CMP £0,R4
        BGT 8$           ;flag is set - illegal coordinate
        ADD @6(R5),R1
        ADD @10(R5),R2
        CLR R4           ;clear flag
        JSR PC,CHECK     ;check that viewport is on screen
        CMP £0,R4        ;flag set -its not on screen !!
        BGT 8$
        print £33
        print £117
        print £126
        MOV @2(R5),R1
        MOV @4(R5),R2
        CMP R1,£0
        BNE 56$
        CMP R2,£0        ;if r1&r2 are 0 then skip asr part
        BEQ 57$
56$:    .REPT 2
        ASR R1           ;divide by 4 to scale for Hirez 100
        ASR R2
        .ENDR
57$:    JSR PC,TRANS     ;transmit the coords for the corner
        MOV @6(R5),R1
```

```
        MOV @10(R5),R2  ;dimensions of box
        CMP R1,£1024
        BNE 58$
        CMP R2,£1414
        BNE 58$
        MOV £10000,R1   ;if r1=1024 and r2=779 then skip asr
        MOV £3000,R2    ;and assign values directly
        BR 59$
58$:    .REPT 2
        ASR R1          ;divide by 4 to scale for Hirez 100
        ASR R2
        .ENDR
59$:    JSR PC,TRANS
8$:     RTS PC
;
TCIRC:: MOV @2(R5),R1
        MOV @4(R5),R2
        JSR PC,TM
        print £33   ;do a tmove to the centre of circle
        print £117  ;transmits sequence ESC O C
        print £103  ;the HIREZ circle plotting command
        MOV @6(R5),R1           ;RADIUS
        MOV @10(R5),R2          ;INC ANGLE
        JSR PC,TRANS
        MOV £0,R1               ;set start angle to 0
        MOV £360.,R2            ;set finish angle to 360
        JSR PC,TRANS
        RTS PC
;
ORIGIN::JSR PC,GRAF  ;print sequence ESC O O
        print £33
        print £117
        print £117
        MOV @2(R5),R1           ;contains ix
        MOV @4(R5),R2           ;contains iy
        JSR PC,TRANS
        CLR R1          ;R1,R2 are arguments passed to trans
        CLR R2
        JSR PC,TRANS    ;sends tektronix vectors 0,0 0,0
        JSR PC,ALPHA
        RTS PC
;
XGAIN:: MOV @2(R5),R1
        MOV @4(R5),R2
        CMP R1,£0
```



```
        BEQ 14$
        ASL R2
        ASL R2
        print £33
        print £117
        print £130
        JSR PC,TRANS
        CLR R1
        CLR R2
        JSR PC,TRANS
14$:    RTS PC
;
YGAIN:: MOV @2(R5),R1
        MOV @4(R5),R2
        CMP R1,£0
        BEQ 15$
        ASL R2
        ASL R2
        print £33   ;ESC O Y
        print £117
        print £131
        JSR PC,TRANS
        CLR R1
        CLR R2
        JSR PC,TRANS
15$:    RTS PC
        ;
FACTOR:: ;
        JSR PC,XGAIN    ;factor scales both gains by the
        JSR PC,YGAIN    ;same amount
        RTS PC
;
TEMP::  PRINT £33       ;write through submode
        PRINT £165      ;esc p
        RTS PC          ;temporary screen display
;
DUMP::  PRINT £33       ;dumps graphics
        PRINT £27
        RTS PC
;
TMODE:: MOV @2(R5),R2   ;value of argument
        CMP R2,£0
        BLT 20$
        CMP R2,£2
        BGT 20$
```

```
        ADD £140,R2
        PRINT £33               ;ESC
        PRINT £117              ;O
        PRINT £127              ;W
        PRINT £40
        PRINT R2
        PRINT £140
        PRINT £40
        PRINT £100
        PRINT £100
20$:    RTS PC
;
TPOINT:: ;                      ;plots  single point at x,y
        MOV @2(R5),R1
        MOV @4(R5),R2
        JSR PC,TM
        JSR PC,TD
        RTS PC
;
TLINE:: MOV @2(R5), R1          ;argument value (must be 1 to 5)
        CMP R1,£1
        BLT 42$
        CMP R1,£5
        BGT 42$
        CMP R1,£1
        BEQ 40$
        ADD £137,R1
        BR 41$
40$:    MOV £134,R1
41$:    PRINT £33               ;ESC
        PRINT R1
42$ :   RTS PC
;
TPRINT:: ;
        MOV @2(R5),R1   ;x coord
        MOV @4(R5),R2   ;y coordinate
        JSR PC,TM       ;move initial plot position
        JSR PC,ALPHA    ;alpha submode
        MOV 6(R5),R3    ;address of first byte in string
31$:    CLR R4
        MOVB (R3)+,R4   ;first byte to r4
        TSTB R4         ;test r4 to see if zero
        BEQ 32$         ;goto end if yes
        PRINT R4
        BR 31$
```



```
32$:    JSR PC,GRAF
        RTS PC
;
TCHAR:: ;
        MOV @2(R5),R4   ;argument in R4
CHR:    CMP £0,R4
        BGE 19$
        CMP R4,£5
        BGE 19$
        ADD £67,R4
        ;add 67(octal) to get correct ESC sequence
        print £33
        print r4
19$:    RTS PC
;
TCROSS:: ;
        MOV @2(R5),R1
        MOV @4(R5),R2
        JSR PC,TM               ;move to ix,iy
        JSR PC,TD               ;draw a point at ix,iy
        DEC R1                  ;move to ix-1,iy-1
        DEC R2
        JSR PC,TM
        JSR PC,TD
        ADD £2,R2               ;move to ix-1,iy+1
        JSR PC,TM
        JSR PC,TD
        ADD £2,R1               ;move to ix+1,iy+1
        JSR PC,TM
        JSR PC,TD
        SUB £2,R2               ;move to ix+1,iy-1
        JSR PC,TM
        JSR PC,TD
        RTS PC
;
TNUM::  MOV @2(R5),R1           ;x co-ordinate
        MOV @4(R5),R2           ;y co-ordinate
        JSR PC,TM               ;move to co-ordinate pair
        MOV @6(R5),R3           ;number to r3
        JSR PC,ALPHA
        TST R3
        BGE 1$
        NEG R3
        print £55 ;minus sign
1$:     JSR PC,OCTDEC
```

```
        ;convert no. to ascii codes and print it
        JSR PC,ALPHA            ;back to graph submode
        RTS PC
;
ESC:    PRINT £33         ;sequence ESC [
        PRINT £133
        RTS PC
;
OCTDEC::
;converts an octal number in r3 to decimal and prints it
        CLR R2                  ;R2= no. of digits
        CMP R3,£23420           ;10000
        BGE FIG5
        CMP R3,£1750            ;1000
        BGE FIG4
        CMP R3,£144             ;100
        BGE FIG3
        CMP R3,£12              ;10
        BGE FIG2
        JMP FIG1                ;units
FIG5:   SUBTR £23420
FIG4:   SUBTR £1750
FIG3:   SUBTR £144
FIG2:   SUBTR £12
FIG1:   ADD £60,R3
        PRINT R3
FINISH: RTS PC
;
CHECK:  CMP £0,R1               ;is ix<0 ?
        BLT 5$
        CMP £1777,R1            ;is ix>1023 ?
        BGT 5$
        CMP £0,R2               ;is iy<0 ?
        BLT 5$
        CMP £1413,R2            ;is iy>779 ?
        BLT 6$
5$:     INC R4                  ;set illegal value flag
6$:     RTS PC
;
TEKON:  PRINT £33       ;transmits ESC 1
        PRINT £61
        RTS  PC
;
TEKOFF: JSR PC,ALPHA    ;alpha submode
        print £33
```



```
        print £62
        RTS PC
;
TRANS: ;
         MOV R2,R3          ;iy to R3
        .REPT 5.
        ASR R3              ;take the 5 most significant bits
        .ENDR
        BIC £177740,R3      ;mask out other bits
        ADD £40,R3          ;add 32
        MOV R3,R0           ;this gives the HI Y byte
        .TTYOUT
        MOV R2,R3           ;iy to r3
        BIC £177740,R3      ;mask out everything except 5 LSB
        ADD £140,R3         ;add 96 to give LO Y byte
        MOV R3,R0
        .TTYOUT
        MOV R1,R3           ;ix to R3
        .REPT 5.
        ASR R3              ;take 5 MSB
        .ENDR
        BIC £177740,R3      ;mask the rest
        ADD £40,R3          ;add 32 to get HI X byte
        MOV R3,R0
        .TTYOUT
        MOV R1,R3
        BIC £177740,R3      ;get 5 LSB
        ADD £100,R3         ;add 64 to get LO X
        MOV R3,R0
        .TTYOUT
        RTS PC
;
ALPHA:  print £37   ;puts in alpha submode
        RTS PC
;
GRAF:   print £35   ;puts in graphics submode
        RTS PC
;
INCP:   print £36   ;put in incremental plot submode
        RTS PC
;
;
CLS::   ;           clears the screen (VT100)
        PRINT £33
        PRINT £133
```

```
        PRINT £62
        PRINT £112
        RTS PC
;
GRON:   JSR PC,TEKON
        JSR PC,RECOV
        RTS PC
;
TPR:    MOV 2(R5),R2
        print £37
30$:    MOVB (R2)+,R1
        CMP R1,£0
        BEQ 33$
        CMP R1,£173
        BNE 31$
        print £33
        print £73
        MOV £0,R1
        MOV £5,R2
        JSR PC,TM
        BR 30$
31$:    CMP R1,£175
        BNE 32$
        print £33
        print £70
        BR 30$
32$:    print r1
        JMP 30$
33$:    RTS PC
;
xhair:: print £33   ;ESC
        print £32   ;CTRL Z (puts in cross hair mode)
        .ttyin          ;status byte
        .ttyin          ;hi x byte
        mov r0,-(sp)    ;on stack
        .ttyin          ;lo x byte
        mov r0,-(sp)
        .ttyin          ;hi y byte
        mov r0,-(sp)
        .ttyin          ;lo y byte
        mov r0,-(sp)
        .TTYIN
        .TTYIN
        mov (sp)+,r0    ;lo y
        bic £177740,r0  ;mask all but lowest 5 bits
```



```
        mov (sp)+,r1    ;hi y
        bic £177740,r1
        .rept 5
        asl r1          ;multiply by 32.
        .endr
        add r1,r0       ;add to lo y
        mov r0,@4(r5)
        mov (sp)+,r0    ;lo x
        bic £177740,r0  ;mask all but lowest 5 bits
        mov (sp)+,r1    ;hi x
        bic £177740,r1
        .rept 5
        asl r1          ;multiply by 32.
        .endr
        add r1,r0       ;add to lo y
        mov r0,@2(r5)
        jsr pc,graf
        rts pc
;
        .END
```

```
        .title scroll
        ; changes the scrolling region on the ansi screen
        ;callable from fortran as CALL  SCROLL(IUPPER,ILOWER)
        ;where iupper and ilower are the top and bottom line
        ;numbers of the new scroll region - note that line
        ;numbers start at the top of the screen and work
        ;down. The subroutine checks that iupper is less than
        ;ilower and will ignore incorrect commands but does
        ;not check the value of the line numbers, so if you
        : use the 48 line display etc make sure that the
        ; values are right !!
        ;
        .mcall .ttyout
        .macro print,val
        mov val,r0
        .ttyout
        .endm
        ;
scroll:: ;
        mov @2(r5),r1           ;contains iupper
        mov @4(r5),r2           ;contains ilower
        cmp r1,r2               ;compare them
        bgt fin                 ;if r1>r2 goto end
        ;
        ;to change scrolling region the escape sequence :
        ; ESC [ Pt ; Pl r  (see Hirez 100 instructions)
        ;
        jsr pc,escs      ;esc [
        mov r1,r3
        jsr pc,octasc    ;convert no. in r3 to ascii code(s)
        print £73
        mov r2,r3
        jsr pc,octasc    ;convert no. in r3 to ascii code(s)
        print £162
;
;       now position cursor at top left of the scroll region
;       escape sequence is ESC [ Pl ; Pc H
        jsr pc,escs
        mov r1,r3       ;r1 holds top line of scroll region
        jsr pc,octasc   ;convert to ascii code(s)
        print £73
        print £61       ;set cursor in column 1
        print £110
fin:    rts pc
```



```
        ;
escs:   print £33               ;ESC
        print £133              ;[
        rts pc
        ;
octasc: clr r4          ;set counter to zero
        cmp r3,£11      ;is there only 1 ascii character ?
        ble 2$          ;yes goto 2$
1$:     sub £12,r3      ;subtract 10
        inc r4          ;remember no. of times 10 subtracted
        cmp r3,£11      ;less than 10 decimal ?
        bgt 1$          ;no subtract another 10
        add £60,r4      ;yes convert to ascii (add 60 octal)
        print r4        ;print this
2$:     add £60,r3      ;remainder converted to ascii
        print r3        ;and printed
        rts pc
        ;
        .end

        .title date
;
;       DATE request,may be interfaced to user programs
;       call from fortran is
;
;       CALL IDATE(IDAY,IMONTH,IYEAR)
;
;       note that we are using the British date convention
;       ,not the US one !
        .mcall .date
;
date::  .date           ;date in r0
        mov r0,r2       ;copy r0
        beq 1$          ;if 0, then no date entered
        bic £^C37,r2    ;clear all but year bits
        add £72.,r2     ;make it current year by adding 72
        mov r2,@6(r5)   ;move year to 3rd arg
        mov r0,r1       ;copy date word again
        asl r1
        asl r1
        asl r1
        ;get day bits on byte boundary by shifting
        swab r1         ;day bits in low order byte
        bic £^C37,r1    ;clear all but day bits
        mov r1,@2(r5)   ;move to first arg
```

```
        swab r0         ;month bits in low byte
        asr r0
        asr r0
        bic £^C37,r0    ;clear all but month bits
        mov r0,@4(r5)   ;month to arg 2
1$:     rts pc
        .end
```



```
        .title  ansi
        ;
        ;does various screen handling routines for the
        ;Hirez 100 terminal whilst it is in ANSI mode
        ;
        ;Version 1.02 Andrew Robinson          29.7.86
        ;
        ;the globals will display characters BOLD,UNDERLINE
        ; characters,make characters BLINK,display in
        ;Reverse VIDEO, or cancel any of these attributes.
        ;
        ;the keyboard may also be locked to prevent any
        ;characters being generated whilst in tek mode
        ;
        .mcall .ttyout
        .macro print,val
        mov val,r0
        .ttyout
        .endm
        ;
        ;the FORTRAN subroutine calls are:
        ; for bold                      CALL BOLD
        ; for underlined                CALL ULINE
        ; for blinking                  CALL BLINK
        ; for reverse video             CALL RVIDEO
        ; to reset to normal            CALL CLEAR
        ; to lock keyboard              CALL LOCK
        ; to unlock keyboard            CALL UNLOCK
        ;
        ;N.B.   the VIDEO attributes are cumulative, so that
        ;is possible to have combinations of effects such as
        ;underlined reverse video or bold blinking characters
        ;
bold::  ;ESC [ 1 m is the escape sequence required by the
        ;terminal to goto bold plotting
        print £33
        print £133
        print £61
        print £155
        rts pc
;
uline:: ;ESC [ 4 m is the escape sequence required by the
        ;terminal to goto underlined characters
        print £33
```

```
        print £133
        print £64
        print £155
        rts pc
;
blink:: ;ESC [ 5 m is the escape sequence required to get the
        ;terminal to blink all following characters
        print £33
        print £133
        print £65
        print £155
        rts pc
rvideo::
        ;ESC [ 7 m is the escape sequence to get the terminal
        ;to goto reverse video printing
        print £33
        print £133
        print £67
        print £155
        rts pc
;
clear::
        ;ESC [ 0 m resets the previous character attribute
        ;to the default (normal printing)
        print £33
        print £133
        print £60
        print £155
        rts pc
;
lock::  print £33       ;ESC [ 2 h locks keyboard
        print £133
        print £62
        print £150
        rts pc
;
unlock:: print £33      ;ESC [ 2 l unlocks keyboard
        print £133
        print £62
        print £154
        rts pc
;
        .end
```



```
        .title cursor
        ;
        ;controls the cursor on the ansi screen
        ;
        .mcall .ttyout
        .macro print,val
        mov val,r0
        .ttyout
        .endm
        ;
cursor:: ;
        mov @2(r5),r1           ;contains iline
        mov @4(r5),r2           ;contains icolumn
        cmp r1,£48.             ;iline>48 ?
        bgt fin
        cmp r2,£132.            ;icolumn>132 ?
        bgt fin
        tst r1                  ;iline < 0?
        blt fin
        tst r2                  ;icolumn<0 ?
        blt fin
        ;
        ;to change scrolling region the escape sequence :
        ; ESC [ Pl ; Pc H  (see Hirez 100 instructions)
        ;
        jsr pc,escs     ;esc [
        mov r1,r3
        jsr pc,octasc   ;convert no. in r3 to ascii code(s)
        print £73
        mov r2,r3
        jsr pc,octasc   ;convert no. in r3 to ascii code(s)
        print £110
;
fin:    rts pc
        ;
escs:   print £33       ;ESC
        print £133      ;[
        rts pc
        ;
octasc: clr r4          ;set counter to zero
        cmp r3,£11      ;is there only 1 ascii character ?
        ble 2$          ;yes goto 2$
1$:     sub £12,r3      ;subtract 10
        inc r4          ;remember no. of times 10 subtracted
```

```
        cmp r3,£11      ;less than 10 decimal ?
        bgt 1$          ;no subtract another 10
        add £60,r4      ;yes convert to ascii (add 60 octal)
        print r4        ;print this
2$:     add £60,r3      ;remainder converted to ascii
        print r3        ;and printed
        rts pc
        .end
```



```
        .TITLE SCREENS
        ;switches the Hirez-100 terminal between 24/48 lines
        ;and 80/132 columns
        ;other values in the arguments are ignored
        ;callable from fortran programs as:
        ;CALL SCREEN(ICOL,ILINE)
        ;ICOL= 80 OR 132 ILINE= 24 OR 48
        .MCALL .TTYOUT
        .MACRO  PRINT,VAL
        MOV VAL,R0
        .TTYOUT
        .ENDM
SCREEN::MOV @2(R5),R1      ;r1 holds value of icol
        MOV @4(R5),R2      ;r2 holds value of iline
        CMP £120,R1        ;120 octal is 80 decimal
        BNE 1$
        JSR PC,COL80       ;transmit 80 column sequence
1$:     CMP £204,R1        ;204 octal is 132 decimal
        BNE 2$
        JSR PC,COL132      ;transmit 132 column sequence
2$:     CMP £30,R2         ;30 octal is 24 decimal
        BNE 3$
        JSR PC,LINE24      ;transmit 24 line sequence
3$:     CMP £60,R2         ;60 octal is 48 decimal
        BNE 4$
        JSR PC,LINE48      ;transmit 48 line sequence
4$:     RTS PC             ;return to fortran
        ;
LINE24: ;terminal must receive the sequence ESC [ ? 0 l
        JSR PC,ESCSEQ      ;this does the ESC [ ? part
        PRINT £60          ;60 octal is ascii code for 0
        PRINT £154         ;154 octal is ascii code for l
        RTS PC
;
LINE48: ;terminal must receive the sequence ESC [ ? 0 h
        ;
        JSR PC,ESCSEQ
        PRINT £60
        PRINT £150
        RTS PC
;
COL80:  ;terminal must receive the sequence ESC [ ? 3 l
        ;
        JSR PC,ESCSEQ
        PRINT £63          ;63 octal is ascii code for 3
```

```
        PRINT £154      ;150 octal is ascii code for l
        RTS PC
;
COL132: ;terminal must receive the sequence ESC [ ? 3 h
        ;
        JSR PC,ESCSEQ
        PRINT £63
        PRINT £150
        RTS PC
;
ESCSEQ: ;transmits the ESC [ ? sequence
        PRINT £33
        PRINT £133
        PRINT £77
        RTS PC
;
        .END
```

APPENDIX EIGHT

Commands recognised by the RAIRS spectrometer control program, IR.FOR.

AUTO

Causes subtraction spectrum to be run with preset parameters, the data saved to disc automatically with the current filename and filenumber and the process repeated with the filenumber incremented by one. This process continues until terminated by typing a CTRL Z characater at the keyboard.

BASE

This command causes a baseline spectrum to be run using the preset run parameters.

CLB

Clears the storage array which holds the data for the baseline spectrum.

CLM

Clears the storage array which holds the co-ordinates for the on-screen markers.

DISP

Erases the alphanumeric data displayed on the screen (the pre-set parameters and the filename and filenumber) and redraws them with their current values.

EXIT

Terminates the program, after having checked that the x10 expand feature on the lock-in amplifier is switched off.

EXP

Toggles the x 10 expand feature on the lock-in amplifier. If expand is on then EXP is displayed at the bottom right of the screen.

FIL=n

Changes the current filenumber to n.

FIN=n

Changes the end frequency of the frequency scan range. The value of n is the new end frequency in wavenumbers.

GFIN

Moves the diffraction grating to the position corresponding to the end frequency in the scan range.

GOTOn

Moves the diffraction grating to the position corresponding to the frequency n (measured in wavenumbers).

GSTA

Moves the diffraction grating to the position corresponding to the starting frequency in the scan range.

INT

Performs a numerical integration on differential spectra acquired whilst running using the wavelength modulation technique. A value of the area beneath the integrated spectrum is also displayed. This routine also has a plotting option to plot the integrated spectrum on the digital plotter.

MAR=n

Switches the Tektronix cross-hair cursor onto the graphics screen. They may be positioned using the cursor keys and the final co-ordinates stored as marker n, where n is 1 to 9. The final x co-ordinate is stored as a frequency (in wavenumbers) and the final y co-ordinate as a height above the baseline (in arbitrary units).

NAME

Responds by asking for a new six character filename and displaying the new name in the top left of the screen.

OFF=n

Changes the voltage offset on the lock-in amplifier. The value of n is in volts.

PLOT

Sends the spectrum displayed on the screen to the digital plotter. Options in plotting include whether to plot the frequency axis or not and whether to plot the currently defined marker points.

PRM

Plots the currently defined markers on the digital plotter.

QUIT

Used to terminate the program when not running the spectrometer.

REA=n

Reads a previously stored file with the current filename and the filenumber n. If n is zero, the file is a baseline spectrum, if n is non-zero it is a subtraction spectrum.

READ

Reads a previously stored file with the current filename and filenumber.

ROL=n

Changes the roll-off parameter on the lock-in amplifier. If the value of n is zero, then the current value of the rolloff is displayed at the top of the screen. If n is 6 or 12 then the rolloff value is changed (the rolloff value is in dB/octave).

RUN

Runs a subtraction spectrum after incrementing the current filenumber by one.

SAVE

Saves the data displayed on the screen, using the current filename and filenumber.

SCRE

Erases the screen and redraws the current spectrum.

SEN=n

Changes the sensitivity scale of the lock-in amplifier to n volts.

SPE=n

Changes the speed at which the linear motion drive moves during a scan. The number n is the speed in arbitrary units, with typical values being in the range 650 (slow) to 900 (fast).

STA=n

Changes the starting point for the current frequency scan range. The units of n are wavenumbers.

STE=n

Changes the distance between points in the frequency scan range and hence the number of points in the spectrum. The units of n are wavenumbers.

TIM=n

Changes the time constant used by the lock-in amplifier. The units of n are seconds.

TITL

Responds by asking for a title for the current spectrum. This is then displayed at the top of the screen.

YOF=n

Controls the y axis position of the displayed spectrum on the Hirez-100 terminal and also on the RY-101 plotter. The range of n is from -550 to 780.

YSC=n

Controls the y axis magnification factor for the spectrum displayed on the terminal

Glossary

AD	Analogue to Digital
AES	Auger Electron Spectroscopy
ARUPS	Angle Resolved Ultra-violet Photo-electron Spectroscopy
DA	Digital to Analogue
EELS	Electron Energy Loss Spectroscopy
ESDIAD	Electron Stimulated Desorption Ion Angular Distribution
FWHM	Full Width at Half Maximum
HREELS	High Resolution Electron Energy Loss Spectroscopy
IR	Infra-red
IRAS	Infra-red Reflection Absorption Spectroscopy (see RAIRS)
LEED	Low Energy Electron Diffraction
LIA	Lock-In Amplifier
MCT	Mercury Cadmium Telluride
QMS	Quadrupole Mass Spectrometer
RAIRS	Reflection Absorption Infra-Red Spectroscopy (also known as IRAS)
TPD	Temperature Programmed Desorption
UHV	Ultra-High Vacuum

References

1 G C Bond and R Burch
Catalysis, Vol 6, Specialist Periodical Reports, Royal Society of Chemistry, London, 1983

2 T J Huang and W O Haag in "Catalytic activation of CO", A.C.S. Symposium series no. 152, editor P C Ford, American Chemical Society, Washington D.C., 1981

3 Articles in "The chemical Physics of Solid Surfaces and Heterogeneous catalysis", Volume 4, editors D A King and D P Woodruff, Elsevier, 1982

4 S M Davis and G A Somorjai in reference 3

5 R W Joyner
Catalysis, Vol 5, Specialist Periodical Reports, Royal Society of Chemistry, London 1982

6 W -D Mross
Catal Rev. -Sci Eng. 25(4),591, (1983)

7 V Ponec
Catal Rev. -Sci. Eng. 18(1), 151, (1978)

8 C M Comrie and R M Lambert
J. C. S. Faraday Trans. 72, 1659, (1976)

9 P Hofmann, S R Bare and D A King
Surface Science 117, 245, (1982)

10 T E Jackman, J A Davies, D P Jackson, P R Norton and W N Unertl
J. Physics (Solid State Physics) C15, L99, (1982)

11 H P Bonzel and S Ferrer
Surface Science 116, L263, (1982)

12 S R Bare, P Hofmann and D A King
Surface Science 144, 347, (1984)

13 P Hofmann, S R Bare, N V Richardson and D A King
Solid State Communications 42, 645, (1982)

14 S R Bare, K Griffiths, P Hofmann, D A King, N L Nyberg and N V Richardson
Surface Science 120, 367, (1982)

15 J Fair and R J Madix
J. Chem. Phys. 73, 3480, (1980)

16 R W McCabe and L D Schmidt
Surface Science 66, 101, (1977)

17 S Ferrer and H P Bonzel
Surface Science 119, 234, (1982)

18 D Reiger, R D Schnell and W Steinmann
Surface Science 143, 157, (1984)

19 P Hofmann, S R Bare and D A King
Physica Scripta T4, 118, (1983)

20 T E Jackman, J A Davies, D P Jackson, W N Unertl and P R Norton
Surface Science 120, 389, (1982)

21 H P Bonzel
J. Vac. Sci. Tech. A2, 866, (1984)
and references therein

22 J Lee, J Arias, C P Hanrahan, R M Martin and H Metiu
Phys. Rev. Lett. 51, 1991, (1983)

23 G P Blyholder
J. Phys. Chem. 68, 2772, (1964)

24 J Arias, J Lee, J Dunaway, R M Martin and H Metiu
Surface Science 159 , L433, (1985)

25 J Lee, C P Hanrahan, J Arias, R M Martin, H Metiu
Phys. Rev. Lett. 51, 1803, (1985)

26 F M Hoffman and R A de Paola
Phys. Rev. Lett. 52, 1697 (1984)

27 R A de Paola, J Hrbek and F M Hoffman
J. Chem, Phys. 82, 2484, (1985)

28 T E Madey and C Benndorf.
Surface Science 164, 602, (1985)

29 F P Netzer, D L Doering, and T E Madey
Surface Science 143, L363, (1984)

30 J J Weimer, E Umbach and D Menzel
Surface Science 155, 83, (1985)

31 J J Weimer, E Umbach and D Menzel
Surface Science 155, 132, (1985)

32 J J Weimer and E Umbach
Phys. Rev. B30, 486, (1986)

33 W Eberhardt, F M Hoffmann, R de Paola, D Heskett, I Strathy, E W Plummer and H R Moser
Phys. Rev. Lett. 54, 1856, (1985)

34 W Eberhardt, F M Hoffmann, R de Paola, D Heskett, I Strathy, E W Plummer and H R Moser
Chem. Phys. Lett. 124, 237, (1986)

35 W A Herrmann, H Biersack, M L Ziegler, K Weidenhammer, R Siegel and D Rehder
J. Am. Chem. Soc. 103, 1692, (1981)

36 D Lackey, M Surman, S Jacobs, D Grider and D A King
Surface Science 152/153, 513 , (1985)

37 E L Garfunkel, J E Crowell and G A Somorjai
J. Phys. Chem. 86, 310, (1982)

38 J E Crowell, E L Garfunkel and G A Somorjai
Surface Science 121, 303, (1982)

39 J E Crowell and G A Somorjai
Appl. Surface Science 19, 73, (1984)

40 L J Whitman and W Ho
J. Chem. Phys. 83, 4808, (1985)

41 K J Uram, L Ng, M Folman and J T Yates Jnr.
J. Chem. Phys. 84, 2891, (1986)

42 K J Uram, L Ng, J T Yates Jnr.
Surface Science 177, 291, (1986)

43 S Holloway and J K Norskov
J Electroanal Chem. 161, 193, (1983)

44 N D Lang, S Holloway, J K Norskov
Surface Science 150, 24, (1985)

45 S Efrima and H Metiu
Surface Science 108, 329, (1981)

46 P J Feibelmann and D R Hamann
Phys. Rev. Lett. 52, 61, (1984)

47 P J Feibelmann and D R Hamann
Surface Science 149, 48, (1985)

48 W Muller and P Bagus
J. Electron. Spectrosc. & Related Phenomena
38, 303,(1986)

49 G Herzberg in "Infrared and Raman Spectra of Polyatomic Molecules", Volume 2, Van Nostrand, New York, 1945

50 F A Cotton, "Chemical Applications of Group Theory", Interscience Publishers, New York and London, 1953

51 F H Read, "Electromagnetic Radiation", John Wiley, London, 1981

52 J D Jackson, "Classical Electrodynamics", 2nd edition, John Wiley, New York, 1975, page 280

53 L D Landau and E M Lifshitz in "Electrodynamics of Continuous Media", Pergamon Press 1975, page 274

54 O S Heavens "Optical Properties of Thin Solid Films", Dover Publications, New York, 1965

55 P Hollins and J Pritchard in "Vibrational Spectroscopy of Adsorbates", editor R F Willis, Springer Series in Chemical Physics 15, Springer-Verlag, Berlin 1980, page 127

56 S A Francis and A H Ellison
J Opt. Soc. Am. 49, 131, (1959)

57 R G Greenler
J. Chem. Phys. 44, 310, (1966)

58 R G Greenler
J. Chem. Phys. 50, 1963, (1969)

59 J D E McIntyre and D E Aspnes
Surface Science 24, 417, (1980)

60 H Ibach
Surface Science 66, 56, (1977)

61 R G Greenler, R R Rahn and J P Schwartz
J. Catalysis 23, 42, (1971)

62 R G Greenler
J. Vac. Sci. Tech. 12, 1410, (1975)

63 R G Greenler
Japan. J. Appl. Phys. Suppl. 2, Part 2, 265, (1974)

64 P A Redhead
Vacuum 12, 203, (1962)

65 D Menzel in "Chemistry and Physics of Solid Surfaces IV", eds R Vanselow and R Howe, Springer Series in Chemical Physics, Springer Verlag 1982, page 391

66 D A King in "Chemistry and Physics of Solid Surfaces II", ed R Vanselow, CRC Press Inc, Boca Raton, Florida, 1979, pages 87-128

67 C G Goymour and D A King
J. C. S. Faraday Trans. I 69, 749, (1973)

68 D L Adams
Surface Science 42, 12, (1974)

69 L C Clarke "Surface Crystallography: An Introduction to LEED", John Wiley, 1985

70 J Riviere
Contemporary Physics 14, 513, (1973)

71 E A Wood
J. Appl. Phys. 35, 1306, (1964)

72 B W Holland and D P Woodruff
Surface Science 36, 488, (1972)

73 R M Lambert
Surface Science 49, 325, (1975)

74 M K Debe and D A King
Phys. Rev. Lett. 39, 708, (1977)

75 M K Debe and D A King
Surface Science 81, 193, (1979)

76 J H Onufurko and D P Woodruff
Surface Science 87, 357, (1979)

77 International Tables for X-ray Crystallography
ed K Lonsdale, Kynoch Press, Birmingham

78 J E Stewart, "Infra Red Specroscopy",
Marcel Dekker, New York, 1970

79 M Czerny and A F Turner
Z. Physik 61, 792, (1930)

80 M Cardona, "Modulation Spectroscopy",
Solid State Physics Suppliment 11, Academic Press
(New York and London) 1969

81 K Horn and J Pritchard
Surface Science, 52, 437, (1975)

82 K Horn and J Pritchard
J. Phys. (Paris) 38, C4, 144, (1977)

83 K Hallam, BSc. Project Report,
University of Bath, 1985

84 R W Hannah and R J Farnum,
"Applied Infrared Spectroscopy", Volume 5, (1973)
Perkin-Elmer Inc.

85 R Ducros and R P Merrill
Surface Science 55, 227, (1976)

86 M Salmeron and G A Somorjai
Surface Science 91, 373, (1980)

87 A Crossley and D A King
Surface Science 68, 528, (1977)

88 A Crossley and D A King
Surface Science 95, 131, (1980)

89 B E Hayden in "Methods in Surface Characterisation"
Volume 1, editors T E Madey and J T Yates Jnr
Plenum Press 1987

90 B E Hayden, K Kretchmar, A M Bradshaw and R G Greenler
Surface Science 149, 394, (1985)

91 R G Greenler, K D Burch, K Kretchmar, R Klauser,
A M Bradshaw and B E Hayden
Surface Science 152/153, 338, (1985)

92 R P Eischens and A L Pliskin
Advances in Catalysis 10, 1, (1958)

93 R Shigeishi and D A King
Surface Science 58, 379, (1976)

94 R M Hammaker, S A Francis and R P Eischens
Spectrochima Acta 21, 1295, (1965)

95 G D Mahan and A A Lucas
J. Chem. Phys. 68, 1344, (1978)

96 M Scheffler
Surface Science 81, 562, (1979)

97 B N J Persson and R Ryberg
Phys. Rev. B24, 6954, (1981)

98 H Ibach and D L Mills in
"Electron Energy Loss Spectroscopy",
Academic Press (1982)

99 M Moskovits and J E Hulse
Surface Science 78, 397, (1978)

100 D P Woodruff, B E Hayden, K Prince and A M Bradshaw
Surface Science 123, 397, (1982)

101 S Efrima and H Metiu
Surface Science 92, 433, (1980)

102 M Tushaus, E Schweizer and A M Bradshaw
J. Electron Spectrosc. and Rel. Phenomena, in press

103 H Pfnur, D Menzel, F M Hoffmann, A Ortega
and A M Bradshaw
Surface Science 93, 431, (1980)

104 A Ortega, PhD Thesis, Berlin Free University, 1980

105 P Hofmann, J Gossler, A Zartner, M Glanz
and D Menzel
Surface Science 161, 303, (1985)

106 E Williams and W H Weinberg
Surface Science 82, 93, (1979)

107 G E Thomas and W H Weinberg
J. Chem. Phys. 70, 954, (1979)

108 H Ueba
Surface Science 188, 421, (1987)

109 B E Hayden, A W Robinson and P M Tucker
Surface Science 192, 163, (1987)

110 W Reidl and D Menzel
Surface Science 163, 59, (1985)

111 J Lee, J Arias, C Hanrahan, R Martin, H Metiu, C Klauber
M D Alvey and J T Yates Jnr
Surface Science 159, L460, (1985)

112 M I Ban, M A Van Hove and G A Somorjai
Surface Science 185, 355, (1987)

113 J P Biberian and M A Van Hove
Surface Science 138, 361, (1984)

114 A W Robinson, B E Hayden and P M Tucker
Vacuum, in press

115 D Hesketh, E W Plummer, R A De Paola, W Eberhardt,
F M Hoffmann and H R Moser
Surface Science 164, 490, (1985)

116 B E Hayden and A M Bradshaw
Surface Science 125, 787, (1983)

117 A M Baro and H Ibach
J. Chem. Phys. 71, 4812, (1979)

118 F M Hoffmann and B N J Persson
Phys. Rev. B34, 4354, (1986)

119 B N J Persson and F M Hoffmann
J. Chem. Phys., submitted

120 C M Chan, K L Luke, M A Van Hove, W H Weinberg and
E D Williams
J. Vac. Sci. Tech. 16, 642, (1979)

121 J C Campuzano, A M Lahee and G Jennings
Surface Science 152/153, 68, (1985)

122 C M Chan and M A Van Hove
Surface Science 171, 226, (1986)

123 C Kittel, "Introduction to Solid State Physics",
John Wiley, London, Second Edition, 1963, page 40

124 L Pauling, "The nature of the chemical bond",
Cornell University Press, Ithaca, 1945, page 346

125 B E Hayden, A W Robinson, P M Tucker
J. Electron Spectrosc. and Related Phenomena
in press

126 A M Bradshaw and F M Hoffmann
Surface Science 72, 513, (1978)

127 J C Campuzano and R G Greenler
Surface Science 83, 301, (1979)

128 K Horn and J Pritchard
Surface Science 55, 70, (1976)

129 K Horn, M Hussain and J Pritchard
Surface Science 63, 244, (1979)

130 B E Hayden, K Kretzschmar and A M Bradshaw
Surface Science 155, 553, (1985)

131 P Hollins and J Pritchard
Surface Science 89, 456, (1979)

132 P Hollins and J Pritchard in "Vibrational
Spectroscopies for Adsorbed Species", ACS Symposium
Series 137 (Am Chem Soc, Washington 1980)

133 B Anton, N R Avery, T E Madey, W H Weinberg
J. Chem. Phys. 85, 507, (1986)

134 J K Norskov
Phys. Rev. B26, 2875, (1982)

135 D K Lambert
J. Vac. Sci. Tech. B3, 1479, (1985)

136 D K Lambert
Solid State Communications 51, 297, (1984)

137 D K Lambert
Phys. Rev. Lett. 50, 2106, (1983)

138 D K Lambert
Phys. Rev. Lett. 51, 2233, (1983)

139 C W Bauschenlicher Jnr
Chem. Phys. Lett. 118, 307, (1985)